

Climate Change Impacts and Projections for the Greater Boston Area

ELLEN DOUGLAS, PhD, PAUL KIRSHEN, PhD



Findings of the Greater Boston Research Advisory Group Report



University of Massachusetts Boston
School for the Environment

Climate Change Impacts and Projections for the Greater Boston Area

Findings of the Greater Boston Research Advisory Group Report

Project Leadership

Ellen Douglas, School for the Environment, UMass Boston; Ellen.Douglas@umb.edu
Paul Kirshen, School for the Environment, UMass Boston; Paul.Kirshen@umb.edu

Project Administrator

Kimberly Starbuck, Urban Harbors Institute, UMass Boston

Stakeholder Engagement and Outreach Team

Kristin Uiterwyk, Urban Harbors Institute, UMass Boston, Team Leader
Kimberly Starbuck, Urban Harbors Institute, UMass Boston
Paul Kirshen, School for the Environment, UMass Boston
Betsy Sweet, Urban Planning and Community Development, UMass Boston
Anna Valdez, School for the Environment, UMass Boston
Darcy Schofield, Metropolitan Area Planning Council

Temperature Team

Evan Kodra, risQ Inc., Team Leader
Kate Duffy, NASA Ames Research Center
Ryan Grieser, risQ Inc.
Ambarish Karmalkar, Department of Geosciences, UMass Amherst
Terry Tabors, risQ Inc.
Mary Warner, Northeastern University

Storms, Precipitation, Flooding, and Groundwater Team

Mathew Barlow, UMass Lowell, Team Leader
Laurie Agel, UMass Lowell
Mathias Collins, National Oceanic and Atmospheric Administration
Art DeGaetano, Cornell University
Jayne Knott, JFK Environmental Services LLC
Ambarish Karmalkar, UMass Amherst

Sea Level Rise Team

Robert DeConto, UMass Amherst, Team Leader
Hannah Baranes, UMass Amherst
Jon Woodruff, UMass Amherst
Anna Ruth Halberstadt, UMass Amherst
Robert Kopp, Rutgers University

GBRAG Steering Committee

Alex Papali, Clean Water Action
 Alison Brizius, City of Boston
 Beth Lambert, Massachusetts Division of Ecological Restoration
 Bud Ris, Green Ribbon Commission
 Caitlin Spence, Metropolitan Area Planning Council
 Carl Spector, City of Boston
 Chris Longchamps, Partners HealthCare
 Darci Schofield, Metropolitan Area Planning Council
 Dr. Paul Biddinger, Massachusetts General Hospital and Partners
 Ellen Mecray, National Oceanic and Atmospheric Administration
 Emily Silda, Barr Foundation
 Ivy Mlsna, Environmental Protection Agency
 J.J. Bartlett, Massachusetts Fishing Partnership
 Jill Horwood, Boston Harbor Now
 Jill Valdes Horwood, Boston Harbor Now
 Joe Christo, City of Boston
 Joy Duperault, Department of Conservation and Recreation
 Julia Knisel, Massachusetts Office of Coastal Zone Management
 Julie Wood, Charles River Watershed Association
 Julie Wormser, Mystic River Watershed Association
 Kathryn Ford, Division of Marine Fisheries
 Kristin Kelleher, Climate Action Business Association
 Margot Mansfield, Massachusetts Office of Coastal Zone Management
 Mark Rousseau, Division of Marine Fisheries
 Mia Mansfield, City of Boston
 Peter DeBruin, MassPort
 Peter Phippen, Great Marsh Coalition
 Peter Weiskel, United States Geological Survey
 Phil Giffee, Neighborhood of Affordable Housing
 Randall Lyons, Massachusetts Marine Trades Association
 Rebecca Herst, University of Massachusetts Boston
 Sasha Shyduroff, Metro Mayers Climate Preparedness Task Force
 Stacy Thompson, Liveable Street Alliance
 Thomas Fitzgerald, National Grid
 Torrie Hanley, Northeastern University
 Yves Torrie, A Better City

Cover Photos, clockwise from upper left:

iStockphoto/Kirkikis, Massachusetts Water Resources Authority, iStockphoto/easywash, Neponset River Watershed Association

Disclaimer:

The scientific results and conclusions, as well as any views or opinions expressed herein, are those of the author(s) and do not necessarily reflect those of the National Oceanographic and Atmospheric Administration or the Department of Commerce.

Table of Contents

Acknowledgements	ix
Executive Summary	1
1. Introduction	6
1.1 The need for scientific consensus on climate projections	6
1.2 The approach and objectives of GBRAG	6
1.3 Introduction references	8
2. Storms, Precipitation, Flooding and Groundwater	9
2.1 Introduction to this chapter	9
2.2 Sources of uncertainty	9
2.3 Storms	10
Key findings	10
Review of existing science	11
Projected changes	12
Knowledge and data gaps	14
2.4 Seasonal precipitation	15
Key findings	15
Review of existing science	15
Projected changes	15
Knowledge and data gaps	18
2.5 Extreme precipitation	18
Key findings	18
Review of existing science	18
Projected changes	21
Knowledge and data gaps	23
2.6 Flooding	24
Key findings	24
Review of existing science	24
Riverine projections	26
Stormwater projections	28
Knowledge and data gaps	28

2.7	Groundwater (summary of groundwater special report)	29
	Key findings	29
	Review of existing science	29
	Groundwater projections	31
	Knowledge and data gaps	34
2.8	Storms, precipitation, flooding, and groundwater references	34
3.	Extreme Temperature	44
3.1	Key findings	44
3.2	Introduction	44
3.3	Review of existing science	45
	Aggregate trends and projections	45
	Extremes and variability	45
3.4	Projections	46
3.5	Open questions and data gaps	52
3.6	Impact sectors: energy	53
	Heating and cooling	53
	Electricity demand	53
3.7	Impact sectors: public health	54
	Heat	54
	Air quality	56
	Vector-borne diseases	57
3.8	Impact sectors: infrastructure and transportation	59
	Roads and care	59
	Public transportation (rail, bus)	59
	Air travel	60
3.9	Impact sectors: economy, society, governance	60
	GDP60	
	Fisheries	61
	Household income	61
3.10	Impact sectors: agriculture and natural resources	61
3.11	Temperature references	62

4. Sea Level Rise	67
4.1 Key findings	67
4.2 Introduction	69
4.3 How fast is Global Mean Sea Level (GMSL) rising and why?	70
4.4 Why is Relative Sea Level (RSL) rising faster in Boston than the global average?	71
4.5 Future sea level projections	74
4.6 Future loss of the Greenland and Antarctic ice sheets	77
4.7 GBRAG versus BRAG sea level projections	77
4.8 GBRAG RSL projections for Boston Harbor	77
4.9 Coastal flooding	80
Mechanisms of coastal flooding	82
2018 Nor'easters	84
Climate-driven changes in extratropical and tropical cyclone characteristics	86
Tidal variability and extreme flooding	86
4.10 Future flooding	86
Flood projections	88
Comparison with BRAG	92
Hydrodynamic models	95
Minor high tide flooding	95
4.11 Outlook and recommendations for using this report	98
4.12 SLR and flooding references	99
5. Appendix	107
Table 4.1	107
Table 4.2	108
Table 4.3	124
Table 4.4	128

TABLES

2. Storms, Precipitation, Flooding, and Groundwater

2.1 Best available estimates for projected changes in storms, with confidence in parentheses.	13
2.2 Total seasonal precipitation over the baseline period (1971 to 2000) and projections relative to baseline for the Suffolk County/Boston Harbor basin.	17
2.3 Comparison of baseline estimates and future projections of days with > 2 in of precipitation and annual average maximum 5-day precipitation accumulation for Boston, based on C-CCVA and Climate Explorer data.	23
2.4 Best available estimates for potential changes in river floods in the Greater Boston area (after Douglas et al., 2016).	27

3. Extreme Temperature

3.1 Projected changes (degrees Fahrenheit or number of days) for counties covering the GBRAG study regions using LOCA Downscaling from The Climate Data Explorer.	47
3.2 County Level Probabilistic LOCA Dowscaled Projections from Karmalkar.	49

4. Sea Level Rise

4.1 Relative sea level probabilities for Boston Harbor relative to a 2000 baseline for three RCP greenhouse gas emissions scenarios.	80
4.2 Metrics describing the two Nor'easters that caused record-breaking flooding on the Massachusetts coast during the winter of 2018.	84
4.3 Projections of 10-year and 100-year winter flood heights, averaged across each nodal cycle phase.	90
4.4 Projections of 10-year and 100-year summer flood heights, averaged across each nodal cycle phase.	90
4.5 Projections of winter season annual exceedances for flood heights of 2.60 m (roughly the present-day 10-year flood height), 2.80 m, and 3.00 m (roughly the present-day 100-year flood height).	91
4.6 Projections of summer season annual exceedances for flood heights of 2.40 m (roughly the present day 10-year flood height), 2.55 m, and 2.70 m (roughly the present-day 100-year flood height).	91
4.7 Comparison of 10 th to 90 th percentile 100-year flood height projections in BRAG (2016) and GBRAG (2021) without Nodal Cycle Tide Changes.	92
4.8 Comparison of relative sea level rise projections since 2000 used by MC-FRM (based on (Kopp et al., 2017) and those developed for GBRAG flood projections.	94

FIGURES

2. Storms, Precipitation, Flooding and Groundwater

2.1	Total annual (top) and warm season (bottom) precipitation in Boston for the period 1936 to 2020.	16
2.2	Model projections for total annual precipitation (in inches) for Suffolk County.	17
2.3	Time series of annual counts of hourly (left) and daily (right) precipitation exceeding the long term (1948 to 2019) 99 th percentile of > 0 hourly rainfall accumulation. The green line is a 10-year running mean.	19
2.4	10-year-centered running means of the percent change in the 10- (red), 25- (blue), and 100- (cyan) year design storm based on partial duration series that include observations through the indicated year relative to that based on a 1948 to 1990 data record.	20
2.5	10-year daily design storm depths (in inches) based on projections (1-day partial duration series) from the BWSC (red), C-CCVA (blue), and NRCC (cyan).	21
2.6	Percent change in the 25- (left) and 100-year (right) design storm relative to the base period using the NRCC approach for Boston (green) and the C-CCVA methodology (blue).	22
2.7	Time series showing increasing flood frequency (peaks-over-threshold per water year) at three gages in eastern New England with near-natural flood conditions.	26
2.8	Monthly recharge rates for Portsmouth and Hampton, New Hampshire, and Dracut and Pepperell, Massachusetts.	30
2.9	Water withdrawals for public drinking water supply in a) Essex County, b) Middlesex County, c) Norfolk County, and d) Plymouth County. Groundwater and surface-water withdrawals are shown with the total withdrawal indicated by the height of the bar.	31
2.10	Projected changes in monthly recharge for four 20-year periods relative to the baseline period (1981 to 2000) under the RCP4.5 emissions scenario for a) Portsmouth, b) Hampton, c) Dracut, and d) Pepperrel.	32
2.11	Projected groundwater rise with RSLR in coastal New Hampshire for four sea level rise scenarios: a) 0.3 m, b) 0.8 m, c) 1.6 m, and d) 2 m.	33

3. Extreme Temperature

3.1	Land cover, impervious surface, and tree canopy cover for Lower Roxbury, from Stawasz et al., 2019.	55
3.2	Key socioeconomic and demographics for Lower Roxbury, from Stawasz et al., 2019.	56
3.3	Urban heat island design proposal for Lower Roxbury, from Stawasz et al., 2019.	57
3.4	Urban heat island scores from the Trust for Public Land (Trust for Public Land, 2020).	58

4. Sea Level Rise

4.1	Relative sea level change at the Boston Harbor tide gauge station (#8443970) over the last century.	71
4.2	Spatial heterogeneity of sea-level change due to gravitational, rotational, and deformational effects arising from an equivalent loss of ice from the Greenland Ice Sheet (GIS; left) versus the West Antarctic Ice Sheet (WAIS; right).	74
4.3	GBRAG time series of RSL projections for Boston Harbor, showing the median (50 th percentile) estimates (solid lines), with the 5 th to 95 th percentile (very likely) ranges in 2100 (top) and 2200 (bottom) indicated by the solid bars at right.	78
4.4	Future rates of sea level rise (mm yr -1) corresponding to the central (50 th percentile) sea level projections shown in Figure 4.3.	81
4.5	Illustration of a nonlinear increase in flood hazard driven by relative sea level rise.	82
4.6	Comparison of flooding during the record-breaking January 2018 Nor'easter and Hurricane Sandy in 2012.	83
4.7	Timing of Boston's top-ten storm tides relative to the 18.6-year tidal nodal cycle.	85
4.8	Seasonal differences and winter dominance in Boston flood hazard.	87
4.9	Historical and projected 10-year (top panels) and 100-year (bottom panels) flood heights in meters above 2000 MSL for the summer (left-hand panels) and winter (right-hand panels) seasons.	89
4.10	Thompson et al. (2021) projections of high tide flooding days per year at the Boston NOAA tide gauge.	96
4.11	Thompson et al. (2021) projections of high tide flooding days per month over 5-year periods at the Boston NOAA tide gauge for the NOAA minor (top panel) and moderate (bottom panel) flood thresholds and under the NOAA Intermediate Low (blue markers) and Intermediate (red markers) sea level rise scenarios.	97

5. Appendix

Supplementary Data: Table 4.1	107
Supplementary Data: Table 4.2	108
Supplementary Data: Table 4.3	124
Supplementary Data: Table 4.4	128

Acknowledgements

When the inaugural Boston Research Advisory Group (BRAG) report was released in 2016, it was recommended that the scientific consensus on climate change risk factors for Boston be updated every three to five years. The Barr Foundation made this update possible. Darci Schofield of the Metropolitan Area Planning Council (MAPC) had noted that the BRAG report offered essential information that was useful to and utilized by many cities and towns outside of the City of Boston and recommended a compilation of more localized information in the update. Subsequent discussions with Bud Ris, Mary Skelton Roberts, Emily Sidla, and Kalila Barnett of the Barr Foundation led to the expansion of the study area to include the 101 towns and cities within the MAPC region. We also acknowledge Ms. Schofield for helping to recruit members of the GBRAG steering committee and to organize our outreach activities within the MAPC domain. We further acknowledge and appreciate the guidance and support we received from John Cleveland and Amy Longsworth of the Green Ribbon Commission in launching the GBRAG.

We gratefully acknowledge the Barr Foundation for funding the GBRAG activities and reporting. We also gratefully acknowledge the competent and steadfast administrative efforts of Kimberly Starbuck of the Urban Harbors Institute at UMass Boston, who organized and managed GBRAG meetings, communications, and the GBRAG report. We further acknowledge the members of the GBRAG Steering Committee for their time and thoughtful feedback during this process.

We gratefully acknowledge the dedication of the following external reviewers of this GBRAG report and special reports; their comments and feedback made for better and more relevant reports:

Maya Buchanan, Senior Climate Policy Analyst, Oregon Department of Energy

David Bjerklie, New England Water Science Center, United States Geological Survey

Mike R. Johnson, Habitat and Ecosystem Services Division, National Oceanographic and Atmospheric Administration

Karen McKinnon, Institute of the Environment and Sustainability, University of California Los Angeles

Jayantha T. Obeysekera, Sea Level Solutions Center, Florida International University

Bhaskar Subramanian, Chesapeake & Coastal Service, Maryland Department of Natural Resources

Gabriele Villarini, Director of IIHR-Hydroscience and Engineering, University of Iowa

Donald Wuebbles, Department of Atmospheric Sciences, University of Illinois Urbana-Champaign

And finally, we gratefully acknowledge the high-quality (and last-minute) final proofreading by Courtney Humphries and the meticulous and patient guidance of David Gerratt, of DG Communications, who produced this document which we are incredibly proud to present.

Ellen Douglas

Paul Kirshen

School for the Environment, University of Massachusetts Boston

Executive Summary

During the writing of the inaugural Boston Research Advisory Group (BRAG) report (Douglas et al., 2016) both NASA and NOAA announced that 2015 was the warmest year on record, beating the previous record set in 2014, by 0.29 °F (Chappell, 2015). Just five years later (during the writing of this report), NASA announced that 2020 had tied 2016 for the warmest year, breaking the previous record by a stunning 1.84 °F, and that the last seven years have been the warmest seven-year period on record (NASA, 2021).

These observations support the assertion made in the sixth and most recent assessment by the Intergovernmental Panel on Climate Change (IPCC, 2021), which states, “*It is unequivocal that human influence has warmed the atmosphere, ocean and land. Widespread and rapid changes in the atmosphere, ocean, cryosphere and biosphere have occurred.*” Hence, the question is not whether the climate is changing, but what we’re going to do about it. At a minimum, we must focus efforts to get to net zero greenhouse gas (GHG) emissions by 2050. It’s not too late to achieve that goal, but time is running out for us to prevent the worst-case scenarios suggested here.

This report is broken into four chapters and summarizes the most recent (as of late 2021) scientific understanding of climate risk factors pertinent to Greater Boston.

Chapter 1

Introduction to the Greater Boston Research Advisory Group

The inaugural BRAG report represented the first scientific consensus on climate change impacts specifically related to the City of Boston. Since its June 2016 release, the report has been used extensively by Boston municipal agencies and climate experts, as well as officials in surrounding communities. Hence, a priority for an update to the BRAG report was to expand the analysis to all of Greater Boston; in this case the 101 cities and towns that make up the Metropolitan Area Planning Commission (MAPC) region, and to present the information in a way that is relevant for communities struggling to plan for the effects of our changing climate. The primary objective of what is now the Greater Boston Research Advisory Group (GBRAG) is to incorporate new findings into the scientific consensus on specific climate risk factors that affect the region.

Chapter 2

Storms, Precipitation, Flooding, and Groundwater

Boston receives more than 43 inches of precipitation annually. Tropical cyclones (TCs; also called hurricanes), extratropical cyclones (ETCs; including Nor’easters), and frontal systems (also called cold or warm fronts) deliver the majority of precipitation. Warm moist air masses from the Atlantic Ocean or Gulf of Mexico contribute to many of the region’s extreme precipitation events. The most extreme precipitation tends to be caused by TCs in the fall and ETCs in the spring, and often exceeds three inches in a single day. This extreme precipitation can generate coastal and urban flooding, as well as impact groundwater.

The BRAG report found no robust evidence of changes in frequency, intensity, or storm track of either TCs or ETCs, although there was limited evidence to suggest a slight northward displacement and increase in intensity for future TCs, and a slight weakening of ETCs. Recent research adds considerably to the BRAG results.

For storms, the key findings are:

- TCs are expected to decrease in frequency overall, but the proportion of stronger storms (Category 4 to 5) will likely increase.
- ETCs will likely be less intense overall (although localized winds near the center and along fronts may increase), and the proportion of precipitation that falls as snow will probably decrease.
- For all storm types, precipitation intensity (e.g., daily precipitation) associated with individual storms is expected to increase.

For seasonal precipitation, which was not considered in the BRAG report, the key findings are:

- Annual precipitation has increased in the Northeast, particularly during the warm season (June to October), and largely due to an increase in high-intensity precipitation.
- Projections also suggest increased precipitation in the winter and spring, although this is highly uncertain, given the range of model projections.
- Although there is a gradual trend toward wetter conditions, precipitation in any given season or year could be significantly lower or higher than the long-term average.

For extreme precipitation, the key findings are:

- Extreme precipitation events have become more frequent and intense in recent decades, and these changes are expected to continue through 2100 under current GHG emission rates.
- Most projections point to a 10 to 20% increase in daily precipitation intensity by 2050 and a 20 to 30% increase by 2100.
- There is currently little evidence to suggest that the intensity of short-duration (hourly precipitation) is changing at a faster rate than daily precipitation extremes.

For flooding, the key findings are:

- River and urban flooding are considered in detail, and new data and modeling studies increase confidence in the earlier BRAG projections.
- River floods are expected to be larger and more frequent, although there is considerable uncertainty about the magnitude of the increases.
- Stormwater is expected to increase with the greater intensity and frequency of heavy precipitation.
- Future regional flooding conditions may be significantly affected by higher groundwater elevations, especially near the coast as the sea level rises (see the Sea Level Rise chapter).
- Historical increases in regional flood frequency have been driven by more frequent warm season events.

Groundwater was not considered in the BRAG report. Because the effects of climate change on groundwater are complex and broad, GBRAG devotes a special report to the topic, which is summarized here. The findings paint an alarming picture of rising water levels near the coast and drought inland that will affect drinking water supply wells. Rising seas will cause coastal groundwater to rise, resulting in septic system failure and other forms of water-quality degradation in some locations. Roads and other foundations, as well as underground infrastructure, are not constructed to withstand groundwater intrusion, which can create very costly problems..

The key findings about groundwater are:

- Long-term monitoring wells show rising groundwater levels in the MAPC communities during the past 50 years.

- Over the next 50 years, groundwater recharge is projected to increase in the late fall and early winter with increases in precipitation but is projected to decrease sharply during late winter and spring due to reduced snowpack and evapotranspiration increases in vegetated areas (annual average recharge rates are projected to decline overall as temperatures continue to rise past mid-century).
- Groundwater levels are projected to rise near the coast as sea levels rise, bringing flooding and consequences for coastal infrastructure and natural resources.

Chapter 3

Temperature

Projected temperature and temperature extremes as a function of GHG scenarios are arguably the most certain and well-understood climate change metrics at the global scale. However, regional uncertainties suggest a range of potential warming scenarios in the Greater Boston area. The primary goal of this chapter is to provide the best available data and resources to a broad range of potential stakeholders, including those assessing socioeconomic vulnerability and aiming to translate data into adaptation and/or mitigation plans.

The average number of days over 90 °F historically ranges between 8 and 10 days per year, depending on the county. The BRAG reported the full range of projected days over 90 °F (maximum and minimum values from several General Circulation Models (GCMs) and emission scenarios) as 25 to 90 days per year. The BRAG *expected* range of days over 90 °F was 30 to 70 days per year (see page 30 of the BRAG report). The GBRAG reports median values for days over 90 °F as 26 to 53 days per year, which compares well with the BRAG-reported *expected* range.

The key findings for temperature projections are:

- **Overview:** This report contains more comprehensive, localized, explicitly probabilistic projections for future temperatures in the region. For example, rather than an average value for the entire region, the distribution of temperature statistics (at 5, 17, 50, 80, and 95th percentiles) are projected for each of the four counties that fall within the study area.
- **Energy:** Energy demands on utility infrastructure and the marginal costs of energy are expected to increase significantly in the summer. Recent weather extremes in California, Texas, and Mississippi make clear the impacts that will be felt, especially by marginalized populations, without significant investment in hardening energy infrastructure for a changing climate. Heatwaves pose analogous challenges for the region.
- **Public Health:** Boston's heat-induced mortality rate will likely increase in coming decades, with marginalized populations and those living in urban heat islands (UHIs) facing higher risk. The report specifically highlights communities in the GBRAG jurisdiction that are socioeconomically vulnerable to urban heat island effects. Air quality hazards and respiratory disease, adverse birth outcomes, and transmission of vector-borne diseases are also likely to increase due to temperature changes.
- **Agriculture and Natural Resources:** Warming winter temperatures and changes in freeze timing may pose a threat to New England agricultural industries (e.g., cranberries and maple syrup) and winter recreation. Projections also suggest a shifting forest composition and increasing spatial range and severity of pest and pathogen species.
- **Infrastructure and Transportation:** Increases in mean and extreme temperatures are expected to place more stress on building materials, as well as jeopardize worker safety and rider comfort. Primarily negative economic and operational impacts are expected on multiple modes of transportation.
- **Economy, Governance, and Society:** Economic impacts of rising air and marine temperatures probably include increased stress on annual incomes and workforce productivity, higher crime, increasing energy costs, and harm to agriculture and fisheries. Massachusetts may see mixed impacts on tourism.

Chapter 4

Sea Level Rise

Since the 2016 publication of the BRAG report, a special IPCC report has appeared, providing updated projections of global and regional sea level rise. These new projections provide the foundational basis for the local sea level projections provided here, adapted to the unique setting of Boston Harbor. Sea level does not change uniformly across the globe, and regional-to-local scale changes in specific places can differ by 30% or more from the global mean. As such, changes in global mean sea level (GMSL) should not be confused with local changes in relative sea level (RSL); it is RSL that impacts coastlines, people, and infrastructure in specific locations like Boston. The distinction between GMSL and RSL is important, because there are places around the world, including the Massachusetts shoreline, where RSL is rising faster than the global average, which will be increasingly consequential for Boston in coming decades.

The key findings of this chapter are:

- RSL in Boston Harbor is rising at an accelerating pace. The average rate of RSL rise between 2001 to 2019 was 0.21 in per year, about twice the average rate over the last century. RSL in Greater Boston is rising faster than the global average due to a combination of regional ocean warming and geodynamical processes (including local vertical land motion) associated with past and current changes in the distribution of land ice around the world.
- Loss of land ice stored in mountain glaciers and ice sheets on Greenland and Antarctica has recently superseded ocean thermal expansion as the primary driver of climate-driven sea level. Melting land ice causes changes in Earth's gravity and rotation that impact regional patterns of sea level rise. When ice is lost from the West Antarctic Ice Sheet, these processes amplify the resulting sea level rise in Boston by about 25% relative to the global average. Future changes in North Atlantic Ocean circulation could also amplify RSL rise in Boston relative to the global average.
- We provide updated probabilistic projections of RSL, adapted specifically to the unique setting of Boston Harbor. The projections account for contributions to RSL from future ocean thermal expansion, ocean dynamics/currents, anthropogenic land water storage, land ice loss from mountain glaciers and Greenland and Antarctic ice sheets, Earth gravitational/rotational/dynamical effects, and local vertical land motion. These new RSL projections differ substantially from those reported in the BRAG report and are lower in the year 2100, mainly because they use the recent assessment of future Antarctic ice loss provided by the IPCC (2019), rather than the single Antarctic modeling study (DeConto and Pollard, 2016) that was previously used.
- Under the most optimistic RCP2.6 scenario, RSL rise in 2100 relative to a 2000 baseline is 35 to 78 cm (17th to 83rd percentile likely range) versus 72 to 146 cm for a more extreme RCP8.5 scenario. Under RCP8.5, 2 m of RSL rise in Boston Harbor is possible by 2100 (192 cm, 95th percentile; 273 cm, 99th percentile). In 2200 the 17th to 83rd likely range of RSL is 184 to 378 cm.
- Increasing uncertainty in the upper tail of the projections over the 21st century and beyond is mainly caused by uncertainty about the response of the Antarctic Ice Sheet to future warming. The Antarctic Ice Sheet contains the ice equivalent of 58 m (190 ft) of sea level rise, so even small changes could be highly impactful. Risk-averse end users of these projections should consider the possibility of sea level outcomes above the likely range, especially under higher GHG emissions. For long-term planning and long-lived coastal assets, we stress that sea level will continue rising beyond 2100 under all GHG emissions scenarios, with the possibility that rates of RSL rise will then exceed 2.5 in per year.
- Most of Greater Boston's extreme flooding events are caused by winter storms (ETCs) that coincide with anomalous high tides. Recent studies have not found significant evidence for future changes in Greater Boston storm surge linked to either changing ETC or TC climatology; however, sea level rise will substantially increase the frequency and magnitude of extreme coastal flooding in the 21st century.

- Under all emissions scenarios, what is now a one in 10-year winter storm flood will likely become an annual event by mid-century. Around 2050, flood projections begin to diverge under different emissions pathways. Beyond 2050, GHG emissions will determine if the increasing flood hazard slows toward the end of the century or continues to accelerate. By 2100, under a high emissions scenario, today's one in 100-year flood event will likely become a yearly event.
- The height of the tide largely controls the severity of flooding during a storm in Greater Boston. Tidal range (the difference between low and high tide) varies year-to-year in the region as a function of natural planetary cycles. Tidal variability should be considered in Greater Boston flood projections.
- Boston Harbor will see an increasing number of high tide “nuisance” flooding days, defined as days when at least one hourly water level measurement exceeds local flooding thresholds defined by NOAA (7.1 feet above 2000 mean sea level for minor flooding or 7.9 feet for moderate flooding). Based on recent projections, Boston’s minor flood threshold will be exceeded on roughly half the days of each year by the early-2050s.

Executive Summary References

“2020 tied for warmest year on record, NASA analysis shows—climate change: Vital signs of the planet.” *NASA*, NASA, 21 Jan. 2021, climate.nasa.gov/news/3061/2020-tied-for-warmest-year-on-record-nasa-analysis-shows.

Chappell, Bill. “A ‘Scorcher’: 2015 Shatters Record as Warmest Year, NASA and NOAA Say.” *NPR*, NPR, 20 Jan. 2016, www.npr.org/sections/thetwo-way/2016/01/20/463709775/a-scorcher-2015-shatters-record-as-warmest-year-nasa-and-noaa-say.

Douglas, E., P. Kirshen, R. Hannigan, R. Herst and A. Palardy. *Climate Change and Sea Level Rise Projections for Boston*. The Boston Research Advisory Group for Climate Ready Boston, 1 June 2016, www.boston.gov/sites/default/files/document-file-12-2016/brag_report_-_final.pdf.

IPCC. “IPCC, 2021: Summary for Policymakers.” *Climate Change 2021: The Physical Science Basis. Contribution of Working Group I to the Sixth Assessment Report of the Intergovernmental Panel on Climate Change*. Cambridge University Press, 2021. www.ipcc.ch/report/ar6/wg1/downloads/report/IPCC_AR6_WGI_Headline_Statements.pdf.

1. *Introduction to the Greater Boston Research Advisory Group (GBRAG)*

1.1 THE NEED FOR SCIENTIFIC CONSENSUS ON CLIMATE PROJECTIONS

During the writing of the inaugural Boston Research Advisory Group (BRAG) report (Douglas et al., 2016) both NASA and NOAA announced that 2015 was the warmest year on record, beating the previous record set in 2014, by 0.29 °F (Chappell, 2015). Just five years later (during the writing of this report), NASA announced that 2020 had tied 2016 for the warmest year, breaking the previous record by a stunning 1.84 °F, and that the last seven years have been the warmest seven-year period on record (NASA, 2021).

Around the same time, the World Meteorological Organization (WMO) reported that 2016, 2019, and 2020 were the top three warmest years on record, with the difference in the global average temperatures reported for those three years being “indistinguishably small” (World Meteorological Organization, 2021). The slight variation in rankings is due to differences in stations and timeframes used in the analyses. Regardless, these observations support the assertion made in the sixth and most recent assessment by the Intergovernmental Panel on Climate Change (IPCC, 2021) that states, “*It is unequivocal that human influence has warmed the atmosphere, ocean and land. Widespread and rapid changes in the atmosphere, ocean, cryosphere and biosphere have occurred.*” Hence, the question at hand is not, is the climate changing but, what are we going to do about it?

Prior to the BRAG report (Douglas et al., 2016), individual cities like Boston had to rely on regional studies, such as the Northeast Climate Impacts Assessment (Frumhoff et al., 2007), to understand the impacts of climate change and develop strategies for adaptation. The inaugural BRAG represented the first scientific consensus on climate change impacts specifically related to the City of Boston. Since its release in June 2016 the BRAG report has been used extensively by Boston agencies, as well as by cities and towns in the surrounding communities, because there was nothing else like it available. In fact, Darcy Schofield of the Metropolitan Area Planning Council (MAPC; personal communication, July 5, 2018) stated that she always uses information from the BRAG in vulnerability assessments, climate action plans, and in Municipal Vulnerability Preparedness (MVP) analysis for MAPC communities. Hence, the greatest need for an update to the BRAG report was to expand the domain of the analysis to the Greater Boston region (the domain for the findings presented herein is the 101 cities and towns that make up the MAPC region) and to present the information in a way that is relevant for communities struggling to plan for our changing climate. This expanded analysis and scientific consensus was called the Greater Boston Research Advisory Group (GBRAG).

1.2 THE APPROACH AND OBJECTIVES OF GBRAG

As noted above, the scientific consensus on climate change impacts to Boston outlined in the inaugural BRAG report were timely and meaningful for communities in the Greater Boston region. To build on the success of the BRAG, the approach for the GBRAG was to:

- a. **Expand the domain of the BRAG** to include the 101 communities within the Metropolitan Area Planning Council (MAPC) region. The relative impacts of climate risk factors vary across the region; as a result, we investigated how this variability affected communities differently. The expanded

domain also provided opportunities for investigating cross-cutting themes, an example of which is the GBRAG Special Report 1 on groundwater (Knott et al, 2022), released under separate cover.

- b. **Create a GBRAG Steering Committee** (SC), comprising more than 30 participants from federal (e.g., USGS, NOAA, EPA), state (e.g., MassEOEEA, MassDEP), regional (e.g., MAPC, MassPort, BostonHarborNow), local (e.g., City of Boston, NOAH) organizations; business representatives (e.g., ABC, National Grid); and academics (e.g., Northeastern, UMass Boston). We held the first SC meeting on Feb 1, 2019 to refine the objectives, identify community participants, and anticipate outcomes. We engaged with community stakeholders and residents using a stakeholder survey and a community outreach campaign from February through April 2019 (draft GBRAG outreach report available on request) and had a second SC meeting to discuss the results. We categorized these results into climate impacts of interest to and design values needed by the GBRAG target communities as guidance to the GBRAG science teams.
- c. **Convene teams of experts (GBRAG science teams)** around relevant climate risk factors defined as 1) Temperature, 2) Storms, Precipitation, Flooding, and Groundwater, and 3) Sea Level Rise. A fourth risk factor, the impacts of climate change on marine temperature and environments, did not ultimately fit within the GBRAG chapter format and will be released as the second GBRAG special report at a later date. Each GBRAG science team had one expert team leader and three to four expert members. A GBRAG science team kickoff meeting was held on September 24, 2019 and a preliminary results meeting was held on January 15, 2020. GBRAG science teams were on schedule to submit team reports by June 15, 2020 when the COVID-19 global pandemic caused an unanticipated year and a half delay. Despite this unprecedented disruption, GBRAG science team reports were finalized and peer-reviewed by September 2021 and the GBRAG report released on June 1, 2022.
- d. **Disseminate GBRAG results widely.** While this GBRAG report represents the primary product of this effort, other outcomes will include presentations to stakeholders and communities, peer reviewed articles, media appearances and interviews by GBRAG management, stakeholder engagement, and science team members focusing on the findings of the GBRAG and special reports.

The primary objective of the GBRAG is an update of the scientific consensus on specific climate risk factors to incorporate new findings in this very active field of research. While at this point, the major sources of uncertainty in climate projections are due to climate model limitations and unknown future emissions, some of this uncertainty is related to an incomplete understanding of the climate system. The rapid advances in scientific understanding of climate change processes (especially with respect to improvements in ice sheet mass loss modeling) infers that process uncertainty will decrease with time; hence in the inaugural BRAG, we recommended that BRAG report be updated at least every two to three years. However, discussions with the City of Boston (Carl Spector, personal communication, May 10, 2018) indicated that an update frequency of four to five years would make new information available within a policy-relevant timeline. Despite the triteness of this statement, we sincerely believe that the findings outlined in this report have been worth the wait.

1.3 INTRODUCTION REFERENCES

“2020 tied for warmest year on record, NASA analysis shows – climate change: Vital signs of the planet.” NASA, 21 Jan. 2021, climate.nasa.gov/news/3061/2020-tied-for-warmest-year-on-record-nasa-analysis-shows.

“2020 was one of three warmest years on record.” World Meteorological Organization, 20 Jan. 2021, public.wmo.int/en/media/press-release/2020-was-one-of-three-warmest-years-record.

Chappell, Bill. “A ‘Scorcher’: 2015 Shatters Record as Warmest Year, NASA and NOAA Say.” *NPR*, NPR, 20 Jan. 2016, www.npr.org/sections/thetwo-way/2016/01/20/463709775/a-scorcher-2015-shatters-record-as-warmest-year-nasa-and-noaa-say.

Douglas, E., P. Kirshen, R. Hannigan, R. Herst and A. Palardy. *Climate Change and Sea Level Rise Projections for Boston*. The Boston Research Advisory Group for Climate Ready Boston, 1 June 2016, www.boston.gov/sites/default/files/document-file-12-2016/brag_report_-_final.pdf.

Frumhoff, P.C., J.J. McCarthy, J.M. Melillo, S.C. Moser, and D.J. Wuebbles. *Confronting Climate Change in the U.S. Northeast: Science, Impacts, and Solutions. Synthesis report of the Northeast Climate Impacts Assessment (NECIA)*. Cambridge, MA: Union of Concerned Scientists (UCS), 2007, www.ucsusa.org/sites/default/files/2019-09/confronting-climate-change-in-the-u-s-northeast.pdf.

IPCC. “Summary for Policymakers. In: Climate Change 2021: The Physical Science Basis. Contribution of Working Group I to the Sixth Assessment Report of the Intergovernmental Panel on Climate Change.” Cambridge University Press, 2021, In Press, www.ipcc.ch/report/ar6/wg1/downloads/report/IPCC_AR6_WGI_Headline_Statements.pdf

Knott, J. F., P. Kirshen and E. Douglas. *Climate-Change Impacts on Groundwater in MAPC Communities. Special Report prepared for Greater Boston Research Advisory Group*. University of Massachusetts Boston, 2022.

2. *Storms, Precipitation, Flooding, and Groundwater*

2.1 INTRODUCTION TO THIS CHAPTER

This chapter reviews and assesses the available literature and projections for the Greater Boston area in terms of precipitation and storms. Coastal flooding is not considered here, as it is included in the Sea Level Rise chapter. Eastern Massachusetts receives over 1,000 mm (over 43 in) of precipitation annually. Tropical storms (TCs), extratropical storms (ETCs), and fronts deliver the majority of precipitation for this area (Kunkel et al., 2012; Agel et al., 2015), with warm moist air masses transported from the Atlantic Ocean or Gulf of Mexico contributing to many of the extreme precipitation events for this region (Agel et al., 2019a). The most extreme precipitation tends to occur in the fall due to TCs, and in the spring due to ETCs, and often exceeds 76 mm (3 in) for a single day. This extreme precipitation can generate coastal and urban flooding, as well as impact groundwater.

This review and assessment considers uncertainty, storms, seasonal precipitation, extreme precipitation, flooding, and groundwater. The discussion of the various factors that can increase or decrease uncertainty in different contexts in Section 2.2 provides important context for the consideration of the different aspects of precipitation and storms. This is followed in Section 2.3 by a consideration of storms and the processes that generate precipitation in terms of the range of storm types and precipitation types important to precipitation in the area. Seasonal precipitation is considered in Section 2.4. Extreme precipitation is then considered in Section 2.5, at daily and hourly timescales, followed by flooding in Section 2.6, both riverine and stormwater. Groundwater is considered in Section 2.7, new to this iteration of the Boston climate reports, and discussed in detail in the *Groundwater Special Report* (Knott et al., 2022). Groundwater is important in eastern Massachusetts for water supply, ponds, and wetland ecosystems, and for sustaining streamflow and water quality during periods of little precipitation. All sections consider both observed and projected changes and identify key knowledge and data gaps.

2.2 SOURCES OF UNCERTAINTY

Uncertainty is an important factor underlying each of the key findings in this chapter. All projections incorporate some level of uncertainty, and there is even uncertainty in aspects of observed changes, due to the limitations of the available observational data. Given the crucial importance of understanding uncertainty when interpreting projections, this section provides a discussion of the multiple factors that increase or decrease uncertainty, to provide context for the projections provided in the following sections. Three key factors in uncertainty (Hawkins and Sutton, 2009) include how well models can reproduce the variable of interest (model uncertainty), the natural variability of the climate system (internal variability), and future decisions about emissions (scenario uncertainty).

Precipitation is a difficult variable to simulate in models. Within the Greater Boston area, precipitation is determined by a wide range of physical mechanisms operating on many different spatial and temporal scales—from localized convection to synoptic-scale frontal systems—which should all be correctly represented in a model for it to produce accurate estimates. Additionally, many aspects of convection and cloud processes that are critical for precipitation cannot be explicitly simulated by General Circulation Models

(GCMs) and are approximated using empirically derived formulae. The nature of such approximations differs between models and can lead to very different precipitation estimates at small spatial and temporal scales. Because of this, a collection (a.k.a. ensemble) of models of different structures and resolutions running the same climate input scenario produces a wide range in precipitation projections for the region (Easterling et al., 2017). This spread represents the *model uncertainty*.

Variations in precipitation in the midlatitude regions are strongly influenced by *internal variability*, generated by the chaotic and unpredictable behavior of the coupled atmosphere-ocean system. For the Northeast, this results in precipitation that is highly variable at small spatial scales and also exhibits large interannual (year-to-year) variability. For a small mid-latitude region such as Boston or the Northeast, internal variability can be much greater than the climate change signal (Deser et al., 2012; Hawkins et al., 2011). For instance, the mid-century precipitation projections over the Northeast show that the spread due to internal variability in a given model can be as large as the ensemble spread (Karmalkar et al., 2019).

Another important factor that contributes to the uncertainty in future climate projections is not knowing the exact greenhouse gas (GHG) emissions trajectory the world will follow in the future. This *scenario uncertainty* is evaluated by simulating the response of the climate system to multiple plausible future GHG concentration scenarios called the Representative Concentration Pathways (RCPs; Meinshausen et al., 2001). The relative importance of scenario uncertainty on regional precipitation, however, is likely to be small compared to other factors (Hawkins and Sutton, 2011). **Indeed, partitioning uncertainty in Northeast precipitation projections (Karmalkar and Bradley, 2017) shows the dominance of internal variability in the short-term and model uncertainty in the long-term with very little to no contribution from scenario uncertainty throughout the 21st century.** This suggests that considering diverse outcomes obtained from a large number of models is more important for risk assessment and downstream studies of runoff and flood projections (Wasko et al., 2021; Giuntoli et al., 2018) than those from multiple emissions scenarios.

Uncertainty is decreased (meaning we have greater confidence in projections) when there is agreement between theoretical expectations, observed changes, and projected changes. For precipitation, the basic physical relationship underlying many theoretical expectations is the fact that the hotter the air becomes, the higher the upper limit on water vapor in the air (for further discussion, see, e.g., the recent reviews of Allan et al., 2020 and Fowler et al., 2021). This increase in water availability increases the upper-limit on precipitation. This theoretical expectation matches both observations (heavy precipitation has already been increasing in the region) and projections (heavy precipitation is projected to continue to increase). **This agreement between theoretical expectations, observations, and projections results in a higher confidence in projections of extreme precipitation than in other aspects of precipitation.**

2.3 STORMS

Key findings

- The previous report found no robust estimates of changes in frequency, intensity, or tracks for both TCs and ETCs, although there was limited evidence to suggest a future slight northward displacement and increase in intensity for TCs and a slight weakening of ETCs. In the current report, more certainty is added to several aspects of storms and storm precipitation.
- TCs are expected to decrease overall in frequency, but the proportion of stronger storms (Category 4 to 5) will likely increase.
- ETCs will likely be less intense overall (although localized winds near the center and along fronts may increase in intensity), and the proportion of precipitation that falls as snow associated with these storms will likely decrease.
- Convective storm activity may increase, especially within TCs and ETCs.

- For all storm types, precipitation intensity (e.g., daily precipitation) associated with individual storms is expected to increase in the future.
- Projections in track changes for Northeast TCs and ETCs continue to be highly uncertain.

Review of existing science

Storms affecting the Greater Boston inland area year-round include TCs, ETCs, and convective storms. Each of these storms can generate heavy or prolonged precipitation, damaging winds, and lightning. Climate change may affect each of these types of storms, by modifying the background environment favorable for development, or directly impacting the storm processes themselves. Each type of storm and our current understanding of observed trends is briefly described in this subsection. For additional information about these storm types, see Ritter (2006).

Extratropical cyclones

ETCs are responsible for 80 to 90% of total precipitation in the Northeast (Hawcroft et al., 2012; Catto et al., 2019). These storms can be quite large in spatial scale. Konrad (2001) found that Northeast storms that generate extreme precipitation can range from 2500 km² to 100,000 km² and impact the region for multiple days with strong winds and precipitation. The Greater Boston area is impacted by strong coastal ETCs (storms that intensify over the waters of the Atlantic Ocean), as well as ETCs that develop over the continental United States (U.S.) and propagate to the Northeast from either the Great Lakes region or the Ohio Valley. An ETC develops in regions of strong horizontal temperature gradients, where instability (moisture and vertical temperature gradients) in the atmosphere and other favorable conditions can lead to large-scale cyclonic motion. Within this cyclonic motion, winds are directed towards a center of minimum surface pressure where the air converges and rises. More intense cyclones generally have lower minimum pressures or rates of pressure drop, and stronger surface winds. As the cyclonic flow moves through the existing temperature gradient, a cold front develops where the flow ushers colder air into warmer regions, and a warm front develops where the flow ushers warmer air towards colder regions. It is along these fronts that the highest winds and precipitation are often found. In addition to winds and precipitation, convection (which can lead to thunderstorms) is often present along cold fronts, and in the region between the warm and cold fronts, especially during the summer.

Currently, there is limited information regarding observed trends in ETC frequency, intensity, and lifecycle. While individual studies may point to observed changes in seasonal intensity and frequency for specific locales, there is little widespread agreement on the sign or magnitude of those changes. However, there has been an observed weakening of the North Atlantic storm track due to increased northeast North American surface temperatures (Wang et al., 2017) and an observed reduction in the 1979 to 2017 mean available potential energy (Gertler et al., 2019), which is required for ETCs to form and intensify. Possibly related to these findings, Chang et al. (2016) found an observed 10% decrease per decade for 1979 to 2014 summer ETC frequency over North America.

Tropical cyclones

TCs (which include hurricanes, tropical storms, and tropical depressions) can cause severe coastal damage, as well as inland flooding and wind damage. TCs that impact the Northeast generally develop in the tropical (between latitudes 0 °N to 25 °N) or subtropical Atlantic (between latitudes 25 °N and 40 °N), where high sea surface temperature, reduced upper-level winds (low vertical wind shear), and abundant warm humid air provide the ingredients for initiation and intensification. A mature TC is characterized by intense cyclonic motion, with strongest winds near the center, and surrounding bands of extreme precipitation, convective activity, and often accompanying storm surge. While coastal regions are most susceptible to wind and surge damage, inland regions are most susceptible to extreme river and flash flooding due to extreme precipitation and soil saturation.

Most Atlantic TCs initially move northwestward and interact with the prevailing flow over the eastern U.S. and western Atlantic, which tends to steer the storms northeastward and away from the U.S. The Greater Boston area is directly hit or brushed by TCs on average every 3 to 4 years; however, the area is also susceptible to tropical systems moving across inland regions after making landfall in other locations. Some TCs moving into higher latitudes undergo extratropical transitioning (ET), that is, taking on some characteristics of ETCs such as frontal regions and expanded wind fields. ETs are especially dangerous for the Northeast in the fall, as they share both the features of TCs (high winds and abundant tropical moisture) and ETCs (fronts and a large spatial scale). Recent TCs that became ETs before affecting the Northeast include Hurricane Irene in 2011 (Jung and Lackmann, 2019), which caused severe flooding in southern and central Vermont, and Hurricane Sandy in 2012, which inundated the New Jersey and New York coastline with a storm surge in excess of 2 m (Evans et al., 2017). TCs and their remnants need not directly pass over the region to be important, as they can increase the likelihood of extreme precipitation over distances more than 500 km from the storm center (Barlow, 2011), and they are often associated with predecessor rain events that can include extreme precipitation (Zielinski and Keim, 2005).

Trends in Northeast U.S. TC frequency and intensity have been difficult to detect in observations, owing in part to the large internal variability of sea surface temperatures (SST) and wind shear that affect the formation and lifecycle of TCs. As one possible explanation, Sobel et al. (2016) suggest that currently the heating effect of greenhouse gases is largely offset by the cooling effect of aerosols, but this is expected to change as the warming signal increases and drowns out the cooling signal associated with aerosols.

Convective Storms

In addition to ETCs and TCs, the Northeast is also susceptible to convective storms, which generally occur during the summer, where strong surface heating combined with moist unstable airmasses can result in isolated thunderstorms or organized systems, such as mesoscale convective complexes and squall lines. In addition to lightning, hail, and torrential rains, these systems can also generate extreme winds such as derechos (intense and widespread straight-line winds). Convective activity can also occur within other storm types (TCs, ETCs, and ETs).

Individual studies have identified several trends in convective activity. Hoogewind et al. (2017) used dynamical downscaling to find an overall increase in 1971 to 2000 U.S. convective activity in spring and fall, which may be related to increasing surface temperatures and moisture availability. Conversely, they found a decrease in convective activity in the summer, which may be due to increased convective inhibition. Tang et al. (2019) found an increase in large hail-producing environments (related to convection) in the eastern U.S. from 1979 to 2017, due to increased mid-tropospheric lapse rates and favorable shear.

Projected changes

One of the expected impacts of climate change is warmer global surface temperatures, and this change is expected to be strongest for the polar regions (IPCC AR5, 2014). There are several consequences of this that will affect inland storms in the Northeast. First, the lower troposphere temperature gradient between the Arctic and mid-latitudes will likely decrease, reducing the kinetic energy for ETCs to both form and intensify. Second, as air temperature rises, so too does the amount of water vapor in the air, in accordance with known constraints (e.g., the Clausius-Claypeyron relationship which predicts an increase in the water holding capacity of air of approximately 7% per degree Celsius rise in temperature). This additional water vapor may lead to more intense precipitation within each storm type (Fowler et al., 2021). Third, additional latent heat released during the conversion of additional water vapor to clouds and precipitation will work to both stabilize (at upper levels) and destabilize (at lower levels) the atmosphere, depending on where it is released, and this in turn could affect the frequency and intensity of ETCs and TCs. Several of these expected changes have already been documented in observations, while others may remain obscured by

natural variability (Sobel et al., 2016; Choi et al., 2017). While climate model projections agree on these basic responses to global warming, there are wide discrepancies on the specific impacts of these consequences on storm frequency, intensity, track, and precipitation. A summary of the state of knowledge of future projections for each inland storm type follows (see also Table 2.1).

Table 2.1

Best available estimates for projected changes in storms, with confidence in parentheses.

Storm Type	Frequency	Intensity (winds)	Precipitation	Track
Extratropical cyclones	Decrease (low)	Decrease (low-med)	Increase w/decrease in % of snow (high)	Uncertain
Tropical cyclones	Decrease (low-med)	Increase (high)	Increase (high)	Uncertain
Convective storms	N/A	N/A	Increase (high)	N/A

Extratropical cyclones

Some climate model projections suggest that mid-latitude ETCs will decrease in frequency, in large part due to decreased horizontal and vertical temperature gradients (Chang et al., 2016; Wang et al. 2017; Gertler and O’Gorman, 2019), but the exact seasonality and sign of these changes remains uncertain (Catto et al., 2019). There is, however, high confidence that precipitation associated with ETCs will increase in intensity due to increased moisture in the air (Michaelis et al., 2017; Zhang and Colle, 2017), and that the overall proportion of winter precipitation that falls as snow will decrease (Catto et al., 2019).

There is less confidence in other aspects of the ETC lifecycle. A number of studies conclude that the intensity of ETCs (low-level winds) will decrease in a warming world, due to the decrease in the mid-latitude surface temperature gradient (e.g., Catto et al., 2019). This would be particularly true at the beginning of their lifecycle, although the intensity may increase at the end of their lifecycle due to enhanced latent heating (Marciano et al., 2015; Michealis et al., 2017; Gertler and O’Gorman, 2019). Latent heating may also enhance low-level winds at the center of ETCs and along fronts (Michaelis et al., 2017; Gertler and O’Gorman, 2019). However, overall frontal intensity may decrease with decreasing temperature gradients (Catto et al., 2014). In addition, convective precipitation (due to latent heating enhancements) may form a larger proportion of overall ETC precipitation (Gertler and O’Gorman, 2019).

There is little agreement on whether ETC tracks will change in the future. Some studies indicate that winter storm tracks may move poleward and increase in density (Parding et al., 2019), while others indicate that summertime storm tracks may move equatorward (Collow et al., 2016). If enhanced downstream blocking occurs in conjunction with these displaced summertime storms, the Northeast may see more intense and longer duration summertime rainstorms. However, while there has been a marked increase in July and August Greenland blocking episodes since 1981 (Hanna et al., 2016), there is very low confidence in future projections of blocking (Muñoz et al., 2020).

The type of precipitation (rain, snow, ice) associated with winter ETCs may change with climate change. There is medium-to-high confidence that total winter snowfall associated with ETCs will decrease, and the proportion of precipitation that falls as rain will increase (Catto et al., 2019; Chen et al., 2019). However, individual storm snowfall may increase at higher latitudes/elevations as conditions remain cold and precipitation related to ETCs increases (Chen et al., 2019; Zarzycki, 2018). There is also some limited

evidence to suggest that snowstorms in much of the mid-latitudes may decrease in areal coverage with climate change (Ashley et al., 2020).

Tropical cyclones

There is high confidence that TCs will generate increased precipitation intensity, directly related to the higher moisture content of the atmosphere (Xu et al., 2016; Sobel et al., 2016; Knutson et al., 2020), and increased storm surge in coastal communities, directly related to the increase in ocean temperature (Knutson et al., 2020; Little et al., 2015). Projections related to TC frequency are less certain. There is low-to-medium confidence in a decrease in the overall number of TCs (−14% median decrease across 27 individual studies, per Knutson et al. (2020)). However, there is widespread agreement in the models that the proportion of the most-intense Northeast TCs (category 4 to 5 hurricanes) will increase in the future (Knutson et al., 2020; Lee et al., 2020). This increase is due to a medium-to-high confidence in an overall increase in the intensity (wind strength or central pressure) of TCs (+5% median increase across 15 individual studies, per Knutson et al. (2020)), combined with the overall decrease in number of TCs.

There is less confidence in any changes in the tracks of TCs. While several studies note a poleward movement of TC tracks in the North Pacific, there is no similar agreement for North Atlantic TCs. If the track does shift northward, the Northeast may be more vulnerable to higher-intensity TCs, or more frequent occurrence of ETs (extratropical-transitioning TCs) (Evans et al., 2017; Liu et al., 2017; Michaelis and Lackmann, 2019). These hybrid storms could produce a large amount of precipitation, due to the projected increase in the proportion of very intense TCs (with stronger wind fields and more tropical moisture).

It is unclear what the combination of lower-frequency, higher-intensity TCs along with possible track changes will mean to the Greater Boston area in terms of total TC frequency. Overall frequency of TCs may remain the same or reduced, but the impact from individual storms may increase, due to increased storm surge (addressed in the Chapter 4), more wind damage, and more extreme precipitation.

Convective Storms

There continues to be widespread uncertainty with respect to convective storms. Due to increased surface temperatures and atmospheric moisture (more low-level instability), there is a potential for convective storms to increase in frequency. However, latent heat release at upper levels may act to inhibit convective activity (Hoogewind et al., 2017). In addition, there is low-to-medium confidence that the frequency and intensity of convective precipitation embedded within ETCs may increase, due to increased surface instability and winds along fronts (Gertler and O’Gorman, 2019).

Knowledge and data gaps

There is high confidence that there will be enhanced precipitation for all types of inland and coastal storms in the Northeast, based on future climate projections. These results are relatively robust despite differences in climate model internal physics, parameterizations of cloud and precipitation processes, and grid resolution. However, many aspects of future inland storms remain uncertain, and this is largely due to inadequacies in the climate models to accurately and consistently simulate the large-scale circulation and environmental feedback processes under which storms form and intensify. Increased model resolution can provide some improvements, particularly with regard to temperature-related factors, but certain processes such as cloud condensation and precipitation that occur at the mesoscale and microscale level will likely continue to be estimated rather than directly resolved in climate models.

Due to these model limitations, current data gaps include estimations of how climate change will impact mid-latitude circulation (shear, blocking, jet strength, and position), which could affect the tracks of both ETCs and TCs. Additionally, there is a lack of understanding of how climate change will impact

troposphere-stratosphere interactions, which has implications for ETC intensity and tracks. It is also undetermined how climate change will impact complicated latent heat feedback mechanisms (which models are currently unable to directly calculate), which has implications for storm intensity, frequency, track, and precipitation.

2.4 SEASONAL PRECIPITATION

Key findings

- Annual precipitation in the Northeast has increased, particularly in the warm season, and largely due to an increase in high-intensity precipitation.
- Model projections for the future also suggest increased precipitation in the winter and spring, although this is highly uncertain, given the range of model projections.
- Precipitation in any given season or year could be significantly lower (drought-like conditions) or higher than long-term average due to internal variability even though there is a gradual trend toward wetter conditions.
- Seasonal precipitation was not considered in the previous report.

Review of existing science

The Northeast region receives abundant and fairly uniform precipitation throughout the year resulting from a southwesterly flow of moisture in the warm season, ETCs in the cold season, and TCs in late summer and early fall. The precipitation annual cycle shows little seasonality in Boston, which receives between 3 to 4 inches of precipitation on average every month (Zielinski and Keim, 2005).

Annual average precipitation in the Northeast has increased over the last century resulting mainly from increases in the warm season, especially in fall (Horton et al. 2014, Easterling et al. 2017). A significant portion of the wetting trend in the warm season and in the fall in particular is shown to be related to an increase in intensity of heavy precipitation events (see also Section 2.5) related to TCs (Barlow, 2011; Aryal et al., 2018) and ETCs (Kunkel et al., 2012). This longer-term increasing trend, however, can be masked at multi-year timescales due to large interannual variability in precipitation. For instance, Boston received below-normal (relative to the 20th century mean) precipitation in the warm season for four consecutive years from 2014 to 2017 (Figure 2.1).

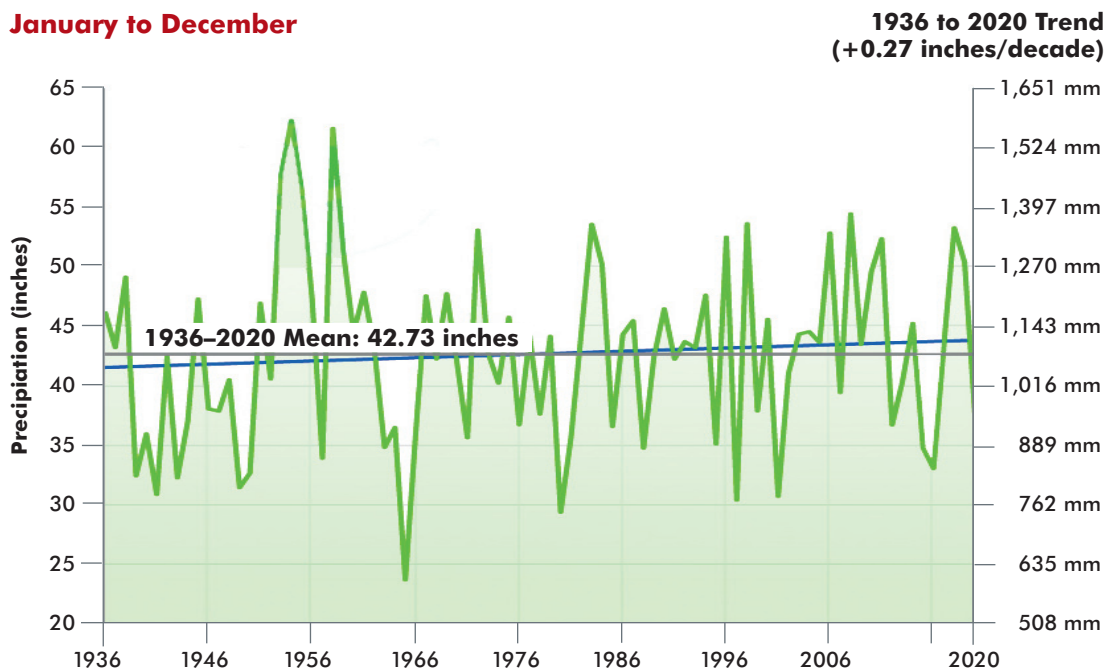
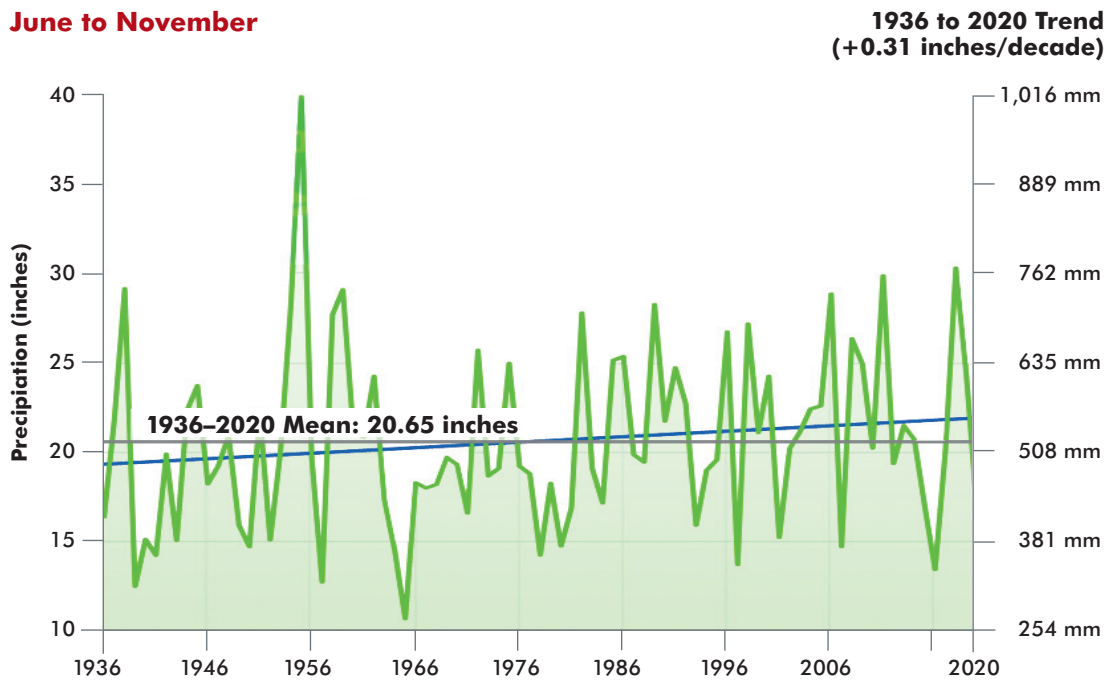
Most Coupled Model Intercomparison Project (CMIP5; Taylor et al., 2012) GCMs are able to simulate the seasonal cycle of precipitation (Lynch et al. 2016) and underpinning physical processes—the large-scale atmospheric circulation features and the associated regional moisture transport and convergence—reasonably well (Sheffield et al., 2013, Thibeault and Seth, 2014). Models also capture the enhanced precipitation in the cool season (November to March) along coastal New England associated with the western Atlantic storm track (Sheffield et al., 2013). In general, however, GCMs as well as Regional Climate Models (RCMs) overestimate precipitation in the Northeast over the historical period mainly in the cool season, whereas they have both wet and dry biases in the warm season (Sheffield et al., 2013; Rawlins et al., 2012; Thibeault and Seth, 2014; Karmalkar et al., 2019). This leads to a more pronounced amplitude in the annual cycle of precipitation in models than observations (Lynch et al. 2016).

Projected changes

The observed trend towards wetter conditions in the Greater Boston area is projected to continue in the future, but model projections remain highly uncertain for the entire 21st century. Projections for Suffolk County (located within the Boston Harbor basin) based on the localized climate anomalies (LOCA; Pierce et al., 2014) statistical downscaling of 14 CMIP5 GCMs is shown in Figure 2.2 and summarized by season in Table 2.2 (the rationale behind selecting a subset of models to provide regional climate

Figure 2.1

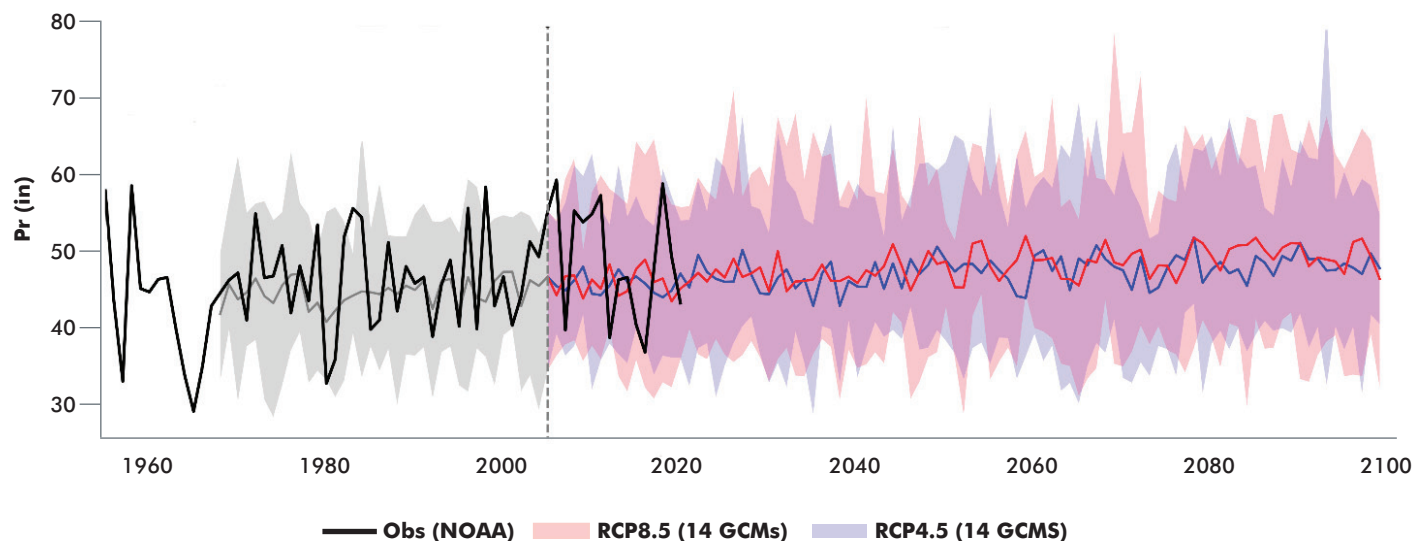
**Total annual (top) and warm season (below) precipitation in Boston
for the period 1936 to 2020.**

January to December**June to November**

Source: National Oceanic and Atmospheric Administration (<https://www.ncdc.noaa.gov/cag>).

Figure 2.2

Model projections for total annual precipitation (in inches) for Suffolk County.



Observed (NOAA) precipitation between 1955 to 2020 is shown in black. The grey plume shows simulated precipitation range across 14 CMIP5 GCMs over the period 1969 to 2005 and the blue and red plumes show ranges for projected precipitation across 14 CMIP5 GCMs for RCP4.5 and RCP8.5, respectively, and the blue and red lines show corresponding ensemble means. The projections are based on LOCA statistically downscaled data for the 14 GCMs used for the ResilientMA project (resilientma.org).

Table 2.2

Total seasonal precipitation over the baseline period (1971 to 2000) and projections relative to baseline for the Suffolk County/Boston Harbor basin.

	Baseline precipitation in inches	Emissions scenario	Projected change in inches relative to the baseline (10 th to 90 th percentile range)	
Season	1971 to 2000		2050s (2040 to 2069)	2090s (2080 to 2099)
Annual	46.07	RCP4.5	+0.7 — +5.4	+1.7 — +5.9
		RCP8.5	+0.4 — +6.7	+0.7 — +9.5
Winter	11.82	RCP4.5	-0.2 — +1.6	+0.2 — +3.5
		RCP8.5	+0.5 — +2.6	+0.7 — +4.7
Spring	11.59	RCP4.5	+0.1 — +1.9	+0.3 — +2.5
		RCP8.5	0 — +2.2	+0.5 — +3.0
Summer	10.51	RCP4.5	+0.1 — +2.7	-0.3 — +2.6
		RCP8.5	-0.6 — +1.5	-1.9 — +1.7
Fall	12.18	RCP4.5	-1.1 — +1.5	-1.7 — +1.1
		RCP8.5	-0.8 — +1.6	-1.5 — +1.9

All values are in inches. The projected changes (in inches relative to the baseline) show the likely ranges (10th and 90th percentiles) across 14 CMIP5 GCMs for 2 RCP scenarios (RCP4.5, RCP8.5). The projections are based on the LOCA statistical downscaling product. (Source: resilientma.org.)

change projections is described in Karmalkar et al. (2019)). Apart from this localized information, most other studies focus on the Northeast region as a whole (e.g., Easterling et al., 2017).

The projected increase in total annual precipitation in the Northeast is dominated by increases in winter and spring (Lynch et al., 2016). The CMIP5 and NA-CORDEX ensembles indicate up to 25% increase in mid-21st century winter precipitation relative to 1980 to 1998 mean for the high emissions scenario (RCP8.5; Karmalkar, 2018). Despite future increase in winter precipitation, the Boston area will likely receive less snowfall in the future due to greater warming in winter months. While the majority of models indicate an increase in summer and fall precipitation as well, the spread across the full ensemble is more uncertain with a few models indicating a decrease in mid-century precipitation.

Knowledge and data gaps

Although annual precipitation has increased in the Northeast, particularly in the warm season, seasonal precipitation projections remain highly uncertain. Previous attempts to constrain precipitation projections over the Northeast (Thibeault and Seth, 2015; Karmalkar et al., 2019) have proved challenging due to a wide-ranging performance across metrics and a lack of a strong relationship between model skill over the historical period and future projections. For instance, the top six CMIP5 models identified based on their better overall performance for a large number of metrics over the Northeast include both increases and decreases in mid-century summer precipitation projections (Karmalkar et al., 2019). Considering the variability in model projections, it is possible that the Northeast may experience more drought-like periods in the future in addition to more extreme precipitation. This aspect of seasonal precipitation will be an important focus of future research.

2.5 EXTREME PRECIPITATION

Key findings

- The previous report considered the 10-year 24-hour design storm and found a consistent signal for increased daily precipitation, but the magnitude of that increase was uncertain. In the current report, the 25-year and 100-year design storms are additionally considered for both sub-daily and daily precipitation. Additional datasets are used to complement and confirm the previous results and provide newer projections.
- Extreme precipitation events have become more frequent and intense in recent decades, and these changes in extreme daily precipitation are expected to continue through 2100 under current greenhouse gas emission rates.
- Most projections point to a 10 to 20% increase in daily precipitation intensity by 2050 and a 20 to 30% increase by 2100, depending on the climate model and downscaling approach.
- There is little current evidence to suggest, based on recent observed data, that the intensity of short-duration (hourly precipitation) is changing at a faster rate than daily precipitation extremes.

Review of existing science

The Northeast has already exhibited notable increases in extreme precipitation. For example, the region that encompasses New England has experienced a greater than 70% increase in the heaviest 1% of daily precipitation events over the period 1958 to 2010, which represents the highest regional increase in the U.S. (Groisman et al., 2012; Kunkel et al., 2013; Walsh et al., 2014). In addition, the Northeast has also experienced a documented increase in flooding and precipitation events that are conducive to flooding, especially in urban environments (Collins, 2009; DeGaetano, 2009; Armstrong et al., 2014; Peterson et al., 2013; Georgakakos et al., 2014). The Northeast U.S. is not the only region that has been experiencing greater extreme precipitation frequency and magnitude. Similar trends are noted in the central and south-

eastern U.S. (Groisman et al., 2012; Cooley and Chang, 2017; Brown et al., 2020) as well as many other regions throughout the world (Groisman et al., 2005; Fisher and Knutti, 2016; Lenderink et al., 2011).

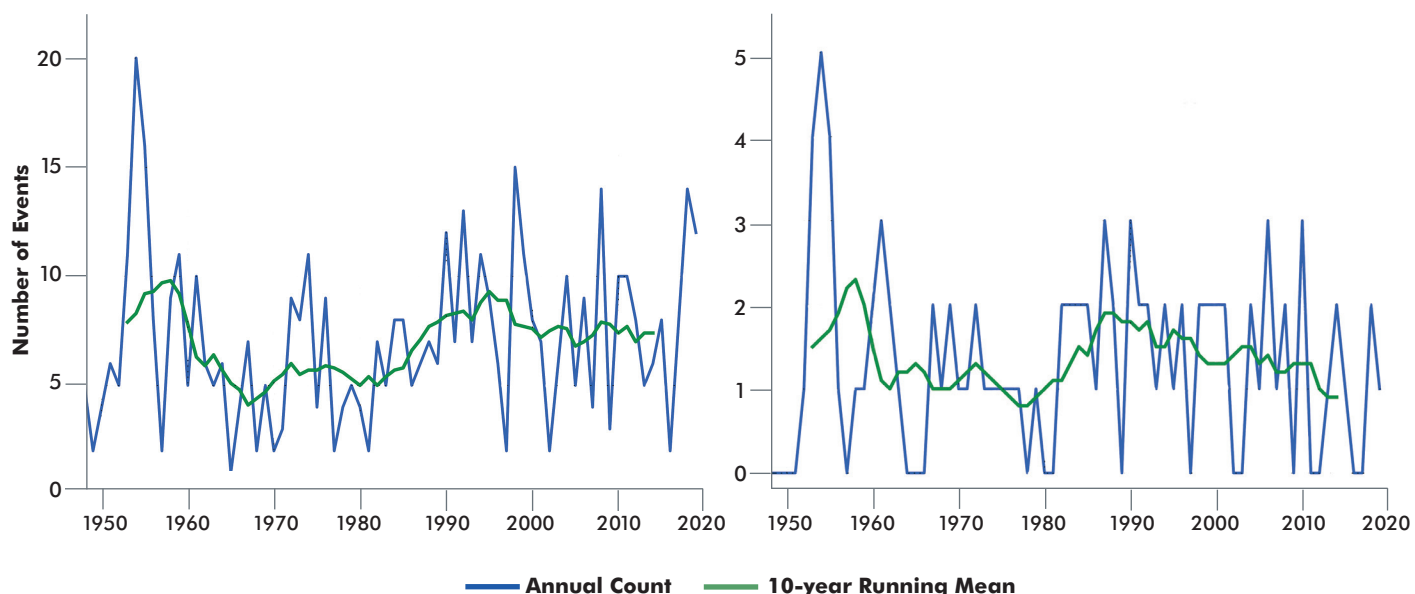
Coumou and Rahmstorf (2012) point to increases in atmospheric water vapor (consistent with increasing average temperature) and increases in the frequency of local convective storm events (also enhanced by warming surface temperatures) as physical reasons for these changes. In addition, changes in frequency, intensity, and tracks of TCs and ETCs contribute to trends in extreme precipitation (as detailed in Section 2.3 of this chapter). However, in some regions, linkages to certain atmospheric circulation patterns have been posed as influencing changes in precipitation extremes (e.g., Kenyon and Hegerl, 2010). Climate model simulations suggest a continuation of these extreme precipitation trends through the 21st century (e.g., Donat et al., 2016; Ning et al., 2015; Sun et al., 2016). While the existence of trends in historical observations does not guarantee trends in future events, the prominence of the extreme precipitation trend, especially in combination with the consistency in the sign of model projections for extreme precipitation, is highly suggestive of future increases and sets a minimum level of what is physically possible.

In the Greater Boston area, trends have been identified in hourly, daily, and multi-day extreme precipitation. For example, Figure 2.3 shows annual counts of the 99th-percentile hourly and daily precipitation rates at Boston, based on data from the NOAA Cooperative Hourly Precipitation Network. Except for an extremely high number of events in 1954 and 1955, there has been an increase of these intense short-duration precipitation events through time such that on average about three more events occur in recent years as compared to the 1950s and 1960s. This increase in events is similar to that reported for extreme daily rainfall (Easterling et al., 2017).

Extreme precipitation has important implications for urban and rural development, public infrastructure, watershed management, agriculture, and human health. These applications have long relied on statistical extreme value analysis of precipitation (Yarnell, 1935), in which an extreme value function is fitted to a relevant observed time series, resulting in a “design storm.” For these design storms, the relevant time

Figure 2.3

Time series of annual counts of hourly (left) and daily (right) precipitation exceeding the long term (1948 to 2019) 99th percentile of > 0 hourly rainfall accumulation. The green line is a 10-year running mean.



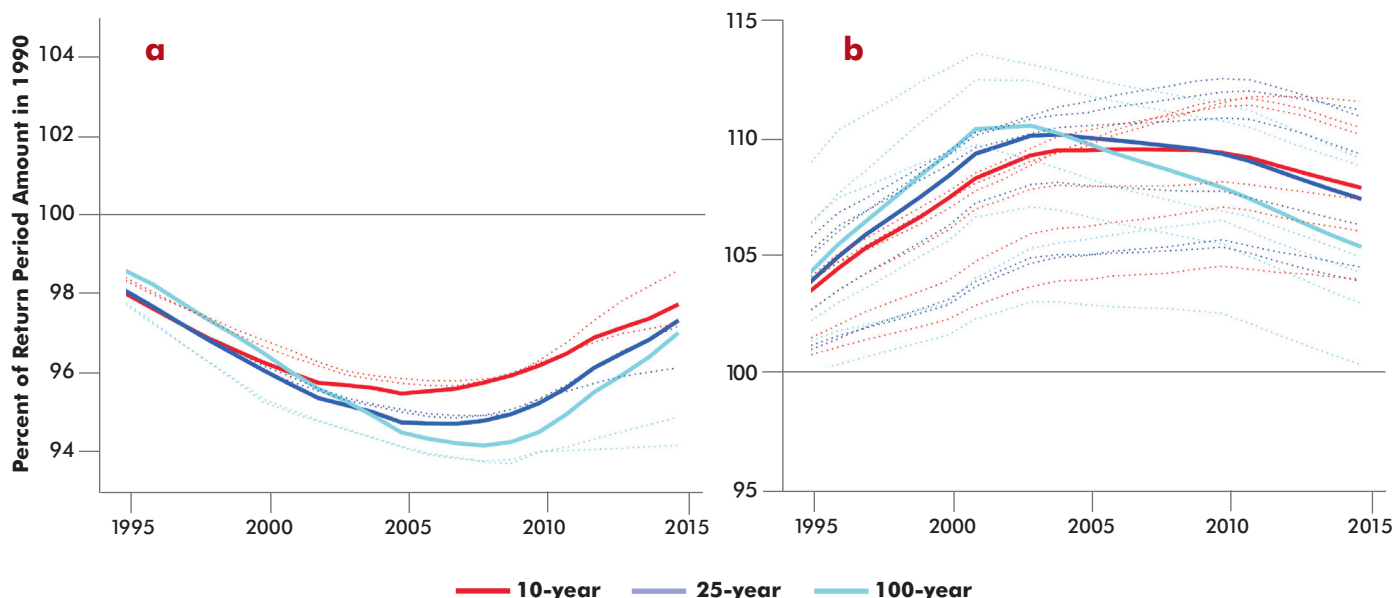
series are commonly a “partial duration series” (PDS), consisting of the n highest values from the observed precipitation record of n years, an “annual maximum series” (AMS) where the highest value for each year is chosen, or less commonly, a “peaks-over-threshold” (POT) time series of all values over a chosen threshold. Each design storm results in a set of accumulated depths associated with different exceedance probabilities (the probability of observing a precipitation event that equals or exceeds this depth). By convention, exceedance probabilities are often reported as average return periods (the long-term average waiting time between extreme events of a specified amount).

An underlying assumption of traditional extreme precipitation analyses has been the stationarity of the climate. Hence, it was expected that past conditions were an adequate guide to the future. However, given the many studies documenting observed and projected increases in extreme precipitation frequency, this assumption may no longer be valid (e.g., Cheng and AghaKouchak, 2014; Myhre et al., 2019). To accommodate trends in precipitation, some extreme value analyses incorporate non-stationarity in the underlying extreme value function.

The benchmarks for this report are the 10-, 25-, and 100-year design storms computed for partial duration series of 1-hourly and daily extreme precipitation for the time period 1948 to 1990. Figure 2.4 shows the time dependent changes for these design storms for various stations, as the ending year for the time series is increased incrementally to 2019, and the next n^{th} highest precipitation value is considered. For hourly precipitation, more recent design storms are consistently lower than the 1948 to 1990 value, indicating a decrease of up to 6% across the stations when data beyond 1990 are considered. However, since 2005 the design storms have tended to increase, although they remain below the baseline level. For 1-day data, the design storms that account for the most recent data are consistently higher than those

Figure 2.4

10-year-centered running means of the percent change in the 10- (red); 25- (blue) and 100- (cyan) year design storm based on partial duration series that include observations through the indicated year relative to that based on a 1948 to 1990 data record.



Panels are for a) 1-hour and b) 1-day durations. The solid lines show values for Boston, MA, and the dotted lines show values for Worcester, MA, and Providence, RI (in panel a) and Blue Hill Observatory, Lowell, Lawrence, Brockton, Franklin, and Middleton, MA (in panel b). The black horizontal line represents no percent change.

based on the 1948 to 1990 period. For the Greater Boston region, the current 25- and 100-year design storms are approximately 5 to 10% higher than the 1948 to 1990 values. While there is considerable variability between stations, the overall temporal changes in the design storms are consistent.

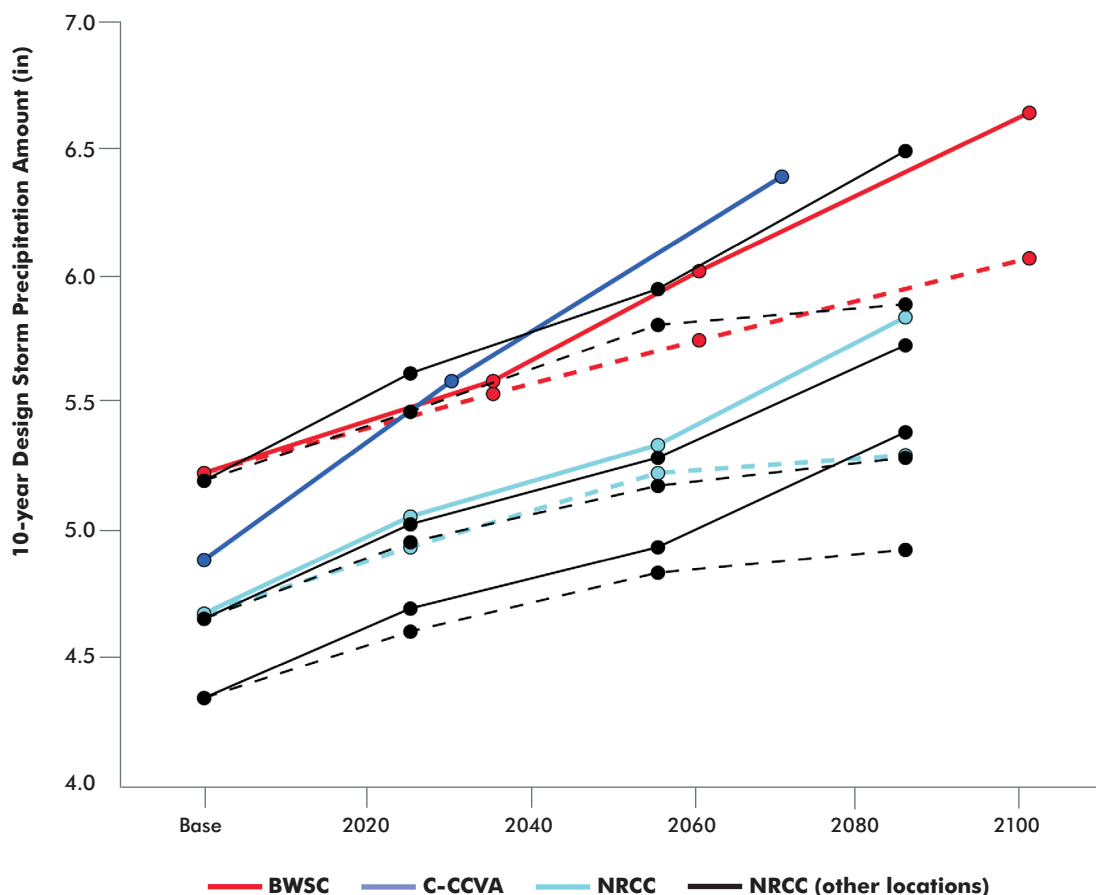
Projected changes

Most efforts to estimate future precipitation extremes using climate model projections have been on a case-by-case basis, often at the city level. The report by the Boston Water and Sewer Commission (BWSC, 2015) provides the most detailed information specifically for Boston. The Cambridge Climate Change Vulnerability Assessment (C-CCVA; City of Cambridge, 2015) provides similar information but did not report projections at 2100. Likewise, the Northeast Regional Climate Center (NRCC), using methods similar to those used in New York State (DeGaetano and Castellano, 2017; 2020), provides estimates of the 10-year design storm for Boston and other locations within the Greater Boston area. Results from each of these studies for the daily 10-year design storm are summarized in Figure 2.5.

The three studies use different baseline periods as well as different future target years, so their results are not directly comparable. The NRCC and C-CCVA studies use shorter base periods that encompass

Figure 2.5

10-year daily design storm depths (in in) based on projections (1-day partial duration series) from the BWSC (red), C-CCVA (blue) and NRCC (cyan). The black lines are NRCC projections for Lawrence, Hingham and Maynard. Solid lines assume high emission scenarios (A1Fi and RCP8.5), dashed line assumes more modest emissions (B2 and RCP4.5).



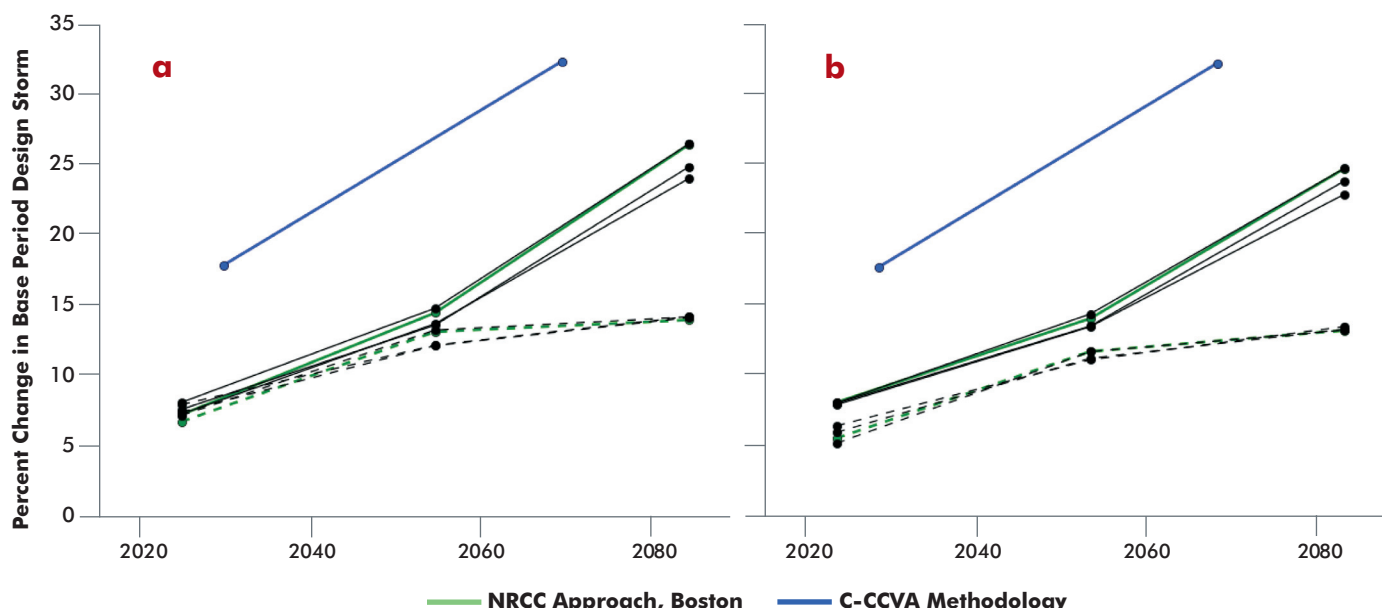
the 1970 to 2000 period, whereas the BWSC uses a longer baseline period that extends from 1948 to 2012. In addition, the three projections use different sets of global climate models and different downscaling approaches. Despite these differences, the changes relative to the baseline are reasonably consistent, especially those projected to occur by the BWSC and NRCC. This is evident in the figure by the similarity in the slopes of the red (BWSC) and cyan and black (NRCC) lines. The C-CCVA projections for 2030 and 2070 match quite closely with BWSC but their baseline value is lower (4.9 in vs 5.24 in, possibly due to the difference in record length analyzed), so that their projections in terms of percentages are nearly twice as large.

By 2050, under the assumption of higher emissions, both the NRCC and BWSC indicate that the 10-year design storm will increase by 15%. As the century progresses, the 10-year design storm continues to increase in both cases, reaching 25% above the baseline value in the 2090s. The lower baseline estimate and steeper slope of the blue C-CCVA line yields larger future changes in this approach. The three solid black curves in Figure 2.5 also show the projected changes in 10-year design storms based on the NRCC approach for three other locations in the Greater Boston area. Baseline precipitation is highest southward along the coast at Hingham (5.21 in) and decreases northward at Lawrence (4.67 in) and inland at Maynard (4.36 in). Nonetheless, the relative rate of change in 10-year design precipitation at these locations is similar to that at Boston, approximately 15% higher by 2050 and nearly 25% higher than the baseline amount in the late 21st century. These similarities are also evident based on lower greenhouse gas emission cases (shown as dashed lines in Figure 2.5). During mid-century NRCC projections as well as those of the BWSC range from an 8 to 10% increase in the 10-year design storm. Later in the century, precipitation increases are in the 13 to 15% range.

The C-CCVA and NRCC also provide projections for future 25- and 100-year design storms. In terms of percent change, there are considerable similarities between the two design storms (Figure 2.6). Using the NRCC approach, Boston, Lawrence, Hingham, and Maynard are projected to experience a 12 to 15%

Figure 2.6

Percent change in the 25- (left) and 100-year (right) design storm relative to the base period using the NRCC approach for Boston (green) and the C-CCVA methodology (blue).



Solid lines assume high emissions (A1Fi and RCP8.5); dashed lines assume more modest emissions (B2 and RCP4.5).

increase in the 25- and 100-year design storm by 2050 and a 22 to 25% increase in these design storms by 2085 under high emissions. The C-CCVA changes are larger with changes of 17 to 18% in 2030 and greater than 30% by 2070. Under the more modest emissions, the NRCC projections indicate a 10 to 12% increase in the 25- and 100-year design storm by 2050, with the increase stabilizing at approximately 12% through 2085. Although larger, the dynamically downscaled projections (C-CCVA) generally lie near the 90th percentile of the ensemble of statistically downscaled projections for Boston used by the NRCC. These projected changes are similar to those noted elsewhere (Wang et al., 2015; Rodriguez et al., 2014).

In addition to these design storms the C-CCVA and NOAA Climate Explorer (<https://crt-climate-explorer.nemac.org>) provide projections of the number of days with precipitation exceeding 2 in (consistent with a 2-year design storm for Boston). Climate Explorer projections are based on a weighted mean of 32 CMIP5 models downscaled using the localized climate anomalies (LOCA) approach of Pierce et al (2014). Table 2.3 summarizes these projections as well as projections of the average annual maximum 5-day precipitation accumulation. Although this variable is not available directly from Climate Explorer, it is based on the same suite of LOCA models and accessed via the Applied Climate Information System (ACIS) which provides underlying database for Climate Explorer.

Although the baseline values are different, the percent increase through time is consistent based on both approaches. By 2070, the number of days receiving more than 2 in of precipitation increases by 50% or more. The difference in the baseline values seems to result from the CMIP 5 model/downscaling combination. Although the median of the LOCA projections in the baseline period is well below that of the C-CCVA data, the C-CCVA baseline value falls within the spread of the LOCA model simulations.

Knowledge and data gaps

Projections of precipitation extremes for durations shorter than 1 day are important for storm water management in urban environments. However current computer capacity generally precludes climate model projections at hourly resolutions. In addition, although theoretical considerations suggest an increase in extremes at the hourly as well as daily durations, there are few actual observations of this trend, in part

Table 2.3

Comparison of baseline estimates and future projections of days with > 2 in of precipitation and annual average maximum 5-day precipitation accumulation for Boston, based on C-CCVA and Climate Explorer data.

	Model	Baseline (1971 to 2000)	2030s (2015 to 2044) Lower	2030s (2015 to 2044) Higher	2070s (2055 to 2084) Lower	2070s (2055 to 2084) Higher
Days with > 2 in of rain	C-CCVA	2	3 (50)	3 (50)	3 (50)	3 (50)
	LOCA	0.8	1.1 (38)	1.1 (38)	1.3 (63)	1.5 (86)
	LOCA-high	3.4	4.0 (18)	4.2 (24)	4.6 (35)	5.1 (50)
Max 5-day precipitation	C-CCVA	6	6.5 (8)	6.6 (10)	7 (17)	7.2 (20)
	LOCA	4.3	4.5 (5)	4.6 (7)	4.6 (7)	4.7 (9)
	LOCA-high	4.7	4.9 (4)	5.2 (11)	5.2 (11)	5.2 (11)

LOCA values refer to the multi-model mean, LOCA-high is the 90th percentile of the model projections. Values in parentheses indicate percent change from the baseline.

due to a lack of availability of relevant long-term hourly timeseries. This further highlights that the science and technology of developing climate-model based downscaled projections of sub-daily precipitation extremes continues to evolve.

Current climate models do not fully resolve multiple physical mechanisms and storm types known to be important to extreme precipitation. The observational data in the Greater Boston area are limited

in terms of both the number of stations and the period of record at each station, and this results in uncertainty both in estimating observed trends—extreme events, by definition, require a long record to adequately capture—and in terms of limiting the capacity to implement statistical downscaling.

Several statistical downscaling products and an ensemble of dynamically downscaled simulations are available that can provide localized climate information for Boston. What is lacking, however, is a systematic analysis of all available data products for their ability to capture characteristics of extreme precipitation in the Greater Boston area. Such an analysis combined with existing station observations is necessary to identify products and information that can be used by planners.

2.6 FLOODING

Key findings

- In the previous report, river flooding was briefly considered but there was little certainty to the projections. In this report, both river and urban flooding are considered in more detail. New data and modeling studies support the previous findings and increase the confidence of these projections.
- River floods are expected to be larger and more frequent although there is considerable uncertainty about the magnitude of the increases. River flooding projections by the BRAG (Douglas et al, 2016) are still relevant but should no longer be considered conservative estimates due to changes in basin hydrology and biases in hydrologic modeling.
- Stormwater is also expected to increase with the greater intensity and frequency of heavy precipitation.
- Future regional flooding conditions may be significantly influenced by increased groundwater elevations, especially near the coast with rising sea level (covered in Chapter 4).
- Historical increases in regional flood frequency have been driven by more frequent warm season (June to October) events.

Review of existing science

When precipitation exceeds the infiltration capacity of the soil or saturates it, or overwhelms urban drainage systems, water ponds on the landscape and flows over land to local waterbodies. This general inundation of the landscape from heavy precipitation is called pluvial flooding. Flooding also occurs when runoff that reaches rivers or lakes raises water surface elevations until they overtop banks and inundate adjacent land areas. Pluvial and river flooding often occur together, but river flooding can happen at locations distant from upstream pluvial flooding or because of upstream snowmelt or other storage releases. This section evaluates changes to pluvial and river flooding associated with changing climate. Coastal flooding, and compound events of river and coastal flooding together, are considered in Chapter 4.

Floods are natural disturbances to which ecosystems, and human communities, are adapted. For example, the size of natural river channels is closely associated with small, frequent floods (Wolman and Miller, 1960). Some species of fish deposit their eggs on stream bottoms during times of year when they are least likely to be flushed downstream by erosive flows (e.g., Kynard, 1997). Human developments are often guided by estimates of where rare floods are likely to inundate (e.g., 100-year floodplains) and some infrastructure is designed to withstand floods of specified magnitudes (e.g., dams and bridges). Changes in floods, particularly increases in magnitude and frequency, can therefore impact people and wildlife.

Increased flood activity in human communities can threaten lives, property, and economic activity directly through inundation (Ashley and Ashley, 2008; Wobus et al., 2017) or indirectly through increased

erosion, sedimentation, or associated changes in river channels (Cook et al., 2015; Renshaw et al., 2019; Yellen et al., 2016). Aquatic and riparian organisms can also be sensitive to physical alterations of river channel and floodplain environments caused by changes in flood magnitude and frequency, and they can be sensitive to shifts in flood seasonality as well (Arias et al., 2013; Robertson et al., 2001).

Pluvial and river floods can change over time through changes in climate (e.g., changes in the magnitude and/or timing of precipitation), but flooding can also be altered by human modifications of the landscape or direct manipulation of rivers. For example, urban development usually increases pluvial and river flooding because large areas of the land surface are made impermeable so precipitation no longer infiltrates the ground but instead accumulates on the land surface and runs off directly to streams. On the other hand, dams can reduce downstream flooding if they are managed to store runoff. While the focus of this section is on changes in river and pluvial flooding associated with climate changes, it is important to remember that floods are affected by human activities on the landscape, too. These activities can magnify or compensate for climate-induced changes.

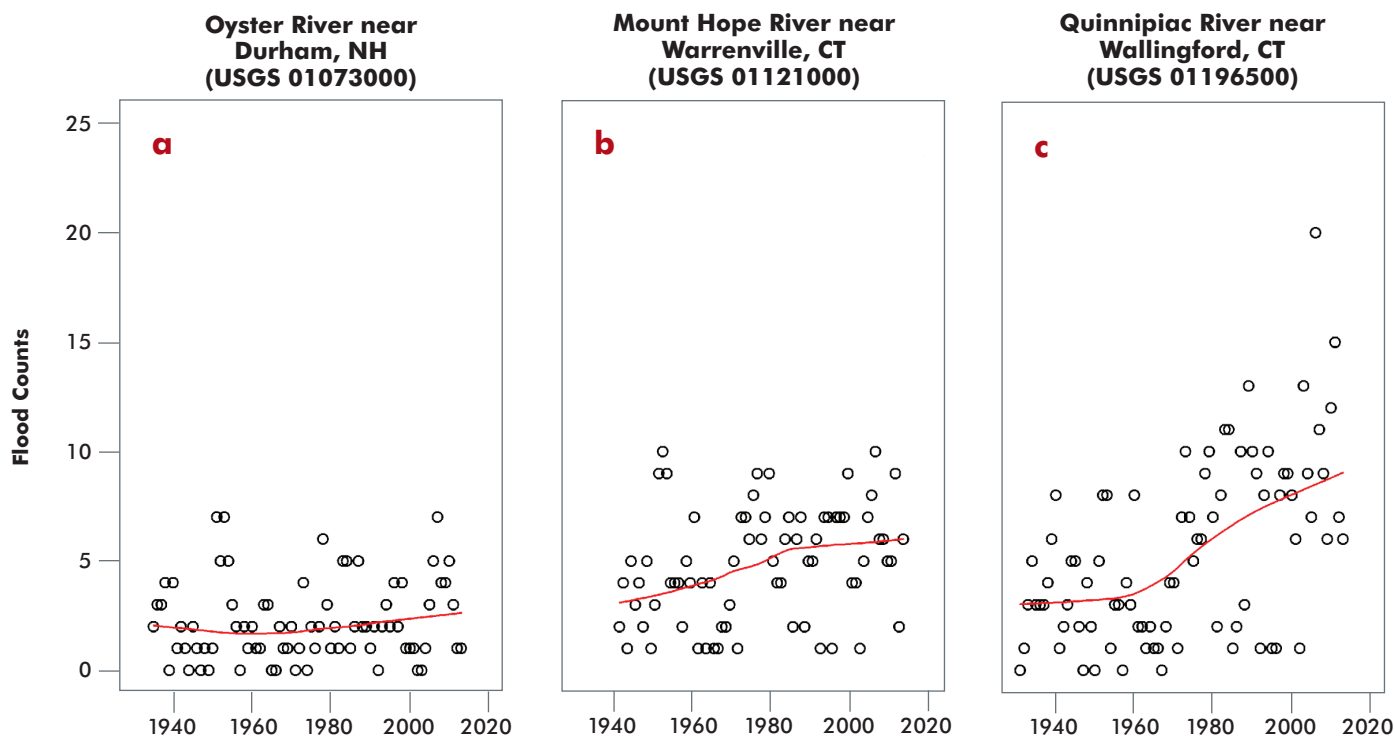
Climatic changes in pluvial flooding are often inferred from changes in extreme precipitation (see Section 2.5), although this should be done with caution because antecedent soil moisture conditions significantly influence runoff generation. Climate-induced changes in river floods are usually assessed by evaluating stream gage records for rivers with natural, or near natural, flooding conditions (Lins, 2012; Slack and Landwehr, 1992). These rivers have limited flow regulation and the land cover is natural, or has changed little, over the period of record. Flood trend studies typically evaluate changes in AMS peaks, the largest event of each year of record, or POT series composed of all events over a specified magnitude. AMS series include many small floods that do not go over bank, as do POT series when thresholds are chosen to identify more than one event per year.

Rivers with near-natural flood-generating conditions in the Northeast U.S. have shown increased flood magnitudes and frequencies in recent decades (Archfield et al., 2016; Armstrong et al., 2012; 2014; Collins, 2009; Frei et al., 2015; Slater and Villarini, 2016). There is generally stronger evidence for increased flood frequency than increased magnitude in the Northeast (Figure 2.7; Archfield et al., 2016; Armstrong et al., 2012; 2014; Frei et al., 2015). Some studies indicate these changes occurred as step increases around 1970 rather than as gradual trends (Armstrong et al., 2012; 2014; Collins, 2009; Glas et al., 2019; Hodgkins, 2010; Villarini and Smith, 2010). Trends in flood seasonality have also been documented. Frei et al. (2015) and Collins (2019) both found increased numbers of floods over time in the warm season (June to October), a time of year that has historically been flood-poor in the Northeast (Collins, 2019).

Hydroclimatic flood trends in the Northeast U.S. generally track regional trends in heavy precipitation, but they are not as pronounced (Frei et al., 2015; Wehner et al., 2017). As the amount of precipitation falling in the heaviest 1% of daily events increased by over 70% for the period 1958–2010, annual maximum flood magnitudes in the region increased by between 20 and 25% over a similar period (Armstrong et al., 2014; Collins, 2009; Walsh et al., 2014). This is not surprising because a number of factors influence whether heavy precipitation generates river floods (Agel et al., 2019b; Collins, 2019; Collins et al., 2014; Ivancic and Shaw, 2015). Particularly important are watershed land cover, soil moisture, and storage conditions (e.g., groundwater heights or snow cover) in the days and weeks preceding a precipitation event. For example, near the end of the cold season, when plants are dormant and soil moisture and water tables are near their annual maxima (Cowell and Urban, 2010; Jasechko et al., 2014), heavy precipitation is likely to cause river flooding because little of it infiltrates the soil and runoff rates are high. These antecedent conditions are characteristic of the late winter and early spring in the Northeast U.S., which is why March, April, and May (MAM) is the dominant flood season in the region (Collins, 2019). Even moderate precipitation can generate river flooding during MAM—especially if it falls on a snowpack or frozen ground. On the other hand, during the warm season when plant growth is greatest, plant transpiration reduces soil moisture and water tables are seasonally low. Under these conditions, heavy rain events can

Figure 2.7

Time series showing increasing flood frequency (peaks-over-threshold per water year) at three gages in eastern New England with near-natural flood conditions.



LOESS smooth trend lines are shown in red. Frequency trends for these stations were first analyzed by Armstrong et al. (2012), but the time series have been extended through 2013 in these plots.

fail to produce river floods because high soil infiltration rates diminish runoff. Moreover, some precipitation never even reaches the ground because it is intercepted by plant leaves and evaporated. Frei et al. (2015) and Huang et al. (2018) show how historical increases in Northeast extreme precipitation have been dominated by warm season events, which partly explains why flood magnitude and frequency increases have been muted in the region compared to the heavy precipitation trends of recent decades (Small et al., 2006). Nonetheless the precipitation trends have been strong enough, through increases in both intensity and areal coverage of heavy events (DeGaetano et al., 2020), to generate enough warm season floods to drive annual flood frequency trends (Collins, 2019; Frei et al., 2015).

Riverine projections

Global- and continental-scale modeling studies are available that provide projections for various measures related to river flooding at a range of time horizons. However, there are considerable uncertainties in these projections that derive from multiple sources in the modeling chain (Giuntoli et al., 2018). Collectively, the available studies give mixed indications of how floods might change in the region under a high radiative forcing scenario (e.g., RCP8.5). Some suggest no change or modest decreases in floods (Asadieh and Krakauer, 2017; Hirabayashi et al., 2013; Villarini and Zhang, 2020), while others suggest modest to relatively large increases (Koirala et al., 2014; Wobus et al., 2017). However, some of these studies use coarse-resolution climate model outputs without bias correction (Hirabayashi et al., 2013; Koirala et al.,

2014; Villarini and Zhang, 2020) while others employ downscaled and bias-corrected outputs coupled with hydrologic models that may have a dry bias as reported by Milly and Dunne (2017) and thus underestimate changes in flood flows (Arnell and Gosling, 2016; Asadieh and Krakauer, 2017; Wobus et al., 2017). Still others like Villarini and Zhang (2020) report changes in runoff rather than routed river flow so riverine flooding is not directly assessed.

The BRAG (Douglas et al., 2016) presented best available estimates for climate-induced changes in river floods in Boston for mid- and late-century assuming a high radiative forcing scenario (e.g., RCP8.5; Table 2.4). The estimates were based on the few regional-scale studies available at the time with river flow projections, and considerations of historical hydroclimatic changes in regional floods. Particularly influential were projections by Demaria et al. (2016) for 22 Northeast U.S. watersheds and Hodgkins and Dudley (2013) for four coastal Maine basins, but the estimates were also informed by flood projections for the City of Boston (Bosma et al., 2016; BWSC, 2015). We believe the projections in Table 2.4

Table 2.4

Best available estimates for potential changes in river floods in the Greater Boston area (after Douglas et al., 2016).

Flood measure	Mid-century (2055)	Late-century (2085)
Small floods (2-year recurrence interval)	0 to +20%	+20% to +50%
Design floods (100-year)	-10% to +35%	+15% to +70%
Flood frequency (floods/year)	Increase	Increase

remain the best estimates for how river floods are likely to change in Boston, and they are applicable to all of eastern Massachusetts because they were developed from regional information—particularly eastern New England. Precipitation and temperature projections have not changed substantially since the Table 2.4 estimates were developed (e.g., Easterling et al., 2017; Lynch et al., 2016; Ning and Bradley, 2015; Vose et al., 2017) and the few regional-scale flood projection studies published afterwards show similar results. Palmer and Siddique (2019) projected the 100-year recurrence interval flood on the Merrimack River in Massachusetts will increase by 14% by mid-century (2021 to 2060) and 21% by late-century (2060 to 2099) under RCP8.5—estimates bracketed by the Table 2.4 projections. Similarly, Wobus et al. (2017) projected that today's 100-year flood magnitudes on eastern Massachusetts rivers will become substantially more frequent by late-century (2090), especially under RCP8.5, and Bjerkli et al. (2015) projected a greater number of high flows annually in nearby New Hampshire under low and high emissions scenarios. The mid-century best estimates shown in Table 2.4 are also broadly supported by historical hydroclimatic trends in regional floods (Armstrong et al., 2012; Collins, 2009).

Although revisions to the quantitative projections are not warranted, the estimates should no longer be considered conservative (i.e., potentially too high). The BRAG (Douglas et al., 2016) characterized the Table 2.4 projections as conservative because they were derived from high radiative forcing scenarios like RCP8.5 (Demaria et al., 2016; Hodgkins and Dudley, 2013). But recent studies suggest the estimates may be too low instead, for two reasons. First, as noted above, climate projections that rely on “offline” hydrologic modeling for river flow estimates often systematically underestimate flow magnitudes because they overestimate evapotranspiration in a changing climate for a variety of reasons including not representing plant physiological changes caused by increased CO₂ (Kooperman et al., 2018; Milly and Dunne, 2017). The models used by Demaria et al. (2016) and Hodgkins and Dudley (2013) are known to have this bias

(Milly and Dunne, 2016; 2011). Indeed, Demaria et al. (2016) reported that their model validation showed river flow extremes were generally underestimated by their simulations.

Second, streamflow and well data indicate groundwater elevations have been rising in many areas of the Northeast in recent decades along with annual and extreme precipitation (Dudley et al., 2020; Easterling et al., 2017; Ficklin et al., 2016; Hodgkins et al., 2017; Weider and Boutt, 2010). This has important implications for river flooding because land areas with shallow water tables, like valley bottoms, produce much of the runoff during rain events through a process called saturation overland flow. This process occurs when infiltrating precipitation raises shallow water tables to the land surface during a storm and makes them impervious to subsequent precipitation (Dunne and Black, 1970). These saturated areas transiently expand during storms and at times of year when water tables are seasonally high, creating larger runoff volumes. They can also expand more permanently if water tables rise as part of a long-term trend, as they have in parts of the Northeast. Although not documented, it is plausible that long-term expansion of saturated areas, and/or more frequent transient expansion, contributed to increased flood magnitudes and frequencies observed in the Northeast in recent decades and could be an important flood-generating factor if water tables continue to rise with increasing precipitation, especially in the winter (Easterling et al., 2017; Jasechko et al., 2014). Coastal areas where water tables are also affected by sea level rise are particularly vulnerable. Groundwater modeling by Knott et al. (2019) showed how sea level rise induces groundwater rise as far as 4 to 5 km inland. The available river flood projection studies for the Northeast do not employ coupled groundwater-surface water models capable of simulating long-term trends in water table elevations (Fowler et al., 2020), so they may systematically underestimate flood risk from shallow groundwater areas that may expand slowly over time. Also, shallow groundwater areas are often relatively small and discontinuous and may not be spatially resolved by comparatively high-resolution models.

Stormwater projections

Pluvial flooding in urban and suburban areas, or “stormwater,” is likely to increase in Greater Boston with expected increases in daily and sub-daily (hourly) precipitation extremes (Section 2.5; Easterling et al. 2017; NASEM, 2019; Prein et al., 2017). More frequent and intense heavy precipitation will produce larger stormwater volumes that more often overwhelm the design capacity of stormwater drainage systems. Figures 2.5 and 2.6 show that systems designed in the late 20th century for a given annual exceedance probability storm will not accommodate a storm of a similar probability at mid- or late-century, increasing stormwater inundations locally. These issues may be compounded in coastal urban areas where storm drain outfalls will be subject to more frequent backwatering associated with sea-level rise. The problem of trying to design infrastructure assuming fixed event probabilities (“stationarity”) when those probabilities are instead changing (“non-stationarity”) has prompted the development of tools like non-stationary intensity-duration-frequency (IDF) curves (DeGaetano and Castellano, 2017; Ragno et al., 2018).

Knowledge and data gaps

The BRAG (Douglas et al., 2016) identified a number of knowledge and data gaps that continue to impact projections for how river floods will change in a changing climate. Broadly speaking, these include an incomplete understanding of flood-generating processes and limited abilities to model them in climate change investigations. Ongoing research has begun to address some of the identified gaps, but it has also illuminated further work needed. For example, whether deciduous plants are dormant has an important effect on flood-generation, and changes in climate are expected to further lengthen the growing season (Collins, 2019; Hibbard et al., 2017). However, many details about how plant phenology and forest composition will change with warming, and how those will affect antecedent soil moisture conditions important for runoff generation, are not fully understood (Knighton et al., 2019; Seyednasrollah et al., 2020).

Another example is the influence of TCs on Northeast U.S. flooding. These systems are known to play an important role in extreme precipitation and floods in the Northeast U.S. (Agel et al., 2019b; Aryal et al., 2018; Barlow, 2011; Dhakal and Jain, 2019; Huang et al., 2018; Kunkel et al., 2010), and TC precipitation rates are expected to increase with warming. But, TC frequency is expected to decrease while changes in tracks are less certain, so it is unclear what the net effect of changes in TCs will mean for Greater Boston-area river floods. Finally, while advances are needed in many components of the modeling process necessary to project floods in a changing climate, the dry bias identified by Milly and Dunne (2017) related to “offline” modeling of evapotranspiration, and the potential solutions they suggest, present a well-defined and tractable opportunity to improve simulations. Additionally, long-term changes in groundwater elevations are likely not well represented in models used by flood projection studies.

2.7 GROUNDWATER (SUMMARY OF GROUNDWATER SPECIAL REPORT)

Key findings

- Groundwater was not covered in the previous report.
- Groundwater levels in the Metropolitan Area Planning Council (MAPC) communities have shown increasing trends in long-term monitoring wells during the past 50 years.
- Over the next 50 years, groundwater recharge is projected to increase in the late fall and early winter with increases in precipitation but is projected to decrease sharply during late winter and spring due to reduced snowpack and evapotranspiration increases in vegetated areas (annual average recharge rates are projected to overall decline as temperatures continue to rise past mid-century).
- Groundwater levels near the coast are projected to rise with sea level rise with consequences for coastal infrastructure, flooding, and natural resources.

Review of existing science

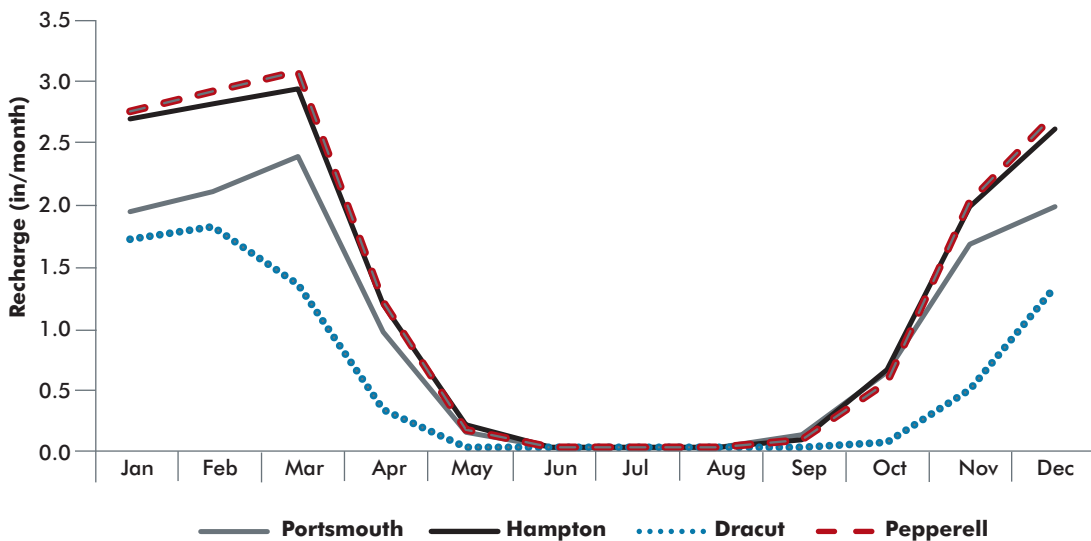
Groundwater is the world’s largest distributed source of fresh water and is important for both ecosystems and human consumption (Pimentel et al., 2004; Taylor et al., 2013). Groundwater is important in eastern Massachusetts for water supply, ponds, and wetlands, and for sustaining streamflow and water quality during periods of little precipitation (Boutt et al., 2010; Kirshen, 2002; Price, 2011). The health of these ecosystems depends on groundwater levels that fluctuate within a normal range of approximately –0.5 m to +0.5 m in alluvial aquifers, for example, throughout the year (Boutt, 2017). Long-term decreases in groundwater levels during periods of drought can cause wetland and stream ecosystems stresses and can reduce drinking water supplies (Hodgkins et al., 2017; Hughes et al., 2012). Likewise, long-term increases in groundwater levels can result in wetland expansion and transition, flooding, and water quality impairment (Cooper et al., 2013; Masterson et al., 2014).

Groundwater levels are directly affected by aquifer recharge and groundwater losses. Aquifer recharge is defined as the rate of water infiltrating the ground surface and traveling through the unsaturated zone to the water table (or saturated zone) (Freeze and Cherry, 1979). Many factors influence the amount of groundwater recharge that occurs. These include precipitation, temperature, physical and biological processes, land cover and use, soil moisture, and topography (Boutt et al., 2019). The annual average groundwater recharge rate in eastern Massachusetts ranges from 37% to 57% of total precipitation (Desimone, 2004; Masterson et al., 2009). Aquifer recharge varies seasonally in response to precipitation, evapotranspiration, and snow melt (Bjerklie and Sturtevant, 2018). This seasonal pattern is shown in Figure 2.8 for four communities in New Hampshire with characteristics similar to the MAPC subregions: Portsmouth (urban), Hampton (coastal community), Dracut (suburban), and Pepperell (rural).

Groundwater recharge is the highest in the winter and early spring and drops to zero from June through September when evapotranspiration rates are the highest. The spatial distribution of recharge

Figure 2.8

Monthly recharge rates for Portsmouth and Hampton, New Hampshire, and Dracut and Pepperell, Massachusetts.



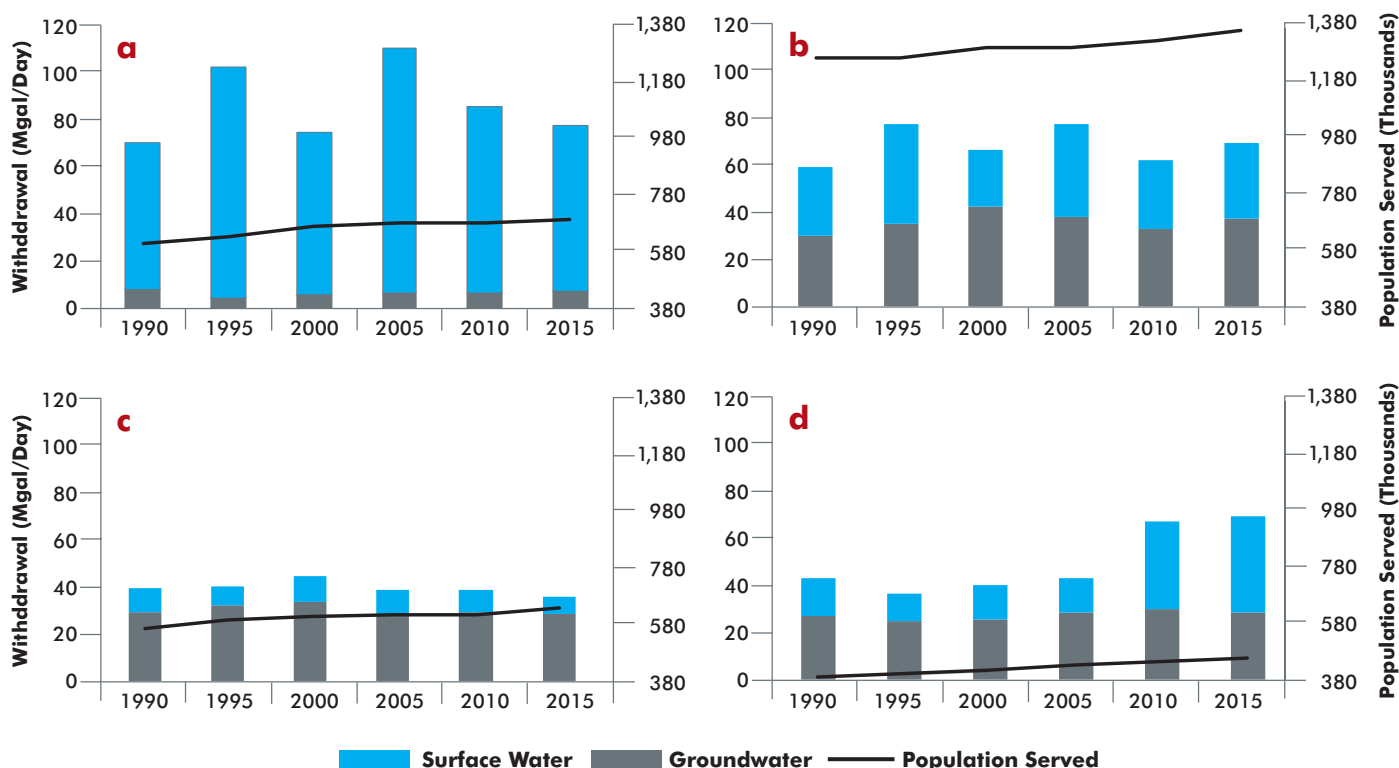
depends on land use and topography. For example, land with a high percentage of impervious area will have lower recharge rates and high runoff potential throughout the year (Bjerkie and Sturtevant, 2018). Groundwater losses occur through groundwater withdrawals from wells, evapotranspiration from the saturated zone, and groundwater discharge to surface-water bodies. Water use from the United States Geological Survey (USGS) records for four counties (Essex, Middlesex, Norfolk, and Plymouth) in eastern Massachusetts from 1990 through 2015 are plotted in Figure 2.9 (*USGS Water Use Data for Massachusetts*, accessed October 16, 2019).

Groundwater withdrawals accounted for a high percentage (ranging from 52 to 76%) of total water withdrawals in Middlesex, Norfolk, and Plymouth counties, but are less important in Essex County where surface-water sources dominate. Groundwater withdrawals are less variable than surface-water withdrawals with the coefficient of variance (COV) ranging from 7% to 18% for groundwater withdrawals versus 17% to 57% for surface-water withdrawals. The population has increased in all four counties from 1990 to 2015, but water withdrawals have remained relatively constant in three of the four counties, possibly due to a reduction in per capita use in Essex, Middlesex, and Norfolk counties or an increase in unreported uses. Water withdrawals increased sharply in Plymouth County from 2005 to 2010 with a corresponding 50% increase of per capita use.

Groundwater levels have been increasing in recent years. Groundwater levels in USGS long-term monitoring wells from 1970 to 2020 in the MAPC area have shown increasing trends. In a study of long-term groundwater level trends in southern New England, nearly all the monitoring wells in glacial till, which are less likely to be influenced by water withdrawals, showed increasing groundwater trends (Boutt, 2017). Stream base flows, seasonal low flows during periods of low or no precipitation, can also be an indicator of groundwater level trends (Bjerkie et al., 2012; Knott, Jacobs, et al., 2018; Masterson and Garabedian, 2007; Walter et al., 2016). In a study of annual 7-day low stream flows, increasing trends over the past 50- and 75-year time periods were observed in Massachusetts stream gages (Dudley et al., 2020).

Figure 2.9

Water withdrawals for public drinking water supply in a) Essex County, b) Middlesex County, c) Norfolk County, and d) Plymouth County. Groundwater and surface-water withdrawals are shown with the total withdrawal indicated by the height of the bar.



Source: Data used in this figure is from USGS (USGS Water Use Data for Massachusetts, accessed October 16, 2019).

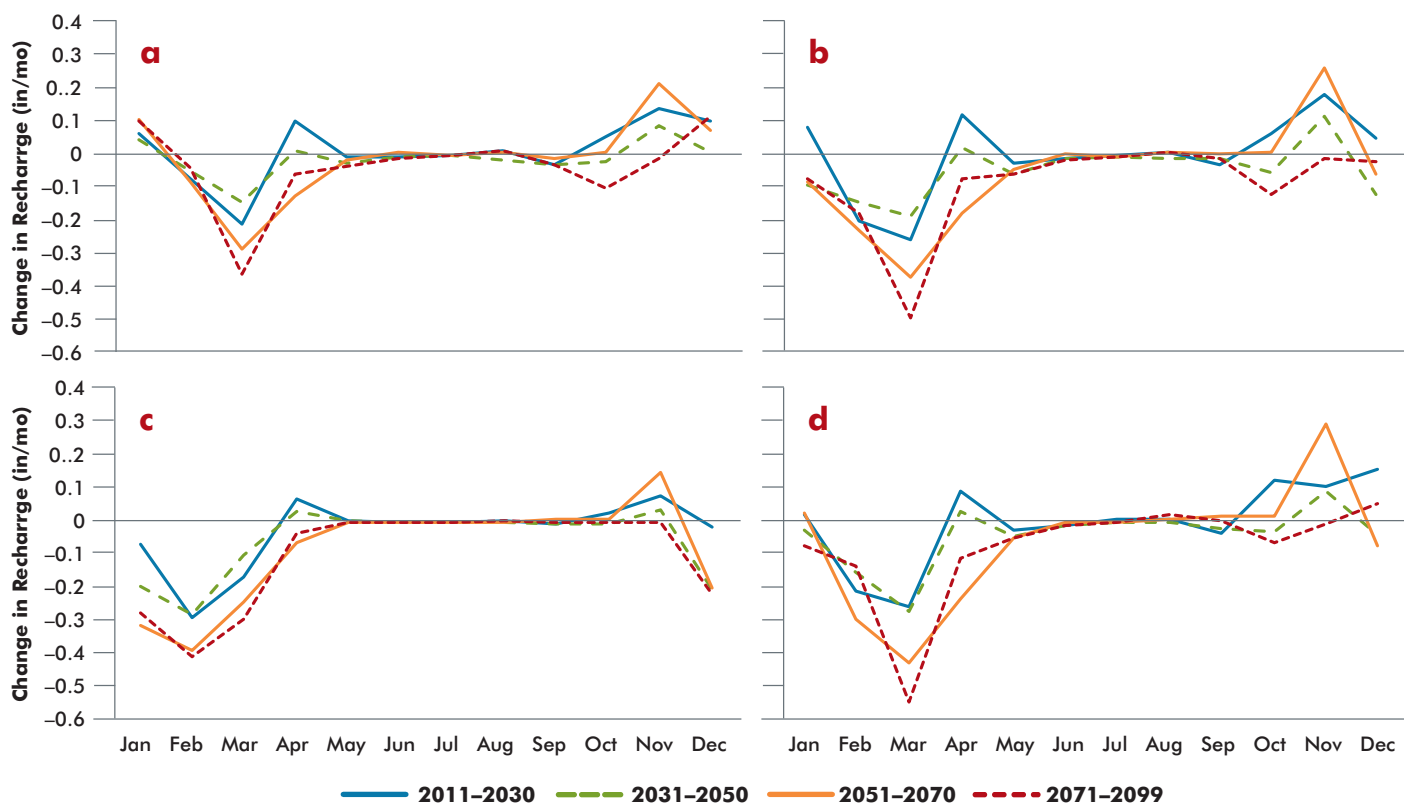
Groundwater projections

Climate change can influence groundwater availability both through changes in both aquifer recharge and water use (Taylor et al., 2013). Precipitation, temperatures, and sea levels are projected to increase in the Northeast due to climate change. Groundwater has been and will continue to be an important drinking water source in eastern Massachusetts and a warming climate is likely to increase demand (Mo et al., 2016). These factors can result in long-term and seasonal changes in groundwater levels potentially impacting drinking-water supplies, water quality, natural resources, and infrastructure (Habel et al., 2020; Knott, Jacobs, et al., 2018; Knott et al., 2019; Walter et al., 2016).

In New Hampshire, the USGS Precipitation Runoff Modeling System (PRMS) was used to simulate changes in streamflow, snowmelt, and aquifer recharge from the present (1981 to 2000) to the end of the century (2081 to 2100) (Bjerkie and Sturtevant, 2018). The results of this study were used to examine projected changes in aquifer recharge in the MAPC study area. Annual average recharge is projected to stay the same or increase slightly before 2030 and decline at increasing rates ranging from a less than 5% reduction to an approximately 18% reduction towards the end of the century (depending on the location) with the RCP4.5 scenario. The magnitude of annual average recharge reductions is projected to be greater with the RCP8.5 emissions scenario. Projected seasonal changes in aquifer recharge for the RCP4.5 scenario are shown in Figure 2.10. These plots show a steep decline in aquifer recharge during late winter and early spring caused by decreases in snow melt and increases in evapotranspiration. Recharge is projected to

Figure 2.10

Projected changes in monthly recharge for four 20-year periods relative to the baseline period (1981 to 2000) under the RCP4.5 emissions scenario for a) Portsmouth, b) Hampton, c) Dracut, and d) Pepperrel.



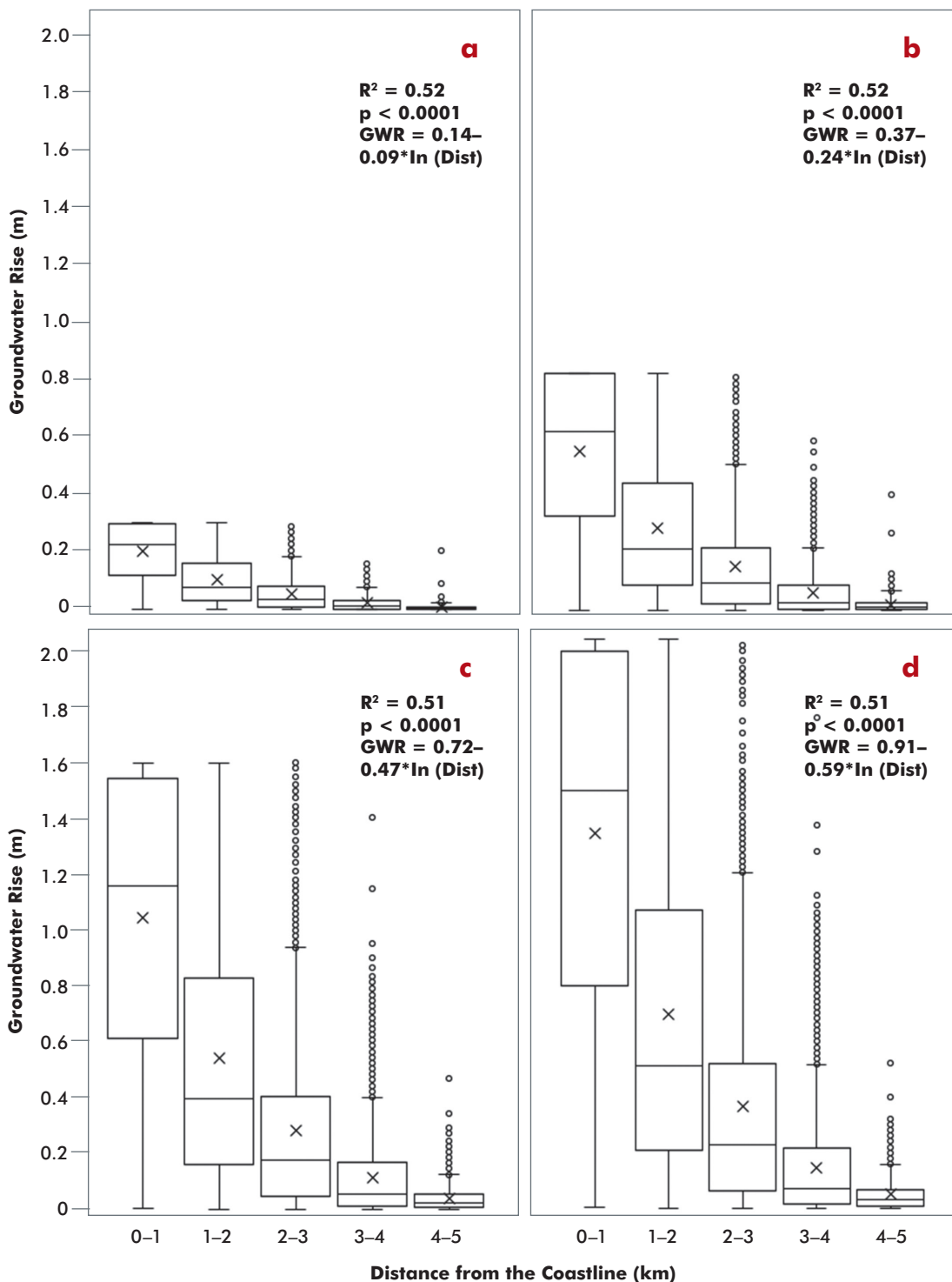
increase in October and November when evapotranspiration is low, increasing the potential for floods when soil moisture is high (Collins, 2019; Collins et al., 2014).

At the coast, groundwater levels are projected to rise with sea level rise (Bjerklie et al., 2012; Habel et al., 2020; Knott, Jacobs, et al., 2018; Manda et al., 2015; Masterson et al., 2014; Oude Essink et al., 2010; Wake et al., 2019; Walter, et al. 2016). In coastal New Hampshire (NH), groundwater levels are projected to rise with relative sea level rise (RSLR) at distances up to 5 km from the shoreline as shown in Figure 2.11 (Knott, Jacobs, et al., 2018). Within the NH Groundwater Rise Zone (GWRZ), mean groundwater rise relative to RSLR is projected to be 66% between 0 and 1 km, 34% between 1 and 2 km, 18% between 2 and 3 km, 7% between 3 and 4 km, and 3% between 4 and 5 km from the coastline (Knott, Jacobs, et al., 2018).

The extent of the GWRZ in coastal areas, including Massachusetts, depends on the surficial geology, the coastline geometry, the surface-water network, and groundwater withdrawals (Knott, Jacobs, et al., 2018; Oude Essink et al., 2010; Walter et al., 2016). Within the GWRZ, RSLR-induced groundwater rise has the potential to damage natural resources, water quality, coastal infrastructure, and historic structures in areas where groundwater is currently shallow, i.e., less than 1.5 m from the ground surface (Flood and Cahoon, 2011; Habel et al., 2020; Knott, Daniel, et al., 2018).

Figure 2.11

Projected groundwater rise with RSLR in coastal New Hampshire for four sea level rise scenarios: a) 0.3 m, b) 0.8 m, c) 1.6 m, and d) 2 m. Each box shows the mean (x), median, interquartile range, and outliers for each 1.0-km distance interval from the coast.



Knowledge and data gaps

More groundwater modeling is needed to assess and plan for climate-change effects on water resources and infrastructure. Three-dimensional groundwater modeling has been used for decades to simulate groundwater systems and groundwater/surface water interactions and is an important tool for investigating climate change impacts and adaptation strategies. Groundwater modeling integrates aquifer recharge, evapotranspiration, water withdrawals, contaminant transport (including saltwater intrusion), groundwater/surface water interactions, and sea level and can be used to simulate the effects of long-term changes in one or more of these parameters. These models can be used to simulate rising groundwater caused by sea level rise, investigate changes in pumping volumes needed to address aquifer recharge reductions, predict groundwater inundation and wetland expansion, investigate saltwater intrusion, and simulate contaminant transport (Bjerkie et al., 2012; DeSimone et al., 2002; Habel et al., 2020; Kirshen, 2002; Knott, Jacobs, et al., 2018; Walter et al., 2016)

Accurate and useful models require data for model calibration. Changes in aquifer recharge with climate change are difficult to quantify. This is due to a limited number of studies integrating climate projections with recharge estimation methods, understanding the influence of changing snowmelt on aquifer recharge, and challenges associated with quantifying aquifer recharge from extreme precipitation events (Bjerkie and Sturtevant, 2018; Meixner et al., 2016). More studies combining climate model output with precipitation-runoff models would be helpful. Boutt (2017) expresses the need for glacial till aquifers to be included in precipitation-runoff models for investigating the impacts of climate change on groundwater since they represent 70% of the active groundwater storage in the glaciated Northeast.

While climate affects groundwater systems, groundwater can also influence the climate. Water-table depths from 2 to 7 m have been found to influence land-energy fluxes suggesting that a more sophisticated modeling of groundwater systems should be integrated into land-surface models used in GCMs (Ferguson and Maxwell, 2010; Taylor et al., 2013).

2.8 STORMS, PRECIPITATION, FLOODING AND GROUNDWATER REFERENCES

Agel, L., M. Barlow, J.-H. Qian, F. Colby, E. Douglas, and T. Eichler. "Climatology of Daily Precipitation and Extreme Precipitation Events in the Northeast United States". *J. Hydrometeorology*, 16, 2015, 2537-2557, <https://doi.org/10.1175/JHM-D-14-0147.1>.

Agel, L., M. Barlow, F. Colby, H. Binder, J. L. Catto, A. Hoell, and J. Cohen. "Dynamical analysis of extreme precipitation in the US northeast based on large-scale meteorological patterns." *Climate Dynamics*, 52, 2019a, 1739-1760, <https://doi.org/10.1007/s00382-018-4223-2>.

Agel, L., Barlow, M., Collins, M.J., Douglas, E., and Kirshen, P. "Hydrometeorological Conditions Preceding Extreme Streamflow for the Charles and Mystic River Basins of Eastern Massachusetts." *Journal of Hydrometeorology*, 20(9), 2019b, 1795–1812.

Alexander, L.V., Arblaster, J.M. "Assessing trends in observed and modelled climate extremes over Australia in relation to future projections." *International Journal Climatology*, 29, 2009, 417–435.

Allan, R., Barlow, M., Byrne, M.P., Cherchi, A., Douville, H., Fowler, H.J., Gan, T.Y., Pendergrass, A.G., Rosenfeld, D., Swann, A.L. and Wilcox, L. "Advances in understanding large-scale responses of the water cycle to climate change." *Annals of the New York Academy of Sciences*, 2020.

Archfield, S.A., Hirsch, R.M., Viglione, A., and Blöschl, G. "Fragmented patterns of flood change across the United States." *Geophysical Research Letters*, 43(19), 2016, 10,232–10,239, <https://doi.org/10.1002/2016GL070590>.

Arias, M.E., Cochrane, T.A., Norton, D., Killeen, T.J., and Khon, P. "The flood pulse as the underlying driver of vegetation in the largest wetland and fishery of the Mekong Basin." *Ambio*, 42(7), 2013, 864–876, https://www.researchgate.net/publication/251235064_The_Flood_Pulse_as_the_Underlying_Driver_of_Vegetation_in_the_Largest_Wetland_and_Fishery_of_the_Mekong_Basin.

- Armstrong, W.H., Collins, M.J., and Snyder, N.P. (2012). "Increased frequency of low magnitude floods in New England." *Journal of the American Water Resources Association (JAWRA)* 48(2), 2012, 306–320.
- Armstrong, W.H., Collins, M.J., and Snyder, N.P. "Hydroclimatic flood trends in the Northeastern United States and linkages with large-scale atmospheric circulation patterns." *Hydrological Sciences Journal*, 59, 2014, 1636–1655, <https://doi.org/10.1080/02626667.2013.862339>.
- Arnell, N.W., and Gosling, S.N. "The impacts of climate change on river flood risk at the global scale." *Climatic Change*, 134(3), 2016, 387–401.
- Aryal, Y.N., Villarini, G., Zhang, W., and Vecchi, G.A. "Long term changes in flooding and heavy rainfall associated with North Atlantic tropical cyclones: Roles of the North Atlantic Oscillation and El Niño-Southern Oscillation." *Journal of Hydrology*, 559, 2018, 698–710.
- Asadieh, B., and Krakauer, N.Y. "Global change in streamflow extremes under climate change over the 21st century." *Hydrology and Earth System Sciences*, 21(11), 2017, 5863.
- Ashley, W.S., Haberlie, A.M. and Gensini, V.A. "Reduced frequency and size of late-twenty-first-century snowstorms over North America." *Nature Climate Change*, 2020, 1–6.
- Ashley, S.T., and Ashley, W.S. "Flood fatalities in the United States." *Journal of Applied Meteorology and Climatology*, 47(3), 2008, 805–818.
- Barlow, M. "Influence of hurricane-related activity on North American extreme precipitation." *Geophysical Research Letters*, 38(4), 2011.
- Bjerklie, D.M., Ayotte, J.D., and Cahillane, M.J. "Simulating hydrologic response to climate change scenarios in four selected watersheds of New Hampshire." *U.S. Geological Survey Scientific Investigations Report 2015–5047*, 2015, 53, <http://dx.doi.org/10.3133/sir20155047>.
- Bjerklie, D. M., Mullaney, J. R., Stone, J. R., Skinner, B. J., and Ramlow, M. A. "Preliminary investigation of the effects of sea-level rise on groundwater levels in New Haven, Connecticut." *U.S. Geological Survey Open-File Report, 2012–1025*, 2012, 46.
- Bjerklie, D. M., and Sturtevant, L. P. "Simulated hydrologic response to climate change during the 21st century in New Hampshire." *USGS Numbered Series No. 2017–5143; Scientific Investigations Report*, 2018, 66, <http://pubs.er.usgs.gov/publication/sir20175143>.
- Bosma, K., Douglas, E., Kirshen, P., McArthur, K., Miller, S., Watson, C. *MassDOT-FHWA Pilot Project Report: Climate Change and Extreme Weather Vulnerability Assessments and Adaptation Options for the Central Artery*. 2016.
- Boston Water and Sewer Commission (BWSC) *Comprehensive-Integrated Sustainable Wastewater and Storm Drainage System Facilities Plan Final Report*. Retrieved from: DVD of the Report. 2015.
- Boutt, D. F. "Assessing hydrogeologic controls on dynamic groundwater storage using long-term instrumental records of water table levels." *Hydrological Processes*, 31(7), 2017, 1479–1497, <https://doi.org/10.1002/hyp.11119>.
- Boutt, D. F., Diggins, P., and Mabee, S. "A field study (Massachusetts, USA) of the factors controlling the depth of groundwater flow systems in crystalline fractured-rock terrain." *Hydrogeology Journal*, 18(8), 2010, 1839–1854, <https://doi.org/10.1007/s10040-010-0640-y>.
- Boutt, D. F., Mabee, S. B., and Yu, Q. "Multiyear Increase in the Stable Isotopic Composition of Stream Water From Groundwater Recharge Due to Extreme Precipitation." *Geophysical Research Letters*, 46(10), 2019, 5323–5330, <https://doi.org/10.1029/2019GL082828>.
- Brown, V.M., Keim, B.D. and Black, A.W. "Trend Analysis of Multiple Extreme Hourly Precipitation Time Series in the Southeast United States." *Journal of Applied Meteorology and Climatology*, 2020.
- Catto, J. L., Nicholls, N., Jakob, C., and Shelton, K. L. "Atmospheric fronts in current and future climates." *Geophysical Research Letters*, 41, 2014, 7642–7650.
- Catto, J.L., Ackerley, D., Booth, J.F. et al. "The Future of Midlatitude Cyclones." *Current Climate Change Reports*, 5, 2019, 407–420, <https://doi.org/10.1007/s40641-019-00149-4>.

- Chang, E. K. M., Ma, C.-G., Zheng, C., and Yau, A. M. W. "Observed and projected decrease in Northern Hemisphere extratropical cyclone activity in summer and its impacts on maximum temperature." *Geophysical Research Letters*, 43, 2016, 2200–2208.
- Chen, G., W. Wang, L. Tao, H. Hsu, C. Tu, and C. Cheng. "Extreme Snow Events along the Coast of the Northeast United States: Analysis of Observations and HiRAM Simulations." *Journal of Climate*, 32, 2019, 7561–7574, <https://doi.org/10.1175/JCLI-D-18-0874.1>.
- Cheng, L. and AghaKouchak, A. "Nonstationary precipitation intensity-duration-frequency curves for infrastructure design in a changing climate." *Scientific Reports*, 4, 2014, 7093.
- Choi, W., C. Ho, D.R. Park, J. Kim, and J.C. Chan. "Near-Future Prediction of Tropical Cyclone Activity over the North Atlantic." *Journal of Climate*, 30, 2017, 8795–8809, <https://doi.org/10.1175/JCLI-D-17-0206.1>.
- City of Cambridge. *Climate Change Vulnerability Assessment*. Cambridge MA, 2015.
- Collins, M.J. "Evidence for changing flood risk in New England since the late 20th century." *Journal of the American Water Resources Association (JAWRA)*, 45(2), 2009, 279–290.
- Collins, M. J. "River flood seasonality in the Northeast United States: Characterization and trends." *Hydrological Processes*, 33(5), 2019, 687–698, <https://doi.org/10.1002/hyp.13355>.
- Collins, M. J., Kirk, J. P., Pettit, J., DeGaetano, A. T., McCown, M. S., Peterson, T. C., Means, T. N., and Zhang, X. "Annual floods in New England (USA) and Atlantic Canada: Synoptic climatology and generating mechanisms." *Physical Geography*, 35(3), 2014, 195–219, <https://doi.org/10.1080/02723646.2014.888510>.
- Collow, A. B. M., M. G. Bosilovich, and R. D. Koster. "Large-Scale Influences on Summertime Extreme Precipitation in the Northeastern United States." *Journal of Hydrometeorology*, 17, 2016, 3045–3061.
- Cook, T. L., Yellen, B. C., Woodruff, J. D., and Miller, D. "Contrasting human versus climatic impacts on erosion." *Geophysical Research Letters*, 42(16), 2015, 6680–6687.
- Cooley, A. and Chang, H. "Precipitation intensity trend detection using hourly and daily observations in Portland, Oregon." *Climate*, 5(1), 2017, 10.
- Cooper, H. M., Chen, Q., Fletcher, C. H., and Barbee, M. M. "Assessing vulnerability due to sea-level rise in Maui, Hawai'i using LiDAR remote sensing and GIS." *Climatic Change*, 116(3–4), 2013, 547–563, <https://doi.org/10.1007/s10584-012-0510-9>.
- Coumou, D., Rahmstorf, S. "A decade of weather extremes." *Nature Climate Change*, 2, 2012, 491–496.
- Cowell, C.M., and Urban, M.A. "The changing geography of the US water budget: Twentieth-century patterns and twenty-first-century projections." *Annals of the Association of American Geographers*, 100(4), 2010, 740–754, <https://doi.org/10.1080/00045608.2010.497117>.
- DeGaetano, A.T., and Castellano, C. M. "Future projections of extreme precipitation intensity-duration-frequency curves for climate adaptation planning in New York State." *Climate Services*, 5, 2017, 23–35.
- DeGaetano, A.T., and Castellano, C. M. *Downscaled Projections of Extreme Rainfall in New York State, Technical Document*. 2020.
- DeGaetano, A.T., Mooers, G., and Favata, T. "Temporal changes in the areal coverage of daily extreme precipitation in the Northeastern United States using high-resolution gridded data." *Journal of Applied Meteorology and Climatology*, 59(3), 2020, 551–565.
- DeGaetano, A.T. "Time-dependent changes in extreme-precipitation return-period amounts in the continental United States." *Journal of Applied Meteorology and Climatology*, 48, 2009, 2086–2099.
- DeGaetano, A.T. and Castellano, C. "Selecting Time Series Length to Moderate the Impact of Non-stationarity in Extreme Rainfall Analyses." *Journal of Applied Meteorology and Climatology*, 57, 2018, 2285–2296.
- Demaria, E.M., Palmer, R.N., and Roundy, J.K. "Regional climate change projections of streamflow characteristics in the Northeast and Midwest US." *Journal of Hydrology: Regional Studies*, 5, 2016, 309–323.
- Deser, C., Knutti, R., Solomon, S., and Phillips, A. S. "Communication of the role of natural variability in future North American climate." *Nature Climate Change*, 2(11), 2012, 775–779.

- Desimone, L. A. *Simulation of ground-water flow and evaluation of water-management alternatives in the Assabet River basin, eastern Massachusetts*. Reston, VA, 2004.
- DeSimone, L. A., Walter, D. A., Eggleston, J. R., and Nimroski, M. T. "Simulation of Ground-Water Flow and Evaluation of Water-Management Alternatives in the Upper Charles River Basin, Eastern Massachusetts." *U.S. Geological Survey Water-Resources Investigations Report 02-4234*, 2002, 94, <https://pubs.usgs.gov/wri/wri024234>.
- Dhakal, N., and Jain, S. "Nonstationary influence of the North Atlantic tropical cyclones on the spatio-temporal variability of the eastern United States precipitation extremes." *International Journal of Climatology*, 2019.
- Donat, M.G., Lowry, A.L., Alexander, L.V., O'Gorman, P.A., Maher, N. "More extreme precipitation in the world's dry and wet regions." *Nature Climate Change*, 6, 2016, 508–513.
- Douglas, E., Kirshen, P., Hannigan, R., Herst, R., Palardy, A., DeConto, R., Ruth, M. "Climate change and sea level rise projections for Boston: The Boston Research Advisory Group Report." *Boston, MA: Climate Ready Boston*, 2016, 54, <http://climateready.boston.gov/findings>.
- Dudley, R.W., Hirsch, R.M., Archfield, S.A., Blum, A.G., and Renard, B. "Low streamflow trends at human-impacted and reference basins in the United States." *Journal of Hydrology*, 580, 2020, 124254.
- Dunne, T., and Black, R.D. "Partial area contributions to storm runoff in a small New England watershed." *Water Resources Research*, 6(5), 1970, 1296–1311.
- Easterling, D.R., K.E. Kunkel, J.R. Arnold, T. Knutson, A.N. LeGrande, L.R. Leung, R.S. Vose, D.E. Wal- iser, and M.F. Wehner. "Precipitation change in the United States." *Climate Science Special Report: Fourth National Climate Assessment, Volume I*, U.S. Global Change Research Program, Washington, DC, USA, 2017, 207–230.
- Ehsani, N., Vörösmarty, C. J., Fekete, B. M., and Stakhiv, E. Z. "Reservoir operations under climate change: Storage capacity options to mitigate risk." *Journal of Hydrology*, 555, 2017, 435–446, <https://doi.org/10.1016/j.jhydrol.2017.09.008>.
- Evans, C., K.M. Wood, S.D. Aberson, H.M. Archambault, S.M. Milrad, L.F. Bosart, K.L. Corbosiero, C.A. Davis, J.R. Dias Pinto, J. Doyle, C. Fogarty, T.J. Galarneau, C.M. Grams, K.S. Griffin, J. Gyakum, R.E. Hart, N. Kitabatake, H.S. Lentink, R. McTaggart-Cowan, W. Perrie, J.F. Quinting, C.A. Reynolds, M. Riemer, E.A. Ritchie, Y. Sun, and F. Zhang. "The Extratropical Transition of Tropical Cyclones. Part I: Cyclone Evolution and Direct Impacts." *Monthly Weather Review*, 145, 2017, 4317–4344, <https://doi.org/10.1175/MWR-D-17-0027.1>.
- Ferguson, I. M., and Maxwell, R. M. "Role of groundwater in watershed response and land surface feedbacks under climate change." *Water Resources Research*, 46(10), 2010, <https://doi.org/10.1029/2009WR008616>.
- Ficklin, D.L., Robeson, S.M., and Knouft, J.H. "Impacts of recent climate change on trends in baseflow and stormflow in United States watersheds." *Geophysical Research Letters*, 43(10), 2016, 5079–5088.
- Fischer, E. M., Knutti, R. "Observed heavy precipitation increase confirms theory and early models." *Nature Climate Change*, 6(11), 2016, 986–991, <http://doi.org/10.1038/nclimate3110>.
- Flood, J.F., and Cahoon, L.B. "Risks to Coastal Wastewater Collection Systems from Sea-Level Rise and Climate Change." *Journal of Coastal Research*, 27(4), 2011, 652–660, <https://doi.org/10.2112/JCOASTRES-D-10-00129.1>.
- Fowler, K., Knoben, W., Peel, M., Peterson, T., Ryu, D., Saft, M., Seo, K., and Western, A. "Many commonly used rainfall-runoff models lack long, slow dynamics: implications for runoff projections." *Water Resources Research*, 2020.
- Fowler, H. J., G. Lenderink, A.F. Prein, S. Westra, R.P. Allan, N. Ban, R. Barbero, P. Berg, S. Blenkinsop, H.X. Do, S.B. Guerreiro, J.O. Haert, E.J. Kendon, E. Lewis, C. Schär, A. Sharma, G. Villarini, C. Wasko, and X. Zhang. "Anthropogenic intensification of short-duration precipitation extremes." *Nature Reviews Earth and Environment*, 2, 2021, 107–122.
- Freeze, R.A., and Cherry, J.A. (1979). "Chapter 6: Groundwater and the Hydrologic Cycle." *Hydrogeologists Without Borders*. 1979.
- Frei, A., Kunkel, K.E., and Matonse, A. "The seasonal nature of extreme hydrological events in the Northeastern United States." *Journal of Hydrometeorology*, 16, 2015, 2065–2085, https://journals.ametsoc.org/view/journals/hydr/16/5/jhm-d-14-0237_1.xml.

- Galarneau, T. J., Jr., Bosart, L. F., and Schumacher, R. S. "Predecessor Rain Events ahead of Tropical Cyclones." *Monthly Weather Review*, 138(8), 2010, 3272–3297.
- Georgakakos, A., Fleming, P., Dettinger, M., Peters-Lidard, C., T.C., Richmond, Reckhow, K., White, K., and Yates, D. "Water resources." *Climate Change Impacts in the United States: The Third National Climate Assessment. Global Change Res. Program*, Washington, D.C., 2014.
- Gertler, C.G. and O'Gorman, P.A. "Changing available energy for extratropical cyclones and associated convection in Northern Hemisphere summer." *Proceedings of the National Academy of Sciences*, 116(10), 2019, 4105–4110, <https://doi.org/10.1073/pnas.1812312116>.
- Giuntoli, I., Villarini, G., Prudhomme, C., and Hannah, D. M. "Uncertainties in projected runoff over the conterminous United States." *Climatic Change*, 150(3), 2018, 149–162.
- Glas, R., Burns, D., and Lautz, L. "Historical changes in New York State streamflow: Attribution of temporal shifts and spatial patterns from 1961 to 2016." *Journal of Hydrology*, 574, 2019, 308–323.
- Groisman, P. Ya., Knight, R.W., Easterling, D. R., Karl, T.R., Hegerl, G.C., Razuvayev, V.N. "Trends in intense precipitation in the climate record." *Journal of Climate*, 18, 2005, 1343–1367.
- Groisman, P. Ya., R. W. Knight, and T. R. Karl. "Changes in intense precipitation over the central United States." *Journal of Hydrometeorology*, 13, 2012, 47–66.
- Habel, S., Fletcher, C.H., Anderson, T.R., and Thompson, P.R. "Sea-Level Rise Induced Multi-Mechanism Flooding and Contribution to Urban Infrastructure Failure." *Scientific Reports*, 10(1), 2020, 1–12, <https://doi.org/10.1038/s41598-020-60762-4>.
- Hanna, E., Cropper, T.E., Hall, R.J. and Cappelen, J. (2016). "Greenland Blocking Index 1851–2015: a regional climate change signal." *International Journal of Climatology*, 36, 2016, 4847–4861.
- Hawcroft, M.K., Shaffrey, L.C., Hodges, K.I., and Dacre, H.F. (2012). "How much Northern Hemisphere precipitation is associated with extratropical cyclones?" *Geophysical Research Letters*, 39, 2012, L24809.
- Hawkins, E., and Sutton, R. "The potential to narrow uncertainty in regional climate predictions." *Bulletin of the American Meteorological Society*, 90(8), 2009, 1095–1108.
- Hawkins, E., and Sutton, R. "The potential to narrow uncertainty in projections of regional precipitation change." *Climate Dynamics*, 37(1–2), 2011, 407–418.
- Hibbard, K.A., Hoffman, F.M., Huntzinger, D., and West, T.O. "Changes in land cover and terrestrial biogeochemistry." *Climate Science Special Report: Fourth National Climate Assessment (ed., Vol. I)*. 2017, 277–302.
- Hirabayashi, Y., Mahendran, R., Koirala, S., Konoshima, L., Yamazaki, D., Watanabe, S., Kanae, S. "Global flood risk under climate change." *Nature Climate Change*, 3(9), 2013, 816–821.
- Hodgkins, G. A., Dudley, R. W., Nielsen, M. G., Renard, B., and Qi, S. L. "Groundwater-level trends in the U.S. glacial aquifer system, 1964–2013." *Journal of Hydrology*, 553, 2017, 289–303, <https://doi.org/10.1016/j.jhydrol.2017.07.055>.
- Hodgkins, G.A. "Historical changes in annual peak flows in Maine and implications for flood-frequency analyses." *U.S. Geological Survey Scientific Investigations Report 2010–5094*, 2010, 38, <http://pubs.usgs.gov/sir/2010/5094>.
- Hodgkins, G.A., and Dudley, R.W. "Modeled future peak streamflows in four coastal Maine rivers." *US Geological Survey Scientific Investigations Report*, 5080, 2013, 18.
- Hoogewind, K.A., M.E. Baldwin, and R.J. Trapp. "The Impact of Climate Change on Hazardous Convective Weather in the United States: Insight from High-Resolution Dynamical Downscaling." *Journal of Climate*, 30, 2017, 10081–10100, <https://doi.org/10.1175/JCLI-D-16-0885.1>.
- Horton R, Yohe G, Easterling W, Kates R, Ruth M, Sussman E, Whelchel A, Wolfe D, Lipschultz F. "Ch. 16: Northeast." *Climate Change Impacts in the United States: The Third National Climate Assessment*, 2014, 371–395.
- Huang, H., Winter, J.M., and Osterberg, E.C. "Mechanisms of abrupt extreme precipitation change over the Northeastern United States." *Journal of Geophysical Research: Atmospheres*, 2018, <https://doi.org/10.1029/2017JD028136>.

- Hughes, J. D., Petrone, K. C., and Silberstein, R. P. "Drought, groundwater storage and stream flow decline in southwestern Australia." *Geophysical Research Letters*, 39(3), 2012, <https://doi.org/10.1029/2011GL050797>.
- IPCC. "Climate Change 2014: Synthesis Report." *Contribution of Working Groups I, II and III to the Fifth Assessment Report of the Intergovernmental Panel on Climate Change*. IPCC, Geneva, Switzerland.
- Ivancic, T.J., and Shaw, S.B. "Examining why trends in very heavy precipitation should not be mistaken for trends in very high river discharge." *Climatic Change*, 133(4), 2015, 681–693, <https://doi.org/10.1007/s10584-015-1476-1>.
- Jasechko, S., Birks, S.J., Gleeson, T., Wada, Y., Fawcett, P.J., Sharp, Z.D., McDonnell, J.J., and Welker, J.M. "The pronounced seasonality of global groundwater recharge." *Water Resources Research*, 50(11), 2014, 8845–8867, <https://doi.org/10.1002/2014WR015809>.
- Jung, C. and G.M. Lackmann. "Extratropical Transition of Hurricane Irene (2011) in a Changing Climate." *Journal of Climate*, 32, 2019, 4847–4871, <https://doi.org/10.1175/JCLI-D-18-0558.1>.
- Karmalkar, A. V. "Interpreting results from the NARCCAP and NA-CORDEX ensembles in the context of uncertainty in regional climate change projections." *Bulletin of the American Meteorological Society*, 99(10), 2018, 2093–2106.
- Karmalkar, A.V., and Bradley, R.S. "Consequences of global warming of 1.5 C and 2 C for regional temperature and precipitation changes in the contiguous United States." *PloS one*, 12(1), 2017, e0168697.
- Karmalkar, A.V., Thibeault, J.M., Bryan, A.M., and Seth, A. "Identifying credible and diverse GCMs for regional climate change studies—case study: Northeastern United States." *Climatic Change*, 154(3–4), 2019, 367–386.
- Kenyon, J., Hegerl, G.C. "Influence of modes of climate variability on global precipitation extremes." *Journal of Climate*, 23(23), 2010, 6248–6262.
- Kirshen, P. H. "Potential Impacts of Global Warming on Groundwater in Eastern Massachusetts." *Journal of Water Resources Planning & Management*, 128(3), 2002, 216.
- Knighton, J., Conneely, J., and Walter, M. T. "Possible Increases in Flood Frequency Due to the Loss of Eastern Hemlock in the Northeastern United States: Observational Insights and Predicted Impacts." *Water Resources Research*, 55(7), 2019, 5342–5359.
- Knott, J. F., Daniel, J. S., Jacobs, J. M., and Kirshen, P. "Adaptation Planning to Mitigate Coastal-Road Pavement Damage from Groundwater Rise Caused by Sea-Level Rise." *Transportation Research Record (Journal Article)*, 2018, 0361198118757441, <https://doi.org/10.1177/0361198118757441>.
- Knott, J. F., Jacobs, J., Daniel, J. S., and Kirshen, P. "Modeling Groundwater Rise Caused by Sea-Level Rise in Coastal New Hampshire." *Journal of Coastal Research*, 35(1), 2018, 143–157, <https://www.jstor.org/stable/26568601>.
- Knott, J. F., Sias, J. E., Dave, E. V., and Jacobs, J. M. "Seasonal and Long-Term Changes to Pavement Life Caused by Rising Temperatures from Climate Change." *Transportation Research Record: Journal of the Transportation Research Board*, 1–12, 2019, <https://doi.org/10.1177/0361198119844249>.
- Knutson, T., S.J. Camargo, J.C. Chan, K. Emanuel, C. Ho, J. Kossin, M. Mohapatra, M. Satoh, M. Sugi, K. Walsh, and L. Wu. "Tropical Cyclones and Climate Change Assessment: Part II: Projected Response to Anthropogenic Warming." *Bulletin of the American Meteorological Society*, 101, 2020, E303–E322, <https://doi.org/10.1175/BAMS-D-18-0194.1>.
- Koirala, S., Hirabayashi, Y., Mahendran, R., and Kanae, S. "Global assessment of agreement among streamflow projections using CMIP5 model outputs." *Environmental Research Letters*, 9(6), 2014, 064017.
- Konrad Ii, C. E. "The Most Extreme Precipitation Events over the Eastern United States from 1950 to 1996: Considerations of Scale." *Journal of Hydrometeorology*, 2, 2001, 309–325.
- Kooperman, G.J., Fowler, M.D., Hoffman, F.M., Koven, C.D., Lindsay, K., Pritchard, M.S., Swann, A.L.S., and Randerson, J.T. "Plant physiological responses to rising CO₂ modify simulated daily runoff intensity with implications for global-scale flood risk assessment." *Geophysical Research Letters*, 45(22), 2018, 12–457.
- Kunkel, K. E., Easterling, D. R., Kristovich, D. A., Gleason, B., Stoecker, L., and Smith, R. "Recent increases in US heavy precipitation associated with tropical cyclones." *Geophysical Research Letters*, 37(24), 2010.

- Kunkel, K. E., D. R. Easterling, D. A. R. Kristovich, B. Gleason, L. Stoecker, and R. Smith. "Meteorological Causes of the Secular Variations in Observed Extreme Precipitation Events for the Conterminous United States." *Journal of Hydrometeorology*, 13, 2012, 1131–1141.
- Kunkel K., et al. "Regional climate trends and scenarios for the U.S. National Climate Assessment: Part 1—Climate of the Northeast U.S." *NOAA Technical Report NESDIS*, 142–1, 2013, 80.
- Kynard, B. "Life history, latitudinal patterns, and status of the shortnose sturgeon." *Acipenser brevirostrum*. *Environmental Biology of Fishes*, 48(1–4), 1997, 319–334.
- Lee, C., S.J. Camargo, A.H. Sobel, and M.K. Tippett. "Statistical-dynamical downscaling projections of tropical cyclone activity in a warming climate: Two diverging genesis scenarios." *Journal of Climate*, 0, 2020, <https://doi.org/10.1175/JCLI-D-19-0452.1>.
- Lenderink, G., Mok, H.Y., Lee, T.C. and Van Oldenborgh, G.J. "Scaling and trends of hourly precipitation extremes in two different climate zones—Hong Kong and the Netherlands." *Hydrology and Earth System Sciences*, 15(9), 2011, 3033–3041.
- Lins, H.F. "USGS hydro-climatic data network 2009 (HCDN–2009)." *U.S. Geological Survey Fact Sheet 2012–3047*, 2012, 4.
- Little, C.M., R.M. Horton, R.E. Kopp, M. Oppenheimer, G. Vecchi, and G. Villarini. "Joint projections of US East Coast sea level and storm surge." *Nature Climate Change*, 5, 2015, 1114–1120.
- Liu, M., G.A. Vecchi, J.A. Smith, and H. Murakami. "The Present-Day Simulation and Twenty-First-Century Projection of the Climatology of Extratropical Transition in the North Atlantic." *Journal of Climate*, 30, 2017, 2739–2756, <https://doi.org/10.1175/JCLI-D-16-0352.1>.
- Lynch, C., Seth, A., and Thibeault, J. "Recent and projected annual cycles of temperature and precipitation in the Northeast United States from CMIP5." *Journal of Climate*, 29(1), 2016, 347–365, <https://doi.org/10.1175/JCLI-D-14-00781.1>.
- Marciano, C.G., G.M. Lackmann, and W.A. Robinson. "Changes in U.S. East Coast Cyclone Dynamics with Climate Change." *Journal of Climate*, 28, 2015, 468–484, <https://doi.org/10.1175/JCLI-D-14-00418.1>.
- Manda, A.K., Sisco, M.S., Mallinson, D.J., and Griffin, M.T. "Relative role and extent of marine and groundwater inundation on a dune-dominated barrier island under sea-level rise scenarios." *Hydrological Processes*, 29(8), 2015, 1894–1904, <https://doi.org/10.1002/hyp.10303>.
- Massachusetts Document Repository. (n.d.-a). Retrieved March 11, 2020, from <https://docs.digital.mass.gov/dataset/massgis-data-massdep-hydrography-125000>.
- Massachusetts Document Repository. (n.d.-b). Retrieved May 15, 2020, from <https://docs.digital.mass.gov/dataset/massgis-data-public-water-supplies>.
- Masterson, D. A., Carlson, C. S., and Walter, D. A. "Hydrogeology and simulation of groundwater flow in the Plymouth-Carver-Kingston-Duxbury aquifer system, southeastern Massachusetts." *U.S. Geological Survey Scientific Investigations Report 2009-5063*, 2009, 110.
- Masterson, J.P., Fienen, M.N., Thieler, E.R., Gesch, D.B., Gutierrez, B.T., and Plant, N.G. "Effects of sea-level rise on barrier island groundwater system dynamics—Ecohydrological implications." *Ecohydrology*, 7(3), 2014, 1064–1071, <https://doi.org/10.1002/eco.1442>.
- Masterson, John P., and Garabedian, S.P. "Effects of Sea-Level Rise on Ground Water Flow in a Coastal Aquifer System." *Groundwater*, 45(2), 2007, 209–217, <https://doi.org/10.1111/j.1745-6584.2006.00279.x>.
- Meinshausen, M., Smith, S. J., Calvin, K., Daniel, J. S., Kainuma, M. L. T., Lamarque, J. F., and Thomson, A. G. J. M. V. "The RCP greenhouse gas concentrations and their extensions from 1765 to 2300." *Climatic Change*, 109(1-2), 2001, 213.
- Meixner, T., Manning, A. H., Stonestrom, D. A., Allen, D. M., Ajami, H., Blasch, K. W., Brookfield, A. E., Castro, C. L., Clark, J. F., Gochis, D. J., Flint, A. L., Neff, K. L., Niraula, R., Rodell, M., Scanlon, B. R., Singha, K., and Walvoord, M. A. "Implications of projected climate change for groundwater recharge in the western United States." *Journal of Hydrology*, 534, 2016, 124–138, <https://doi.org/10.1016/j.jhydrol.2015.12.027>.

Michaelis, A.C., J. Willison, G.M. Lackmann, and W.A. Robinson. "Changes in Winter North Atlantic Extratropical Cyclones in High-Resolution Regional Pseudo-Global Warming Simulations." *Journal of Climate*, 30, 2017, 6905–6925, <https://doi.org/10.1175/JCLI-D-16-0697.1>.

Michaelis, A.C. and G.M. Lackmann. "Climatological Changes in the Extratropical Transition of Tropical Cyclones in High-Resolution Global Simulations." *Journal of Climate*, 32, 2019, 8733–8753, <https://doi.org/10.1175/JCLI-D-19-0259.1>.

Milly, P.C.D., and Dunne, K.A. "On the hydrologic adjustment of climate-model projections: The potential pitfall of potential evapotranspiration." *Earth Interactions*, 15(1), 2011, 1–14.

Milly, P.C.D., and Dunne, K.A. "Potential evapotranspiration and continental drying." *Nature Climate Change*, 6(10), 2016, 946–949.

Milly, P.C.D., and Dunne, K.A. "A hydrologic drying bias in water-resource impact analyses of anthropogenic climate change." *Journal of the American Water Resources Association*, 53(4), 2017, 822–838.

Mo, W., Wang, H., and Jacobs, J. M. "Understanding the influence of climate change on the embodied energy of water supply." *Water Research*, 95, 2016, 220–229, <https://doi.org/10.1016/j.watres.2016.03.022>.

Muñoz, C., D. Schultz, and G. Vaughan. "A Midlatitude Climatology and Interannual Variability of 200- and 500-hPa Cut-Off Lows." *Journal of Climate*, 33, 2020, 2201–2222, <https://doi.org/10.1175/JCLI-D-19-0497.1>.

Myhre, G., Alterskjær, K., Stjern, C.W., Hodnebrog, Ø., Marelle, L., Samset, B.H., Sillmann, J., Schaller, N., Fischer, E., Schulz, M. and Stohl, A. "Frequency of extreme precipitation increases extensively with event rareness under global warming." *Scientific Reports*, 9(1), 2019, 1–10.

National Academies of Sciences, Engineering, and Medicine (NASEM). *Framing the Challenge of Urban Flooding in the United States*. Washington, DC: The National Academies Press, 2019, <https://doi.org/10.17226/25381>.

Ning, L., Riddle, E.E., Bradley, R.S. "Projected changes in climate extremes over the northeastern United States." *Journal of Climate*, 28, 2015, 3289–3310.

Oude Essink, G.H.P., van Baaren, E.S., and de Louw, P.G.B. "Effects of climate change on coastal groundwater systems: A modeling study in the Netherlands." *Water Resources Research*, 46(10), 2010, <https://doi.org/10.1029/2009WR008719>.

Palmer, R., and Siddique, R. "Estimating Future Changes in 100-year, 24-hour Flows on the Connecticut and Merrimack Rivers." MassDOT, 19-003, 2019.

Parding, K.M., R. Benestad, A. Mezghani, and H.B. Erlandsen. "Statistical Projection of the North Atlantic Storm Tracks." *Journal of Applied Meteorology and Climatology*, 58, 2019, 1509–1522, <https://doi.org/10.1175/JAMC-D-17-0348.1>.

Peterson, T., Heim, R., Hirsch, R., Kaiser, D., Brooks, H., Diffenbaugh, N., Dole, R., Giovannettone, J., Guirguis, K., Karl, T., Katz, R., Kunkel, K., Lettenmaier, D., McCabe, G., Paciorek, C., Ryber, K., Schubert, S., Silva, V., et al. "Monitoring and Understanding Changes in Heat Waves, Cold Waves, Floods and Droughts in the United States: State of Knowledge." *Bulletin of the American Meteorological Society*, 94(6), 2013, 821–834.

Pierce, D. W., D. R. Cayan, and B. L. Thrasher. "Statistical Downscaling Using Localized Constructed Analogs (LOCA)." *Journal of Hydrometeorology*, 15, 2014, 2558–2585.

Pimentel, D., Berger, B., Filiberto, D., Newton, M., Wolfe, B., Karabinakis, E., Clark, S., Poon, E., Abbott, E., and Nandagopal, S. "Water Resources: Agricultural and Environmental Issues." *BioScience*, 54(10), 2004, 909–918, [https://doi.org/10.1641/0006-3568\(2004\)054\[0909:WRAAEI\]2.0.CO;2](https://doi.org/10.1641/0006-3568(2004)054[0909:WRAAEI]2.0.CO;2).

Prein, A.F., Rasmussen, R.M., Ikeda, K., Liu, C., Clark, M.P., and Holland, G.J. "The future intensification of hourly precipitation extremes." *Nature Climate Change*, 7(1), 2017, 48–52.

Price, K. "Effects of watershed topography, soils, land use, and climate on baseflow hydrology in humid regions: A review." *Progress in Physical Geography: Earth and Environment*, 35(4), 2011, 465–492. <https://doi.org/10.1177/0309133311402714>.

- Ragno, E., AghaKouchak, A., Love, C.A., Cheng, L., Vahedifard, F., and Lima, C.H. "Quantifying changes in future intensity-duration-frequency curves using multimodel ensemble simulations." *Water Resources Research*, 54(3), 2018, 1751–1764.
- Rawlins, M., R. S. Bradley, and H. Diaz. "Assessment of regional climate model simulation estimates over the northeast United States." *Journal of Geophysical Research*, 117, 2012, D23112, <https://doi.org/10.1029/2012JD018137>.
- Renshaw, C.E., Magilligan, F.J., Doyle, H.G., Dethier, E. N., and Kantack, K.M. "Rapid response of New England (USA) rivers to shifting boundary conditions: Processes, time frames, and pathways to post-flood channel equilibrium." *Geology*, 47(10), 2019, 997–1000.
- Ritter, Michael E. "The Physical Environment: an Introduction to Physical Geography." 2006, <http://www.thephysicalenvironment.com>.
- Robertson, A.I., Bacon, P., and Heagney, G. "The responses of floodplain primary production to flood frequency and timing." *Journal of Applied Ecology*, 38(1), 2001, 126–136. www.thephysicalenvironment.com.
- Rodríguez, R., Navarro, X., Casas, M.C., Ribalaygua, J., Russo, B., Pouget, L., Redaño, A. "Influence of climate change on IDF curves for the metropolitan area of Barcelona (Spain)." *International Journal of Climatology*, 34, 2014, 643–654.
- Seyednasrollah, B., Young, A. M., Li, X., Milliman, T., Ault, T., Frolking, S., et al. "Sensitivity of deciduous forest phenology to environmental drivers: Implications for climate change impacts across North America." *Geophysical Research Letters*, 47, 2020, e2019GL086788. <https://doi.org/10.1029/2019GL086788>.
- Sheffield J, Barrett AP, Colle B, Nelun Fernando D, Fu R, Geil KL, Hu Q, Kinter J, Kumar S, Langenbrunner B et al. "North American climate in CMIP5 experiments. Part I: evaluation of historical simulations of continental and regional climatology." *Journal of Climate*, 26(23), 2013, 9209–9245.
- Slack, J.R., and Landwehr, J.M. "Hydro-climatic data network: A U.S. Geological Survey streamflow data set for the United States for the study of climate variations." *U.S. Geological Survey Open-File Report*, 92–129, 1992, 1874–1988.
- Slater, L.J., and Villarini, G. "Recent trends in US flood risk." *Geophysical Research Letters*, 43(24), 2016, 12428–12436.
- Small, D., Islam, S., and Vogel, R. "Trends in precipitation and streamflow in the eastern U.S.: paradox or perception?" *Geophysical Research Letters*, 33, 2006, L03403.
- Sobel, A.H., S.J. Camargo, T.M. Hall, C.-Y. Lee, M.K. Tippett, and A.A. Wing. "Human influence on tropical cyclone intensity." *Science*, 353, 6296, 2016, 242–246, <https://pubmed.ncbi.nlm.nih.gov/27418502>.
- Sun, Q., Miao, C. and Duan, Q. "Extreme climate events and agricultural climate indices in China: CMIP5 model evaluation and projections." *International Journal of Climatology*, 36, 2016, 43–61.
- Tang, B.H., Gensini, V.A. and Homeyer, C.R. "Trends in United States large hail environments and observations." *npj Climate and Atmospheric Science*, 2, 2019, 45. <https://doi.org/10.1038/s41612-019-0103-7>.
- Taylor, K.E., R.J. Stouffer, and G.A. Meehl. "An overview of CMIP5 and the experiment design." *Bulletin of the American Meteorological Society*, 93, 2012, 485–498, <https://doi.org/10.1175/BAMS-D-11-00094.1>.
- Taylor, R. G., Scanlon, B., Döll, P., Rodell, M., van Beek, R., Wada, Y., Longuevergne, L., Leblanc, M., Famiglietti, J. S., Edmunds, M., Konikow, L., Green, T. R., Chen, J., Taniguchi, M., Bierkens, M. F. P., MacDonald, A., Fan, Y., Maxwell, R. M., Yechieli, Y., ... Treidel, H. "Ground water and climate change." *Nature Climate Change*, 3(4), 2013, 322–329. <https://doi.org/10.1038/nclimate1744>.
- Thibeault, J.M., and Seth, A. "Changing climate extremes in the Northeast United States: Observations and projections from CMIP5." *Climatic Change*, 127(2), 2014, 273–287, <http://doi:10.1007/s10584-014-1257-2>.
- Thibeault JM, Seth A. "Toward the credibility of Northeast United States summer precipitation projections in CMIP5 and NARCCAP simulations." *Journal of Geophysical Research: Atmospheres*, 120(19), 2015, 10050–10073. <https://doi.org/10.1002/2015JD023177>.
- USGS Water Use Data for Massachusetts. (n.d.). Retrieved May 22, 2020, from https://waterdata.usgs.gov/ma/nwis/water_use.

- Villarini, G., and Smith, J.A. "Flood peak distributions for the eastern United States." *Water Resources Research*, 46, 2010, W06504.
- Villarini, G., and Zhang, W. "Projected changes in flooding: a continental US perspective." *Annals of the New York Academy of Sciences*, 2020.
- Vose, R.S., D.R. Easterling, K.E. Kunkel, A.N. LeGrande, and M.F. Wehner (2017). "Temperature changes in the United States." *Climate Science Special Report: Fourth National Climate Assessment*, I, 2017, 185–206, <https://doi.org/10.7930/J0N29V45>.
- Wake, C., Knott, J., Lippmann, T., Stampone, M., Ballesteros, T., Bjerkle, D., Burakowski, E., Glidden, S., Hosseini-Shakib, I., and Jacobs, J. "New Hampshire Coastal Flood Risk Summary Part 1: Science." *University of New Hampshire*, 2019, <https://doi.org/10.34051/p/2019.1>.
- Walsh, J., Wuebbles, D., Hayhoe, K., Kossin, J., Kunkel, K., Stephens, G., Thorne, P., Vose, R., Wehner, M., Willis, J., Anderson, D., Doney, S., Feely, R., Hennon, P., Kharin, V., Knutson, T., Landerer, F., Lenton, T., Kennedy, J., and Somerville, R. "Ch. 2: Our Changing Climate." *Climate Change Impacts in the United States: The Third National Climate Assessment*, 2014, 19–67, <https://doi.org/10.7930/J0KW5CXT>.
- Walter, D.A., McCobb, T.D., Masterson, J.P., and Fienen, M.N. "Potential effects of sea-level rise on the depth to saturated sediments of the Sagamore and Monomoy flow lenses on Cape Cod, Massachusetts." *U.S. Geological Survey Scientific Investigations Report*, 2016–5058, 2016, 55.
- Wang, X., Huang, G., Liu, J., Li, Z., Zhao, S. "Ensemble projections of regional climatic changes over Ontario, Canada." *Journal of Climate*, 28, 2015, 7327–7346.
- Wang, J., H. Kim, and E.K. Chang. "Changes in Northern Hemisphere Winter Storm Tracks under the Background of Arctic Amplification." *Journal of Climate*, 30, 2017, 3705–3724, <https://doi.org/10.1175/JCLI-D-16-0650.1>.
- Wasko, C., S. Westra, R. Nathan, H.G. Orr, G. Villarini, R. Villalobos Herrera, and H.J. Fowler. "Incorporating climate change in flood estimation guidance." *Philosophical Transactions*, 379(2195), 2021, 1–24.
- Wehner, M.F., Arnold, J.R., Knutson, T., Kunkel, K.E., and LeGrande, A.N. "Droughts, floods, and wildfires." *Climate Science Special Report: Fourth National Climate Assessment*, I, 2017, 231–256, <https://doi.org/10.7930/J0CJ8BNN>.
- Weider, K., and Boutt, D. F. "Heterogeneous water table response to climate revealed by 60 years of ground water data." *Geophysical Research Letters*, 37(24), 2010. <https://doi.org/10.1029/2010GL045561>.
- Wolman, G.M., and Miller, J.P. "Magnitude and frequency of forces in geomorphic processes." *Journal of Geology*, 68, 1960, 54–74. <https://doi.org/10.1086/626637>.
- Wobus, C., Gutmann, E., Jones, R., Rissing, M., Mizukami, N., Lorie, M., ... and Martinich, J. "Climate change impacts on flood risk and asset damages within mapped 100-year floodplains of the contiguous United States." *Natural Hazards and Earth System Sciences*, 17(12), 2017, 2199. <https://doi.org/10.5194/nhess-17-2199-2017>.
- Xu, J., Y. Wang, and Z. Tan. "The Relationship between Sea Surface Temperature and Maximum Intensification Rate of Tropical Cyclones in the North Atlantic." *Journal of the Atmospheric Sciences*, 73, 2016, 4979–4988, <https://doi.org/10.1175/JAS-D-16-0164.1>.
- Yarnell, D.L. *Rainfall Intensity-Frequency Data*. U.S. Department of Agriculture, S04, 1935, 68.
- Yellen, B., Woodruff, J.D., Cook, T.L., and Newton, R.M. "Historically unprecedented erosion from Tropical Storm Irene due to high antecedent precipitation." *Earth Surface Processes and Landforms*, 41(5), 2016, 677–684, https://www.researchgate.net/publication/288918424_Historically_unprecedented_erosion_from_Tropical_Storm_Irene_due_to_high_antecedent_precipitation.
- Zarzycki, C.M. "Projecting Changes in Societally Impactful Northeastern U.S. Snowstorms." *Geophysical Research Letters*, 45, 2018, 12,067–12,075.
- Zhang, Z. and B.A. Colle. "Changes in Extratropical Cyclone Precipitation and Associated Processes during the Twenty-First Century over Eastern North America and the Western Atlantic Using a Cyclone-Relative Approach." *Journal of Climate*, 30, 2017, 8633–8656, <https://doi.org/10.1175/JCLI-D-16-0906.1>.
- Zielinski, G.A., and Keim, B.D. "New England Weather, New England Climate." *UPNE*, 2005.

3. *Temperature*

3.1 KEY FINDINGS

- **Temperature Projections:** This report contains more comprehensive, localized, explicitly probabilistic projections for selected metrics at a regional scale at the county level, from downscaled Coupled Model Intercomparison Project Phase 5 (CMIP5) Global Climate Models (GCMs). While the climate modeling community is currently analyzing Phase 6 (CMIP6) GCMs, of which some models project higher temperatures, the range of potential outcomes in the new generation of climate models is roughly similar.
- **Energy:** Projections are expanded to include a more specific discussion surrounding the likely impacts of increasing energy demand in terms of utility infrastructural impacts and marginal cost of energy demand, which is expected to increase significantly in the summer. Recent weather extremes in California, Texas, and Mississippi make clear the impacts that can be felt, especially by marginalized populations, without significant investment in hardening energy infrastructure for changing climate. Heatwaves pose analogous challenges for the GBRAG region.
- **Public Health:** Boston's heat-induced mortality rate will likely increase in the coming decades, with unequally vulnerable populations and those living in Urban Heat Islands (UHI) facing higher risk. Compared to the 2016 BRAG report, we point to multiple new publications related to the UHI and two new high-resolution datasets that measure the UHI effect, one from the Trust for Public Land (TPL) and one from NOAA. We provide the TPL dataset cropped to the MAPC region available as a supplemental dataset for mitigation investment planning. This report specifically highlights communities in the GBRAG jurisdiction that are socioeconomically vulnerable to UHI effects. The air quality hazards and respiratory disease, adverse birth outcomes, and transmission of vector-borne diseases are also likely to increase under temperature changes.
- **Agriculture and Natural Resources:** Warming winter temperatures and changes in freeze timing throughout the 21st century may pose a threat to New England area agricultural industries (e.g., cranberries and maple syrup) and winter recreation. Projections also suggest a shifting forest composition and increasing spatial range and severity of pest and pathogen species.
- **Infrastructure and Transportation:** Increases in mean and extreme temperatures are expected to present a greater stress to building materials, as well as jeopardize worker safety and rider comfort. Primarily negative economic and practical impacts are expected on multiple modes and aspects of transportation.
- **Economy, Governance, and Society:** Economic impacts of increasing air and marine temperatures notably include probable increased stress to annual incomes of populations and workforce productivity, as well as increasing energy costs, agricultural losses, fisheries, and crime. Mixed impacts on tourism are possible in Massachusetts.

3.2 INTRODUCTION

Projected temperatures and extremes as a function of Greenhouse Gas (GHG) emissions scenarios are arguably the most certain, well-understood, and well-projected climate change metrics at the global scale.

However, uncertainties at the regional scale suggest a range of potential warming scenarios in the Greater Boston area. In this follow-on to the original 2016 Boston Resilience Advisory Group (BRAG) temperature section, we (1) summarize findings that have not changed significantly since this original report, (2) highlight new findings in the context of the original report, (3) expand the impact sectors and geographic coverage to those of the Greater Boston area, and (4) expand the topical coverage to include projections and impacts of air quality given its relationship to temperature. Where possible, this section provides and highlights projections specific to the Greater Boston area, delineating differences between regions (usually counties) when available. When projections for this region are not available in literature, we highlight other relevant projections, insights, and impacts at global or regional scales and put them in the context of the challenges of the Greater Boston area. The primary goal of this section is to provide the best available data and resources to a broad range of potential downstream stakeholders, including those assessing socio-economic vulnerability and aiming to translate data into adaptation and/or mitigation plans. In light of this goal, in many cases we highlight impact sectors that best contextualize the projections included.

3.3 REVIEW OF EXISTING SCIENCE

Aggregate trends and projections

There is strong scientific consensus that anthropogenic emissions are the primary cause of the upward trend in global temperature (Pachauri et al., 2008; Pachauri et al., 2014; Dupigny-Giroux et al., 2018; World Meteorological Organization, 2021). Observed changes in temperature-related signals have been accurately reproduced in historical model simulations and are projected to intensify into the future (Hayhoe, 2007). However, uncertainties in magnitudes of temperature projections remain at the regional and local scales (Stott et al., 2016). At increasing spatio-temporal resolutions, uncertainty increases and trends become progressively more difficult to distinguish from natural variability for near-term horizons (Kumar et al., 2014; Ganguly et al., 2015; Deser et al., 2020). At long-term horizons, projected warming is highly dependent on the trajectory of global emissions, represented in climate models by International Panel on Climate Change (IPCC) Representative Concentration Pathways (RCPs). For example, average temperature in the Northeast is projected to rise by 4 °F by 2050 under RCP4.5 (moderate emissions scenario) and 5.1 °F by 2050 under RCP8.5 (business-as-usual scenario) relative to near present temperatures (1975 to 2005) (Dupigny-Giroux et al., 2018). Uncertainty related to climate models, in terms of their biases and their spread, are the third main source of uncertainty. From 1984 to 2016, sea surface temperatures have increased approximately 2 degrees Fahrenheit in the summer and less than 1 °F over the Northeast Continental shelf, which carries implications for marine ecosystems and economies as well as the increased probability of tropical cyclone landfall (Dailey et al., 2009; BlackRock Investment Institute, 2019).

Extremes and variability

Projections of temperature extremes and variability are generally expected to scale with mean temperature, but not linearly: “small” increases in global temperature can have outsized implications for extremes (e.g., Wang et al., 2017a). Temperature variability and, in particular, extremes generally relate to the most acute impacts in most sectors; as such they will be a heavier focal point in this report compared to changes in average temperature behavior.

Extremes are often measured by exceedances (or shortfalls) of high (and low) thresholds, often over a defined consecutive number of days or nights (e.g., Ganguly et al., 2009; Kharin et al., 2013; Kodra et al., 2014; Perkins-Kirkpatrick and Lewis, 2020). Heat waves may be defined through threshold exceedance, which may be especially useful if the thresholds are meaningful for impacts (e.g., for survival of crops, Schlenker and Roberts, 2009; Asseng et al., 2015) or human comfort levels and mortality (Hajat et al., 2007; Greene et al., 2011; Raymond et al., 2020). A large number of indices have been developed and

used to assess climate conditions in the context of human health (Blazejczyk et al., 2012). This report leverages GCM projections from both classes of approaches. Examples of hot or cold indices that combine variables include heat index (City of Cambridge, 2015) or wind chill (Hajat et al., 2007), which consider temperature with relative humidity or wind speed, respectively. This report leverages multiple classes of metrics and contextualizes them in terms of relevant Greater Boston area impact sectors. Unsurprisingly, at a high level, metrics driven by extreme hot temperature are broadly expected to increase in severity, duration, and frequency (e.g., Ganguly et al., 2009; Dupigny-Giroux et al., 2018).

Cold snaps may similarly consider frost thresholds such as number of frost days (Kodra et al., 2011). Given the acute impact of Nor'easters as well as snow and snowmelt to the region to multiple sectors, characterizing the future of cold extremes and variability is also important. While extreme cold is expected to decrease on average, research projects regional cold snaps as or more intense than those present, even late into the 21st century (Kodra et al., 2011).

3.4 PROJECTIONS

Downscaling methods are used to provide local scale details from climate models run at larger scales. No consensus in the scientific community has accepted a single downscaling method. Rather, different downscaling approaches are suitable for different climate impact applications. The Cambridge Climate Change Vulnerability Assessment (CCVA) applied the Asynchronous Regional Regression Model (ARRM) method to downscale projections to 1/8th degree and was the source of the temperature projections in the BRAG report. Rasmussen et al. (2016) employed Bias Corrected Spatial Disaggregation (BCSD) to downscale projections to the county level. ARRM and BCSD both rely on matching of observed and modeled historical distributions to learn a quantile mapping, which is then applied to future simulations. In the ARRM method, 20-year distributions are matched in an asynchronous mode, meaning values regressed against each other do not necessarily occur at the same time, while distributions for BCSD are constructed from the same month. Rasmussen et al. (2016) additionally provide projections in a probabilistic mode using MAGICC6, which allows a quantification of likely ranges of values at the county level. Finally the method of Localized Constructed Analogs (LOCA) matches the field to be down-scaled with the most similar analog among a set of observed days. LOCA (Pierce et al., 2014) differs from previous methods of constructed analogs by reducing averaging, which results in a more realistic depiction of spatial variation. As a result, LOCA produces better estimates of extreme days than methods like ARRM and BCSD, which may perform better for means than extremes. We used the results of the LOCA method to develop temperature projections for the GBrag.

Table 3.1 synthesizes a wide range of LOCA projected values and metrics relating to temperature and temperature extremes. All data in Table 3.1 were accessed and downloaded via *The Climate Explorer*, a tool built to support the U.S. Climate Resilience Toolkit (Lipschultz et al., 2020). Data from this project were selected for two main reasons. First, from a spatial scale perspective, these downscaled projections are designed to reflect meteorological and hydrological features that vary among the counties in the Metropolitan Area Planning Council (MAPC) study region. Second, the available metrics are relatively comprehensive in service of the key impact sectors highlighted in this section. Projections in Table 3.1 illustrate the two potential futures represented by low (RCP4.5) and high (RCP8.5) global atmospheric GHG concentration pathways, which increasingly diverge toward the late 21st century. Under both pathways, temperature projections indicate increasing numbers of hot days with maximum temperatures greater than 90-, 95-, and 100-degrees Fahrenheit and a reduction in days with below-freezing temperatures. A shift in energy demand will occur with more Cooling- Degree- Days and fewer Heating- Degree- Days.

The data source for Table 3.1 does not treat uncertainty in projections probabilistically. Therefore Dr. Ambarish Karmalkar, a member of the GBrag temperature team, developed county level probabilistic projections by downscaling using the LOCA method temperature values from fourteen carefully selected

CMIP5 models and two pathways of future greenhouse gas (GHG) concentrations RCP4.5 and RCP8.5. The fourteen models were carefully selected from a large ensemble of CMIP5 models based on their ability to provide reliable climate information for the Northeast U.S., while maintaining diversity in future projections consistent with known uncertainties (Karmalkar et al., 2019).

The observed values for the period 1986 to 2015 are derived from the Climate Prediction Center (CPC) Global Temperature dataset. The daily data are available at $0.5^\circ \times 0.5^\circ$ resolution and are provided by the NOAA/OAR/ESRL PSL, Boulder, Colorado, from their website at <https://www.psl.noaa.gov/data/gridded/data.cpc.globaltemp.html>. The data are linearly interpolated to the LOCA grid before computing values for temperature metrics. The relatively lower resolution of the CPC data in comparison to LOCA means that estimates do not fully account for the spatial variability in temperature in the study region.

The projections cited in Table 3.2 below describe the 5th, 17th, 50th (median), 83rd, and 95th percentiles of 30-year means across 14 model projections and across all LOCA grid-points within the country for each RCP. The percentiles are calculated across all grid-points within every county (and not for spatially averaged values) to capture the spatial variability in temperature metrics. Note that the projected values are *not forecasts*, but instead capture a wide range of plausible outcomes consistent with uncertainties in future trajectory of greenhouse gas concentrations and climate modeling.

Table 3.1

Projected changes (degrees Fahrenheit or number of days) for counties covering the GBRAG study regions using LOCA Downscaling from The Climate Data Explorer. (<https://crt-climate-explorer.nemac.org>)

Parameter	County	Baseline		Projections			Projections (change from historical baseline)				Scenario	Source
		1990–2010	2020–2040	2040–2060	2060–2080	2080–2100	2020–2040	2040–2060	2060–2080	2080–2100		
Average Daily Max Temp (°F)	Essex	59.7	62.4	64.3	66.6	68.9	2.6	4.5	6.9	9.1	RCP8.5	1
	Middlesex	59.6	62.6	64.5	66.9	69.1	2.9	4.9	7.3	9.5		
	Suffolk	59.9	62.6	64.5	66.8	69.0	2.7	4.6	7.0	9.2		
	Norfolk	60.2	62.7	64.6	66.9	69.1	2.4	4.4	6.7	8.9		
	Essex	59.7	62.3	63.3	64.2	64.8	2.5	3.6	4.5	5.0	RCP4.5	1
	Middlesex	59.6	62.5	63.6	64.4	65.0	2.8	3.9	4.8	5.3		
	Suffolk	59.9	62.5	63.6	64.4	65.0	2.6	3.7	4.6	5.1		
	Norfolk	60.2	62.6	63.7	64.5	65.1	2.4	3.5	4.3	4.8		
Average Daily Min Temp (°F)	Essex	39.5	42.6	44.5	47.0	49.3	3.0	5.0	7.4	9.8	RCP8.5	1
	Middlesex	38.3	41.1	43.1	45.5	47.9	2.7	4.7	7.2	9.5		
	Suffolk	42.4	44.6	46.6	49.0	51.3	2.2	4.1	6.5	8.8		
	Norfolk	40.5	42.5	44.4	46.9	49.2	2.0	3.9	6.4	8.6		
	Essex	39.5	42.4	43.6	44.5	45.1	2.9	4.0	5.0	5.5	RCP4.5	1
	Middlesex	38.3	40.9	42.1	43.0	43.6	2.6	3.7	4.7	5.2		
	Suffolk	42.4	44.5	45.6	46.5	47.1	2.1	3.2	4.1	4.7		
	Norfolk	40.5	42.4	43.5	44.4	45.0	1.8	2.9	3.9	4.5		

Table 3.1 (continued)

Projected changes (degrees Fahrenheit or number of days) for counties covering the GBRAG study regions using LOCA Downscaling from The Climate Data Explorer.

Parameter	County	Baseline	Projections				Projections (change from historical baseline)				Scenario	Source
		1990–2010	2020–2040	2040–2060	2060–2080	2080–2100	2020–2040	2040–2060	2060–2080	2080–2100		
Days w/ max > 90 (°F)	Essex	8.0	17.9	28.1	43.0	59.0	9.8	20.1	35.0	51.0	RCP8.5	1
	Middlesex	8.7	21.3	33.7	50.2	66.7	12.6	25.0	41.5	58.1		
	Suffolk	9.5	20.7	31.7	46.9	62.5	11.1	22.2	37.4	53.0		
	Norfolk	8.4	19.3	30.8	46.9	62.9	10.9	22.5	38.5	54.5		
	Essex	8.0	17.4	22.7	27.9	29.9	9.4	14.7	19.8	21.9	RCP4.5	1
	Middlesex	8.7	20.8	26.8	32.8	35.3	12.1	18.1	24.1	26.6		
	Suffolk	9.5	20.2	26.0	31.2	33.9	10.7	16.5	21.7	24.3		
	Norfolk	8.4	18.8	24.9	30.3	33.0	10.5	16.6	21.9	24.6		
Days w/ max > 95 (°F)	Essex	1.0	4.2	8.7	17.4	28.9	3.3	7.7	16.5	27.9	RCP8.5	1
	Middlesex	1.2	5.5	11.4	22.6	35.7	4.3	10.3	21.4	34.5		
	Suffolk	1.4	5.4	11.1	21.5	32.7	4.0	9.7	20.1	31.3		
	Norfolk	1.3	4.6	9.6	20.1	32.0	3.3	8.3	18.8	30.7		
	Essex	1.0	4.0	6.1	8.4	9.4	3.1	5.1	7.5	8.5	RCP4.5	1
	Middlesex	1.2	5.2	7.7	10.8	12.2	4.0	6.6	9.6	11.0		
	Suffolk	1.4	5.2	8.1	11.0	12.3	3.8	6.7	9.6	10.9		
	Norfolk	1.3	4.4	6.8	9.4	10.8	3.1	5.5	8.1	9.5		
Days w/ max > 100 (°F)	Essex	0.0	0.5	1.7	4.9	10.2	0.5	1.7	4.9	10.2	RCP8.5	1
	Middlesex	0.0	0.8	2.5	7.1	14.0	0.8	2.5	7.1	14.0		
	Suffolk	0.0	0.8	2.5	6.8	13.0	0.8	2.5	6.8	13.0		
	Norfolk	0.1	0.6	1.9	5.8	11.7	0.5	1.9	5.8	11.7		
	Essex	0.0	0.5	0.8	1.5	1.9	0.5	0.8	1.5	1.9	RCP4.5	1
	Middlesex	0.0	0.7	1.3	2.2	2.8	0.7	1.3	2.2	2.8		
	Suffolk	0.0	0.8	1.5	2.4	2.9	0.8	1.5	2.4	2.9		
	Norfolk	0.1	0.5	1.1	1.8	2.3	0.5	1.0	1.8	2.2		
Days w/ max < 32 (°F)	Essex	23.3	15.0	10.0	5.5	3.0	-8.4	-13.3	-17.9	-20.3	RCP8.5	1
	Middlesex	27.2	17.8	12.5	7.5	4.5	-9.4	-14.6	-19.7	-22.7		
	Suffolk	21.4	14.4	10.0	5.8	3.4	-7.0	-11.4	-15.6	-18.0		
	Norfolk	21.1	14.9	10.3	6.0	3.4	-6.2	-10.8	-15.2	-17.8		
	Essex	23.3	15.6	12.5	10.0	9.0	-7.7	-10.9	-13.3	-14.4	RCP4.5	1
	Middlesex	27.2	18.4	15.2	12.6	11.4	-8.8	-12.0	-14.6	-15.7		
	Suffolk	21.4	14.8	12.2	10.1	9.1	-6.6	-9.2	-11.3	-12.3		
	Norfolk	21.1	15.3	12.6	10.5	9.4	-5.8	-8.5	-10.7	-11.7		
Cooling degree days	Essex	595.5	916.0	1142.8	1467.0	1813.9	320.4	547.3	871.4	1218.4	RCP8.5	1
	Middlesex	583.7	903.7	1146.1	1485.3	1837.4	320.1	562.5	901.6	1253.8		
	Suffolk	720.7	1050.2	1310.6	1665.2	2027.1	329.5	590.0	944.5	1306.4		
	Norfolk	651.2	941.9	1185.6	1528.2	1874.8	290.7	534.4	877.0	1223.6		
	Essex	595.5	900.0	1023.8	1138.4	1191.8	304.5	428.2	542.9	596.3	RCP4.5	1
	Middlesex	583.7	885.2	1011.3	1132.5	1190.7	301.6	427.7	548.8	607.0		
	Suffolk	720.7	1034.7	1176.3	1299.0	1366.4	314.0	455.7	578.4	645.7		
	Norfolk	651.2	924.8	1059.3	1177.2	1240.3	273.6	408.1	526.0	589.1		

Table 3.1 (continued)

Projected changes (degrees Fahrenheit or number of days) for counties covering the GBrag study regions using LOCA Downscaling from The Climate Data Explorer.

Parameter	County	Baseline	Projections					Projections (change from historical baseline)					Scenario	Source
		1990–2010	2020–2040	2040–2060	2060–2080	2080–2100	2020–2040	2040–2060	2060–2080	2080–2100	2020–2040	2040–2060		
Heating degree days	Essex	6198.7	5479.3	4992.7	4439.8	3950.9	-719.4	-1206.0	-1758.9	-2247.8	RCP8.5	1	RCP8.5	1
	Middlesex	6421.5	5704.6	5213.4	4668.0	4201.6	-716.8	-1208.0	-1753.5	-2219.8				
	Suffolk	5771.4	5197.1	4750.1	4233.9	3778.2	-574.3	-1021.3	-1537.5	-1993.1				
	Norfolk	5985.7	5466.1	4996.6	4463.9	3997.0	-519.7	-989.2	-1521.8	-1988.8				
	Essex	6198.7	5507.4	5225.0	5005.9	4856.0	-691.3	-973.7	-1192.8	-1342.7	RCP4.5	1	RCP4.5	1
	Middlesex	6421.5	5730.9	5446.4	5230.3	5086.7	-690.6	-975.1	-1191.2	-1334.7				
	Suffolk	5771.4	5214.2	4959.9	4761.9	4621.8	-557.2	-811.4	-1009.5	-1149.6				
	Norfolk	5985.7	5485.5	5214.6	5010.6	4866.1	-500.3	-771.1	-975.1	-1119.6				
Growing degree days	Essex	2646.2	3226.4	3621.7	4150.9	4697.5	580.1	975.5	1504.7	2051.2	RCP8.5	1	RCP8.5	1
	Middlesex	2601.5	3185.6	3596.6	4133.8	4668.9	584.1	995.1	1532.3	2067.4				
	Suffolk	2896.0	3474.1	3895.4	4446.9	5001.5	578.1	999.4	1550.9	2105.4				
	Norfolk	2767.6	3275.6	3685.6	4226.8	4763.4	508.1	918.0	1459.2	1995.8				
	Essex	2646.2	3204.6	3426.2	3612.1	3718.8	558.3	779.9	965.9	1072.6	RCP4.5	1	RCP4.5	1
	Middlesex	2601.5	3161.7	3385.0	3576.2	3683.1	560.2	783.5	974.7	1081.6				
	Suffolk	2896.0	3453.2	3688.6	3877.8	3997.8	557.2	792.5	981.8	1101.7				
	Norfolk	2767.6	3253.7	3486.9	3672.0	3787.3	486.1	719.3	904.5	1019.7				

Source: The Climate Data Explorer (<https://crt-climate-explorer.nemac.org/>), using methodology from Pierce et al. 2014

Table 3.2

County Level Probabilistic LOCA Downscaled Projections from Karmalkar.

RCP4.5

Average Temperature (Annual)

	Obs. Baseline (°F)	Project RCP4.5 (abs, °F)																			
Counties	2000s (1986–2015)	2030s (2016–2045)					2050s (2036–2065)					2070s (2056–2085)					2080s (2070–2099)				
Counties/Percentile		5	17	50	83	95	5	17	50	83	95	5	17	50	83	95	5	17	50	83	95
Essex	49.7	50.9	51.5	52.4	53.3	53.7	51.5	52.4	53.4	54.7	55.3	52.1	52.8	54.3	55.6	56.7	52.2	52.9	54.5	56.3	57.2
Middlesex	49.3	49.6	50.7	51.8	52.9	53.3	50.4	51.5	52.8	54.2	54.9	50.9	52.0	53.6	55.1	56.2	51.2	52.2	53.9	55.8	56.8
Norfolk	50.2	50.8	51.4	52.4	53.4	54.1	51.5	52.3	53.5	54.7	55.6	51.8	52.7	54.3	55.7	56.7	52.1	53.0	54.7	56.5	57.3
Suffolk	50.1	52.2	52.7	53.5	54.2	54.6	52.6	53.5	54.5	55.7	56.1	53.1	53.8	55.3	56.4	57.8	53.4	53.9	55.5	57.2	58.2

RCP8.5

	Obs. Baseline (°F)	Project RCP8.5 (abs, °F)																			
Counties	2000s (1986–2015)	2030s (2016–2045)					2050s (2036–2065)					2070s (2056–2085)					2080s (2070–2099)				
Counties/Percentile		5	17	50	83	95	5	17	50	83	95	5	17	50	83	95	5	17	50	83	95
Essex	49.7	51.1	51.9	52.8	53.6	54.2	52.1	53.5	54.6	55.8	56.7	53.6	55.0	56.7	58.5	60.3	54.8	56.0	58.4	60.5	62.4
Middlesex	49.3	49.9	51.0	52.3	53.2	53.8	51.3	52.6	54.0	55.3	56.3	52.7	54.2	56.1	58.1	60.0	53.9	55.3	57.8	60.1	62.1
Norfolk	50.2	51.0	51.8	52.7	53.7	54.3	52.4	53.3	54.6	55.9	56.8	53.7	54.8	56.8	58.9	60.3	54.8	55.8	58.6	60.8	62.1
Suffolk	50.1	52.2	53.0	53.9	54.6	55.1	53.1	54.5	55.7	56.7	57.5	54.5	55.9	57.9	59.4	61.1	55.7	57.0	59.4	61.4	63.0

Table 3.2 (continued)**County Level Probabilistic LOCA Downscaled Projections from Karmalkar.**

RCP4.5

Minimum Temperature (Annual)

Counties	Obs. Baseline (°F)	Project RCP4.5 (abs, °F)																				Project RCP4.5 (abs, °F)				
		2000s (1986–2015)					2030s (2016–2045)					2050s (2036–2065)					2070s (2056–2085)					2080s (2070–2099)				
Counties/Percentile		5	17	50	83	95	5	17	50	83	95	5	17	50	83	95	5	17	50	83	95	5	17	50	83	95
Essex	40.7	40.4	41.3	42.6	43.9	44.6	41.2	42.2	43.7	45.2	46.2	41.7	42.7	44.5	46.1	47.1	42.0	43.0	44.8	46.8	48.0					
Middlesex	39.6	38.4	39.7	41.1	42.4	43.1	39.3	40.6	42.2	43.8	44.9	39.9	41.2	42.9	44.7	46.0	40.2	41.5	43.3	45.3	46.8					
Norfolk	40.7	39.6	40.6	42.3	44.0	45.0	40.5	41.6	43.4	45.2	46.5	40.9	42.2	44.1	46.3	47.6	41.2	42.4	44.5	46.8	48.3					
Suffolk	40.5	42.7	43.3	44.3	45.5	46.5	43.5	44.0	45.4	46.8	47.8	43.7	44.5	46.3	47.7	48.9	43.9	44.9	46.6	48.4	49.4					

RCP8.5

Counties	Obs. Baseline (°F)	Project RCP8.5 (abs, °F)																				Project RCP8.5 (abs, °F)				
		2000s (1986–2015)					2030s (2016–2045)					2050s (2036–2065)					2070s (2056–2085)					2080s (2070–2099)				
Counties/Percentile		5	17	50	83	95	5	17	50	83	95	5	17	50	83	95	5	17	50	83	95	5	17	50	83	95
Essex	40.7	40.8	41.7	43.0	44.2	45.0	42.2	43.3	44.8	46.3	47.5	43.9	45.0	46.9	49.2	51.1	45.1	46.3	48.6	51.2	53.2					
Middlesex	39.6	38.9	40.1	41.6	42.7	43.7	40.4	41.7	43.4	44.9	46.2	42.0	43.5	45.5	47.7	49.8	43.3	44.7	47.1	49.6	51.9					
Norfolk	40.7	40.1	40.9	42.6	44.4	45.4	41.5	42.7	44.5	46.4	47.6	43.0	44.4	46.7	49.3	50.8	44.2	45.6	48.2	51.1	52.8					
Suffolk	40.5	42.9	43.7	44.6	46.0	46.7	44.5	45.2	46.6	47.9	49.0	45.8	46.8	48.7	51.0	52.1	46.9	47.8	50.4	53.1	54.1					

RCP4.5

Maximum Temperature (Annual)

Counties	Obs. Baseline (°F)	Project RCP4.5 (abs, °F)																				Project RCP4.5 (abs, °F)				
		2000s (1986–2015)					2030s (2016–2045)					2050s (2036–2065)					2070s (2056–2085)					2080s (2070–2099)				
Counties/Percentile		5	17	50	83	95	5	17	50	83	95	5	17	50	83	95	5	17	50	83	95	5	17	50	83	95
Essex	58.8	60.7	61.4	62.2	63.2	63.5	61.2	62.1	63.2	64.6	64.9	61.7	62.6	64.1	65.4	66.5	61.9	62.7	64.4	66.1	66.9					
Middlesex	59.0	60.6	61.5	62.4	63.5	63.9	61.2	62.3	63.5	64.8	65.2	61.8	62.7	64.3	65.6	66.6	62.0	62.8	64.6	66.4	67.2					
Norfolk	59.7	61.2	61.7	62.6	63.4	63.9	61.6	62.5	63.7	64.8	65.2	62.1	62.9	64.4	65.5	66.7	62.3	63.0	64.6	66.3	67.2					
Suffolk	59.8	61.1	61.7	62.6	63.5	63.8	61.5	62.4	63.5	64.8	65.3	62.1	62.8	64.3	65.6	66.4	62.2	62.9	64.6	66.4	66.9					

RCP8.5

Counties	Obs. Baseline (°F)	Project RCP8.5 (abs, °F)																				Project RCP8.5 (abs, °F)				
		2000s (1986–2015)					2030s (2016–2045)					2050s (2036–2065)					2070s (2056–2085)					2080s (2070–2099)				
Counties/Percentile		5	17	50	83	95	5	17	50	83	95	5	17	50	83	95	5	17	50	83	95	5	17	50	83	95
Essex	58.8	60.7	61.7	62.7	63.5	63.9	61.8	63.3	64.4	65.7	66.4	62.9	64.7	66.5	68.4	70.1	64.0	65.7	68.0	70.4	72.0					
Middlesex	59.0	60.8	61.8	62.9	63.7	64.2	61.9	63.4	64.7	65.9	66.6	63.0	64.9	66.8	68.7	70.2	64.1	66.0	68.4	70.7	72.2					
Norfolk	59.7	61.2	62.2	63.0	63.7	64.1	62.1	63.5	64.9	65.9	66.4	63.1	65.0	66.9	68.7	70.0	64.1	66.0	68.6	70.6	71.7					
Suffolk	59.8	61.2	62.1	62.9	63.7	64.2	62.2	63.6	64.7	65.8	66.5	63.3	64.8	66.7	68.7	70.2	64.4	65.8	68.4	70.7	72.0					

Table 3.2 (continued)**County Level Probabilistic LOCA Dowscaled Projections from Karmalkar.**

RCP4.5

Number of Days with $T_{max} > 90^{\circ}\text{F}$ (Annual)

	Obs. Baseline (days)	Project RCP4.5 (days)																			
Counties	2000s (1986–2015)	2030s (2016–2045)					2050s (2036–2065)					2070s (2056–2085)					2080s (2070–2099)				
Counties/Percentile		5	17	50	83	95	5	17	50	83	95	5	17	50	83	95	5	17	50	83	95
Essex	8.7	9.9	12.5	16.8	21.6	25.0	11.8	15.5	21.8	28.4	31.3	14.4	17.3	25.6	34.4	39.7	14.9	17.8	28.3	38.9	44.5
Middlesex	9.2	12.0	15.2	20.1	25.8	29.7	14.2	18.3	25.9	33.0	36.5	17.2	20.5	30.3	40.4	46.0	17.4	20.9	33.0	45.4	50.4
Norfolk	9.9	10.7	14.0	18.4	22.8	27.2	13.1	17.0	24.3	30.6	35.1	15.8	18.8	28.0	37.8	44.6	16.4	19.4	31.1	41.9	49.4
Suffolk	10.0	12.8	15.7	19.9	24.4	27.9	15.4	18.6	25.0	32.2	35.8	17.3	20.4	28.9	38.4	46.3	17.5	21.5	32.2	43.2	49.1

RCP8.5

Number of Days with $T_{max} > 90^{\circ}\text{F}$ (Annual)

	Obs. Baseline (days)	Project RCP8.5 (days)																			
Counties	2000s (1986–2015)	2030s (2016–2045)					2050s (2036–2065)					2070s (2056–2085)					2080s (2070–2099)				
Counties/Percentile		5	17	50	83	95	5	17	50	83	95	5	17	50	83	95	5	17	50	83	95
Essex	8.7	10.7	14.3	18.4	23.1	25.7	15.4	22.3	29.1	37.9	42.8	17.9	29.6	44.9	59.2	66.5	23.4	35.8	58.4	73.9	81.4
Middlesex	9.2	13.4	17.6	22.1	26.8	30.6	17.6	26.1	34.7	43.4	50.5	19.8	34.8	52.3	65.3	74.1	26.7	42.2	67.4	81.0	88.0
Norfolk	9.9	12.2	16.5	19.7	24.2	28.7	15.9	25.2	32.4	40.7	46.8	18.3	32.6	48.9	62.7	69.9	25.4	40.7	63.8	76.8	83.4
Suffolk	10.0	15.2	17.4	20.7	25.6	29.3	20.3	25.3	33.0	42.1	49.1	23.7	32.9	49.1	62.3	73.3	29.1	38.1	63.9	79.6	86.5

RCP4.5

Number of Days with $T_{max} > 95^{\circ}\text{F}$ (Annual)

	Obs. Baseline (days)	Project RCP4.5 (days)																			
Counties	2000s (1986–2015)	2030s (2016–2045)					2050s (2036–2065)					2070s (2056–2085)					2080s (2070–2099)				
Counties/Percentile		5	17	50	83	95	5	17	50	83	95	5	17	50	83	95	5	17	50	83	95
Essex	1.2	1.8	2.3	3.6	5.8	7.3	1.9	3.2	5.5	8.5	10.2	2.8	4.0	6.7	11.5	16.3	3.0	4.3	8.0	13.7	19.2
Middlesex	1.2	2.3	3.1	4.6	7.5	9.1	2.6	4.0	6.6	10.6	12.4	3.7	4.9	8.6	15.2	19.0	4.0	5.5	10.1	18.0	22.7
Norfolk	1.5	2.0	2.8	4.1	6.2	7.8	2.3	3.8	6.2	9.4	11.6	3.3	4.4	7.7	12.7	17.4	3.7	4.8	9.1	15.7	21.1
Suffolk	1.5	2.7	3.2	5.0	6.9	8.7	3.0	4.6	7.1	11.1	13.2	4.4	5.0	9.1	15.0	19.7	4.5	5.6	10.9	18.7	23.7

RCP8.5

Number of Days with $T_{max} > 95^{\circ}\text{F}$ (Annual)

	Obs. Baseline (days)	Project RCP8.5 (days)																			
Counties	2000s (1986–2015)	2030s (2016–2045)					2050s (2036–2065)					2070s (2056–2085)					2080s (2070–2099)				
Counties/Percentile		5	17	50	83	95	5	17	50	83	95	5	17	50	83	95	5	17	50	83	95
Essex	1.2	1.7	2.8	4.4	6.6	8.4	3.1	5.5	8.5	14.7	18.0	4.1	8.6	17.1	30.9	35.7	6.2	11.8	26.8	43.0	50.1
Middlesex	1.2	2.3	3.7	5.5	8.4	10.1	4.1	7.3	11.2	17.8	22.4	5.2	11.0	22.4	35.7	42.6	7.8	15.5	34.1	49.7	57.6
Norfolk	1.5	2.1	3.3	4.7	6.9	8.7	3.6	6.7	9.7	15.7	19.1	4.4	9.9	20.1	32.8	37.7	7.0	14.4	31.0	44.8	51.4
Suffolk	1.5	2.9	4.0	5.5	8.0	9.8	5.1	7.4	10.9	17.8	22.0	7.3	11.1	21.1	31.5	41.5	10.2	14.9	31.6	44.9	55.0

Table 3.2 (continued)**County Level Probabilistic LOCA Dowscaled Projections from Karmalkar.**

RCP4.5

Number of Days with $T_{max} > 100^{\circ}\text{F}$ (Annual)

Counties	Obs. Baseline (days)	Project RCP4.5 (days)															2070s (2056–2085)			2080s (2070–2099)		
		2000s (1986–2015)					2030s (2016–2045)					2050s (2036–2065)					2070s (2056–2085)			2080s (2070–2099)		
Counties/Percentile		5	17	50	83	95	5	17	50	83	95	5	17	50	83	95	5	17	50	83	95	
Essex	0.0	0.0	0.1	0.3	0.9	1.4	0.1	0.2	0.6	1.6	2.4	0.2	0.3	0.8	2.2	5.3	0.2	0.4	1.1	2.6	6.9	
Middlesex	0.0	0.1	0.2	0.5	1.2	1.9	0.1	0.3	0.8	2.3	3.3	0.3	0.5	1.1	3.8	6.7	0.4	0.6	1.5	4.4	8.8	
Norfolk	0.1	0.1	0.2	0.4	0.9	1.2	0.1	0.4	0.8	1.8	2.7	0.3	0.5	1.0	2.8	5.1	0.4	0.5	1.3	4.0	7.1	
Suffolk	0.1	0.2	0.3	0.6	1.1	1.6	0.2	0.5	1.0	2.3	3.5	0.5	0.6	1.3	3.7	6.8	0.5	0.8	1.9	4.6	8.5	

RCP8.5

Counties	Obs. Baseline (days)	Project RCP8.5 (days)															2070s (2056–2085)			2080s (2070–2099)		
		2000s (1986–2015)					2030s (2016–2045)					2050s (2036–2065)					2070s (2056–2085)			2080s (2070–2099)		
Counties/Percentile		5	17	50	83	95	5	17	50	83	95	5	17	50	83	95	5	17	50	83	95	
Essex	0.0	0.0	0.2	0.5	1.1	1.8	0.2	0.7	1.4	4	6.1	0.5	1.3	3.7	10.3	17.1	0.9	2.0	8.2	19.1	26.9	
Middlesex	0.0	0.1	0.3	0.7	1.6	2.6	0.3	1.1	2.0	5.7	7.6	0.6	2.0	5.7	15.2	20.5	1.0	3.2	11.1	25.1	31.4	
Norfolk	0.1	0.1	0.3	0.6	1.1	1.8	0.2	1.1	1.8	4.5	6.2	0.5	1.6	4.8	12.1	17.2	0.8	2.6	9.6	19.9	26.0	
Suffolk	0.1	0.2	0.4	0.7	1.4	2.3	0.5	1.2	2.2	5.5	7.5	1.0	2.3	5.8	14.1	19.6	1.5	3.5	10.4	21.4	29.5	

3.5 OPEN QUESTIONS AND DATA GAPS

While the temperature changes are a relatively well-understood aspect of climate change, irreducible uncertainties remain in near-term projections due to natural variability and in long-term projections due to unknown future emissions and development pathways, plus structural uncertainties related to differences across climate models.

Projections referenced in this report are largely generated from CMIP5 era climate simulations. Preliminary analysis of the next generation of climate models (CMIP6) suggests climate sensitivity, or surface warming in response to doubling CO₂ concentration, is higher in CMIP6 models: 1.8 to 5.6 K across 27 models rather than 1.5 to 4.5 K (Zelinka et al., 2020). However, there is active scientific discussion about how to interpret these and how plausible higher-end climate sensitivities are. Benchmarking against paleoclimate records suggests that this elevated CMIP6 sensitivity may be incompatible with geological evidence (Zhu et al., 2020). Assessment and interpretation of CMIP6 projections are active areas of research. Additionally, trends in the higher-order statistics of temperature, such as autocorrelation, are relatively less well described than changes in mean. Increasing trends in temporal autocorrelation of air temperature may result in increasingly persistent runs of unfavorable conditions, such as heat waves (Di Cecco and Gouhier, 2018).

While this section focuses on projections and impacts of temperature change, complex interactions with other climate variables are also important to consider. For example, coastal communities like those in the Boston area could experience drinking water risk into the future, as the combination of drought and sea level rise could impact ground and surface water resources, respectively (e.g., Roehl et al., 2013). Many stakeholders, especially those seeking climate adaptation solutions with estimable cost-risk tradeoffs, would be best equipped with probabilistic climate projections rather than simply best estimates. With several exceptions, these rarely exist as data, tools, or in literature.

3.6 IMPACT SECTORS: ENERGY

Climate projections for a large number of temperature-derived metrics are shown in the next section and are connected to the impact sectors discussed in the following subsections. The potential for devastating impacts of weather extremes that utilities are not prepared for have been made clear by recent megafires and heatwaves in California as well as 2021's extreme winter storm Uri in Texas and Mississippi. All of these events disproportionately impacted marginalized communities (Davies et al., 2018; Ura and Garnam, 2021; Diaz and Vance, 2021) and have collectively exacted billions in losses (Smith, 2020; Wood, 2021). Like the rest of the U.S., the Greater Boston area's energy infrastructure has been constructed to deal with historical climate and as such heatwaves pose an analogous challenge for the GBRAG region, threatening especially underserved, at risk, and marginalized neighborhoods such as those highlighted in Stawasz et al. (2019).

Heating and cooling

One of the primary impact sectors of focus in the original temperature section of the BRAG report was energy. In that report, the key metrics Heating and Cooling Degree Days (HDD and CDD) were highlighted given near linear relationships with average daily temperature as well as their prevalence in estimating per capita energy demand in practice. As a refresher, HDD and CDD (Amato et al., 2005; Petri and Caldeira, 2015) are measures that relate to energy usage for climate control for cold or hot weather, respectively. Typically, a balance point temperature is defined as the temperature above which cooling takes place and below which heating takes place. It is standard practice to set 65 °F (18.3 °C) as the balance point temperature to allow for comparisons across time or space, holding the reference temperature constant (e.g., Petri & Caldeira, 2015). In reality, however, heating and cooling are adjusted gradually within ranges around separate balance points for cold and hot conditions (Amato et al., 2005), and different places exhibit different temperature sensitivities. For example, one study (Amato et al., 2005) estimated balance point temperatures specifically in metro Boston for electricity consumption in the residential and commercial sectors of 60 °F (15.6 °C) and 55 °F (12.8 °C), respectively, owing to adaptation of the building stock, proliferation of air conditioning, and behavioral parameters. Longer and hotter periods associated with climate change are responsible for increasing CDD and decreasing HDD (Alola et al., 2019). Table 3.1 provides these projections as well as others provided by The Climate Explorer (Lipschultz et al., 2020).

Electricity demand

We expand on this projection and discuss implications in terms of increasing energy expenditure. Using RCP8.5 (worst-case-scenario), Veliz et al. (2017) projects that electricity expenses for residential and commercial customers in Massachusetts aggregated over three load zones are projected to increase by ~\$5.9 to 6 billion and \$5 to 5.1 billion, respectively, between 2013 and 2057-centered (2044 to 2070) climatology. In total, these extra costs would be a 12% increase for residential customers and 9.3% increase for commercial customers. Increasingly electrified cars and buildings are also expected to increase electricity's share in total energy demand as many fossil fuel technologies are phased out in the coming decades (Fox-Penner, 2020). An increase in electricity demand not only leads to higher individual expenditures for consumers and businesses, but it can also shift the market equilibrium price of electricity given that it drives the need to utilize more expensive peak energy sources more frequently (Veliz et al., 2017). In some areas of the country, Texas for example (DiSavino, 2015), spikes in demand have already been observed during acute heatwaves and have incurred significant utility-side electricity generation costs. On the other hand, demand for heating is expected to decrease owing to warmer winters, potentially alleviating some winter season pressure for utilities in the Greater Boston area.

3.7 IMPACT SECTORS: PUBLIC HEALTH

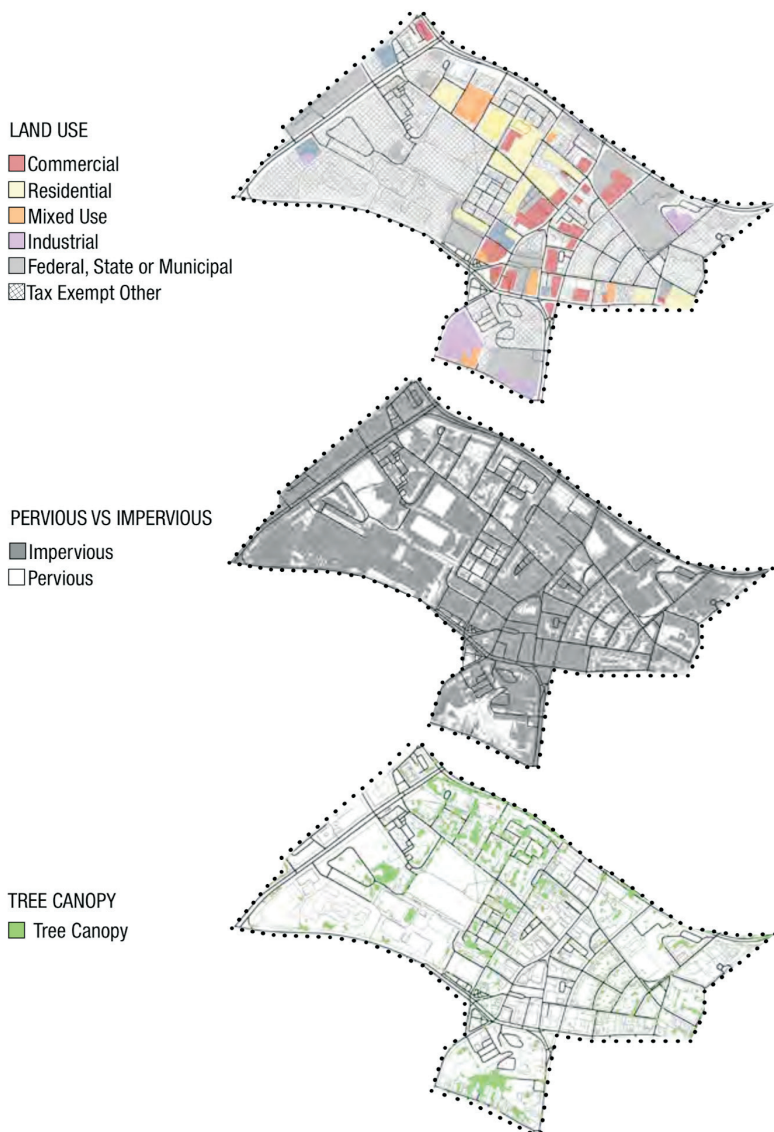
The temperature section of the first BRAG report also focused on public health, primarily on mortality, referencing two studies (Greene et al., 2011; Petkova et al., 2013). In this iteration, we expand slightly on mortality projections, referencing more literature. In addition, we widen the scope of the public health discussion to include respiratory and cardiovascular illnesses, birth outcomes, and vector-borne diseases.

Heat

Temperature as well as humidity, cloudiness, and wind conditions can collectively characterize the air conditions that are associated with public health concerns and mortality (Greene et al., 2011). A new study suggests that, globally, between 20.5 to 76.3% of warm season heat-related mortalities from 1991 to 2018 can be attributed to climate change (Vicedo-Cabrera et al., 2021). Petkova et al. (2013) estimate that Boston's heat-induced mortality rate may triple over the next three decades. One recent study (Greene et al., 2011) developed projections for summertime Excessive Heat Events (EHEs) specifically for Boston among a collection of other cities in the U.S. The study's projections reflect that, rather than responding in isolation to individual weather elements (e.g., maximum temperature), human health (mortality) is affected by the simultaneous interactions from a combination of meteorological conditions (e.g., temperature, humidity, cloud cover, and wind speed). As such, EHEs are defined based on combinations of weather elements which contribute to increased mortality. In comparison to an annual average of 11 EHE days between 1975 and 1995, Greene projected 51 EHE days annually by mid-century (2045 to 2055) under a high-emissions scenario. Daily minimum temperatures and the length of heatwaves are as or more important than daily maximum temperatures, as human physiology cannot endure extended high temperatures without cool breaks.

Another recent initiative, which examined Greater Boston's vulnerability to extreme heat, described the heightened health risk where heat waves are historically rare and populations have not assimilated heat-adaptive behaviors (Stawasz et al., 2019). Unequally vulnerable populations, including the young, elderly, and those experiencing poverty, also face higher risk. Stawasz et al., (2019) focuses on four key communities in the Boston metro area exposed to urban heat islands (UHI): East Boston, Lower Roxbury, Somerville, and Chelsea/Everett. The report notes that the human and economic consequences of *not* investing in addressing the UHI in these communities are expected to exponentially outweigh the financial costs of mitigation. These sites were chosen given that all four are currently undergoing significant redevelopment, offering a window of opportunity for simultaneously mitigating the UHI effect. In addition, each neighborhood hosts a large percentage of at-risk and marginalized populations that are all experiencing soaring housing costs as well as growing inequality, gentrification, poverty, and unemployment—all of which accelerated in the wake of COVID-19. (The same populations devastated by the pandemic tend to live in UHI hot spots, showing the multiplicative toll of joint disasters on at-risk communities, highlighted by this year's coincident heat in Southern California (Colliver and McCaskill, 2021)). For each neighborhood, Stawasz et al., (2019) provides high resolution spatial detail on current land use, impervious surface cover, tree canopy cover, and mitigation design proposals for each neighborhood. For convenience, Figures 3.1 through 3.3 highlight these details for Lower Roxbury: Figure 3.1 shows detailed land cover, impervious surface, and tree canopy cover; Figure 3.2 covers key socioeconomics and demographics; Figure 3.3 lays out a UHI design proposal. We strongly recommend stakeholders downstream of this section to refer to Stawasz et al., (2019) for more: <https://ulidigitalmarketing.blob.core.windows.net/ulidcnc/2019/11/Living-With-Heat-Report-for-web.pdf>.

We have identified two other UHI datasets as well. The first, highlighted in Figure 3.4, is a UHI score constructed by the Trust for Public Land at a 30-meter resolution ultimately derived from 2019 and 2020 summer NASA LANDSAT data. The score ranges from 1 to 5 based on temperature anomalies, with

Figure 3.1**Land Cover, Impervious Surface, and Tree Canopy Cover for Lower Roxbury, from Stawasz et al., 2019.****LAND USE**

Nearly half of the Lower Roxbury project site is dedicated to Tax-Exempt land uses. This means that the land is dedicated open space, transportation, State or City facilities including schools, higher education, and the Boston Housing Authority. The remainder of the site is residential and commercial with few industrial uses. Tax-Exempt property is dedicated to providing a mix of services to residents, visitors, and workers in the neighborhood and its surroundings, making accessibility an important focus.

IMPERVIOUS GROUND COVERAGE

One major contributor to urban heat island is the dark, impervious ground cover that retains and slowly releases heat, offering little opportunity for cooling. The existing conditions in Lower Roxbury offer many opportunities to address this as a majority of the site is impervious ground coverage.

TREE CANOPY AND SHADING

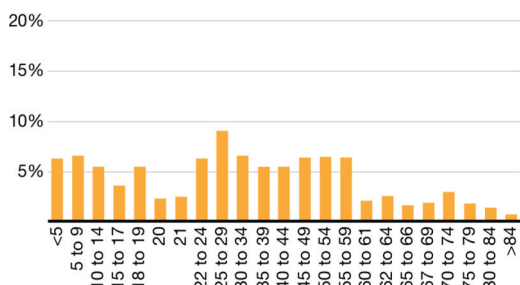
Canopy coverage in Lower Roxbury is mainly concentrated in or at the boundary of residential areas. The main commercial and transit center of Dudley Square lacks any significant tree coverage and could prove an opportunity connecting the pockets of tree canopy.

LEFT Site Diagrams

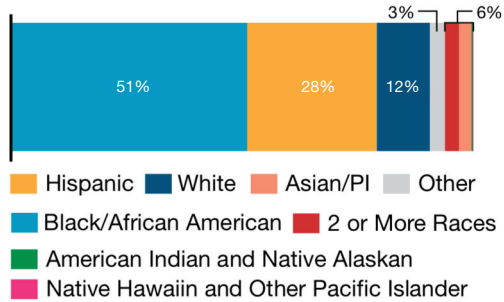
Image credit: Arrowstreet

Data source: Trust for Public Land, Climate Smart Cities

1 being a relatively mild heat area (slightly above the mean for the city), and 5 being a severe heat area (significantly above the mean for the city). See TPL (n.d.) for details on this score. We have cropped the TPL dataset to the four MAPC counties and provide it in “geotiff” format as a supplemental resource (available upon request), along with tract and county boundaries; the former is useful for analyzing needs for investment in mitigation at a community level. In summer 2021, NOAA mapped UHI in cities across the U.S. (<https://nibhis.cpo.noaa.gov/Urban-Heat-Islands/Mapping-Campaigns/Campaign-Cities>), with the Boston metro area among them; results are forthcoming. We also point the reader to the 2019 UHI mapping campaign led by Boston’s Museum of Science (MoS; see CAPA Strategies, 2019 for details). Compared to the TPL scoring data, the MoS-led campaign’s results are more detailed because they include information collected by remote sensors on the

Figure 3.2**Key Socioeconomics and Demographics for Lower Roxbury, from Stawasz et al., 2019.****Age**

U.S. Census Bureau,
2013-2017 American Community Survey 5-Year Estimates
Data are for Census Block Group Approximations
of the Roxbury Neighborhood

Race & Ethnicity

U.S. Census Bureau, 2010 Census
Data are for Census Block Group Approximations
of the Roxbury Neighborhood

BPDA Approved Housing

Boston Planning & Development Agency - Neighborhood Profiles, August 2017

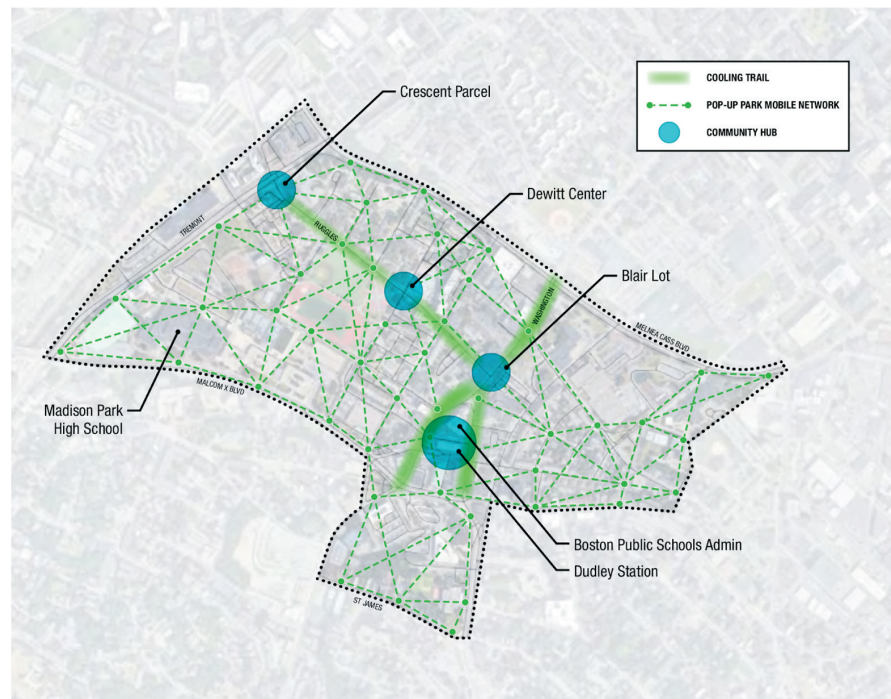
cars of volunteers, in addition to LANDSAT-derived products. Both datasets lead to very similar qualitative conclusions (e.g., which communities need investment in urban canopy cover the most) but the MoS campaign data may take more work to interpret depending on the needs of GBRAG stakeholders.

Addressing the UHI will be crucial not only from an economic perspective but also in terms of climate justice and restorative investment. These datasets are similar in terms of implications and can be used to prioritize investments in mitigation for communities, e.g., at a tract level.

Ambient air temperature during pregnancy has been positively associated with negative outcomes in a study population in Massachusetts (Kloog et al., 2015). Increased air temperature is suggested to increase the risk of low birth weight preterm delivery. Heat events are associated with a day-of increase in deliveries and accelerated births for up to two weeks (Barreca and Schaller, 2020).

Air quality

New to this iteration, we summarize understanding of the linkage between temperature and air quality and in turn their implications for public health. Two key air pollutants related to adverse health effects are ozone and Particulate Matter (PM). In total, the impacts of climate change on air quality in Massachusetts are uncertain and deserve further attention in literature. One study (Tagaris et al., 2009) examined economic and health impacts of changes in air quality (BenMAP). Children and patients with chronic lung/heart disease, and asthmatics, are impacted by PM. Adverse impacts include respiratory symptoms and illness, decreased lung function, increased asthma exacerbation, and premature mortality. A study of Medicare beneficiaries in Massachusetts from 2000 to 2012 suggested that long-term exposure to PM_{2.5} and ozone are causally associated with mortality, even at pollution levels below national standards (Wei et al., 2020). Tagaris et al. (2009) showed a significant increase in PM in Massachusetts and consequently increases in premature mortality, but little to no change in ozone.

Figure 3.3**Urban Heat Island Design Proposal for Lower Roxbury, from Stawasz et al., 2019.**

LEFT Concept diagram for the Lower Roxbury site showing the proposed network of cooling trails, pop-up parks and community hubs
Image credit: Arrowstreet

BELLOW Street view of existing conditions on Ruggles Street in Lower Roxbury
Image credit: Google Maps



There is a positive correlation between surface ozone and temperature in polluted regions (Fu and Tian, 2019). On the other hand, higher water vapor linked to temperature increase (O’Gorman and Schneider, 2009) is expected to *decrease* ozone background (Jacob and Winner, 2009). This duality potentially explains the little to no change in downstream ozone health impacts estimated in Massachusetts (Tagaris et al., 2009). The EPA (U.S. EPA, 2017) projected relatively small increases in ozone concentrations by 2050 and 2090 in Massachusetts under RCP8.5. More recent research suggests that across the U.S. as a whole, without intervention, climate change will increase MDA8 ozone by 3.6 ppb and that more stringent climate and air pollution control policies will be necessary to meet the current National Ambient Air Quality Standard (Moghani and Archer, 2020).

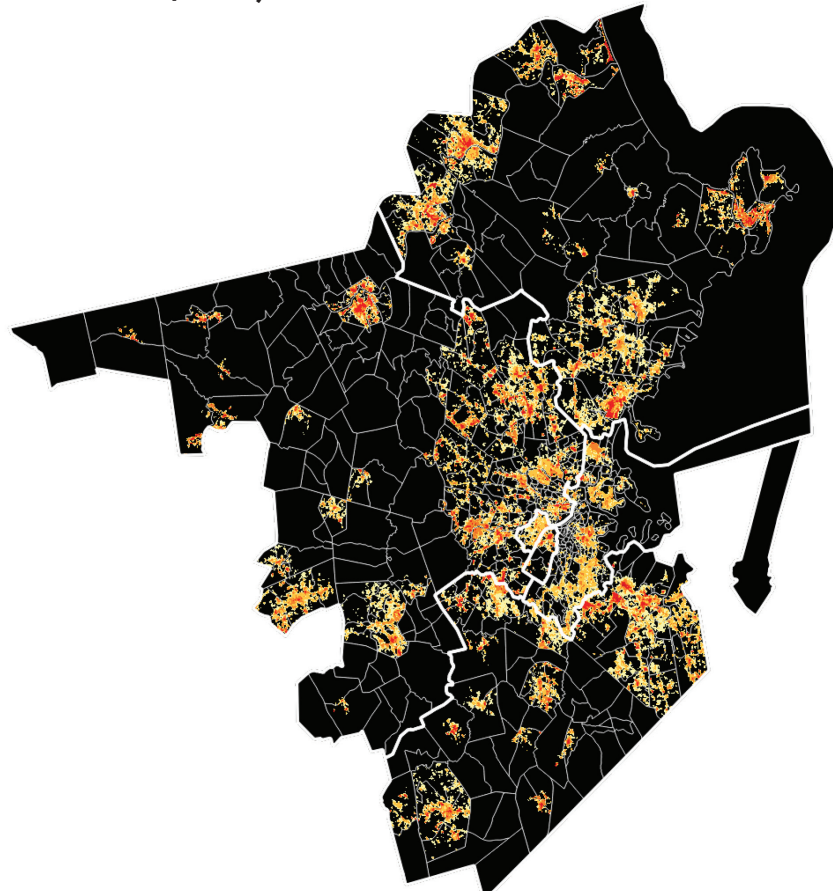
The effect of climate change on particulate matter (PM) is even more complicated and uncertain than for ozone and is dependent on precipitation, among other factors (Jacob and Winner, 2009). Tai et al. (2010) performed a regression analysis between PM and historical *observed* climate variables. Tai found a significant and positive correlation between PM and historical temperature over Massachusetts, thus clarifying the marginal relationship between temperature and PM. However, the relationship between precipitation and PM is negative and stronger in magnitude. Heavy precipitation has increased in the Northeast since 1901, and climate models suggest with high confidence that heavy precipitation will continue to increase in the Northeast over the 21st century (Tai et al., 2010; Easterling et al., 2017). Given PM’s complex response to temperature and precipitation, it is still unclear how PM will evolve in the region.

Vector-borne Diseases

Infectious diseases are also a growing health concern in the GBRAG region. Lyme disease is the most common vector-borne disease (VBD) in the U.S. Its occurrence and case rate is highly seasonal, and the

Figure 3.4

**Urban Heat Island scores from the Trust for Public Land
(Trust for Public Land, 2020).**



Scores range from 1 to 5 (yellow to red) at a 30-meter resolution. Thinner white lines define census tract boundaries. Thicker white lines define the boundaries of the 4 counties of the MAPC region. These data are available as a supplementary upon request. Source data: <https://www.arcgis.com/home/item.html?id=339c93a11b7d4cf7b222d60768d32ae5>

annual onset of timing of cases is modulated by meteorological conditions in prior months. One recent study (Monaghan et al., 2015) used 5 CMIP5 GCMs and multiple future GHG scenarios to estimate trends in Lyme Onset Week (LOW). Given that GCMs project warmer temperatures and (usually) more precipitation in the Northeast, research shows a strong consensus of significant earlier Lyme Onset Week dates (-0.3 weeks for RCP2.6 multi-model mean, -1.1 weeks for RCP8.5 multi-model mean) (Monaghan et al., 2015). This implies an earlier and potentially annually increased caseload in Lyme disease in Massachusetts. Indeed, the U.S. Global Climate Research Program (Beard et al., 2016) shows significant observed increases in spatial extent and count from year 2001 to 2014 in the Northeast. A more recent paper that does not use GCMs extrapolates another regression by assuming a 2 °C (3.6 °F) change (which is projected to occur somewhere between -2036 to 2065, depending on RCP choice) and estimates that the number of LD cases will increase significantly over the next several decades (Dumic and Severnini, 2018). The balance of evidence suggests that, in large part driven by increasing temperature, Lyme disease (and by proxy other less tick-related VBDs) is likely to increase significantly. This implies increases in hospitalizations, health costs, and the need for promoting public health awareness. Results are less certain for mosquito-driven VBDs like West Nile Virus (Beard et al., 2016).

3.8 IMPACT SECTORS: INFRASTRUCTURE AND TRANSPORTATION

Infrastructure and transportation have been grouped together given their thematic similarity and overlap. The Climate Ready Boston report (2016) highlighted one study that used one CMIP3 GCM to examine the effect of CO₂ and temperature increases on the carbonation and chloride-induced corrosion of concrete structures in the Boston metropolitan area. The results suggest that concrete construction projects could undergo carbonation and chlorination depths that exceed the current code-recommended cover thickness by the ~2070s (carbonation) and ~2050s (chlorination), respectively, potentially requiring extensive repairs (Saha and Eckelman, 2014). The remainder of the relevant details can be found in the BRAG report.

A range of critical infrastructure related to transportation is also at risk to projected changes in temperature (Chester et al., 2020). There exist several primary threats to the transportation sector, both through direct and indirect sources. Extreme heat and extreme cold conditions threaten workers and safe working conditions, especially for construction employees, who are 13 times more likely to suffer heat-related mortality compared to workers in other industries (Gubernot et al, 2019, Acharya et al., 2018). In addition, these extremes could place extra burdens on road transportation with greater stress to building material (e.g., cement) as well as create a likely increase in individual car drivers looking to avoid exposure to extreme heat or extreme cold conditions. Simultaneously, this requires public transportation sectors to adapt to crowds of people exposed to extreme temperatures.

Roads and cars

Using ~2.69 million Twitter geolocations, a study of mobility during the severe winter storms in the East during 2015 examined how they impacted different dimensions of traffic, such as traffic demand, traffic safety, traffic operations, and flow. The effect of snowstorms was shown to vary by trip purposes, distances, types of vehicles, different areas impacted, and time. Notably, unlike other acute disasters (such as earthquakes, or hurricanes and floods), severe winter weather may not force residents to evacuate their homes on a large scale (Wang et al., 2017b). Chinowsky (2013) suggests that climate change, if unchecked, will increase the annual costs of keeping U.S. paved and unpaved roads in service by \$785 million in present value terms by 2050 (the percentage of which is specific to Massachusetts not stated). Policies to reduce greenhouse gas emissions are estimated to reduce these costs by approximately \$280 million in present value terms. In a similar vein, a recent study (Stoner et al., 2019) coupling one GCM with a pavement performance model showed a permanent degradation of asphalt concrete primarily related to temperature increases by the end of the 21st century across the country, reinforcing a likely “infrastructure deficit” above and beyond normal road maintenance. This approach could be useful in conducting cost benefit analyses in investing in improving highways and local roads in Massachusetts.

Public transportation (rail, bus)

A 2011 U.S. DOT study/report (Hodges, 2011) details likely physical and socioeconomic impacts of climate change related to public transportation. Infrastructure-wise, heat waves (however specifically measured) stress materials, buckle rails, and jeopardize customer and worker safety and comfort. Qualitatively, this gives rise to issues like additional downtime/increased transit wait time, inefficiency, and increased maintenance cost. Socioeconomically vulnerable and oppressed populations—persons of color, persons with disabilities, older adults, immigrant populations, and low-income individuals—are groups who disproportionately depend on public transportation and suffer disproportionately from disruptions and degradation in service. As one of several examples, the study points out that during an East Coast heat wave, the Boston MBTA’s “T” experienced rail kinks that caused them to slow trains and to remove and replace enlarged sections of rail. In another, heat waves in New Jersey and Los Angeles stretched overhead catenary, disrupting power supply to rail vehicles. In yet another, electronic train control equipment and farebox machines

in Portland overheated during high-heat days. In IPCC-like uncertainty characterization terms, extreme heat is a “very likely” (> 90%) dimension of concern related to: (1) track buckling; (2) customer comfort issues; and (3) worker safety issues. Related to the UHI effect (covered to the extent possible in the BRAG report), this same 2011 study also highlights that urban areas, which form the core of transit services, tend to be hotter than surrounding areas. Dark rooftops and asphalt-paved surfaces, which absorb and re-radiate heat, combine with less tree canopy coverage to create the UHI phenomenon. To cast this in terms of one useful metric in Table 1, these problems will likely become more common with increases in terms of the number of days over 90 °F.

Air travel

Cities like Phoenix are already experiencing days hot enough that airplanes are forced to stay grounded (Wichter, 2017). Massachusetts airports specifically aside, the airline business is inherently a network, meaning if this phenomenon only directly impacts airports in hotter cities in the short term, in net, stakeholders like MassPort will be adversely impacted as well. A 2015 paper attempts to quantify this idea (Stamos et al., 2015) in one form using a network science/graphical approach combining multiple modes of transportation (air, road, and rail). We have not found projections for air transit specific to Massachusetts, but given the adverse impacts of cold waves and heat waves on air transit delays and efficiency, it is reasonable to at least extrapolate that the increase in heat in other cities may be expected to, via network effects, increase problems in terms of “macro” economics (via delays, cancellations, lost goodwill, and increased maintenance) in the airline industry, especially in hotter seasons.

3.9 IMPACT SECTORS: ECONOMY, SOCIETY, GOVERNANCE

This section is new in this GBRAG report. Given the wide scope of possible topics here, we begin “top down” and focus on the high-level expected impacts of increases in temperature on these three sectors. To the extent possible via literature, we then drill down to Massachusetts-specific insights and projections.

At a high level, all of these three topics are tightly interrelated and are often 2nd or 3rd order impact sectors. Financial and economic concerns, in particular, are leading to accelerating and very broad private sector interest in the risks (and opportunities) of climate change. Prime examples include recently announced plans for divesting from fossil fuels from the CEO of BlackRock (Sorkin, 2020)—the world’s largest money manager, with ~\$7T in assets under management. A report released by a team of leading physical scientists and economists from the same firm details the economic risks of climate change in light of a wide range of dimensions (BlackRock Investment Institute, 2019). The report estimates net impacts of climate change given a 2060 to 2080 climatology from RCP8.5 at a county level across the contiguous 48 U.S. states, using a composite index based on marrying a multitude of climate risks (hurricanes, wildfires, extreme temperature, floods, droughts) to key financial service sectors (municipal bonds, GDP, mortgage-backed securities, energy generation). In index fashion, Massachusetts is projected to experience relatively moderate net negative economic impacts from climate change, with the most severe negative category of impacts in the Cape Cod area.

GDP

Hsiang et al. (2017) provides more granular insight into the types of economic impacts to expect nationally and specific to Massachusetts’ counties. It does so by coupling a probabilistic, downscaled county level median of multi-model ensemble projections for temperature and precipitation (Rasmussen et al., 2016) with damage functions estimated from historical models. For most Massachusetts counties, under the worst-case scenarios (RCP8.5, 2080 to 2099 climatology) the study estimates that the net impact of climate change to GDP could even be moderately positive (up to +5%). The key exception is the Boston

area, where the coastal concentration of assets and their exposure to urban heat and flooding is higher. Here GDP impacts are expected to be moderately negative (up to -5%). Violent crime (+3 to 4%), property crime (+1 to 2%), and high-risk (outdoor) labor (-0.5 to -1.5%, higher risk in the Boston area) are all expected to increase across the state. All of these changes are functions of increasing temperature. Energy expenditures from electricity are expected to increase moderately as well, in line with research covered earlier. Given that statistical significance and spread in GCM projections are not detailed in these two studies, they should be interpreted directionally but with caution.

As of 2012, health costs accounted for ~10% of total domestic product in Massachusetts. That percentage is rising because the long-term rate of increase in health costs has been about double that of the overall state economy. Climate change will not only compromise the health of the population but will also impose a heavier burden on the state (Repetto, 2012). While the net mortality is expected to decrease in Massachusetts, primarily through a reduction in deaths from cold weather, an increase in certain VBDs (see Public Health) and heat-related health risks in the summer are expected to indirectly increase health-care-related costs, especially in warmer months.

Fisheries

The value of commercial and recreational fishing and shellfish landings in Massachusetts is more than \$1 billion annually (Repetto, 2012). Under global warming, the waters south of Cape Cod may become too warm to support a lobster population. Warmer waters also promote shell diseases, parasites, and algal blooms that can damage important marine ecosystems and advance instability of coastal economic sectors.

Household income

One econometric study (Albouy et al., 2016) estimated annual welfare losses of ~1 to 4% in terms of household income by 2100 using two business-as-usual CMIP3 scenarios (A1Fi and A2), holding technology and population purchasing preferences constant and controlling for demographics. Household costs are expected to increase as a means of avoiding excessive heat. The Greater Boston area was placed on the lower end of that spectrum (up to 1%), whereas the entire state of Florida by contrast was on the high end (4% or more).

On the other hand, Bloesch and Gourio (2015) suggest that anomalously cold weather has reduced certain types of economic output. Economic indicators published in 2014, including industrial production, employment, and automobile sales, showed that economic activity had slowed substantially during an unusually cold 2013 to 2014 winter in the Northeast. Holding all else constant, the study estimates that a one standard deviation increase in a temperature index during the winter leads nonfarm employment to grow by 0.04%, while a one standard deviation increase in a snowfall index leads to a *decline* of 0.03%.

3.10 IMPACT SECTORS: AGRICULTURE AND NATURAL RESOURCES

This section focuses on the ecological impacts of temperature changes relevant to the natural resource-based economies and traditions of the Northeast. Projected trends in temperature and temperature extremes are expected to have direct and indirect effects on forest composition and health, prevalence of pests and invasive species, recreation, and the economics of traditional agricultural industries.

Increasing mean annual and seasonal temperatures are expected to lengthen the growing season by 29 to 43 days by 2100 (Rustad et al., 2011) by altering the timing of first and last frosts and increasing the accumulation Growing Degree Days (GDD) (Kukal and Irmak, 2018). However, potential benefits of a longer growing season may be attenuated by increasing stresses, such as summer drought, and increased springtime flooding due to higher-precipitation events. Heavy precipitation has increased in the U.S. Northeast since 1901, and climate models suggest with high confidence that heavy precipitation will continue to increase over the 21st century, especially in winter and spring (Easterling et al., 2017).

Shortages in soil moisture owing to decreasing snowpack and increasing evapotranspiration have profound impacts on productivity if they occur during critical portions of the growing season (Hayhoe et al., 2007). Dominant tree species in regional forests are expected to shift under an increasingly warm temperature regime, although uncertainty exists in the ability of trees to migrate at the rate at which climate zones are shifting.

Increasing winter temperatures also pose a threat to agriculture. Cranberries and maple syrup, two iconic New England agricultural products, depend on accumulation of winter chilling days (Ellwood et al., 2014). Cold-limited nuisance species may increase in range and severity and cause increased ecological and economic damage as the freeze-free period is projected to lengthen by 2 to 3 weeks by the mid-century (Dupigny-Giroux et al., 2018). Warmer temperatures are generally thought to benefit pests, pathogens, and invasive species as such temperatures accelerate their movement, consumption, dispersion, and generation time (Dukes et al., 2009). Warmer waters also promote shell diseases, parasites, and algal blooms that can damage important marine ecosystems and advance instability of coastal economic sectors (Griffith and Gobler, 2020).

A shift toward winter precipitation occurring as rain decreases snow cover and long-term water storage in reservoirs and aquifers. Adverse effects on winter recreation (snowmobiling, snowboarding, and skiing) are likely to include reduced season length and increased operating costs (Wobus et al., 2017).

3.11 TEMPERATURE REFERENCES

- Acharya, Payel, Bethany Boggess, and Kai Zhang. "Assessing heat stress and health among construction workers in a changing climate: a review." *International Journal of Environmental Research and Public Health*, 15(2), 2018, 247.
- Albouy, David, et al. "Climate amenities, climate change, and American quality of life." *Journal of the Association of Environmental and Resource Economists*, 3(1), 2016, 205–246.
- Alola, Andrew Adewale, et al. "Cooling and heating degree days in the US: the role of macroeconomic variables and its impact on environmental sustainability." *Science of the Total Environment*, 695, 2019, 133832.
- Amato, Anthony D., et al. "Regional energy demand responses to climate change: methodology and application to the commonwealth of Massachusetts." *Climatic Change*, 71(1–2), 2005, 175–201.
- Asseng, Senthil, Frank Ewert, Pierre Martre, Reimund P. Rötter, David B. Lobell, Davide Cammarano, Bruce A. Kimball et al. "Rising temperatures reduce global wheat production." *Nature Climate Change*, 5(2), 2015, 143–147.
- Barreca, Alan, and Jessamyn Schaller. "The impact of high ambient temperatures on delivery timing and gestational lengths." *Nature Climate Change*, 10(1), 2020, 77–82.
- Beard, C.B., et al. "Ch. 5: Vectorborne Diseases. The Impacts of Climate Change on Human Health in the United States: A Scientific Assessment." U.S. Global Change Research Program, Washington, DC, 2016, 129–156.
- BlackRock Investment Institute. "Getting physical: Scenario analysis for assessing climate-related risks." 2019, <https://www.blackrock.com/us/individual/literature/whitepaper/bii-physical-climate-risks-april-2019.pdf>.
- Blazejczyk, Krzysztof, et al. "Comparison of UTCI to selected thermal indices." *International Journal of Biometeorology*, 56(3), 2012, 515–535.
- Bloesch, Justin, and Francois Gourio. "The effect of winter weather on US economic activity." *Economic Perspectives*, 39(1), 2015.
- CAPA Strategies, 2019. "Heat watch report, Boston, Massachusetts." Report available at <https://osf.io/kbsa4/download>. Dataset is available for download at <https://osf.io/f6xyd/download>. Accessed Mar 9, 2022.
- Chester, Mikhail V., B. Shane Underwood, and Constantine Samaras. "Keeping infrastructure reliable under climate uncertainty." *Nature Climate Change*, 2020, 1–3.
- Chinowsky, Paul S., Jason C. Price, and James E. Neumann. "Assessment of climate change adaptation costs for the US road network." *Global Environmental Change*, 23(4), 2013, 764–773.
- City of Cambridge Community Development Department. *Cambridge Climate Change Vulnerability Assessment (CCVA) Report—Part 1*. 2015.

- Colliver, Victoria and Nolan D. McCaskill. "A complicating factor in combating Covid hot spots: Heat." *Politico*, 2021, <https://www.politico.com/news/2021/03/03/coronavirus-heat-472624>.
- Coutts, Erin, K. Ito, C. Nardi, and T. Vuong. "Planning urban heat island mitigation in Boston." *Tufts University Urban Environmental Policy Plan*, 2015.
- Dailey, Peter S., et al. "On the relationship between North Atlantic sea surface temperatures and US hurricane landfall risk." *Journal of Applied Meteorology and Climatology*, 48(1), 2009, 111–129.
- Davies, Ian P., Ryan D. Haugo, James C. Robertson, and Phillip S. Levin. "The unequal vulnerability of communities of color to wildfire." *PloS One* 13(11), 2018, e0205825.
- Deese, Brian et al. "Getting physical—Scenario analysis for assessing climate-related risks" *BlackRock*, 2011.
- Deser, Clara., et al. "Insights from Earth system model initial-condition large ensembles and future prospects." *Nature Climate Change*, 2020, 1–10.
- Di Cecco, Grace J., and Tarik C. Gouhier. "Increased spatial and temporal autocorrelation of temperature under climate change." *Scientific Reports*, 8(1), 2018, 1–9.
- Diaz, Jaclyn, and Kobee Vance. "Like 'Peanut Brittle': Mississippi Water Crisis Highlights Infrastructure Problems." *NPR*, 2021, <https://www.npr.org/2021/03/03/973175017/like-peanut-brittle-mississippi-water-crisis-highlights-infrastructure-problems>.
- DiSavino, Scott. "Texas Power Demand Breaks Record during Heat Wave, Prices Spike." *Reuters*, Thomson Reuters, 2015.
- Douglas, E., P. Kirshen, R. Hannigan, R. Herst and A. Palardy. *Climate Change and Sea Level Rise Projections for Boston*. The Boston Research Advisory Group for Climate Ready Boston, 1 June 2016, www.boston.gov/sites/default/files/document-file-12-2016/brag_report_-_final.pdf.
- Dukes, Jeffrey S., et al. "Responses of insect pests, pathogens, and invasive plant species to climate change in the forests of northeastern North America: What can we predict?" *Canadian Journal of Forest Research*, 39(2), 2009, 231–248.
- Dumic, Igor, and Edson Severini. "'Ticking Bomb': the impact of climate change on the incidence of lyme disease." *Canadian Journal of Infectious Diseases and Medical Microbiology*, 2018.
- Dupigny-Giroux, L.A., et al. "Northeast—Impacts, Risks, and Adaptation in the United States: Fourth National Climate Assessment." U.S. Global Change Research Program, Washington, DC, USA, II, 018, 669–742.
- Easterling, David R., et al. "Precipitation change in the United States." U.S. Global Change Research Program. U.S. Global Change Research Program, Washington, DC, 2017, 301–335.
- Ellwood, Elizabeth R., et al. "Cranberry flowering times and climate change in southern Massachusetts." *International Journal of Biometeorology*, 58(7), 2014, 1693–1697.
- Fox-Penner, Peter. *Power after carbon: Building a clean, resilient grid*. Harvard University Press, 2020.
- Fu, Tzung-May, and Heng Tian. "Climate change penalty to ozone air quality: review of current understandings and knowledge gaps." *Current Pollution Reports*, 5(3), 2019, 159–171.
- Ganguly, Auroop R., Karsten Steinhaeuser, David J. Erickson, Marcia Branstetter, Esther S. Parish, Nagendra Singh, John B. Drake, and Lawrence Buja. "Higher trends but larger uncertainty and geographic variability in 21st century temperature and heat waves." *Proceedings of the National Academy of Sciences*, 106(37), 2009, 15555–15559.
- Ganguly, Auroop R., et al. "Climate adaptation informatics: water stress on power production." *Computing in Science & Engineering*, 17(6), 2015, 53–60.
- Greene, Scott, et al. "An examination of climate change on extreme heat events and climate–mortality relationships in large US cities." *Weather, Climate, and Society*, 3(4), 2011, 281–292.
- Griffith, Andrew W., and Christopher J. Gobler. "Harmful algal blooms: a climate change co-stressor in marine and freshwater ecosystems." *Harmful Algae*, 91, 2020, 101590.

- Gubernot, Diane M., et al. "Characterizing occupational heat-related mortality in the United States, 2000–2010: An analysis using the census of fatal occupational injuries database." *American Journal of Industrial Medicine*, 58(2), 2015, 203–211.
- Hajat, Shakoor, et al. "Heat-related and cold-related deaths in England and Wales: who is at risk?." *Occupational and Environmental Medicine*, 64(2), 2007, 93–100.
- Hardin, Aaron. "Assessment of urban heat islands during hot weather in the US Northeast and linkages to microscale thermal and radiational properties." *Doctoral dissertation, Texas Tech University*, 2015.
- Hayhoe, Katharine, et al. "Past and future changes in climate and hydrological indicators in the US Northeast." *Climate Dynamics*, 28(4), 2007, 381–407.
- Hodges, Tina. "Flooded Bus Barns and Buckled Rails: Public transportation and climate change adaptation." *No. FTA Report No. 0001. United States. Federal Transit Administration. Office of Budget and Policy*, 2011.
- Hsiang, Solomon, et al. "Estimating economic damage from climate change in the United States." *Science*, 356.6345, 2017, 1362–1369.
- Jacob, Daniel J., and Darrell A. Winner. "Effect of climate change on air quality." *Atmospheric Environment*, 43(1), 2009, 51–63.
- Karmalkar, A. V., Thibeault, J. M., Bryan, A. M., & Seth, A. "Identifying credible and diverse GCMs for regional climate change studies—case study: Northeastern United States." *Climatic Change*, 154(3), 2019, 367–386.
- Kharin, Viatcheslav V., et al. "Changes in temperature and precipitation extremes in the CMIP5 ensemble." *Climatic Change*, 119(2), 2013, 345–357.
- Kloog, Itai, et al. "Using satellite-based spatiotemporal resolved air temperature exposure to study the association between ambient air temperature and birth outcomes in Massachusetts." *Environmental Health Perspectives*, 123(10), 2015, 1053–1058.
- Kodra, Evan, et al. "Persisting cold extremes under 21st-century warming scenarios." *Geophysical Research Letters*, 38(8), 2011.
- Kodra, Evan, Subimal Ghosh, and Auroop R. Ganguly. "Evaluation of global climate models for Indian monsoon climatology." *Environmental Research Letters*, 7(1), 2012, 014012.
- Kodra, Evan, et al. "Asymmetry of projected increases in extreme temperature distributions." *Scientific Reports*, 4, 2014, 5884.
- Kodra, Evan, et al. "Physics-guided probabilistic modeling of extreme precipitation under climate change." *Scientific Reports*, 10(1), 2020, 1–11.
- Kukal, Meetpal S., and Suat Irmak. "US agro-climate in 20 th century: growing degree days, first and last frost, growing season length, and impacts on crop yields." *Scientific Reports*, 8(1), 2018, 1–14.
- Kumar, Devashish, and Auroop R. Ganguly. "Intercomparison of model response and internal variability across climate model ensembles." *Climate Dynamics*, 51(1), 2018, 207–219.
- Kumar, Devashish et al. "Regional and seasonal intercomparison of CMIP3 and CMIP5 climate model ensembles for temperature and precipitation." *Climate Dynamics*, 43(9–10), 2014, 2491–2518.
- Lipschultz, Fredric, et al. "Climate Explorer: Improved Access to Local Climate Projections." *Bulletin of the American Meteorological Society*, 101(3), 2020, E265–E273.
- Mitchell, Daniel M., et al. "The effect of climate change on the variability of the Northern Hemisphere stratospheric polar vortex." *Journal of the Atmospheric Sciences*, 69(8), 2012, 2608–2618.
- Moghani, Mojtaba, and Cristina L. Archer. "The impact of emissions and climate change on future ozone concentrations in the USA." *Air Quality, Atmosphere & Health*, 13(12), 2020, 1465–1476.
- Monaghan, Andrew J., et al. "Climate change influences on the annual onset of Lyme disease in the United States." *Ticks and Tick-Borne Diseases*, 6(5), 2015, 615–622.
- Moore, Sean M., et al. "Meteorological influences on the seasonality of Lyme disease in the United States." *The American Journal of Tropical Medicine and Hygiene*, 90(3), 2014, 486–496.

O’Gorman, Paul A., and Tapio Schneider. “The physical basis for increases in precipitation extremes in simulations of 21st-century climate change.” *Proceedings of the National Academy of Sciences*, 106(35), 2009, 14773–14777.

Pachauri, R. K., and A. Reisinger. Climate change 2007. *Synthesis report. Contribution of Working Groups I, II and III to the fourth assessment report of the Intergovernmental Panel on Climate Change*. Cambridge University Press, Cambridge, 2008.

Pachauri, Rajendra K., et al. *Climate change 2014: Synthesis report. Contribution of Working Groups I, II and III to the fifth assessment report of the Intergovernmental Panel on Climate Change*. IPCC, 2014.

Perkins-Kirkpatrick, S. E., and S. C. Lewis. “Increasing trends in regional heatwaves.” *Nature Communications*, 11(1), 2020, 1–8.

Petkova, Elisaveta P., et al. “Projected heat-related mortality in the US urban northeast.” *International Journal of Environmental Research and Public Health*, 10(12), 2013, 6734–6747.

Petri, Yana, and Ken Caldeira. “Impacts of global warming on residential heating and cooling degree-days in the United States.” *Scientific Reports*, 5, 2015, 12427.

Pierce, David W., et al. “Selecting global climate models for regional climate change studies.” *Proceedings of the National Academy of Sciences*, 106(21), 2009, 8441–8446.

Pierce, D. W., Cayan, D. R., & Thrasher, B. L. “Statistical downscaling using localized constructed analogs (LOCA).” *Journal of Hydrometeorology*, 15(6), 2014, 2558–2585

Rasmussen, D. J. et al. “Probability-weighted ensembles of US county-level climate projections for climate risk analysis.” *Journal of Applied Meteorology and Climatology*, 55(10), 2016, 2301–2322.

Raymond, Colin, Tom Matthews, and Radley M. Horton. “The emergence of heat and humidity too severe for human tolerance.” *Science Advances*, 6(19), 2020, eaaw1838.

Repetto, Robert. “Massachusetts’ Rising Economic Risk from Climate Change.” *Better Future Project*, 2012.

Roehl Jr, Edwin A., Ruby C. Daamen, and John B. Cook. “Estimating seawater intrusion impacts on coastal intakes as a result of climate change.” *Journal-American Water Works Association* 105(11), 2013, E642-E650.

Rustad, Lindsey, et al. “Changing climate, changing forests: The impacts of climate change on forests of the northeastern United States and eastern Canada.” Gen. Tech. Rep. NRS-99. Newtown Square, PA: US Department of Agriculture, Forest Service, Northern Research Station. 99, 2012, 1–48.

Saha, Mithun, and Matthew J. Eckelman. “Urban scale mapping of concrete degradation from projected climate change.” *Urban Climate*, 9, 2014, 101–114.

Santer, Benjamin D., et al. “Incorporating model quality information in climate change detection and attribution studies.” *Proceedings of the National Academy of Sciences*, 106(35), 2009, 14778–14783.

Schlenker, Wolfram, and Michael J. Roberts. “Nonlinear temperature effects indicate severe damages to US crop yields under climate change.” *Proceedings of the National Academy of Sciences*, 106(37), 2009, 15594–15598.

Smith, Ryan. “Billions in insured losses for 2020 wildfires—RMS.” *Insurance Business America*, 2020.

Sorkin, Andrew Ross. “BlackRock CEO Larry Fink: Climate crisis will reshape finance.” *The New York Times*, January 14, 2020.

Stamos, Iraklis, et al. “Impact assessment of extreme weather events on transport networks: A data-driven approach.” *Transportation Research Part D: Transport and Environment*, 34, 2015, 168–178.

Stawasz, Arlen et al. *Living with Heat Urban*. Land Institute: Boston/New England, 2019.

Stoner, Anne MK, et al. “Quantifying the impact of climate change on flexible pavement performance and lifetime in the United States.” *Transportation Research Record*, 2673(1), 2019, 110–122.

Stott, Peter A., et al. “Attribution of extreme weather and climate-related events.” *Wiley Interdisciplinary Reviews: Climate Change*, 7(1), 2016, 23–41.

- Street, Michael, Christoph Reinhart, Leslie Norford, and John Ochsendorf. "Urban heat island in Boston—An evaluation of urban air-temperature models for predicting building energy use." *In Proceedings of the BS2013: 13th Conference of International Building Performance Simulation Association, Chambéry, France*, 2013, 26–28.
- Sunyer, Maria Antonia, et al. "A Bayesian approach for uncertainty quantification of extreme precipitation projections including climate model interdependency and nonstationary bias." *Journal of Climate*, 27(18), 2014, 7113–7132.
- Tagaris, Efthimios, et al. "Potential impact of climate change on air pollution-related human health effects." *Environmental Science & Technology*, 43(13), 2009, 4979–4988.
- Tai, Amos PK, Loretta J. Mickley, and Daniel J. Jacob. "Correlations between fine particulate matter (PM_{2.5}) and meteorological variables in the United States: Implications for the sensitivity of PM_{2.5} to climate change." *Atmospheric Environment*, 44(32), 2010, 3976–3984.
- Trust for Public Land. The Heat is On. 2020, https://www.tpl.org/sites/default/files/The-Heat-is-on_A-Trust-for-Public-Land_special-report.pdf.
- Ura, Alexa, and Juan Pablo Garnam. "Already hit hard by pandemic, Black and Hispanic communities suffer the blows of an unforgiving winter storm." *The Texas Tribune*, February 19, 2021.
- US Environmental Protection Agency. *Multi-model framework for quantitative sectoral impacts analysis: A technical report for the Fourth National Climate Assessment*. 2017.
- Vélez, Karina D., et al. "The effect of climate change on electricity expenditures in Massachusetts." *Energy Policy*, 106, 2017, 1–11.
- Vicedo-Cabrera, Ana Maria, et al. "The burden of heat-related mortality attributable to recent human-induced climate change." *Nature Climate Change*, 11(6), 2021, 492–500.
- Wang, Guiling, Dagang Wang, Kevin E. Trenberth, Amir Erfanian, Miao Yu, Michael G. Bosilovich, and Dana T. Parr. "The peak structure and future changes of the relationships between extreme precipitation and temperature." *Nature Climate Change*, 7(4), 2017a, 268–274.
- Wang, Yan, Qi Wang, and John E. Taylor. "Aggregated responses of human mobility to severe winter storms: An empirical study." *PloS One*, 12(12), 2017b, e0188734.
- Wei, Yaguang, et al. "Causal effects of air pollution on mortality rate in Massachusetts." *American Journal of Epidemiology*, 189(11), 2020, 1316–1323.
- Wichter, Zach. "Too Hot to Fly? Climate Change May Take a Toll on Air Travel." *The New York Times*, June 20, 2017.
- Wobus, Cameron, et al. "Projected climate change impacts on skiing and snowmobiling: A case study of the United States." *Global Environmental Change*, 45, 2017, 1–14.
- Wood, Charlie. "US winter storm Uri set to inflict record-breaking, multi billion-dollar industry losses." *Reinsurance News*, 2021, <https://www.reinsurancene.ws/us-winter-storm-uri-set-to-inflict-record-breaking-multi-billion-dollar-industry-losses>.
- World Meteorological Organization. *The State of the Global Climate 2020*. World Meteorological Organization, 2021, <https://public.wmo.int/en/our-mandate/climate/wmo-statement-state-of-global-climate>.
- Zelinka, Mark D., et al. "Causes of higher climate sensitivity in CMIP6 models." *Geophysical Research Letters*, 47(1), 2020, e2019GL085782.

4. Sea Level Rise

4.1 KEY FINDINGS

- **Relative Sea Level (RSL) in Boston Harbor is rising at an accelerating pace.** The average rate of RSL rise between 2001 to 2019 was 5.4 mm/yr (0.21 in/yr), about twice the rate averaged over the last century. RSL in Greater Boston is rising faster than the global average due to a combination of regional ocean warming and geodynamical processes (including local vertical land motion) associated with past and current changes in the distribution of land ice around the world.
- **Loss of land ice stored in mountain glaciers and ice sheets on Greenland and Antarctica has recently superseded ocean thermal expansion as the primary driver of climate-driven sea level.** Melting land ice causes changes in Earth's gravity and rotation that impact regional patterns of sea level rise. When ice is lost from the West Antarctic Ice Sheet, these processes amplify the resulting sea level rise in Boston by about 25% relative to the global average. Notably, the rate of ice loss in West Antarctica increased by a factor of three in the decade spanning 2007 to 2017 relative to the previous decade. Future changes in North Atlantic ocean circulation could also amplify RSL rise in Boston relative to the global average.
- **We provide updated probabilistic projections of RSL, adapted specifically to the unique setting of Boston Harbor.** The projections account for contributions to RSL from future ocean thermal expansion, ocean dynamics/currents, anthropogenic land water storage, land ice loss from mountain glaciers and Greenland and Antarctic ice sheets, Earth gravitational/rotational effects, and local vertical land motion. These new RSL projections differ substantially from Climate Ready Boston (2016) and are lower in the year 2100, mainly because they use a more recent assessment of future Antarctic ice loss provided by the IPCC (2019), rather than the single Antarctic modeling study (DeConto and Pollard, 2016) used previously.
- **Projections of RSL rise in Boston Harbor vary widely as a function of future greenhouse gas emissions.** Under the most optimistic RCP2.6 scenario, RSL rise in 2100 relative to a 2000 baseline is 35 to 78 cm (17th to 83rd percentile likely range), versus 72 to 146 cm for a more extreme RCP8.5 scenario. Under RCP8.5, two meters of RSL rise in Boston Harbor is possible by 2100 (192 cm, 95th percentile; 273 cm, 99th percentile). In 2200, the 17th to 83rd percentile likely range of sea level rise is 184 to 378 cm.
- **Increasing uncertainty in the upper tail of the projections over the 21st century and beyond is mainly caused by deep uncertainty in the response of the Antarctic Ice Sheet to future warming, which remains difficult to model.** The Antarctic Ice Sheet contains the ice-equivalent of 58 m (190 ft) of sea level rise, so even small changes there could be highly impactful. Risk adverse end users of these projections should consider the possibility of sea level outcomes above the likely range, especially under higher greenhouse gas emissions. For long-term planning and long-lived coastal assets, we stress that sea level will continue rising beyond 2100 under all greenhouse gas emissions scenarios, with the possibility that rates of RSL rise will exceed 1 cm per year. In some cases, the future rate of sea level rise may be a more impactful metric than its absolute height. Due to the long thermal memory of the ocean, slow regrowth of ice sheets, and ongoing (downward) vertical land motion, any sea level rise (and land loss) that does occur should be considered permanent on century and possibly millennial timescales.

- **Most of Greater Boston's extreme flooding events are caused by winter storms (extratropical cyclones) coinciding with anomalous high tides.** Recent studies have not found significant evidence for future changes in Greater Boston storm surge linked to changing storm climatology; however, sea level rise will substantially increase the frequency of extreme coastal flooding in the 21st century. Therefore changes in storm frequency are not considered in future estimates of storm surge flooding.
- **Under all emissions scenarios, what is now a one in 10-year winter storm flood will likely become an annual event by mid-century.** Flood projections begin to diverge under different emissions pathways around 2050. Beyond 2050, greenhouse gas emissions will determine if increasing flood hazard slows toward the end of the century (RCP2.6) or continues to accelerate. The equivalent of today's one in 100-year flood event will likely become an annual event by 2100 under RCP8.5.
- **The height of the tide largely controls the severity of flooding during a given storm in Greater Boston.** Tidal range (the difference between low and high tide) varies year-to-year in the region as a function of natural planetary cycles, dominated by an 18.6-yr lunar nodal cycle related to motion of the moon's elliptical orbit. Eight of Boston's top-ten historic flood events over the past 200 years (including two record-setting Nor'easters in January and March of 2018) occurred during a peak in this 18.6-year cycle, indicating the need for tidal variability to be considered in Greater Boston flood projections.
- **Future increases in flood hazard driven by sea level rise will slow during decades when the lunar nodal cycle is in a negative phase and the reduced tide range counteracts sea level rise (2019 to 2027 and 2037 to 2046).** However, as the nodal cycle enters a positive phase in the following decade (2028 to 2036 and 2047 to 2055), the larger tide range combined with sea level rise will amplify flood hazard. Beyond mid-century, the influence of these tidal variations on flood projections becomes less important, as background sea level rise becomes the dominate control on flooding.
- **Boston Harbor will see an increasing number of high tide "nuisance" flooding days,** defined as days when at least one hourly water level measurement exceeds local flooding thresholds defined by NOAA (215 cm above 2000 mean sea level for minor flooding or 241 cm for moderate flooding). Based on recent projections (Thompson et al., 2021), Boston's minor flood threshold will be exceeded on roughly half the days of each year by the early 2050s under the NOAA Intermediate sea level rise scenario, which is between the median RCP4.5 and RCP8.5 sea level projections provided in this report. Under the NOAA Intermediate Low sea level rise scenario (close to median RCP2.6 projections in this report), this will occur between 2070 and 2090. Boston's moderate flood threshold will be exceeded on half of days around 2070 under the NOAA Intermediate sea level rise scenario, but will only reach 48 to 87 exceedance days per year (10th to 90th percentile range) by the end of the century (2100) due to the lunar nodal cycle being in a negative phase.
- **Seasonal-to-decadal sea level fluctuations unrelated to background sea level rise cause inevitable extreme months of clustered high tide flooding.** Over a given five-year period, the peak flooding month often experiences more than double the number of high tide flooding days than the average month. As a result, we stress that planning for the "typical" future month or year leads to substantial underestimation of flood hazard in the occasional, yet inevitable periods of severe flooding, when cyclical contributions to sea level constructively combine.

4.2 INTRODUCTION

This Greater Boston Research Advisory Group (GBRAG) report provides 1) an update of recent trends in sea level change in Boston Harbor, and 2) revised projections of future sea level rise relative to those provided in the previous Boston Research Advisory Group (BRAG) report (Douglas et al., 2016). These revised sea level projections reflect the rapidly evolving science of sea level change (Hamlington et al., 2020). This is especially true for projections of future contributions to sea level rise, arising from the loss of glacial ice on Antarctica (Oppenheimer et al., 2019).

Since the publication of the BRAG report in 2016, a special report of the Intergovernmental Panel on Climate Change (IPCC) has appeared (Pörtner et al., 2019), providing updated projections of global and regional sea level rise. This IPCC Special Report on the Oceans and Cryosphere in a Changing Climate (SROCC) differs substantially from previous IPCC sea level assessments including IPCC AR5 (Church et al., 2013), especially in the late 21st century and beyond (Oppenheimer et al., 2019). As discussed below, these new IPCC projections provide the foundational basis for the local sea level projections provided here, adapted to the specific and unique setting of Boston Harbor.

The concept of ‘sea level’ is not as simple as often assumed, warranting some background and clarification. In most instances, GBRAG follows the standard sea-level terminology adopted by the 2016 BRAG report. Additional details on terminology and definitions are provided by (Gregory et al., 2019). Most importantly, sea level does not change uniformly across the globe, and regional-to-local scale changes in specific places like Boston Harbor can differ by 30% or more from the global mean. As such, changes in global mean sea level (GMSL) should not be confused with local changes in relative sea level (RSL). Here, we define RSL as the difference in elevation between the sea surface and land surface at a specific place and time (Ferrell and Clark, 1976). It is the change in RSL (not GMSL) that impacts coastlines, people, and infrastructure in specific locations like Boston. The distinction between GMSL and RSL is important, because there are places around the world, including the Massachusetts shoreline, where RSL is rising faster than the global average, which will be increasingly consequential for Boston in the coming decades.

While this report provides guidance on present and future changes in RSL in Boston Harbor, the global context of GMSL provides a useful starting point for understanding climate-driven sea level rise. The organizational approach followed here is to 1) describe the processes that drive changes in GMSL; 2) discuss why changes in RSL in Boston Harbor diverge from (are greater than) the global average; 3) provide an updated set of probabilistic RSL projections for Boston Harbor up to the year 2200; and 4) provide an assessment of time-evolving flood hazard.

In line with the BRAG report, we continue to use a 19-year average of sea level centered on the year 2000 as our reference “baseline.” This averaging reduces influences of tidal and seasonal cycles, and inter-annual climate variability on the reference level, although as discussed below, seasonal to decadal cycles in tidal range are important for projections of the expected frequency of future flood events in Boston Harbor (Baranes et al., 2020; Ray and Foster, 2016; Talke et al., 2018). The impact of Boston’s time-varying tidal range was not considered by the 2016 BRAG report, but is considered here, representing a substantial advance of the science.

This GBRAG sea level assessment focuses on Boston Harbor. The projected magnitude of future sea level rise in Boston Harbor is broadly representative (within a few percent) of sea level rise expected between the Cape Cod Canal and the New Hampshire border. However, we caution that the projected frequency and magnitude of extreme flood events reported here are specific to the location of the Boston Harbor NOAA tide gauge. Relative impacts of storm surge, waves, and tides vary even within the confines of Boston Harbor, so there will also be spatial variability in future flood hazard within the harbor.

This report maintains consistency with the 2016 BRAG report by considering the widely used Representative Concentration Pathways (RCPs) (Meinshausen et al., 2011; van Vuuren et al., 2011) to represent

a plausible range of future climate scenarios over the coming decades and centuries. The RCPs (RCP2.6, RCP4.5 and RCP8.5) refer to the approximate radiative forcing (added surface energy flux) in Watts per square meter (W m^{-2}) in the year 2100, resulting from aggregated, anthropogenically caused changes in the concentration of radiatively important atmospheric trace gasses and aerosols including CO₂, CH₄, N₂O, and tropospheric ozone. As a general guide, RCP2.6 assumes strict reductions in greenhouse emissions by the mid 20th century and net zero emissions by 2080, broadly consistent with the aspirations of the Paris Climate Agreement to limit global warming to < 2 °C in 2100 relative to pre-industrial conditions. In contrast, RCP8.5 is a more extreme but possible scenario (Schwalm et al., 2020), assuming ongoing, fossil-fuel driven economic growth. RCP4.5 is an intermediate scenario assuming a slow reduction in greenhouse gas emission after 2050. Based on the IPCC AR5 report (Stocker et al., 2013) that relied on an earlier generation of climate models known as CMIP5 (the 5th phase of the Coupled Model Intercomparison Project (Taylor et al., 2012)), global warming in 2100 is forecast to be 1.3 to 2.2 °C under RCP2.6, 1.9 to 3.3 °C under RCP4.5, and 3.3 to 5.5 °C under RCP8.5. An updated suite of climate model simulations (CMIP6) (Eyring et al., 2016) was not available in time to be used in the sea level analysis reported here.

4.3 HOW FAST IS GLOBAL MEAN SEA LEVEL (GMSL) RISING AND WHY?

Over most of the 20th Century, GMSL rose at an average rate of around 1.1 to 1.3 mm yr⁻¹ (Dangendorf et al., 2017; Hay et al., 2015). Since ~1990, the pace of sea level rise has accelerated sharply (Nerem et al., 2018). The IPCC SROCC (Oppenheimer et al., 2019) assessed the average rate of GMSL rise between 1993 and 2015 to be 3.16 mm yr⁻¹ (50th percentile), increasing to nearly 3.6 mm yr⁻¹ over the decade between 2006 and 2015. As described below, much of this late 20th century and early 21st century acceleration has been attributed to increasing ice loss on Greenland (Nerem et al., 2018; Shepherd et al., 2020), although Antarctica has the potential to become an even greater contributor in future decades (DeConto and Pollard, 2016; Oppenheimer et al., 2019; Pattyn et al., 2018).

On decadal to century timescales, trends in GMSL are dominated by changes in the volume of water in the ocean basins. The volume of ocean water can change in one of two ways. Water can be added (or lost) to (from) the ocean through changes in the amount of ice stored on land (in glaciers and ice sheets) and water stored in lakes and groundwater. Alternatively, ocean volume can increase in response to changes in the average density of sea water. Water density decreases (volume increases) with ocean warming, freshening, or both. As a result, sea level can rise without inputs of water from melting land ice or other sources. The oceans are absorbing ~90% of the excess heating associated with greenhouse gas emissions, especially in the upper 2000 m of the water column (Pörtner et al., 2019). The resulting thermal expansion of the ocean was the dominant contributor to GMSL rise (~14 cm) over the 20th century (Hay et al., 2015). The oceans continue to warm and the last five years (2016 to 2019) are the warmest in the instrumental record of ocean temperature (Cheng et al., 2020), yet the loss of land ice has recently (since ~2006) superseded thermal expansion as the primary contributor to sea level rise (Oppenheimer et al., 2019). This signifies an important change in the Earth system, in part because the loss of land ice has far greater potential to raise sea level than thermal expansion, especially on century and longer timescales.

Over the last decade, the Greenland Ice Sheet and its peripheral glaciers has begun to dominate contributions to GMSL rise from land ice. According to the IPCC SROCC (Oppenheimer et al., 2019), between 2006 and 2015, Greenland's contribution to GMSL rise was 0.77 mm yr⁻¹ (0.72 to 0.82 mm yr⁻¹, 5 to 95% range), versus 0.61 mm yr⁻¹ (0.72 to 0.82 mm yr⁻¹) from mountain glaciers, and ~0.43 mm yr⁻¹ (0.34 to 0.52 mm yr⁻¹) from Antarctica. While mountain glaciers are still contributing almost as much to GMSL as the Greenland Ice Sheet, their potential to cause sea level rise is limited to < 40 cm. In sharp contrast, the Greenland Ice Sheet contains enough ice to cause 7.4 m of GMSL rise if entirely lost (Morlighem et al., 2014). The small current contribution to sea level rise from Antarctica belies its

potential to become the single greatest contributor to sea level rise in the future. The Antarctic Ice Sheet contains the equivalent of 58 m of sea level rise (Morlighem et al., 2020); and while it is currently contributing less sea level rise than mountain glaciers or Greenland, Antarctica's pace of ice loss tripled between 2012 and 2017 relative to the previous two decades (Shepherd et al., 2018). Even a small fractional loss of the Antarctic Ice Sheet in the future will present significant challenges for the New England coastline.

In addition to thermal expansion and the loss of land ice, anthropogenic changes in land water storage and groundwater pumping also contribute to changes in GMSL. The net effect of land-water storage over the last decade or so (2006 to 2015) has produced a negative contribution to GMSL rise of about -0.21 mm yr^{-1} (WCRP Global Sea Level Budget Group (WCRP, 2018)), but this negative contribution is small relative to the positive contributions from thermal expansion and loss of land ice that dominate the signal.

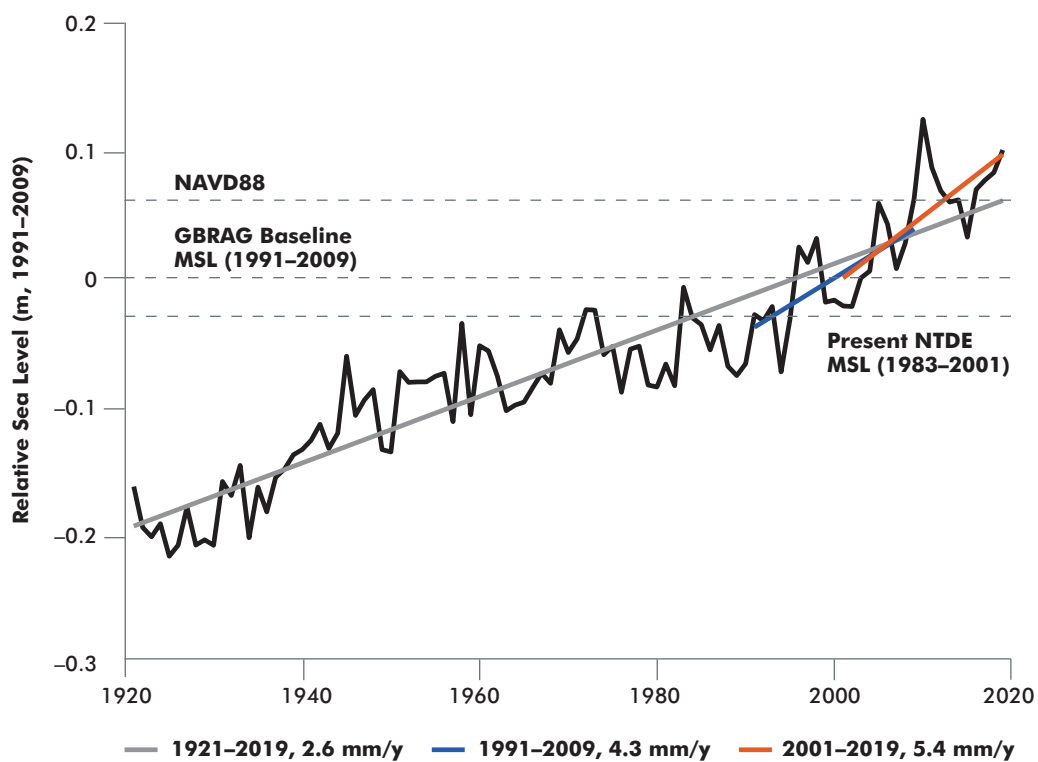
On shorter (annual and interannual) timescales, climate-driven fluctuations in rainfall patterns and the fraction of rain falling (and temporarily stored) on land versus the ocean can also change ocean volume (Cazenave et al., 2012; Hamlington et al., 2020; Nerem et al., 2018). These ephemeral influences on GMSL are also small relative to longer-term trends, and because they are influenced by coupled ocean-atmospheric oscillations such as El Niño, they are difficult to predict so they are ignored here as in most other future sea level assessments.

4.4 WHY IS RELATIVE SEA LEVEL (RSL) RISING FASTER IN BOSTON THAN THE GLOBAL AVERAGE?

RSL at specific locations like Boston Harbor is the complex sum of multiple processes operating at global, regional, and local spatial scales, and over a wide range of timescales. Changes in RSL deviate from GMSL due to regional and local effects that influence local sea surface heights, the elevation of the underlying

Figure 4.1

Relative sea level change at the Boston Harbor tide gauge station (#8443970) over the last century.



GBRAG uses a mean sea level reference based on a 19-year average from 1991 to 2009. The NAVD 88 (North American Vertical Datum of 1988), and NOAA's standard NTDE (National Tidal Datum Epoch) are shown for comparison. Note the substantial interannual variability and accelerating pace of RSL rise in recent decades. This Boston Harbor tide gauge station provides the reference location for the sea level projections provided here.

land surface, or both. Importantly, the sum of these processes (described briefly below) is causing RSL in Boston Harbor to rise faster than the global average.

RSL at the Boston Harbor tide gauge station rose at an average pace of around 4.3 mm yr^{-1} over the 1991 to 2009 reference period, albeit with considerable interannual variability (Figure 4.1). Boston's faster-than-average pace of sea level rise can largely be attributed to vertical land motion (VLM) of the Massachusetts coastline. VLM is driven by geodynamical processes largely unrelated to current climate change. The land surface in Eastern Massachusetts and the adjacent sea floor is currently sinking (Piecuch et al., 2018), because it was on an elevated flexural "forebulge" during the last glacial period (around 20,000 years ago), near the margin of the Laurentide Ice Sheet that covered much of North America. Flexural loading and subsequent unloading of the ice sheet on the Earth's crust, viscous flow of the underlying mantle, and redistribution of mass (which effects the Earth's gravitational field and Earth's rotation) continue today, long after the disappearance of the ice sheet (Peltier, 2004). Model calculations of these ongoing, viscoelastic glacio-isostatic adjustments (GIA) report an ongoing contribution to RSL of $\sim 1.0 \text{ mm yr}^{-1}$ in the vicinity of Boston, with a trend toward higher values south of Cape Cod, and lower values North of Boston in the Gulf of Maine (Piecuch et al., 2018). Analysis of geological records of VLM over the last several millennia (Engelhart and Horton, 2012; Kopp et al., 2016) are broadly consistent with the geophysical models, indicating an ongoing GIA contribution to VLM in the Greater Boston area of $0.8 \pm 0.3 \text{ mm yr}^{-1}$ (Kopp et al., 2013). This estimate of $0.8 \pm 0.3 \text{ mm yr}^{-1}$, determined by a statistical model applied to a global compilation of RSL trends designed to extract local trends, is fully consistent with the independent estimate of Zervas et al. (2013), who used RSL measurements at the Boston Harbor tide gauge, adjusted for monthly ocean-driven changes and an assumed long-term (20th to early 21st century) GMSL rise of 1.7 mm yr^{-1} (Church et al., 2013). This residual method results in a VLM estimate of 0.84 mm yr^{-1} . Based on the consistency of these published estimates, we continue to use $0.8 \pm 0.3 \text{ mm yr}^{-1}$ (Kopp et al., 2013) as the non-climatic, VLM contribution to RSL rise in Boston Harbor. It is worth emphasizing that the rates of these post-glacial GIA processes are not expected to change over the next few centuries, so RSL in Boston Harbor will continue to rise by nearly a mm yr^{-1} , regardless of climate change.

Other geological and anthropogenic factors can contribute to VLM, including plate tectonics (Van De Plassche et al., 2014), and mantle convective processes that cause "dynamic topography" (Moucha et al., 2008), but these processes can be considered negligible over the next few centuries in Boston, so they are ignored here as they were by the 2016 BRAG report. Sediment compaction and groundwater extraction can be highly impactful on VLM in many places around the world (Oppenheimer et al., 2019). However, these processes are likely to be localized in the Greater Boston region. Furthermore, the Boston Harbor tide gauge is anchored on bedrock rather than compacting sediment, where we can assume GIA is the dominant contributor to the $0.8 \pm 0.3 \text{ mm yr}^{-1}$ of VLM.

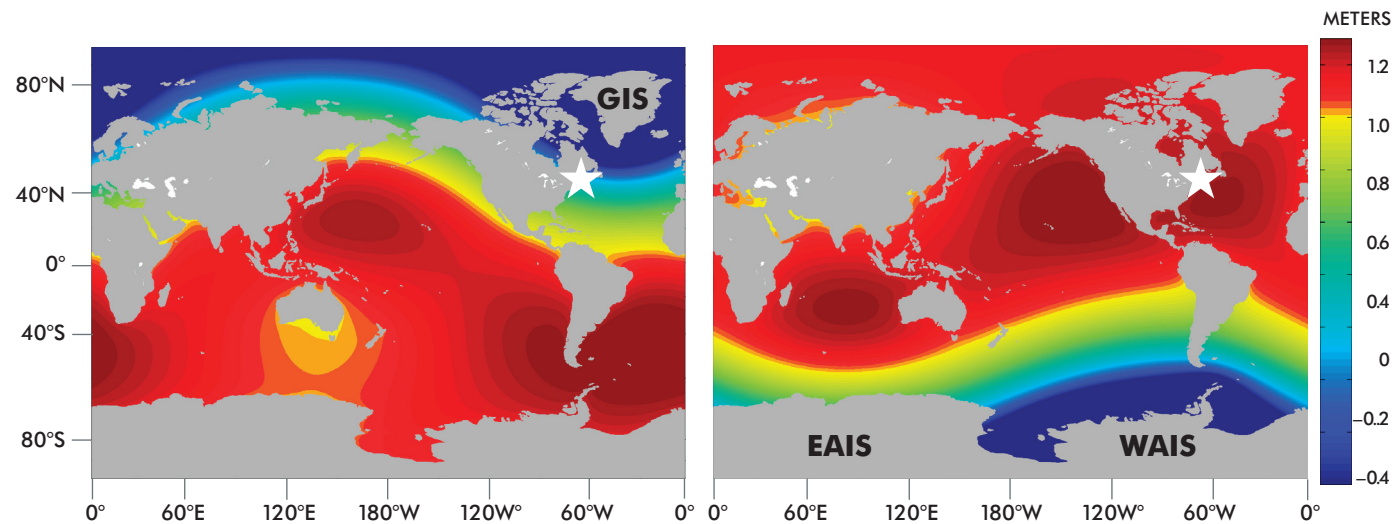
Departures in RSL from GMSL are also caused by regional-to-local changes in sea surface heights, in addition to VLM. The dominant processes include changes in prevailing winds and ocean currents, and changes in the distribution of heat and salt within the ocean (Yin, 2012; Yin and Goddard, 2013; Yin et al., 2009). Collectively, these processes control "dynamic" sea level changes. The Northeast U.S. is especially sensitive to changes in the strength and position of the Gulf Stream and more broadly in the strength of the Atlantic Meridional Overturning Circulation (AMOC). Under the high emissions RCP8.5 scenario, persistent dynamical changes have the potential to cause $> 10 \text{ cm}$ of sea level rise along the New England coast by 2100, and $> 30 \text{ cm}$ by 2300 (Yin, 2012). Because of their large potential magnitude, these processes are considered in the future sea level projections provided here. Dynamic climate processes can also cause considerable year-to-year variability in sea level at specific locations like Boston. For example, the dominant peak in RSL in 2009 to 2010 clearly seen in Figure 4.1 has been associated with a temporary slowdown in the Atlantic Meridional Overturning ocean Circulation (AMOC) and a northeasterly anomaly in offshore winds associated with a strongly negative North Atlantic Oscillation (NAO) index

(Goddard et al., 2015). Northeasterly winds tend to push more surface waters toward the New England coast. Such influences of interannual climatic variability in RSL change are not directly accounted for in the sea level projections provided here, but it should be acknowledged that year-to-year variations around the long-term trend (Figure 4.1) will continue.

Lastly, global redistributions of mass as glaciers and ice caps gain and lose ice not only deform the shape of the Earth (which can contribute to long-term trends in VLM as noted above), they also affect the Earth's gravitational field and its pole of rotation (Mitrovica et al., 2011). These latter, near-instantaneous effects can cause departures in regional sea level relative to the global average by up to ~30% (Oppenheimer et al., 2019). Close to the source of ice loss (within ~2000 km), the relaxing gravitational attraction between land ice and the proximal ocean causes a drop in RSL, even though the ice loss causes a globally averaged rise in sea level (Figure 4.2). Distal from the source of ice loss (beyond ~6000 km), regional sea level rise becomes amplified relative to the global average. These patterns or "fingerprints" of sea level rise are further modified by adjustments in the Earth's pole of rotation (Mitrovica et al., 2011). Because of Boston's proximity to the Greenland Ice Sheet, Boston only "feels" about 30% of the sea level rise contributed by the loss of ice on Greenland. In contrast, Boston experiences 125% of the sea level rise contributed by ice loss in West Antarctica (Figure 4.2), the sector of the Antarctic Ice Sheet where ice loss is currently accelerating (Shepherd et al., 2019). Because these gravitational, rotational, and deformation processes have such a strong modifying influence on sea level rise in Massachusetts, fingerprint calculations based on the future projected loss of Greenland vs. Antarctic ice must also be considered. Sea level fingerprints were accounted for in the future sea level projections provided by the BRAG (Douglas et al., 2016), and the same methodology is adopted here.

Figure 4.2

Spatial heterogeneity of sea level change due to gravitational, rotational, and deformational effects arising from an equivalent loss of ice from the Greenland Ice Sheet (GIS; left) versus the West Antarctic Ice Sheet (WAIS; right). Boston's location is indicated by the white star.



Colors show meters of sea level rise that would occur if each ice sheet were to lose enough ice to cause a 1-meter rise in GMSL. Locations with values greater than 1 (orange-red) experience more sea level rise than the global average, while locations with values less than 1 (blue-yellow) experience less. Dark blue colors (proximal to the ice sheet losing mass) indicate a sea level fall despite a globally averaged rise. The pattern can be scaled up or down for more or less ice loss. Boston is clearly more vulnerable to sea level rise caused by an equivalent loss of ice on West Antarctica than on Greenland. Most (~90%) Antarctic ice is stored in the East Antarctic Ice Sheet (EAIS). However, the smaller WAIS, which contains enough ice to raise GMSL by ~5 m, is currently losing ice (Shepherd et al., 2019) and is particularly vulnerable to future warming (DeConto et al., 2021), adding to Boston's sea level exposure. Adapted from Hay et al., 2014.

As a net result of the regional processes described above, the pace of RSL in Boston Harbor has increased to 5.4 mm yr⁻¹ over the last two decades, contributing about 4.9 cm (~2 in) of sea level rise relative to the 2000 baseline. As discussed below, this accelerating rise in RSL (Figure 4.1) is already creating significant challenges for the Boston area, including a sharp increase in the number of tidally driven, clear sky “nuisance” flooding events (Sweet et al., 2020), and increased risk of extreme flooding during tropical cyclone (TC) and winter storm events (Baranes et al., 2020).

4.5 FUTURE SEA LEVEL PROJECTIONS

A range of methodologies have been used to project future sea level rise (see Horton et al. (2018) for a recent review). These include the extrapolation of recent trends into the future (Nerem et al., 2018), semiempirical methods (Rahmstorf et al., 2012) that apply statistical relationships between observed changes in climate and sea level, structured expert judgment (Bamber et al., 2019), and more physically based approaches using computer models that directly simulate changes in the components of the climate system that contribute to sea level change (Church et al., 2013; Moore et al., 2013; Oppenheimer et al., 2019). These components include the atmosphere that impacts surface mass balance of glaciers and ice sheets, ocean temperatures and currents that contribute to thermal expansion and dynamic sea level rise, and the melting and seaward flow (glacial dynamics) of the ice sheets on Greenland and Antarctica.

Limitations of semiempirical methods include reliance on limited observational data, and, perhaps more importantly, the assumption that past relationships between climate change and sea level will be similar in the future (Moore et al., 2013). Physically based models of the Earth’s climate system and ice sheets have the advantage that the models represent the individual components of the sea level budget, including the processes that contribute to regional departures in sea level from the global mean (Kopp et al., 2017; Kopp et al., 2014). Multi-model climate ensembles, like those relied upon by the IPCC (Taylor et al., 2012), provide global projections of future temperature and precipitation over land areas, and temperature, salinity, and currents in the ocean. These climate model simulations can be used in ‘offline’ calculations of future contributions to sea level from mountain glaciers (in response to predicted changes in temperature and precipitation), and regional contributions from ocean thermal expansion, and ocean dynamics (Kopp et al., 2014). Corresponding contributions to sea level rise from the Greenland and Antarctic ice sheets, the largest potential contributors to future sea level, can be provided directly by ice sheet models, under the same RCP emissions scenarios considered by climate models. However, we emphasize that uncertainty in the future climate projections that provide the basis for estimating these individual components of sea level change is considerable. This uncertainty is largely due to unknown future greenhouse gas emissions (which will be the result of future human decision making), and to a lesser extent, ongoing uncertainties in model representations of specific processes such as clouds and precipitation (Flato et al., 2013) and interactions between ice sheets and the ocean (Asay-Davis et al., 2017), among others.

At their core, the GBRAG sea level projections provided here are physically based. Structured expert judgement (SEJ), using calibrated responses (best guesses) from leading climate and cryosphere scientists (Bamber and Aspinall, 2013; Bamber et al., 2019), provides a complementary approach to physically based estimates of future sea level rise. SEJ has been considered by the IPCC along side physically based estimates of future sea level rise (Church et al., 2013; Oppenheimer et al., 2019). As explained below, SEJ is considered here for comparison with our physically based approach and to inform the shape of the tails of future sea level probability distributions outside the likely range of available projections.

4.6 FUTURE LOSS OF THE GREENLAND AND ANTARCTIC ICE SHEETS

The current generation of Greenland and Antarctic ice sheet models capture changes in the surface mass balance of ice sheets (precipitation minus sublimation and melting) in response to changing temperatures and precipitation (provided by global and regional climate models), the dynamic flow of glacial ice into the ocean where marine-terminating glacial ice is added to the ocean through melting and calving of icebergs, and interactions between the flowing ice and the underlying bedrock. The fidelity of Greenland and Antarctic ice sheet models has improved markedly over recent years (Bulthuis et al., 2019; Fürst et al., 2015; Schlegel et al., 2018) and they are increasingly used in future sea level projections and assessments (Kopp et al., 2017; Levermann et al., 2020; Oppenheimer et al., 2019).

Greenland's current ice loss (Shepherd et al., 2020) is dominated (~60%) by surface mass balance processes (mainly melting and runoff), rather than dynamic discharge to the ocean (van den Broeke et al., 2016) and this trend is expected to continue into the future (Oppenheimer et al., 2019). As a result, uncertainties in Greenland Ice Sheet model projections mainly stem from uncertainties in future trends in Greenland's temperature, precipitation, and clouds (Edwards et al., 2014; Pattyn et al., 2018; Van Tricht et al., 2016). Greenland air temperatures are warming at about twice the rate of the global average. This amplified warming or "Arctic amplification" is largely attributed to a positive feedback between the loss of Arctic sea ice and absorption of solar energy (Dai et al., 2019). Large-scale atmospheric circulation patterns are also impactful on year-to-year melt patterns on Greenland (Tedesco et al., 2016b), and sustained future trends in circulation could become important on longer timescales. Positive feedbacks between warming and melt on Greenland are also critically important. These warming-melt feedbacks are associated with the lowering of the ice sheet surface into warmer altitudes, darkening of the ice surface caused by expanding meltwater ponds, changes in the water content (and albedo) of snow and firn (the transitional stage between snow and the underlying ice), and microbial/algal material accumulating on the ice-sheet surface (Pattyn et al., 2018; Ryan et al., 2018; Tedesco et al., 2016a). As a result of these positive melt feedbacks, a critical threshold might be exceeded, whereby the ice sheet continues to melt over thousands of years until it is lost almost entirely (Gregory et al., 2020), regardless of a future stabilization in temperature (Pattyn et al., 2018).

Greenland's projected contribution to GMSL in recent modeling studies (Aschwanden et al., 2019; Calov et al., 2018; Fürst et al., 2015; Golledge et al., 2019; Vizcaino et al., 2015) appearing since the publication of the IPCC AR5 (Church et al., 2013) have changed little. Because of this consistency, the IPCC SROCC assessment (Oppenheimer et al., 2019) found no reason to update the earlier AR5 estimates for Greenland's future contribution to sea level. The projected Greenland contributions (17th to 83rd percentile likely range) in 2100 are 4 to 10 cm under the RCP2.6 scenario, 4 to 13 cm under RCP4.5, and 7 to 21 cm under RCP8.5. The wide range of values mainly stems from uncertain regional climate trends around Greenland and the strength of the warming-melt feedbacks mentioned above.

While uncertainty in Greenland's future contribution to GMSL is considerable, uncertainty in the Antarctic contribution to future sea level is far greater. This is especially true in the second half of the 21st century and beyond (Kopp et al., 2017). The larger sea level uncertainty associated with Antarctica is largely dynamic in nature (DeConto and Pollard, 2016) rather than climatic as it is for Greenland. As discussed in detail in the IPCC SROCC (Oppenheimer et al., 2019), the Antarctic Ice Sheet is fundamentally different from the Greenland Ice Sheet. Most of the Greenland ice sheet margin terminates on land, with marine-terminating valley glaciers reaching the ocean in relatively narrow (~5 to 10 km) fjords. In contrast, most of the much larger and thicker Antarctic Ice Sheet margin terminates directly in the ocean, with the edges of the ice sheet in direct contact with relatively warm ocean water that melts the ice from below. In addition, much of the underlying bed of the Antarctic Ice Sheet (Morlighem et al., 2020) is far below sea level (more than 2000 meters in places). This is especially true in West Antarctica, where most

of the West Antarctic Ice Sheet sits in a deep, bowl-shaped subglacial basin, with the bedrock sloping downwards (landward) from the marine-terminating edge of the ice sheet toward the ice sheet interior. In the absence of floating ice shelves (seaward flowing extensions of marine terminating ice) that can touch down or “pin” on underlying irregularities on the sea floor or scrape along the rock walls of fjords and embayments to offer some resistive stress (buttressing) to the glacial ice upstream, unbuttressed marine-terminating ice margins on reverse sloped bedrock are conditionally unstable (Gudmundsson et al., 2012). This instability is caused by rapidly increasing seaward ice flow as a function of the ice thickness at the “grounding line,” the point where the seaward flowing ice margin begins to float to form an ice shelf (Schoof, 2007; Weertman, 1974). Once an Antarctic ice margin begins to retreat and back up into a deep basin, the ice thickness increases as does ice flow into the ocean. This positive feedback between ice thickness and ice loss is called the “marine ice sheet instability (MISI),” and it makes much of the Antarctic Ice Sheet margin vulnerable to rapid ice loss. The main trigger for the onset of MISI is the initial loss of buttressing ice shelves. Antarctic ice shelves are observed to be thinning in many places today as a result of warm subsurface ocean waters attacking the shelves from below (Paolo et al., 2015). MISI has been attributed to accelerating ice loss in West Antarctica (Rignot et al., 2014) and since the publication of the IPCC AR5 (Church et al., 2013), observations and supporting numerical modeling have increased confidence that MISI will continue to contribute to future sea level rise. As a result, Antarctic ice sheet models that account for MISI dynamics were included in the updated IPCC SROCC sea level projections (Oppenheimer et al., 2019), which substantially increases future sea level relative to AR5 under RCP8.5 forcing, especially beyond 2100.

Another process was recently proposed (DeConto and Pollard, 2016; Pollard et al., 2015) that could cause even faster rates of Antarctic ice loss than MISI. This latter process is related to brittle ice processes (meltwater enhanced crevassing and calving) rather than the ductile (flow) dominated processes related to MISI. These brittle processes can be initiated by the appearance of surface meltwater that can quickly break up buttressing ice shelves as has been observed to occur in Antarctica (Scambos et al., 2017). The loss of buttressing ice shelves is followed by the onset of MISI in the seaward flowing glaciers that are no longer buttressed, and possibly the onset of very rapid calving where thick ice fronts terminate in deep water (Parizek et al., 2019). The potential for runaway structural failure of thick, unbuttressed ice margins is called the marine ice cliff instability (MICI), to differentiate between flow-driven MISI and fracture-driven MICI (DeConto and Pollard, 2016).

MICI processes are currently the focus of intense study by the glaciological community. To date, MICI has only been incorporated into one continental-scale ice sheet model (DeConto and Pollard, 2016) and the potential for this process to drive rapid sea level rise remains very uncertain (Edwards et al., 2019; Pattyn et al., 2018). Despite this uncertainty (DeConto and Pollard, 2016; DeConto et al., 2021) showed that if Antarctic glaciers reaching the ocean someday lose their buttressing ice shelves and begin to calve at the same rate as their smaller counterparts on Greenland, the combination of MISI and MICI could contribute > 5 cm per year of GMSL rise from Antarctica alone, possibly beginning in the late 21st century. This possibility of the MICI process becoming widespread on a warming Antarctica creates deep uncertainty on the upper bound of sea level projections at the end of the 21st century and beyond, particularly under RCP8.5 (Oppenheimer et al., 2019). Onset of widespread MICI within the 21st century is generally considered unlikely, but it would be globally devastating, with the potential to cause multi-meter sea level rise on century timescales. Boston would be impacted more than many other coastal cities, because of the fingerprint pattern associated with ice loss on West Antarctica (Figure 4.2).

The 2016 BRAG report used the time-evolving RCP2.6, 4.5 and 8.5 projections of the Antarctic contribution to GMSL rise that considered a combination of MISI and MICI processes (DeConto and Pollard, 2016). However, due to ongoing uncertainties in the MICI process and the timing when it might be triggered, the IPCC SROCC Antarctic results (Oppenheimer et al., 2019), did not include

the (DeConto and Pollard, 2016) directly in their sea level projections. Nonetheless, IPCC SROCC did emphasize that the onset of MICI in Antarctica as described in (DeConto and Pollard, 2016) could produce future rates of sea level rise much higher than the top of the likely range (83rd percentile) reported by SROCC and we emphasize that assessment again here. IPCC SROCC's reliance on process-based Antarctic ice sheet models that account for MISI (Bulthuis et al., 2019; Golledge et al., 2019; Golledge et al., 2015; Levermann et al., 2014; Ritz et al., 2015), but not MICI (DeConto and Pollard, 2016), still results in a substantial increase in high emissions sea level projections, relative to those provided by IPCC AR5 (Church et al., 2013). SROCC projections (median and 17th to 83rd percentiles) of GMSL in 2100 under RCP8.5 are 0.84 (0.61 to 1.10), about 10 cm higher than AR5. On longer timescales, IPCC SROCC assessed the likely range of GMSL rise in 2300 to be 2.3 to 5.4 m, higher than in AR5 (0.92 to 3.59 m), but far less than estimates including MICI in Antarctica.

4.7 GBRAG VERSUS BRAG SEA LEVEL PROJECTIONS

We emphasize that an important difference between this GBRAG report and the 2016 BRAG report is this report's use of the new IPCC SROCC projections of Antarctica's contribution to future RSL rise in Boston, rather than using the more extreme (DeConto and Pollard, 2016) Antarctic estimates directly accounting for MICI. As shown below, this has slightly increased our GBRAG projections in the early 21st century, but it has substantially reduced our RSL estimates in the late 21st and 22nd centuries. With that said, we note that the upper bound of the uncertainty range remains high, largely due to ongoing uncertainties related to the Antarctic component.

We also emphasize that because of the positive warming-melt feedbacks on Greenland (Pattyn et al., 2018) and the Antarctic Ice Sheet's direct interaction with the surrounding (warming) ocean with a long thermal response time (Garbe et al., 2020), sea level rise contributed by both ice sheets should be considered irreversible and permanent on century timescales. The ice sheets will require a return to preindustrial and possibly colder (glacial-like) conditions to recover, and even then, the recovery may take thousands of years (Oppenheimer et al., 2019). This important point (that projected sea level rise should be considered permanent) is often underappreciated when assessing sea level impacts and when considering adaptation pathways.

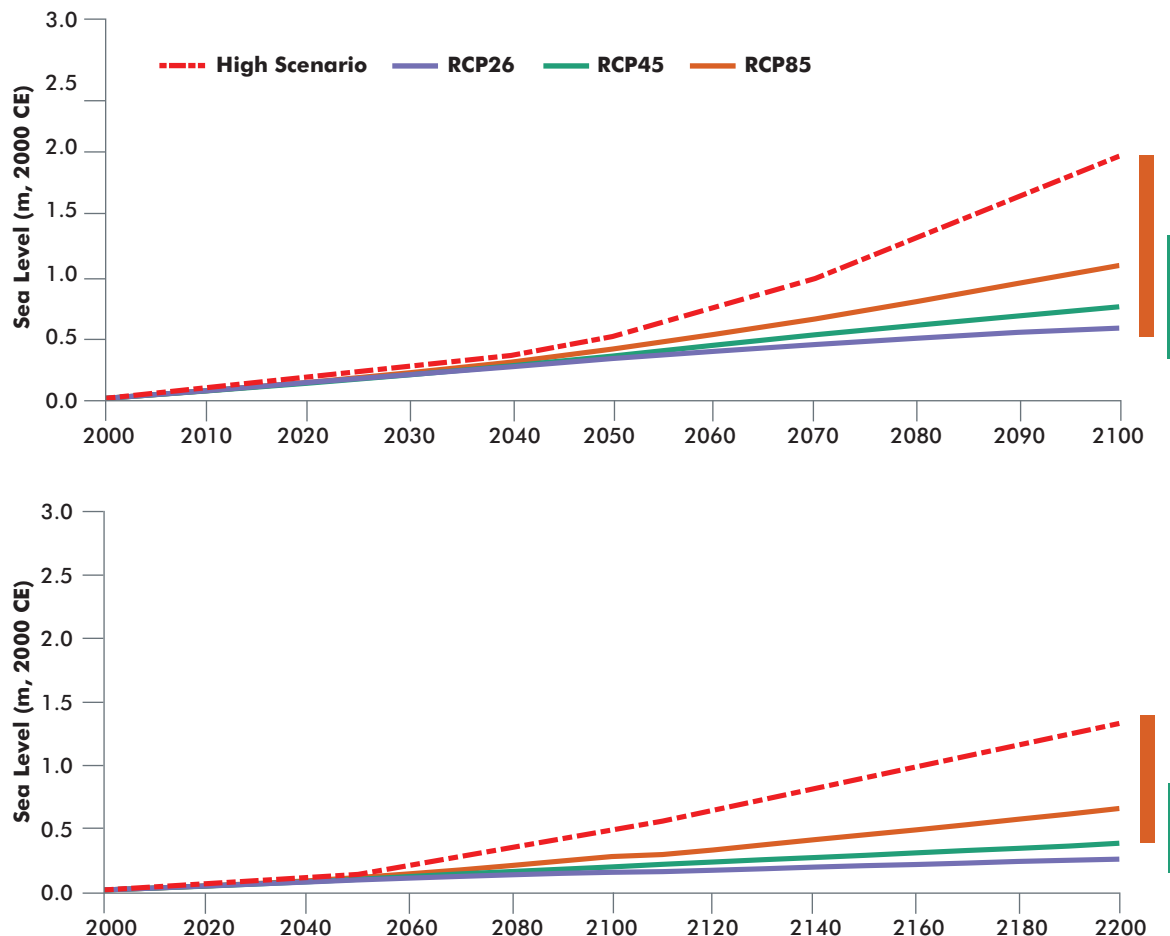
4.8 GBRAG RSL PROJECTIONS FOR BOSTON HARBOR

We follow the same statistical methodology (Kopp et al., 2017; Kopp et al., 2014) used in the 2016 BRAG report (Douglas et al., 2016), to generate updated probabilistic projections of future sea level rise in Boston Harbor. Probabilities (percentiles) of expected sea level rise provide a robust alternative to discrete sea level scenarios (Parris et al., 2012), sometimes described as "lowest," "intermediate low," "intermediate high," or "highest," as adapted for use by NOAA and in previous reports on Boston sea level rise (e.g., Bosma et al., 2015; CZM, 2013). The projections provided here are specific to the Boston Harbor tide gauge location which is anchored on bedrock and not susceptible to sediment compaction, unlike much of the Greater Boston coastline, and in particular, sections of the city built on fill. Due to a general lack in highly resolved data on the composition, age, and loading (construction) history of these areas, we do not consider the effect of compaction on the spatial heterogeneity of future rates in RSL.

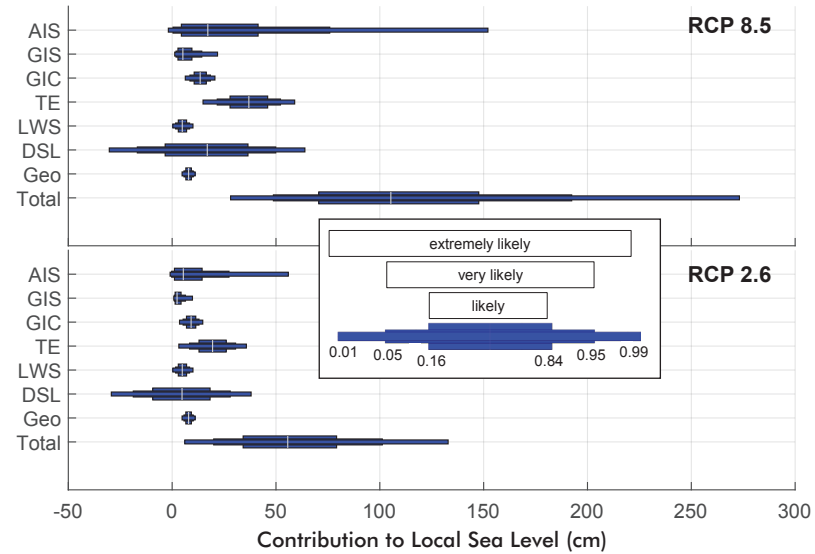
As noted above, the GBRAG projections of RSL (Figure 4.3,) are relative to the 19-year average, sea level baseline line, centered on the year 2000. The tabulated values (Table 4.1) are the departure of sea level relative to the baseline, calculated over 19-year periods centered on 2020, 2030, 2050, 2070, 2100, and 2200. Unlike the BRAG report, we provide an analysis of the time-evolving rate of sea level rise in addition to RSL heights (Figure 4.4). In some instances, the rate of sea level rise at a given time may be more informative for planning and engineering purposes than the absolute height of the sea surface.

Figure 4.3

GBRAG time series of RSL projections for Boston Harbor, showing the median (50th percentile) estimates (solid lines), with the 5th to 95th percentile (very likely) ranges in 2100 (top) and 2200 (bottom) indicated by the solid bars at right. These projections are equivalent to those shown in Table 1.



The high scenario (red dashed line) replaces the IPCC SROCC Greenland and Antarctic contributions used in our primary estimates, with probabilistic estimates from (Bamber et al., 2019) based on structured expert judgment and a conditional filter that produces 2 m of sea level rise by 2100, roughly equivalent to the 95th percentile outcome in Table 4.1. The inset at right, shows the relative contribution of each sea level component to the total uncertainty. Note the extreme uncertainty of the Antarctic Ice Sheet (AIS) component under RCP8.5, which is particularly relevant for Boston because of the gravitational/rotational/dynamical effects shown in Figure 4.2. AIS (Antarctic Ice Sheet), GIS (Greenland Ice Sheet), GIC (Glaciers and Ice Caps), TE (Thermal Expansion), LWS (Land Water Storage), DSL (Dynamic Sea Level), Geo (Geological Factors).



The RSL sea level projections (Figure 4.3; Table 4.1) are the time-averaged change in the vertical distance from the seabed and the sea surface at the Boston tide gauge site. With the exception of places where extreme compaction is underway, these RSL projections can be considered representative of Greater Boston. These RSL projections provide the background sea levels used to calculate projected changes in the frequency and height of future flood events (see “Coastal Flooding,” p. 80). Unlike the background RSL estimates (Figure 4.3), the extreme flood heights and frequencies provided later in the report are specific to the Boston Harbor tide gauge location and do not provide reliable guidance distal from the inner harbor.

The GBRAG RSL projections follow a well-established probabilistic approach (Kopp et al., 2017; Kopp et al., 2014) that aggregates the individual components of sea level change most relevant to Boston. The statistical methods used here are consistent with the 2016 BRAG report (DeConto et al., 2016), and recent sea level assessments provided for the State of California (Griggs et al., 2019) and New Jersey (Kopp et al., 2019). The individual components of RSL considered in the analysis include 1) projected changes in ocean thermal expansion, 2) North Atlantic Ocean dynamics, 3) ice lost from the Antarctic Ice Sheet, 4) ice lost from the Greenland Ice Sheet, 5) ice lost from mountain glaciers and ice caps, 6) global land water storage, and 7) vertical land motion at Boston Harbor. As in the BRAG report, projections of ocean thermal expansion and regional dynamic changes come from the ocean model component of CMIP5 (Taylor et al., 2012) Global Climate Models (GCMs). The sea level change contributed by anthropogenic land water storage is based on historical observations combined with population projections (Church et al., 2013; United Nations, 2012, 2014). Estimates of mountain glacier and ice cap loss are based on CMIP5 GCM projections of atmospheric warming over the global distribution of glaciers and ice caps. Greenland Ice Sheet melt is provided by the IPCC SROCC (2019) assessment, which is unchanged from the IPCC AR5 (2013) assessment used by the BRAG report. The most significant departure from the BRAG report is the replacement of the Antarctic sea level component (DeConto and Pollard, 2016), which is updated with the physically based assessment reported in the IPCC SROCC (2019). As in the BRAG report, we use SEJ (Bamber and Aspinall, 2013; Bamber et al., 2019) for guidance on the shapes of the tails outside the likely ranges of Greenland and Antarctic sea level contributions.

The individual contributions of sea level rise are combined along with their respective uncertainties, and Latin hypercube sampling (10,000 samples) is used to generate time-evolving probability distributions of RSL change at the Boston Harbor tide gauge location. Gravitational/rotational/dynamical effects (fingerprints) from varying contributions to sea level rise from ice loss in mountain glaciers and Greenland and Antarctic Ice Sheets are fully accounted for, as is the 0.8 ± 0.3 mm/yr of RSL rise caused by VLM. The probabilistic analysis is applied to RCP2.6, RCP4.5, and RCP8.5 greenhouse gas emissions scenarios, providing three discrete emissions-dependent probability distributions of sea level change from 2000 to 2200 (Figure 4.3). Importantly, updating the Antarctic component (DeConto and Pollard, 2016) used by BRAG with the new IPCC SROCC Antarctic projections (Oppenheimer et al., 2019) has reduced the central estimate of relative sea level rise in 2100 in the high emissions RCP8.5 scenario from 1.5 m (4.9 ft) to 1.05 m. However, it is important to stress that because of the deeply uncertain Antarctic component, sea level rise in 2100 in excess of 2 m (6.6 ft; 5% probability) cannot be ruled out (Table 4.1; Figure 4.3). The central estimate (median) of the rate of sea level rise in 2100 under RCP8.5 is approximately 1.5 cm yr^{-1} , which would be particularly challenging from a coastal resilience perspective (see Figure 4.4). The 95th percentile rate of sea level rise (top of the *very likely* range) is nearly 5 cm yr^{-1} in 2100, which would likely result in substantial parts of the Greater Boston coastline becoming difficult to manage. Because of the Antarctic uncertainty, we provide a time-evolving “high end” sea level rise scenario (Figure 4.3) roughly consistent with the 95th percentile of our main projections.

Table 4.1

Relative sea level probabilities for Boston Harbor relative to a 2000 baseline for three RCP greenhouse gas emissions scenarios.

				Likely range					
		0.99	0.95	0.83	0.5	0.17	0.05	0.01	0.001
RCP8.5	2020	1	5	8	13	17	21	25	31
	2030	4	9	14	20	27	33	40	54
	2050	12	19	27	39	52	65	83	127
	2070	19	31	44	63	85	109	145	239
	2100	28	49	72	105	146	192	273	476
	2200	118	148	184	257	378	550	904	1,690
RCP4.5	2020	3	6	8	12	15	18	21	25
	2030	6	10	14	19	24	28	33	43
	2050	9	16	23	34	44	54	66	95
	2070	13	23	34	50	68	84	105	161
	2100	16	31	48	73	100	129	173	290
	2200	23	54	89	147	230	335	543	1,050
RCP2.6	2020	3	6	9	13	16	19	22	27
	2030	4	8	13	19	25	30	35	44
	2050	4	12	20	32	43	53	64	85
	2070	6	16	27	43	59	73	90	130
	2100	6	20	35	56	78	101	133	214
	2200	41	54	69	97	143	208	341	680

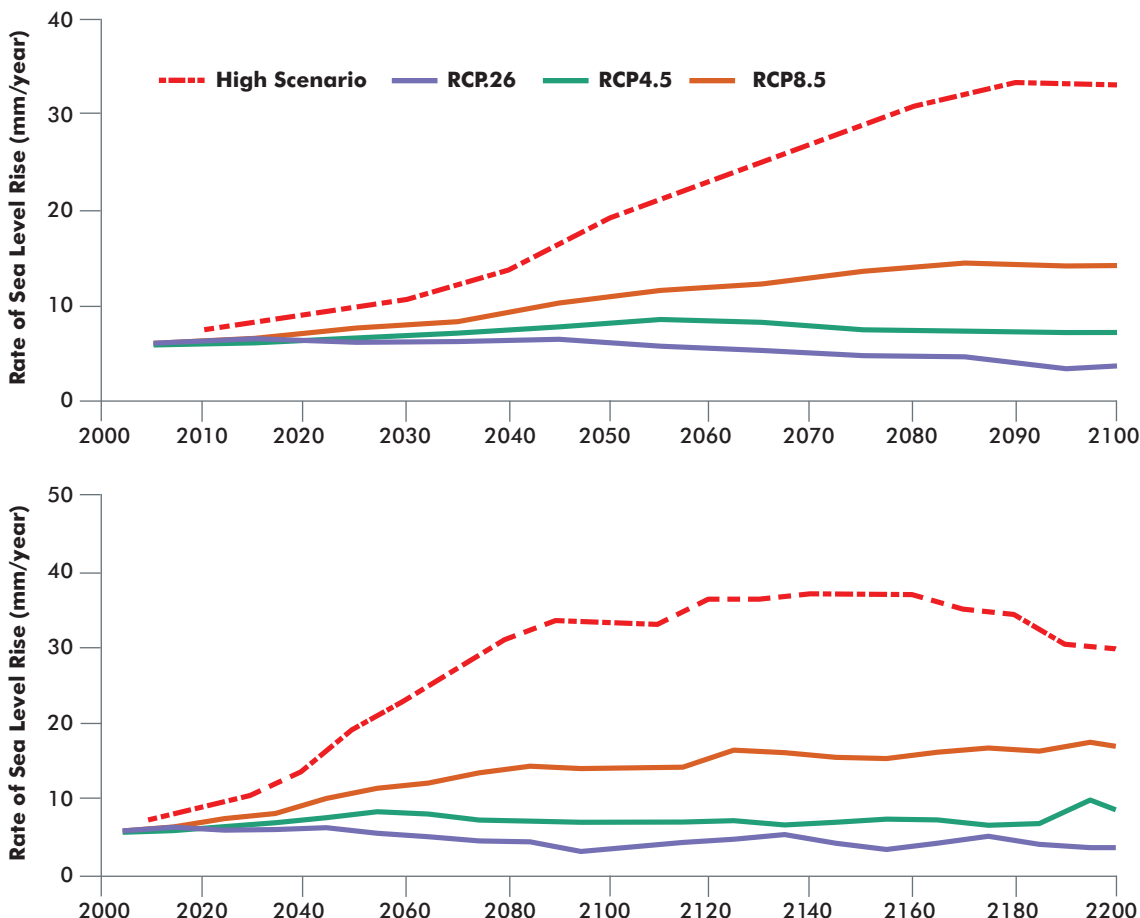
Values are in cm and columns show percentiles. 0.5 represents the 50th percentile (median) estimate, while 0.83 to 0.17 represent the 17th to 83rd percentile “likely range” of possible outcomes. There is a 66% likelihood that sea level will fall within the likely range (light blue columns), while there is a 5% chance that sea level will exceed the 0.05 (95th percentile) value.

4.9 COASTAL FLOODING

Relative sea level rise is increasing the frequency of coastal flooding on a global scale (e.g., Oppenheimer et al., 2019). Even under a regime of slow and steady sea level rise, flood frequency increases rapidly because lower-magnitude events with higher probabilities (i.e., routine storms that commonly impact the region) can cross flood thresholds on top of a higher baseline sea level (see Figure 4.5 for an illustration of this nonlinear response). Much of the discussion on specific mechanisms of coastal flooding in the 2016 BRAG report remains valid. Here, we use recent advances in flood hazard research to provide updated flood projections that incorporate the new probabilistic sea level rise scenarios presented above. Advances

Figure 4.4

Future rates of sea level rise (mm yr^{-1}) corresponding to the central (50th percentile) sea level projections shown in Figure 4.3.

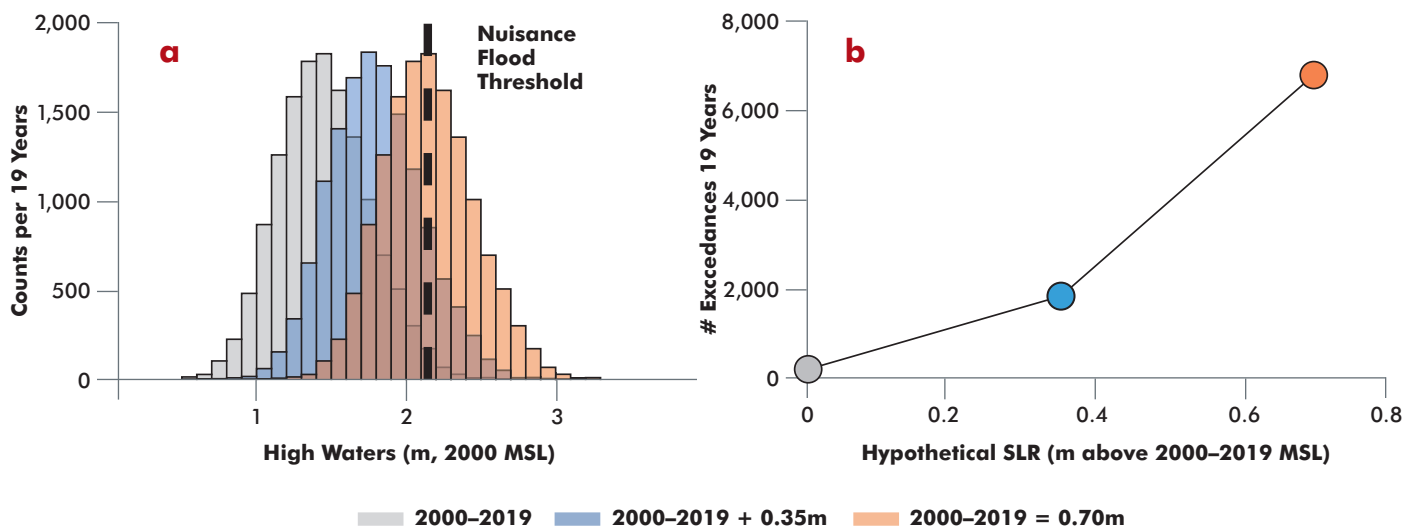


since the 2016 report include a reconstruction of Boston tidal and extreme water level measurements extending back to 1825 (Talke et al., 2018); statistical methods that incorporate the impact of Boston's large and time-varying tides on extreme flood frequencies (Baranes et al., 2020); updated extreme flooding projections for all of Massachusetts based on hydrodynamic modeling from Woods Hole Group; an improved understanding of mechanisms driving minor high tide flooding (also called "nuisance" flooding) in Boston (Ray & Foster, 2016); high tide flooding projections for Boston (Thompson et al., 2019; Sweet et al., 2018, 2020); and regional projections for the impacts of future changes in storm climatology on flood heights for both extratropical (Lin et al., 2019) and tropical cyclones (Marsooli et al., 2019).

Here, we 1) outline mechanisms of extreme coastal flooding in the Boston region; 2) describe the impacts of climatic and tidal variability on flood hazard; 3) provide context for two extreme flood events that impacted the region in January and March of 2018; and 4) provide projections of extreme flooding through 2100 at the location of the Boston tide gauge by combining the Baranes et al. (2020) methodology with probabilistic sea level rise projections (Figure 4.3). Lastly, we discuss mechanisms and recent projections of high tide "nuisance" flooding in Boston (e.g., Thompson et al., 2019; Sweet et al., 2020).

Figure 4.5

Illustration of a nonlinear increase in flood hazard driven by relative sea level rise.



(a) Binned counts of high-water elevations per 19 years relative to the Boston threshold for high tide flooding (2.15 m above 2000 MSL; (Sweet et al., 2018)). 2001 to 2019 high waters are measured values from the Boston tide gauge (grey-shading). Blue and red shading show hypothetical future high-water elevations with 0.35 and 0.70 m of sea-level rise relative to 2001 to 2019 (similar to median RCP4.5 projections for 2050 and 2100, Table 4.1). Sea level rise causes the high-water distributions to shift to the right, such that each 0.35-m shift increases the number of high water events that exceed the nuisance flood threshold. This non-linear response is represented by an increasingly large area under the curve falling to the right of the flood threshold line. (b) Hypothetical sea level rise versus 19-year total number of high waters exceeding the nuisance flood threshold (i.e., area under curve to the right of the flood threshold line in a). The steeper slope between the blue and red points illustrates the nonlinear increase in flood hazard driven by a constant rate of sea level rise.

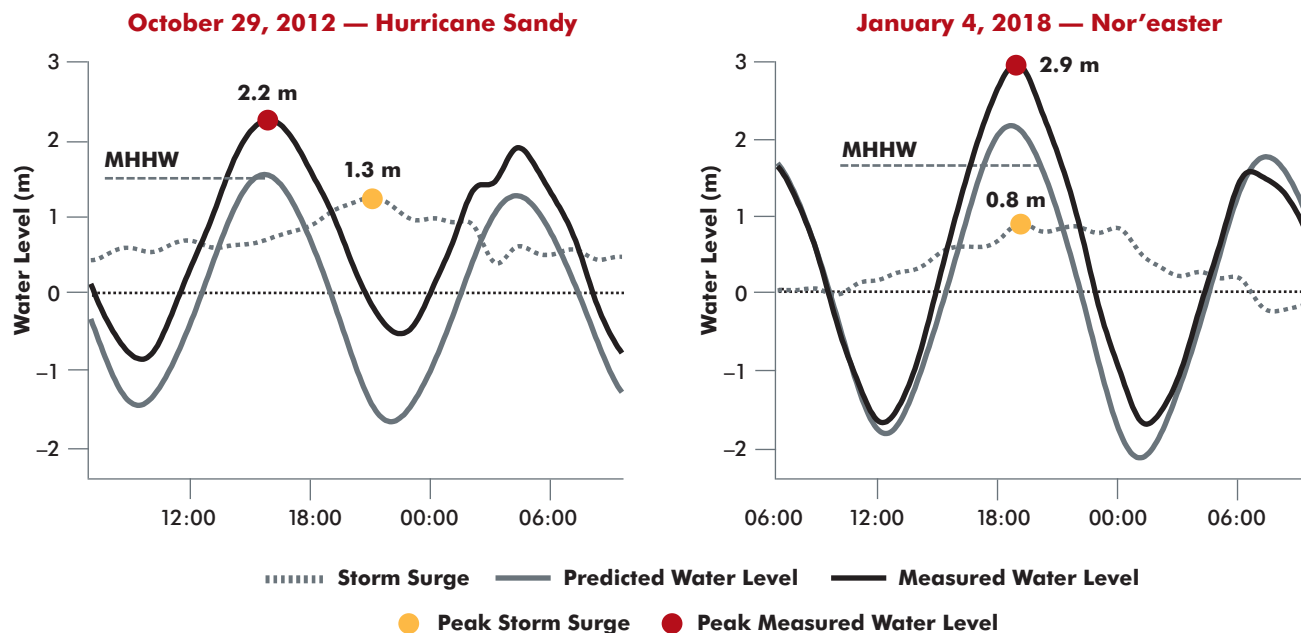
Mechanisms of coastal flooding

Extreme sea levels are caused by the combined impacts of rising sea level, high tides, storm surge, and waves. *Storm surge* is the rise in water level above the predicted tide, caused by storms centered off the coast driving ocean water toward land. Low atmospheric pressure, wave set-up, wave run-up, and rainfall can further contribute to observed storm-induced increases in water elevation (Harris and Bureau, 1963). The term *storm tide* refers to the combined impact of storm surge and the astronomical tide. Note the difference between peak measured high water and peak predicted high tide is defined as *skew surge*, which is often employed for developing flood statistics because the more standard *storm surge* term can include a partial dependence on tidal stage (e.g. (Williams et al., 2016)).

The largest storm surge recorded in Boston over the last 100 years is 1.9 m (e.g., Catalano and Broccoli, 2018), and the largest recorded skew surge is 1.3 m (Talke et al., 2018); however, the 3.1-m rise and fall of sea level twice per day due to tides is significantly larger. Most of Boston's extreme coastal flooding events are therefore caused by the overlap of storm surge with an anomalously high tide (Baranes et al., 2020; Kirshen et al., 2008; Talke et al., 2018). This is in contrast to the south-facing shoreline of Massachusetts and New York City, where tide range is smaller and the most extreme storm surges are greater due to coastal orientation and morphology (Boldt et al., 2010; Castagno et al., 2020; Orton et al., 2012). Comparing the relatively minor flooding in Boston caused by Hurricane Sandy in 2012 to severe flooding during the January 4, 2018 Nor'easter (which set the record for highest water level recorded at the Boston tide gauge in 100 years) illustrates the relative impacts of high tide and storm surge on total flood height

Figure 4.6

Comparison of flooding during the record-breaking January 2018 Nor'easter and Hurricane Sandy in 2012.



Measured water level relative to annual mean sea level (i.e. storm tide; black curve) is broken down into predicted water level (i.e. the tidal contribution; gray curve) and storm surge (calculated as observed water level minus the predicted tidal level; gray dashed curve). Annual mean higher high water (MHHW) is shown to compare high tide on the day of the storm to average high tide conditions. Water level measurements are from tidesandcurrents.noaa.gov.

(Fig. 4.6). Maximum storm surge during Hurricane Sandy was 50 cm higher than the 2018 event, yet maximum storm tide was 70 cm lower. This is because storm surge peaked around low tide during Sandy, whereas in 2018, peak surge coincided with a significantly larger-than-average high tide.

While multiple conditions can produce storms across the Northeastern U.S., the primary drivers of coastal flooding are large, synoptic-scale (hundreds of miles) atmospheric disturbances, or cyclones, with surface winds that rotate counter-clockwise around low-pressure centers. Cyclones can originate from various dynamic processes. Tropical cyclones (TCs) form at low latitudes over warm water where atmospheric conditions are favorable to convection. Near-surface winds spiral inward toward a low-pressure center and draw moisture from the ocean upward into the cyclone. In the North Atlantic, tropical cyclones are called hurricanes once they reach a sustained wind speed of more than 74 mph. Extratropical cyclones (ETCs) form at mid-latitudes and are generally driven by latitudinal (north-south) temperature gradients that give rise to strong winds between cold and warm air masses. The term Nor'easter is commonly used in the Northeast to describe ETCs because the most damaging winds often come from the northeast on the western side of the passing low.

TCs typically impact the Northeast between August and October, while ETCs are most common in the cold-season months of November through April. ETCs have historically been the dominant flooding mechanism in Boston and the rest of northern New England, as they are 1) more frequent, 2) follow tracks more favorable to intense flooding north of Cape Cod, and 3) generally have longer durations that make them more likely to overlap with high tides (e.g., Kirshen et al., 2008; Talke et al., 2018)). Along the south-facing shorelines of Massachusetts, Rhode Island, Connecticut, and New York, ETC-induced

Table 4.2

Metrics describing the two Nor'easters that caused record-breaking flooding on the Massachusetts coast during the winter of 2018.

	January 4, 2018 Nor'easter	March 3, 2018 Nor'easter
Storm tide, • m above 2018 MHHW • m above 2018 MSL	1.36 m 2.95 m	1.22 m 2.81 m
Storm tide rank, 1921 to 2020 (i.e. not including SLR)	2	3
Total water level rank, 1921 to 2020 (i.e. including SLR)	1	3
Maximum storm surge	0.85 m	1.08 m
Storm surge rank, 1921 to 2020	79	20
Predicted high water at peak storm tide, • m above 2018 MHHW • m above 2018 MSL	0.55 m 2.14 m	0.43 m 2.02 m
Predicted high water rank, 2018 winter storm season	3	12

flooding is also most common for all but the most extreme flood events (Catalano and Broccoli, 2018). However, TCs have caused the largest historical flood events for locations like New York City (Talke et al., 2014), because of the region's coastal morphology, position relative to direct TC landfalls, and significantly smaller tidal range.

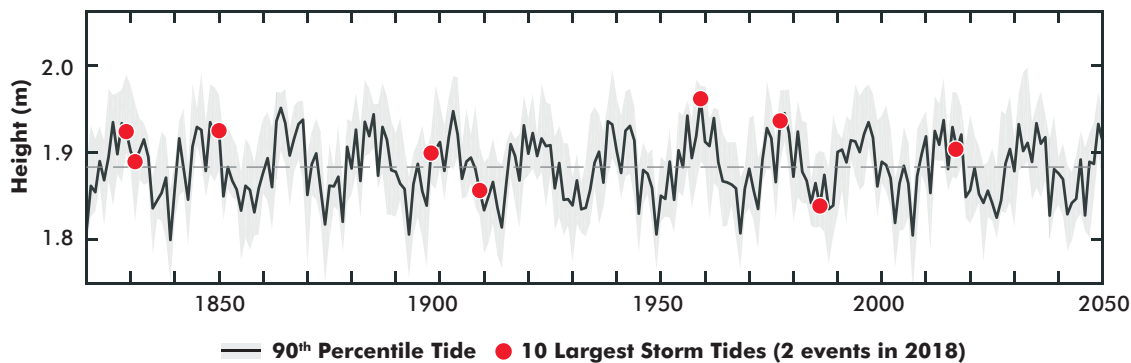
2018 Nor'easters

Extreme coastal flooding caused by two Nor'easters in 2018 illustrate the primary influence of tides in determining flood severity around Boston. Table 4.2 describes the January 4th and March 3rd floods by various metrics; notably, the two storms caused the highest and third-highest water levels recorded within the ~100-year-long record from the Boston National Oceanic and Atmospheric Administration (NOAA) tide gauge. Although sea level rise has increased the frequency of extreme flooding over the past century (Talke et al., 2018), adjusting the 100-year NOAA water level time series to annual MSL (i.e. comparing storm tides) only decreases the 2018 flood ranks from first and third to second and third (with the Blizzard of 1978 beating out the January 2018 Nor'easter in the annual MSL-adjusted storm tide time series). The metrics in Table 4.2 also show that storm surge was not the primary cause of the record-breaking flooding, particularly for the January storm. The 0.85-m January surge ranks 79th within the NOAA record (close to the annual storm), and the 1.08-m March surge ranks 20th.

It was the unusually high tides coinciding with the storms that caused severe flooding in 2018. The two storms' timing was unfortunate in three respects: 1) they occurred in 2018, near the peak of the 18.6-year nodal cycle (Figure 4.7); 2) the January and March storms coincided with the 3rd and 12th-highest tides of the 2018 storm season respectively, which were 0.55 m and 0.43 m above the year's mean higher high water (MHHW; the average of the higher high tide for each day); and 3) the timing of peak surge was nearly aligned with the timing of high tide during both events (Figure 4.6). Using the Baranes

Figure 4.7

Timing of Boston's top-ten storm tides relative to the 18.6-year tidal nodal cycle.



The annual 90th percentile of high waters relative to annual MSL (black curve) are plotted as a function of time and clearly show the influence of the 18.6-year nodal cycle. Red circles mark the years of the 10 largest historical Boston storm tides. Eight of the top 10 events (including the two 2018 floods) occurred in years where the nodal cycle was in its positive phase (indicated by red circles falling above the horizontal dashed line) (Talke et al., 2018).

et al. (2020) methodology, which accounts for the known high tides in 2018, we calculate that there was only a 0.056% chance of both events occurring during that storm season; thus, although the storms themselves were not record-breaking, their timing relative to the anomalously large tides was unprecedented.

Climate-driven changes in extratropical and tropical cyclone characteristics

While there is evidence for future changes in ETC and TC activity globally, most recent studies have not found statistically significant evidence for future changes in Boston storm surge linked to either changing ETC (Lin et al., 2019) or TC (Marsooli et al., 2019) climatology. Marsooli et al. (2019) uses a well-vetted hurricane and hydrodynamic model to generate a large number of representative North Atlantic TCs and resulting storm tides under both present (1980 to 2005) and late-21st-century (2070 to 2095, RCP8.5) conditions. These TC ensembles include changes in TC frequency, intensity, and size. Future changes in flood heights due solely to projected TC activity are compared to changes associated with both TC activity and future regional sea level rise based on the sea level rise projections by Kopp et al. (2014). TC contributions to increasing flood heights are found to be substantial along the Gulf and southern East Coast of the U.S.; however, their contribution decreases northward along the eastern seaboard, particularly for points north of Cape Cod, where TC impacts become minimal. Specific to coastal counties in the Greater Boston region, changing TC activity accounts for roughly 1% of the total increase in the 100-yr flood height, with the remaining 99% due to projected sea level rise. The exception to this result is Plymouth County, where TC contributions increase to roughly 9%, mainly due to the fraction of the county being located south of Cape Cod at the head of Buzzards Bay, where the morphology and southern-facing orientation of the coast substantially enhances TC-induced storm surges (Boldt et al., 2010; Cheung et al., 2007; Redfield and Miller, 1957). TC-related contributions were found to be less for higher-frequency events impacting Plymouth county, including a contribution of 2% to the 10-yr flood height.

Lin et al. (2019) investigates future climate-driven changes in ETC storm surge by comparing hydrodynamic simulations of Boston flooding for the historical (1979 to 2012) and mid-to-late-21st-century

(2054 to 2079) periods. Results suggest a modest 5% increase in the 10-year storm surge height and a 1% increase in the 50-year storm surge height between the historical and future time periods due to changing ETC climatology. However, depending on the climate model used to define future ETC characteristics, results vary significantly with a range of -2% to +21% for the 10-year storm surge and -11% to +20% for 50-year storm surge.

Tidal variability and extreme flooding

Natural planetary cycles cause tidal magnitude (the vertical distance between high and low tide) to vary year-to-year in Boston, enhancing flood hazard in years when tides are larger (Baranes et al., 2020; Eliot, 2010; Haigh et al., 2020; Peng et al., 2019; Ray and Foster, 2016; Talke and Jay, 2020; Talke et al., 2018; Woodworth et al., 2019). The moon's elliptical orbit revolving in space (the *lunar nodal cycle*) causes Boston's largest high tides to cyclically increase and decrease by ~7 cm (just under a quarter foot) every 18.6 years (Ray and Merrifield, 2019), which is roughly equivalent to 25% of the total relative sea level rise that has occurred in Boston over the last 100 years. Eight of Boston's top-ten storm tides over the past 200 years have occurred during decades when the 18.6-year nodal cycle's positive phase forces a larger tidal range (Figure 4.7) (Talke et al., 2018).

There has also been a secular increase in tide range throughout the Gulf of Maine (the basin between Cape Cod and the Bay of Fundy), widening the difference between low and high tide elevations by ~4 cm in Boston over this past century (Godin, 1992, 1995; Ray, 2006; Ray and Foster, 2016; Ray and Merrifield, 2019). The increase in tides has increasing impact north of Boston toward the Bay of Fundy. In Greater Boston, future flood risk is dominated by projected rates of background sea level rise followed by secondary impacts associated with the nodal cycle (Baranes et al., 2020).

Recent work by Baranes et al. (2020) focusing on Boston and the greater Gulf of Maine region presents a new statistical approach for assessing flood hazard that accounts for tidally driven interannual variability associated with the 18.6-year nodal cycle. The technique demonstrates the effect of the nodal cycle in driving significant historical oscillations in flood hazard metrics, such as the height of the 100-year flood. Interaction between the nodal cycle and sea level rise also has significant implications for future flood hazard in Boston. Currently (in 2022), the negative phase of the nodal cycle is counteracting the sea level rise-induced increase in flood hazard; however, in 2025, the nodal cycle will reach a minimum in the region and then begin to accelerate flood hazard as it moves toward its maximum over the subsequent decade when both sea level rise and larger tides are constructional.

4.10 FUTURE FLOODING

Similar to the 2016 BRAG report, the frequency of extreme coastal flood heights at the Boston tide gauge we project under three future RCP emission scenarios: RCP2.6, RCP4.5, and RCP8.5. Probabilistic sea level rise projections for each scenario (Table 4.1) are combined with future predicted high tides and tide gauge-derived extreme value statistics of skew surge. Like many tide gauges, the Boston gauge is located in a wave-sheltered harbor and measures the contributions of storm surge, tides, and mean sea level to flood level but excludes direct wave impacts. Thus, the projections provided here are for extreme still water levels and do not include waves. These projections also do not include seasonal-to-decadal fluctuations in sea level caused by temperature, salinity, wind, atmospheric pressure, and ocean currents (see the below section on *Minor High Tide Flooding* for a more in-depth discussion of these drivers of sea level variability).

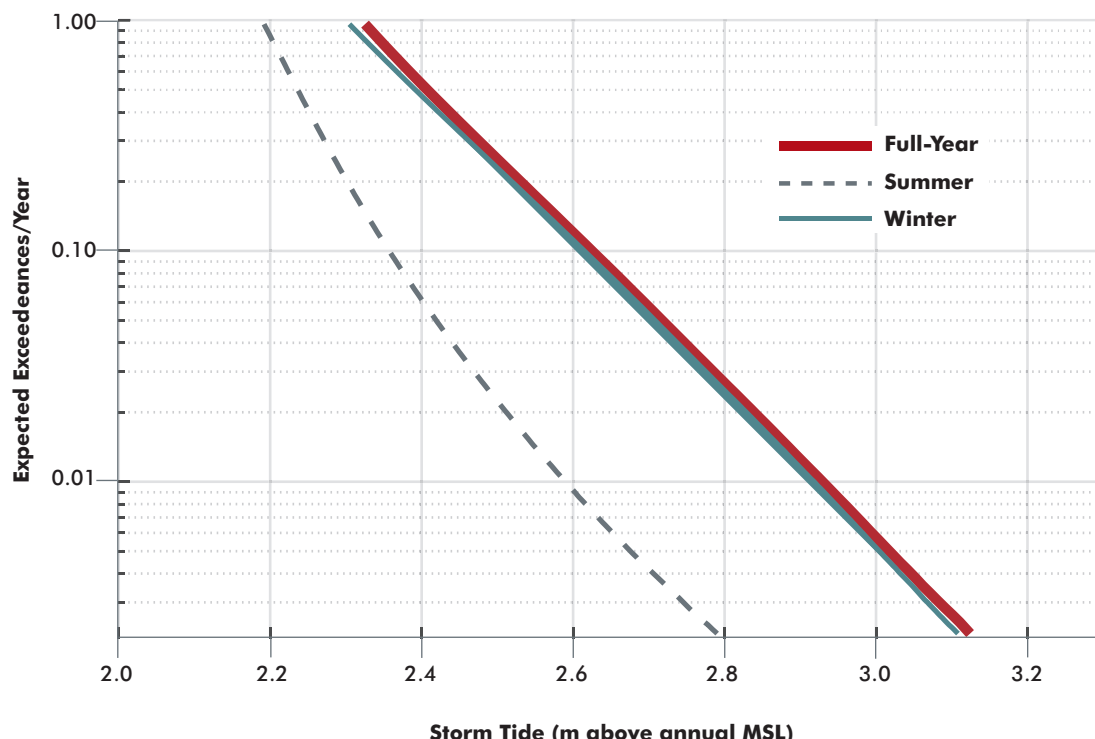
We substantially improve upon the 2016 BRAG projections by applying a quasi-nonstationary joint probability approach (Baranes et al., 2020) that 1) provides more accurate estimates of annual flood exceedances, which is the expected number of times extreme sea levels will exceed a given height in a year; and 2) yields an annually varying flood height–annual exceedance relationship (hereafter referred to as a

“flood exceedance curve”) that changes based on the predicted tides for each year. Note that exceedances/year is the inverse of recurrence interval (or return period); for example, a storm tide with a 100-year recurrence interval has 0.01 expected exceedances/year. We also separate winter and summer season projections because the region’s large storm events mostly occur in the winter season (Talke et al., 2018), while summertime tide levels are larger on average (Ray and Foster, 2016). At present, the summer season contribution to annual extreme flood hazard is negligible (Figure 4.8; Baranes et al., 2020), so it is important to view full-year flood exceedance curves for Boston with that caveat in mind. We define the winter storm season as October 31 to April 30 and the summer season as May 1 to October 20 (consistent with Talke et al., 2018 and Baranes et al., 2020).

The joint probability approach employed here fits separate probability distributions to predicted high tides and the 100-year record of skew surge from the Boston NOAA tide gauge following methods in Baranes et al. (2020). The joint tide-surge distribution thus accounts for the possibility of storm surges aligning with any tidal condition. Projections are quasi-nonstationary because each future year’s flood exceedance curve is calculated by combining projected mean sea level and tides specific to that year with the probability distribution fit to all historical skew surges observed over the 100-year NOAA record. Annual tide predictions at the Boston gauge for 1921 to 2100 are from Ray and Foster (2016). Thus, we allow tides and sea level to vary through time but consider storm characteristics to be stationary. This approach reflects our assessment that 1) future impacts to the Boston region by changes in extratropical

Figure 4.8

Seasonal differences and winter dominance in Boston flood hazard.



The summer season flood frequency curve (dashed line) has a negligible contribution to the full-year curve (thick red line), whereas the winter season curve (grey line) nearly matches the full year. Flood frequency distributions represent average flood hazard over the past 100 years relative to annual mean sea level and are calculated following Baranes et al. (2020).

and tropical cyclone activity are at present considered minimal, albeit with ongoing uncertainty (see above); and 2) the largest drivers of future change in coastal flood hazard are sea level rise and natural tidal cycles.

Uncertainty ranges in our projections include both statistical uncertainty in the skew surge distribution that characterizes their probabilities based on a limited 100-year record of observations, and probabilistic uncertainty in sea level rise projections. As discussed in Douglass et al. (2016), using probabilities of sea level rise in flood risk assessment is extremely important because uncertainty in background sea level increases the median estimate of extreme flood levels. Steady sea level rise forces a nonlinear increase in flood hazard (Figure 4.5), so the number of additional flood exceedances introduced by the possibility of larger-than-expected sea level rise is greater than the reduction in flood exceedances due to smaller-than-expected sea level rise.

Statistical uncertainty in the skew surge distribution is represented by 1,000 Generalized Pareto Distributions (GPDs) with equal probabilities, while sea level rise uncertainty is represented by 10,000 scenarios with equal probabilities under each RCP. For each season (summer and winter) and for each RCP, we 1) use a Latin hypercube sampling scheme to sample 1,000 sets of skew surge GPDs and sea level rise scenarios, 2) add the 1,000 selected sea level rise scenarios to future predicted tides, and 3) calculate annually varying flood exceedance projections for each of the 1,000 selected GPD and sea level rise projection sets (Baranes et al., 2020).

Flood projections

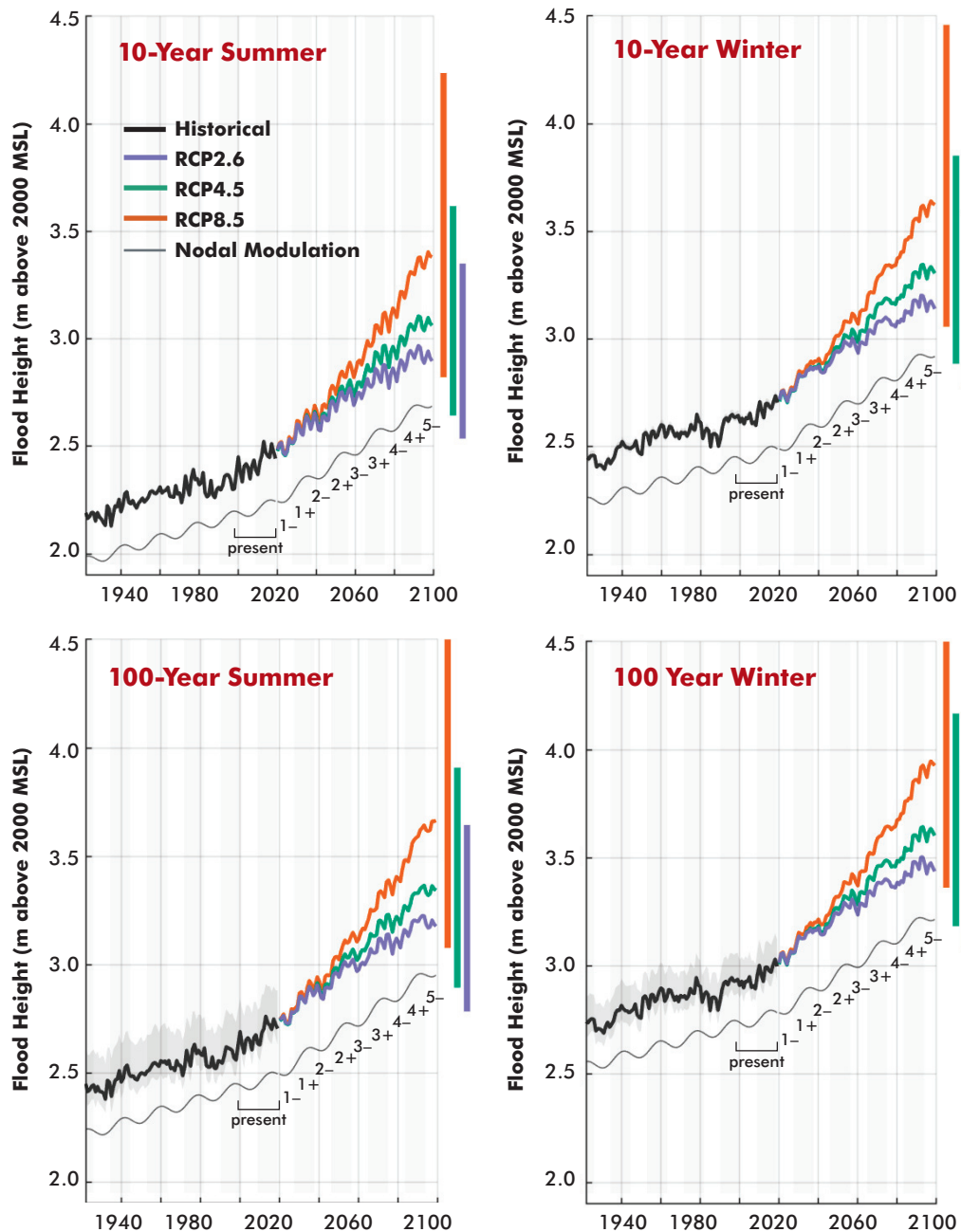
Figure 4.9 shows historical (1921 to 2019) and projected (2020 to 2100) winter and summer season flood heights for the 10-year flood (0.1 expected exceedances/year) and the 100-year flood (0.01 expected exceedances/year). An illustration of the 18.6-year tidal modulation of storm tides is plotted below the flood height curves in each panel of Figure 4.9. Tables 4.2 and 4.3 show present-day and projected flood heights, averaged over each nodal cycle phase (labeled present, 1-, 1+, 2-, etc. in Figure 4.9; with minus and plus signs denoting negative and positive nodal phases). Note that present-day flood levels are determined by averaging over 2000 to 2019, a time period that encompasses a full 18.6-year nodal cycle. All flood heights are relative to 2000 MSL (Figure 4.1; Table 4.1).

Sea level rise has clearly been driving an accelerating increase in flood hazard since the early 20th century. Flood projections do not begin to diverge under different emissions pathways until about 2050, after which human decision-making determines whether the increase in flood hazard slows at the end of the century (RCP2.6), or continues to accelerate (RCP8.5). The decadal, cyclical variation in flood heights through 2100 also demonstrates the impact of the 18.6-year nodal cycle on flood hazard. Importantly, the long-term increase in flood hazard driven by sea level rise temporarily slows during decades when the nodal cycle is in a negative phase, and the smaller tide range counteracts sea level rise. However, as the nodal cycle enters a positive phase in the following decade, the increased tide range on top of sea level rise leads to a more rapid increase in flood hazard. Progressing forward from present (year 2020), the nodal cycle will be in a negative phase until 2027, so flood hazard will remain steady compared to the previous decade even though sea level is continuing to rise. However, one should expect flood hazard to increase more rapidly over the 2028 to 2036 decade when the nodal cycle switches to its positive phase. Figure 4.9 also shows a 4.4-year cycle of variation in the 10 and 100-year flood heights. This is also due to predictable interannual variation in the magnitude of Boston's tides, caused by perigean spring tides coinciding with the winter or summer solstice on a 4.4-year cycle (see Ray & Foster, 2016 for a detailed explanation). We do not focus on this 4.4-year effect because in practice, it would be drowned out by inter-annual variability in MSL, which has historically been on the order of several cm (Baranes et al., 2020).

Tables 4.5 and 4.6 provide guidance on the annual exceedances of future flood levels (we use 2.6 to 3.0 m for future flood levels for the winter season and 2.4 to 2.7 m for future flood levels for the summer season relative to 2000 MSL) that currently have recurrence intervals between ~10 and ~100 years under

Figure 4.9

Historical and projected 10-year (top panels) and 100-year (bottom panels) flood heights in meters above 2000 MSL for the summer (left-hand panels) and winter (right-hand panels) seasons.



Purple, green, and orange lines show median projections for RCP2.6, RCP4.5, and RCP8.5 emissions concentration pathways, and bars on the right-hand-side show the central 90% ranges at 2100. These ranges include both statistical uncertainty in storm tides and uncertainty in sea level rise projections. Thick black lines show historical flood heights, and grey shading represents the central 90% range of statistical uncertainty (shading is not visible in the upper panels because there is less uncertainty in estimating the 10-year flood). The thin grey sinusoid is an illustration of 18.6-year nodal cycle amplitude and phase (note that positive-phase years are shaded in light grey), offset from the flood height curves for visualization. Nodal cycle phase labels (present, 1-, 1+, etc.) correspond to Tables 4.2 and 4.3.

Table 4.3

Projections of 10-year and 100-year winter flood heights, averaged across each nodal cycle phase (see Figure 4.9).

		Heights for 10-year Winter Flood (m. 2000 MSL)			Heights for 100-year winter flood (m. 2000 MSL)		
Nodal Period	Years	RCP2.6	RCP4.5	RCP8.5	RCP2.6	RCP4.5	RCP8.5
Present	2000–2018	2.43 (2.36–2.50)			2.69 (2.59–2.85)		
1–	2019–2027	2.74 (2.66–2.83)	2.74 (2.66–2.82)	2.75 (2.65–2.86)	3.04 (2.93–3.19)	3.04 (2.94–3.18)	3.05 (2.93–3.21)
1+	2028–2036	2.83 (2.71–2.96)	2.83 (2.72–2.95)	2.85 (2.72–3.00)	3.13 (2.99–3.31)	3.13 (3.00–3.30)	3.15 (3.00–3.34)
2–	2037–2046	2.86 (2.71–3.03)	2.87 (2.74–3.03)	2.91 (2.74–3.11)	3.17 (3.00–3.37)	3.18 (3.02–3.37)	3.21 (3.03–3.44)
2+	2047–2055	2.95 (2.75–3.17)	2.98 (2.80–3.19)	3.04 (2.83–3.31)	3.26 (3.05–3.51)	3.28 (3.09–3.53)	3.34 (3.12–3.64)
3–	2056–2064	2.98 (2.74–3.24)	3.02 (2.80–3.29)	3.11 (2.94–3.46)	3.28 (3.03–3.56)	3.33 (3.10–3.62)	3.42 (3.15–3.78)
3+	2065–2074	3.06 (2.80–3.36)	3.14 (2.87–3.47)	3.27 (2.97–3.72)	3.37 (3.09–3.69)	3.44 (3.16–3.80)	3.57 (3.24–4.04)
4–	2075–2083	3.08 (2.79–3.42)	3.18 (2.86–3.58)	3.36 (3.27–3.92)	3.38 (3.08–3.75)	3.48 (3.15–3.90)	3.67 (3.27–4.24)
4+	2084–2091	3.14 (2.82–3.55)	3.27 (2.90–3.74)	3.51 (3.05–4.19)	3.45 (3.11–3.87)	3.57 (3.20–4.06)	3.82 (3.35–4.50)
5–	2092–2100	3.17 (2.82–3.60)	3.32 (2.91–3.84)	3.61 (3.09–4.40)	3.47 (3.11–3.92)	3.62 (3.21–4.16)	3.92 (3.39–4.72)

Table 4.4

Projections of 10-year and 100-year summer flood heights, averaged across each nodal cycle phase (see Figure 4.9).

		Heights for 10-year Winter Flood (m. 2000 MSL)			Heights for 100-year winter flood (m. 2000 MSL)		
Nodal Period	Years	RCP2.6	RCP4.5	RCP8.5	RCP2.6	RCP4.5	RCP8.5
Present	2019–2027	2.50 (2.41–2.59)	2.49 (2.41–2.58)	2.50 (2.40–2.61)	2.75 (2.64–2.93)	2.75 (2.64–2.92)	2.76 (2.63–2.95)
1–	2028–2036	2.58 (2.45–2.72)	2.58 (2.47–2.72)	2.60 (2.46–2.77)	2.85 (2.69–3.05)	2.85 (2.70–3.05)	2.87 (2.70–3.09)
1+	2037–2046	2.61 (2.45–2.79)	2.62 (2.48–2.79)	2.66 (2.49–2.87)	2.88 (2.69–3.11)	2.89 (2.72–3.12)	2.93 (2.73–3.18)
2–	2047–2055	2.71 (2.51–2.93)	2.73 (2.55–2.96)	2.79 (2.59–3.08)	2.98 (2.75–3.24)	3.00 (2.80–3.28)	3.06 (2.83–3.38)
2+	2056–2064	2.74 (2.50–3.00)	2.79 (2.56–3.06)	2.87 (2.61–3.23)	3.00 (2.74–3.30)	3.05 (2.81–3.36)	3.14 (2.87–3.52)
3–	2065–2074	2.82 (2.55–3.12)	2.89 (2.61–3.24)	3.02 (2.69–3.48)	3.09 (2.80–3.42)	3.16 (2.87–3.53)	3.29 (2.94–3.77)
3+	2075–2083	2.84 (2.54–3.19)	2.94 (2.62–3.35)	3.12 (2.74–3.69)	3.11 (2.79–3.48)	3.21 (2.87–3.63)	3.40 (2.99–3.97)
4–	2084–2091	2.91 (2.58–3.31)	3.03 (2.66–3.51)	3.27 (2.82–3.96)	3.18 (2.83–3.60)	3.31 (2.92–3.80)	3.54 (3.07–4.24)
4+	2092–2100	2.92 (2.57–3.36)	3.08 (2.67–3.60)	3.37 (2.85–4.17)	3.20 (2.82–3.64)	3.35 (2.92–3.89)	3.64 (3.09–4.44)
5–	2000–2018	2.74 (2.66–2.83)	2.74 (2.66–2.83)	2.74 (2.66–2.83)	2.74 (2.66–2.83)	2.74 (2.66–2.83)	2.74 (2.66–2.83)

We show median flood heights and central 90% ranges (values in parentheses). All flood heights are in meters above 2000 MSL.

Table 4.5

Projections of winter season annual exceedances for flood heights of 2.60 m (roughly the present-day 10-year flood height), 2.80 m, and 3.00 m (roughly the present-day 100-year flood height).

		2.60 m		2.80 m		3.00 m	
Nodal Period	Years	RCP2.6	RCP8.5	RCP2.6	RCP8.5	RCP2.6	RCP8.5
Present	2000–2018	0.13–0.19		0.03–0.04		0.004–0.011	
1–	2019–2027	0.20–0.43	0.19–0.47	0.04–0.10	0.04–0.11	0.01–0.02	0.01–0.02
1+	2028–2036	0.32–ann.	0.35–ann.	0.07–0.21	0.08–0.27	0.01–0.05	0.02–0.06
2–	2037–2046	0.35–ann.	0.47–ann.	0.08–0.32	0.10–0.49	0.02–0.07	0.02–0.11
2+	2047–2055	0.57–ann.	annual	0.12–0.81	0.22–ann.	0.03–0.18	0.05–0.38
3–	2056–2064	0.56–ann.	annual	0.12–ann.	0.30–ann.	0.03–0.25	0.07–0.87
3+	2065–2074	annual	annual	0.21–ann.	0.71–ann.	0.05–0.56	0.16–ann.
4–	2075–2083	0.98–ann.	annual	0.21–ann.	annual	0.05–0.72	0.24–ann.
4+	2084–2091	annual	annual	0.29–ann.	annual	0.06–ann.	0.52–ann.
5–	2092–2100	annual	annual	0.31–ann.	annual	0.07–ann.	0.85–ann.

Table 4.6

Projections of summer season annual exceedances for flood heights of 2.40 m (roughly the present-day 10-year flood height), 2.55 m, and 2.70 m (roughly the present-day 100-year flood height).

		2.40 m		2.55 m		2.70 m	
Nodal Period	Years	RCP2.6	RCP8.5	RCP2.6	RCP8.5	RCP2.6	RCP8.5
Present	2000–2018	0.09–0.19		0.02–0.05		0.005–0.015	
1–	2019–2027	0.17–0.77	0.17–0.98	0.03–0.10	0.03–0.12	0.01–0.02	0.01–0.03
1+	2028–2036	0.37–ann.	0.44–ann.	0.06–0.41	0.07–0.66	0.02–0.06	0.02–0.09
2–	2037–2046	0.48–ann.	0.88–ann.	0.07–0.90	0.11–ann.	0.02–0.11	0.02–0.22
2+	2047–2055	annual	Annual	0.17–annual	0.47–ann.	0.03–0.58	0.07–annual
3–	2056–2064	annual	annual	0.18–annual	annual	0.04–ann.	0.13–annual
3+	2065–2074	annual	annual	0.41–ann.	annual	0.07–ann.	0.50–annual
4–	2075–2083	annual	annual	0.47–ann.	annual	0.07–ann.	annual
4+	2084–2091	annual	annual	annual	annual	0.13–ann.	annual
5–	2092–2100	annual	annual	annual	annual	0.13–ann.	annual

Flood heights are relative to 2000 MSL, and ranges of exceedances represent the central 66% “likely” range. Note that “annual” represents an exceedance value greater than or equal to 1.

low and high-emissions scenarios. The tables show the central 66% “likely” range of projected annual exceedances (where, for example the 100-year flood has 0.01 expected annual exceedances), and do not extend beyond exceedances of 1 (i.e., the annual event). As an example, it is projected that for the period between 2047 to 2055 (nodal cycle “2+”), the present-day winter season 100-year flood (at ~3 m above 2000 MSL) will likely have a recurrence interval of 6 to 33 years under the low-emissions RCP2.6 scenario (0.03 to 0.18 annual exceedances), and 3 to 20 years under the RCP8.5 high-emissions scenario (0.05 to 0.38 annual exceedances), where recurrence interval is the inverse of annual exceedances (Table 4.5). By 2100, this same 3-m flood level will likely be the annual event under RCP8.5 (0.85 to > 1 annual exceedances), or between the annual and 14-year event under RCP2.6 (0.07 to > 1 annual exceedances). Note that the projected range of exceedances reported in Tables 4.5 and 4.6 can be wide, because at extreme flood levels in Boston, small changes in flood height lead to large variation in exceedances (Buchanan et al., 2016).

Comparison with BRAG

Table 4.7 compares projections of the winter 100-year flood height from this report to projections from the 2016 BRAG report (Table 2.1 in Douglas et al., 2016). The winter season flood exceedance curve almost exactly matches the annual curve (Figure 4.8), supporting our comparison of winter season results to the annually derived statistics in BRAG. It is important to note that the 2016 report provided *mean* projected flood heights, whereas in Tables 4.3 and 4.4, we provide *median* (50th percentile) flood heights. As explained above, the number of additional flood exceedances introduced by the possibility of larger than expected sea level rise is not offset by the reduction of exceedances introduced by the possibility of smaller than expected sea level rise, even if the sea level rise distribution is near-normal; thus, those additional positive exceedances will cause mean projected flood heights to exceed the median. Differences between median and mean values are generally within a few cm, reaching a maximum of 4 cm at the end of the 21st century under RCP8.5.

Table 4.7

Comparison of 10th to 90th percentile 100-year flood height projections in BRAG (2016) and GBRAG (2022) without Nodal Cycle Tide Changes.

		2016 BRAG		GBRAG	50 th percentile difference (GBRAG minus BRAG, m)	Nodal cycle phase
		100-y flood height 10 th –90 th percentile		Winter 100-y flood height 10 th –90 th percentile		
		ft, NAVD88	m, 2000 MSL	m, 2000 MSL		
Present		9.2	2.87	2.88–3.08		
2030	RCP4.5	9.5–10.1	2.96–3.14	3.03–3.28	+0.04	Positive
	RCP8.5	9.5–10.1	2.96–3.14	3.02–3.32	+0.05	
2050	RCP4.5	9.8–10.8	3.05–3.35	3.07–3.51	+0.02	Positive
	RCP8.5	9.8–10.8	3.05–3.35	3.10–3.61	+0.01	
2100	RCP4.5	10.8–14.1	3.35–4.36	3.19–4.16	-0.37	Neutral
	RCP8.5	12.1–17.4	3.75–5.37	3.67–4.78	-0.44	

BRAG values are reported in feet relative to NAVD88 and meters relative to 2000 MSL while GBRAG values are only reported in meters relative to 2000 MSL. We also compare median (50th percentile) sea level estimates, with positive values indicating higher GBRAG estimates and negative values indicating higher BRAG estimates.

Our present-day 100-year flood height estimate is slightly higher in part due to our including the two 2018 Nor'easters in our extreme value statistical analysis. Through 2050, our projected flood heights are *higher* than the 2016 projections (2 to 16 cm higher under RCP4.5 and 5 to 26 cm for RCP8.5), whereas in 2100, our projections are *lower* (16 to 20 cm lower for RCP4.5 and 8 to 59 cm for RCP8.5). As discussed above, these differences are mainly caused by our revised GBRAG baseline sea level projections that use updated land ice contributions provided by IPCC SROCC (Oppenheimer et al., 2019). In 2030 and 2050, the nodal cycle is in its positive phase which also contributes to higher GBRAG flood projections.

Hydrodynamic models

In this report, we estimate extreme flood frequencies by fitting probability distributions to measured skew surges at the Boston tide gauge and combining those distributions with tide predictions and probabilistic sea level projections. Flood frequencies can also be estimated from hydrodynamic model simulations of water levels (Lin et al., 2019; Marsooli et al., 2019). Hydrodynamic modeling has the advantages of 1) providing spatially continuous flood elevations and flow velocities down to the spatial scales (<1 m) relevant to specific infrastructure such as roads and bridges, 2) explicitly modeling wave impacts, 3) accounting for nonlinear impacts on tides and surge from rising sea level, and 4) considering potential changes in storm climatology. However, these models are computationally intensive (particularly when implemented at the infrastructure scale), and as is the case with most numerical models, rely on uncertain parameterizations, bathymetry, and assumptions (Lin et al., 2010; Vousdoukas et al., 2016). Furthermore, generating a modeled flood exceedance distribution requires an ensemble of many simulations representing essentially all possible flood scenarios. Thus, individual flood statistics at infrastructure and community scales for the entire Greater Boston region is currently only feasible by combining hydrodynamic modeling ensembles with a limited set of tidal conditions and discrete sea level scenarios, rather than full sets of probabilistic sea level projections.

The Massachusetts Coast Flood Risk Model (MC-FRM) is currently the most sophisticated hydrodynamic model for assessing future changes in flood hazard along the Massachusetts coastline due to the combination of sea level rise and changing storm climatologies. The MC-FRM was developed by Woods Hole Group for the Massachusetts Department of Transportation (MassDOT) under a larger University of Massachusetts Boston contract on the vulnerability of MassDOT assets to present and increased coastal flooding and is an expansion of the Boston Harbor Flood Risk Model (Bosma et al., 2015). MC-FRM simulations are in progress, and results are being distributed through MassDOT, Massachusetts CZM, and MassGIS as they become available. The U.S. Army Corps of Engineers North Atlantic Coast Comprehensive Study (NACCS) also provides hydrodynamic modeling-based flood statistics for the Greater Boston area (Nadal-Caraballo et al., 2015). However, the NACCS only considers a 1-m sea level rise scenario, and its domain includes Virginia through Maine, so the model is not optimized for Massachusetts like the MC-FRM. Thus, we focus our discussion on the MC-FRM.

The MC-FRM is a coupled ADCIRC-UnSWAN model that includes the impacts of sea level, tides, storm surge, wave setup, riverine flows, and dam operations on coastal flooding. Its domain includes all Massachusetts coastlines and estuaries and has horizontal spatial resolution reaching 5 to 10 feet in populated overland regions. The model also includes dynamic wave run-up and accounts for wave overtopping of coastal structures such as seawalls. MC-FRM results provide flood heights and flood frequencies across the model domain for the present-day and for future time horizons in 2030, 2050, and 2070. The model uses the 99.5th percentile RCP8.5 relative sea level rise projections because it evaluates MassDOT critical infrastructure, such as Boston's central artery highway/tunnel system. Baseline sea level projections used in the MC-FRM analysis are shown in Table 4.8 and are the same as those in Kopp et al. (2017). For practitioners using both MC-FRM flood projections (as they become available) and the GBRAG projections

provided here, we compare baseline sea levels at 2030, 2050, and 2070 relative to both the MC-FRM and GBRAG vertical datums (feet above NAVD88 and meters above 2000 MSL, respectively). We offer this comparison of baseline sea levels because GBRAG sea level projections are higher than those used by the MC-FRM beyond 2030. Note, however, that it is not appropriate to compare the two sets of flood projections, as the MC-FRM is designed to give a detailed assessment of a few discrete scenarios, whereas GBRAG projections are designed to describe all possible scenarios at a single location.

For each future climate horizon, the MC-FRM evaluates flooding from both TCs and ETCs. Modeled ETCs are based on storms observed within instrumental and historical records, an approach that is consistent with our evaluation of there being no clear evidence for future changes in extratropical frequency or intensity. Modeled TCs, however, are drawn from a set of over 500,000 synthetic storms with characteristics that vary over time as climatological conditions change, following a similar methodology to Marsooli et al. (2019). MC-FRM and Marsooli et al. (2019) are consistent in their projections for future increases in tropical cyclone activity contributing to the increase in future flood hazard along Massachusetts' south-facing shorelines, where TCs are the primary cause of severe flooding.

For ETC simulations, the MC-FRM randomly phases storms with the tidal cycle such that flood projections account for the possibility of peak storm surge occurring over a range of tidal levels. However, the modeled tides used in the MC-FRM are from a single month in 2008. The 2018 Nor'easters demonstrated that the height of high tide on the particular day a storm hits is an important determination of flood severity. Therefore, proper statistical representation of 2018-type events requires sampling from a full nodal cycle (18.6 years) of tidal conditions. This is not computationally feasible for a hydrodynamic modeling study with a storm set as large as the MC-FRM's.

Compared with hydrodynamic model-based projections, the tide gauge-based flood projections (Figure 4.9, Tables 4.3 through 4.6) have the advantages of 1) incorporating full probability distributions of sea level rise under multiple emissions scenarios, 2) providing a statistically robust treatment of tides, and 3) being grounded in observations. However, the analysis only provides flood hazard information at a single wave-sheltered location (the Boston tide gauge). These GBRAG tabulated flood heights can be used for decision-making near the tide gauge and as validation for hydrodynamic flood modeling. The MC-FRM results also have the potential to provide complementary guidance on the impact of waves and spatial variability in flood magnitude between the Boston tide gauge and specific locations of interest within the Greater Boston domain. The MC-FRM results also include surges increasing in height as water levels increase. At present, there are no flood projections that are both spatially continuous and fully probabilistic. Synthesizing computationally expensive hydrodynamic model output with more complete

Table 4.8

Comparison of relative sea level rise projections since 2000 used by MC-FRM (based on Kopp et al., 2017) and those developed for GBRAG flood projections.

Year	MC-FRM Sea-Level Rise RCP8.5, 99.5 th Percentile		GBRAG RCP8.5, 99.5 th Percentile		GBRAG Percentile of MC-FRM 99.5 th Percentile SLR (RCP8.5)
	ft, NAVD88	m, 2000 MSL	ft, NAVD88	m, 2000 MSL	
2030	1.2	0.43	1.24	0.44	99.4
2050	2.4	0.79	2.95	0.96	98.6
2070	4.2	1.34	5.34	1.69	98.5

Note that sea level projections are not influenced by tides.

(statistically based) tidal and sea level rise distributions is an ongoing area of research that will improve flood projections in the future.

Minor high tide flooding

High tide flooding, also often called “nuisance” flooding, is defined as more routine, low-magnitude flooding that is not a serious threat to public safety, but can overwhelm stormwater drainage systems, close roads, and deteriorate infrastructure not designed to be submerged or exposed to salt (Moftakhari et al., 2015; Sweet et al., 2020; Sweet et al., 2018; Sweet and Park, 2014; Thompson et al., 2021). In Boston, the NOAA-defined threshold for minor flooding is 63 cm above the present MHHW datum (where “present” is the 1983 to 2001 average), or 215 cm above 2000 MSL.¹ The Boston moderate flooding threshold is 89 cm above present MHHW.

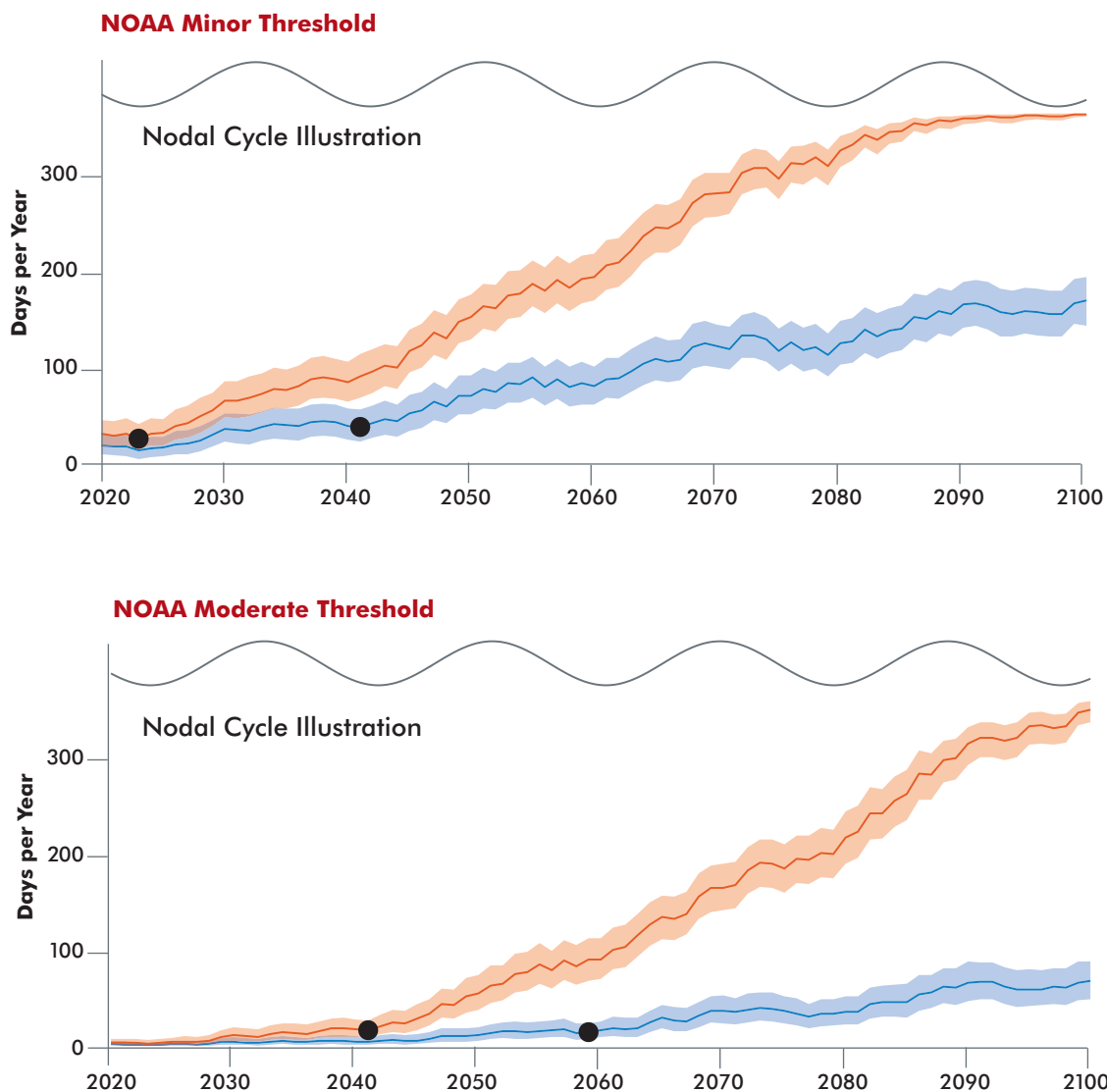
Astronomical (i.e. tidal) and climatic processes that modulate sea level over seasonal to decadal timescales control the frequency of high tide flooding. In Boston, the relative amplitudes of the major tidal constituents cause high tide flooding events to occur most often around the summer solstice (see Ray & Foster, 2016 for a detailed explanation). On interannual timescales, the 18.6-year nodal cycle (Fig. 4.7) and the 4.4-year cycle of lunar perigee, caused by perigean spring tides coinciding with the winter or summer solstice twice per 8.85 years, also cause high tide flood events to cluster in certain years when the two cycles constructively interfere (reinforce) to increase high tide levels (Ray and Foster, 2016; Thompson et al., 2019, 2021). Interannual and higher-frequency fluctuations in temperature, salinity, wind, atmospheric pressure, and ocean currents also change sea level and impact the timing of flooding (e.g. Thompson et al., 2021). For example, at the Boston Harbor tide gauge, the present amplitude of the seasonal sea-level cycle is ~3.5 cm (such that June sea level is ~7 cm higher than January sea level). On decadal timescales, Boston sea level can vary by an additional 10 to 15 cm (Figure 4.1). However, it is difficult to attribute this longer-timescale variability to a particular forcing mechanism, because multiple, interacting processes are at play (Sweet et al., 2009).

The long-term secular increase in sea level rise underlies all above-mentioned cyclical variations in water level and is accelerating the frequency of high tide flood events (see Figure 4.5 for an explanation of the nonlinear flood response). In Boston, 2011 was the first year that spring high tides alone exceeded the city’s local nuisance flood threshold without the additional influence of storms. Using the empirical, 63-cm threshold, Sweet et al. (2020) found that in 2017, near the peak of the 18.6-year nodal cycle, Boston experienced a record-breaking 22 high tide flood events. In 2019, the nodal cycle entered its negative phase, and they found that high tide flood events were reduced to 7 flood days in 2019 and a projected 11 to 18 flood days in 2020. Thompson et al. (2021) provide the best available projections of future high tide flooding at 89 U.S. tide gauge locations, including Boston. They combine three discrete sea level rise scenarios with localized ensemble projections of 21st century monthly mean sea level and astronomical tides. Sea level projections are the NOAA Intermediate Low, Intermediate, and Intermediate High local relative sea level rise scenarios for Boston, which include local effects of glacial isostatic adjustment and gravitational and rotational effects from ice melt (Sweet et al., 2017; Supplementary Data Table 4.1). In comparison with the updated sea level projections provided in this report (Table 4.1), the NOAA Intermediate Low scenario is similar to our median (50th percentile) RCP2.6 projections, and the

¹ This threshold is based on an empirical relationship between tide range and high tide flooding, which was developed by NOAA for consistently determining minor flood thresholds across U.S. tide gauges (Sweet et al., 2018). The estimated 63-cm Boston threshold for nuisance flooding is used in recently published projections (Thompson et al., 2019, 2021; Sweet et al., 2020); however, an observation-based Boston minor flood threshold of 68 cm above MHHW has also been established by the NOAA National Weather Service (NWS) Weather Forecasting Office (WFO) based on available flood observations for the city. This 68-cm threshold is used in Sweet et al. (2014), Spanger-Siegfried et al. (2014), and Ray & Foster (2016); however, NOAA prefers the empirically derived, nationally consistent threshold because local thresholds are often only valid in particular parts of a city (Sweet et al., 2018).

Figure 4.10

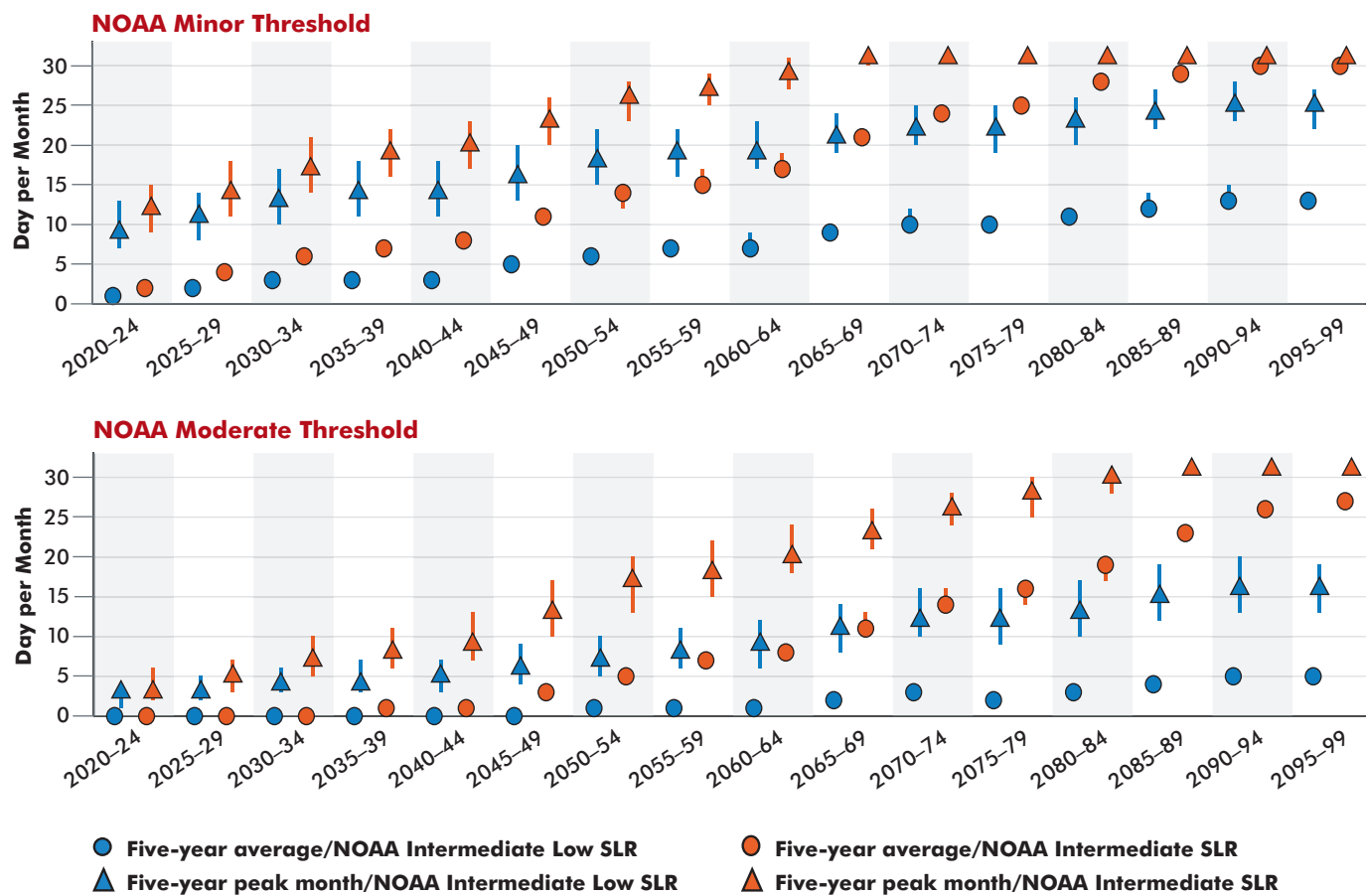
Thompson et al. (2021) projections of high tide flooding days per year at the Boston NOAA tide gauge.



Projections are shown for the NOAA minor flood threshold (63 cm above MHHW; top panel) and the NOAA moderate flood threshold (89 cm above MHHW; bottom panel) under two future sea level rise scenarios: NOAA Intermediate Low (blue) and NOAA Intermediate (red). The 50th percentile from the ensemble of projections (line) and 10th to 90th percentile range (shaded regions) show the number of high tide flooding days increasing with time for both flood thresholds and both sea level rise scenarios. The 18.6-year nodal cycle (grey line) clearly modulates high tide flooding days, with the most rapid increases occurring over decades when the nodal cycle is increasing from its minimum to maximum amplitude. This is consistent with the year of inflection (black circle; see text for an explanation) occurring at a nodal cycle minimum for all projection scenarios. Data shown here are tabulated in Supplementary Data Table 4.2.

Figure 4.11

Thompson et al. (2021) projections of high tide flooding days per month over 5-year periods at the Boston NOAA tide gauge for the NOAA minor (top panel) and moderate (bottom panel) flood thresholds and under the NOAA Intermediate Low (blue markers) and Intermediate (red markers) sea level rise scenarios.



Over each five-year period, circles show the average high tide flooding days per month, and triangles show the number of high tide flooding days in the peak flooding month within the five years. Markers represent the 50th percentile for each ensemble of projections, and lines are the 10th to 90th percentile range. Data shown here are tabulated in Supplementary Data Table 4.3.

NOAA Intermediate and Intermediate High scenarios fall between our median RCP4.5 and RCP8.5 projections. In sum, the high tide flooding projections in Thompson et al. (2021) account for sea level rise (comparable to GBRAG projections) and daily-to-decadal timescale sea level variability driven by tides, atmosphere-ocean dynamics, and internal climatic variability. Note that the projection ensembles do not represent the full range of uncertainty in flooding, given that each ensemble only considers a single sea level rise scenario (rather than a set of probabilistic projections, such as those provided in this report).

Figure 4.10 shows projections of high tide flooding days per year (i.e., days where at least one hourly sea level value exceeds a flood threshold) at the location of the Boston tide gauge. Projections for the NOAA Intermediate Low and Intermediate sea level rise scenarios are included for both the NOAA minor and moderate flood thresholds (Supplementary Data Table 4.2 contains tabulated annual projections and includes the additional NOAA Intermediate High sea level rise scenario). Under all sea level rise scenarios, Boston can expect an acceleration in the number of high tide flooding days throughout the century.

Boston's minor flood threshold will be exceeded on roughly half the days of each year by the early 2050s under the NOAA Intermediate sea level rise scenario. Under the Intermediate Low scenario, this will occur between 2070 and 2090. Boston's moderate flood threshold will be exceeded on half of days around 2070 under the Intermediate sea level rise scenario, but will only reach 48 to 87 exceedance days per year (10th to 90th percentile range) by the end of the century (2100).

Thompson et al. (2021) define the year of inflection as the year marking a transition from a regime of gradually increasing flooding to one of rapidly increasing flooding. They identify the decade that experiences a quadrupling or more of the number of high tide flooding days compared to the prior decade, based on the 50th percentile curve from each projection ensemble. The year of inflection divides these two decades, and Thompson et al. (2021) suggest that it should be a decision point for updating policy and management strategies to prepare for future rapid increases in flooding. Under the NOAA Intermediate Low sea level rise scenario, the year of inflection is 2041 for the minor flood threshold and 2059 for the moderate flood threshold. The number of high tide flooding days per year increases by 39 days for the minor threshold and 22 days for the moderate threshold in the decade following the year of inflection. Under the NOAA Intermediate sea level rise scenario, years of inflection are 2023 for the minor threshold and 2041 for the moderate threshold. Annual high tide flooding days increase by 46 days per year for both thresholds in the decade following the year of inflection. In Boston, the 18.6-year nodal cycle strongly modulates interannual variation in high tide flooding (Figure 4.10). Years of inflection for all scenarios therefore occur near nodal cycle minima, where tide range is near its minimum and will increase over the subsequent decade.

Seasonal to decadal sea level fluctuations unrelated to background sea level rise cause inevitable extreme months of clustered high tide flooding (Thompson et al., 2019, 2021). Because high tide flooding impacts are cumulative (Moftakhari et al., 2018; Ghanbari et al., 2020), only considering projected high tide flooding days per year (or per some longer time interval) for decision-making will underestimate flood impacts during extreme months (Thompson et al., 2021). In addition to annual projections, Thompson et al. therefore also provide projections of high tide flooding days per month for both an average month and the most extreme month in each future five-year period (Figure 4.11). Over five-year periods in Boston, the peak flooding month often experiences more than double the number of high tide flooding days than the average month. Thus, we reinforce that planning for the “typical” future month or year leads to substantial underestimation of flood hazard in the occasional, yet inevitable, periods of severe flooding, when cyclical contributions to sea level constructively interfere (Thompson et al., 2019, 2021).

4.11 OUTLOOK AND RECOMMENDATIONS FOR USING THIS REPORT

Sea level and flooding projections continue to evolve as illustrated by the difference between this GBRAG assessment and the previous BRAG report. Departures between this report and prior assessments are mainly caused by the revised projections of Antarctica's future contribution to sea level rise provided by the IPCC SROCC (Oppenheimer et al., 2019). The Antarctic Ice Sheet is the single greatest potential source of sea level rise, but it remains difficult to model, mainly because of its complex interaction with the surrounding ocean. Possible instabilities in the ice sheet have been identified that could produce multi-meter sea level rise within the 22nd century, particularly in the high emissions RCP8.5 scenario (DeConto et al., 2021). This “deep uncertainty” in the Antarctic contribution to future sea level rise presents a serious ongoing challenge for future planning (Oppenheimer et al., 2019) that has yet to be resolved. This issue is particularly relevant for Boston because of the gravitational and rotational amplification of sea level rise along the Northeast coastline caused by the loss of ice on West Antarctica (Figure 4.2), the sector of the ice sheet currently losing the most ice (Shepherd et al., 2019).

Sea level science and projections of future ice sheet behavior in particular are evolving rapidly. This necessitates regular updates to projections like the ones provided here. A key advantage of our probabilistic

framework for sea level and flooding projections is that the projections can be readily updated as revisions to the individual contributions to sea level rise become available.

Reliable flood projections in Greater Boston must properly account for tidal variation while incorporating the most up-to-date sea level guidance. We provide such projections at a single location (the Boston Harbor tide gauge); however, these projections have three important disadvantages: 1) they become less reliable with increasing distance from the tide gauge, 2) the methodology is not directly applicable to wave-affected areas, and 3) they do not account for nonlinear impacts on tides and storm surge from rising sea level. Meteorologic-hydrodynamic models can provide spatially continuous flood hazard information at fine spatial scales, while accounting for waves and nonlinear interactions among tides, surge, and sea level. However, they are too computationally intensive to incorporate probabilistic sea level rise (i.e., the full range of possible sea level scenarios, rather than a few discrete scenarios) and sufficient assessment of the timing of storms relative to tides. Hybrid methods are required that provide the spatial coverage of detailed hydrodynamic modeling studies, while taking advantage of computationally inexpensive probabilistic approaches that jointly combine tide-surge probabilities with updated sea level rise projections and associated uncertainties.

These GBRAG sea level and flood projections are intended to provide practitioners with a probabilistic perspective of time-evolving exposure to inundation and flood risk, based on the latest science. We recognize that the choice of planning horizon will vary on a case-by-case basis. Because our projections become strongly emissions-dependent in the second half of the 21st century and beyond (Figure 4.3), we stress that decisions pertaining to natural systems or infrastructure with a long (> 30-year) lifespan should consider the full range of low, medium, and high RCP emissions scenarios. GBRAG makes no attempt to assign a probability to which future emissions scenario is most likely to be followed by society. Furthermore, we stress that sea level uncertainty increases sharply in the second half of the 21st century, especially under the high emissions RCP8.5 scenario. Risk averse practitioners and/or those considering high-value assets with great community and/or ecological value, or a mix of assets with a wide range of importance, may find low exceedance probability values (95th or 99th percentile; 0.05 or 0.01 column in Table 4.1) to be the most appropriate for planning purposes. In other instances, when considering impacts on less vital infrastructure, landforms, or ecosystems, the “17th to 83rd percentile likely range” may be sufficient. In sum, GBRAG does not explicitly recommend one planning approach over another, which will vary as a function of planning horizon, community and practitioner values, and the consequences of losing a particular natural or built asset.

4.12 REFERENCES

- Asay-Davis, X.S., Jourdain, N.C., Nakayama, Y. “Developments in Simulating and Parameterizing Interactions Between the Southern Ocean and the Antarctic Ice Sheet.” *Current Climate Change Reports*, 3, 2017, 316–329.
- Aschwanden, A., Fahnestock, M.A., Truffer, M., Brinkerhoff, D.J., Hock, R., Khroulev, C., Mottram, R., Khan, S.A. “Contribution of the Greenland Ice Sheet to sea level over the next millennium.” *Science Advances*, 5, 2019, eaav9396.
- Bamber, J.L., Aspinall, W. “An expert judgement assessment of future sea level rise from the ice sheets.” *Nature Climate Change*, 3, 2013, 424–427.
- Bamber, J.L., Oppenheimer, M., Kopp, R.E., Aspinall, W.P., Cooke, R.M. “Ice sheet contributions to future sea-level rise from structured expert judgment.” *Proceedings of the National Academy of Sciences*, 116, 2019, 11195–11200.
- Baranes, H.E., Woodruff, J.D., Talke, S.A., Kopp, R.E., Ray, R.D., DeConto, R.M. “Tidally driven interannual variation in extreme sea level frequencies in the Gulf of Maine.” *Journal of Geophysical Research: Oceans*, 125, 2020, e2020JC016291.
- Boldt, K.V., Lane, P., Woodruff, J.D., Donnelly, J.P. “Calibrating a sedimentary record of overwash from Southeastern New England using modeled historic hurricane surges.” *Marine Geology*, 275, 2010, 127–139.

- Bosma, K., Douglas, E., Kirshen, P., McArthur, K., Miller, S., Watson, C. *Climate Change and Extreme Weather Vulnerability Assessments And Adaptation Options for the Central Artery*. Massachusetts DOT, 2015.
- Buchanan, M.K., Kopp, R.E., Oppenheimer, M., Tebaldi, C., 2016. Allowances for evolving coastal flood risk under uncertain local sea-level rise. *Climatic Change*, 137, 347–362.
- Bulthuis, K., Arnst, M., Sun, S., Pattyn, F. “Uncertainty quantification of the multi-centennial response of the Antarctic ice sheet to climate change.” *The Cryosphere*, 13, 2019, 1349–1380.
- Calov, R., Beyer, S., Greve, R., Beckmann, J., Willeit, M., Kleiner, T., Rückamp, M., Humbert, A., Ganopolski, A. “Simulation of the future sea level contribution of Greenland with a new glacial system model.” *The Cryosphere*, 12, 2018, 3097–3121.
- Castagno, K.A., Donnelly, J.P., Woodruff, J.D. “Grain-Size Analysis of Hurricane-Induced Event Beds in a New England Salt Marsh, Massachusetts, USA.” *Journal of Coastal Research*, 2020.
- Catalano, A.J., Broccoli, A.J. “Synoptic Characteristics of Surge-Producing Extratropical Cyclones along the Northeast Coast of the United States.” *Journal of Applied Meteorology and Climatology*, 57, 2018, 171–184.
- Cazenave, A., Henry, O., Munier, S., Delcroix, T., Gordon, A.L., Meyssignac, B., Llovel, W., Palanisamy, H., Becker, M. “Estimating ENSO Influence on the Global Mean Sea Level, 1993–2010.” *Marine Geodesy*, 35, 2012, 82–97.
- Cheng, L., Abraham, J., Zhu, J., Trenberth, K.E., Fasullo, J., Boyer, T., Locarnini, R., Zhang, B., Yu, F., Wan, L., Chen, X., Song, X., Liu, Y., Mann, M.E. “Record-Setting Ocean Warmth Continued in 2019.” *Advances in Atmospheric Sciences*, 37, 2020, 137–142.
- Cheung, K.F., Tang, L., Donnelly, J.P., Scleppi, E.M., Liu, K.-B., Mao, X.-Z., Houston, S.H., Murnane, R.J. “Numerical modeling and field evidence of coastal overwash in southern New England from Hurricane Bob and implications for paleotempestology.” *Journal of Geophysical Research: Earth Surface*, 112, 2007.
- Church, J.A., Clark, P.U., Cazenave, A., Gregory, J.M., Jevrejeva, S., Levermann, A., Merrifield, M.A., Milne, G.A., Nerem, R.S., Nunn, P.D., Payne, A.J., Pfeffer, W.T., D., S., Unnikrishnan, A.S. “Chapter 13: Sea Level Change.” *Climate Change 2013: the Physical Science Basis*. Cambridge University Press, 2013
- CZM, 2013. “Sea Level Rise: Understanding and Applying Trends and Future Scenarios for Analysis and Planning.” Massachusetts Office of Coastal Zone Management, 2013, 18.
- Dai, A., Luo, D., Song, M., Liu, J. “Arctic amplification is caused by sea-ice loss under increasing CO₂.” *Nature Communications*, 10, 2019, 121.
- Dangendorf, S., Marcos, M., Wöppelmann, G., Conrad, C.P., Frederikse, T., Riva, R. “Reassessment of 20th century global mean sea level rise.” *Proceedings of the National Academy of Sciences*, 2017, 201616007.
- DeConto, R.M., Pollard, D. “Contribution of Antarctica to past and future sea-level rise.” *Nature*, 531, 2016, 591–597.
- DeConto, R.M., Pollard, D., Alley, R.B., Velicogna, I., Gasson, E., Gomez, N., Sadai, S., Condron, A., Gilford, D.M., Ashe, E.L., Kopp, R., Li, D., Dutton, A. “The Paris Climate Agreement and future sea level rise from Antarctica.” *Nature*, 593, 2021, 83–89.
- Douglas, E., Kirshen, P., Hannigan, R., Herst, R., Palardy, A. *Climate Change and Sea Level Rise Projections for Boston: The Boston Research Advisory Group Report*, 2016.
- Edwards, T.L., Brandon, M.A., Durand, G., Edwards, N.R., Golledge, N.R., Holden, P.B., Nias, I.J., Payne, A.J., Ritz, C., Wernecke, A. “Revisiting Antarctic ice loss due to marine ice-cliff instability.” *Nature*, 566, 2019, 58–64.
- Edwards, T.L., Fettweis, X., Gagliardini, O., Gillet-Chaulet, F., Goelzer, H., Gregory, J.M., Hoffman, M., Huybrechts, P., Payne, A.J., Pergo, M., Price, S., Quiquet, A., Ritz, C. “Effect of uncertainty in surface mass balance–elevation feedback on projections of the future sea level contribution of the Greenland ice sheet.” *The Cryosphere*, 8, 2014, 195–208.
- Eliot, M. “Influence of interannual tidal modulation on coastal flooding along the Western Australian coast.” *Journal of Geophysical Research: Oceans*, 115, 2010.
- Engelhart, S.E., Horton, B.P. “Holocene sea level database for the Atlantic coast of the United States.” *Quaternary Science Reviews*, 54, 2012, 12–25.

- Eyring, V., Bony, S., Meehl, G.A., Senior, C.A., Stevens, B., Stouffer, R.J., Taylor, K.E. "Overview of the Coupled Model Intercomparison Project Phase 6 (CMIP6) experimental design and organization." *Geoscientific Model Development*, 9, 2016, 1937–1958.
- Ferrell, W.E., Clark, J.A. "On post glacial sea-level." *Geophysical Journal of the Royal Astronomical Society*, 46, 1976, 647–667.
- Flato, G., Marotzke, J., Abiodun, B., Braconnot, P., Chou, S.C., Collins, W., Cox, P., Driouech, F., Emori, S., Eyring, V., Forest, C., Gleckler, P., Guilyardi, E., Jakob, C., Kattsov, V., C., R., Rummukainen, M. "Evaluation of climate models, Climate Change 2013: The Physical Science Basis. Contribution of Working Group I to the Fifth Assessment Report of the Intergovernmental Panel on Climate Change." *Cambridge University Press, Cambridge, United Kingdom and New York, NY, USA*, 2013.
- Fürst, J.J., Goelzer, H., Huybrechts, P. "Ice-dynamic projections of the Greenland ice sheet in response to atmospheric and oceanic warming." *The Cryosphere*, 9, 2015, 1039–1062.
- Garbe, J., Albrecht, T., Levermann, A., Donges, J.F., Winkelmann, R. "The hysteresis of the Antarctic Ice Sheet." *Nature*, 585, 2020, 538–544.
- Ghanbari, M., Arabi, M., & Obeysekera, J. "Chronic and Acute Coastal Flood Risks to Assets and Communities in Southeast Florida." *Journal of Water Resources Planning and Management*, 146(7), 2020, 04020049.
- Goddard, P.B., Yin, J., Griffies, S.M., Zhang, S. "An extreme event of sea-level rise along the Northeast coast of North America in 2009–2010." *Nature Communications*, 2015.
- Godin, G. "Possibility of rapid changes in the tide of the Bay of Fundy, based on a scrutiny of the records from Saint John." *Continental Shelf Research*, 12, 1992, 327–338.
- Godin, G. "Rapid evolution of the tide in the Bay of Fundy." *Continental Shelf Research*, 15, 1995, 369–372.
- Golledge, N.R., Keller, E.D., Gomez, N., Naughten, K.A., Bernales, J., Trusel, L.D., Edwards, T.L. "Global environmental consequences of twenty-first-century ice-sheet melt." *Nature*, 566, 2019, 65–72.
- Golledge, N.R., Kowalewski, D.E., Naish, T.R., Levy, R.H., Fogwill, C.J., Gasson, E. "The multi-millennial Antarctic commitment to future sea-level rise." *Nature*, 526, 2015, 421–425.
- Gregory, J.M., George, S.E., Smith, R.S. "Large and irreversible future decline of the Greenland ice sheet." *The Cryosphere*, 14, 2020, 4299–4322.
- Gregory, J.M., Griffies, S.M., Hughes, C.W., Lowe, J.A., Church, J.A., Fukimori, I., et al. "Concepts and Terminology for Sea Level: Mean, Variability and Change, Both Local and Global." *Surveys in Geophysics*, 2019.
- Griggs, G., Whiteman, E., Arvai, J., Cayan, D., DeConto, R., Fox, J., Fricker, H., Kopp, R., Tebaldi, C. "Rising Seas in California—An Update on Sea-Level Rise Science." *Encyclopedia of Climate Change*, 2019.
- Group, W.G.S.L.B. "Global Sea Level Budget 1993–Present." *Earth System Science Data*, 10, 2018, 1551–1590.
- Gudmundsson, G.H., Krug, J., Durand, G., Favier, L., Gagliardini, O. "The stability of grounding lines on retrograde slopes." *The Cryosphere*, 6, 2012, 1497–1505.
- Haigh, I.D., Pickering, M.D., Green, J.A.M., Arbic, B.K., Arns, A., Dangendorf, S., Hill, D.F., Horsburgh, K., Howard, T., Idier, D., Jay, D.A., Jänicke, L., Lee, S.B., Müller, M., Schindeleger, M., Talke, S.A., Wilmes, S.-B., Woodworth, P.L. "The Tides They Are A-Changin': A Comprehensive Review of Past and Future Nonastronomical Changes in Tides, Their Driving Mechanisms, and Future Implications." *Reviews of Geophysics*, 58, 2020, e2018RG000636.
- Hamlington, B.D., Gardner, A.S., Ivins, E., Lenaerts, J.T.M., Reager, J.T., Trossman, D.S., Zaron, E.D., Adhikari, S., Arendt, A., Aschwanden, A., Beckley, B.D., Bekaert, D.P.S., Blewitt, G., Caron, L., Chambers, D.P., Chandanpurkar, H.A., Christianson, K., Csatho, B., Cullather, R.I., DeConto, R.M., Fasullo, J.T., Frederikse, T., Freymueller, J.T., Gilford, D.M., Girotto, M., Hammond, W.C., Hock, R., Holschuh, N., Kopp, R.E., Landerer, F., Larour, E., Menemenlis, D., Merrifield, M., Mitrovica, J.X., Nerem, R.S., Nias, I.J., Nieves, V., Nowicki, S., Pangaluru, K., Piecuch, C.G., Ray, R.D., Rounce, D.R., Schlegel, N.-J., Seroussi, H., Shirzaei, M., Sweet, W.V., Velicogna, I., Vinogradova, N., Wahl, T., Wiese, D.N., Willis, M.J. "Understanding of Contemporary Regional Sea-Level Change and the Implications for the Future." *Reviews of Geophysics*, 58, 2020, e2019RG000672.
- Harris, D.L., Bureau, U.S.W. *Characteristics of the Hurricane Storm Surge*. Department of Commerce, Weather Bureau, 1963.

- Hay, C., Mitrovica, J. X., Gomez, N., Creveling, J. R., Austermann, J., & E. Kopp, R. "The sea-level fingerprints of ice-sheet collapse during interglacial periods." *Quaternary Science Reviews*, 87, 2014, 60–69.
- Hay, C., Morrow, E.D., Kopp, R.E., Mitrovica, J.X. "Probabilistic reanalysis of twentieth-century sea-level rise." *Nature*, 517, 2015, 481–484.
- Horton, B.P., Kopp, R.E., Garner, A.J., Hay, C.C., Khan, N.S., Roy, K., Shaw, T.A. "Mapping Sea-Level Change in Time, Space, and Probability." *Annual Review of Environment and Resources*, 43, 2018, 481–521.
- Kirshen, P., Knee, K., Ruth, M. "Climate change and coastal flooding in Metro Boston: impacts and adaptation strategies." *Climatic Change*, 90, 2008, 453–473.
- Kopp, R.E., Andrews, C., Broccoli, A., Garner, A., Kreeger, D., Leichenko, R., Lin, N., Little, C., Miller, J.A., Miller, J.K., Miller, K.G., Moss, R., Orton, P., Parris, A., Robinson, D., Sweet, W., Walker, J., Weaver, C.P., White, K., Campo, M., Kaplan, M., Herb, J., Auermuller, L. *New Jersey's Rising Seas and Changing Coastal Storms: Report of the 2019 Science and Technical Advisory Panel*. Rutgers, The State University of New Jersey, 2019.
- Kopp, R.E., DeConto, R.M., Bader, D.A., Hay, C.C., Horton, R.M., Kulp, S., Oppenheimer, M., Pollard, D., Strauss, B.H. "Evolving understanding of Antarctic ice-sheet physics and ambiguity in probabilistic sea-level projections." *Earth's Future*, 2017, 1217–1233.
- Kopp, R.E., Horton, R.M., Little, C.M., Mitrovica, J.X., Oppenheimer, M., Rasmussen, D.J., Strauss, B.H., Tebaldi, C. "Probabilistic 21st and 22nd century sea-level projections at a global network of tide-gauge sites." *Earth's Future*, 2, 2014, 383–406.
- Kopp, R.E., Kemp, A.C., Bittermann, K., Horton, B., Donnelly, J., Gehrels, W.R., Hay, C., Mitrovica, J., Morrow, E.D., Rahmstorf, S. "Temperature-driven global sea-level variability in the Common Era." *Proceedings of the National Academy of Sciences*, 113, 2016, E1434–E1441.
- Kopp, R.E., Simons, F.J., Mitrovica, J.X., Maloof, A.C., Oppenheimer, M. "A probabilistic assessment of sea level variations within the last interglacial stage." *Geophysical Journal International*, 193, 2013, 711–716.
- Levermann, A., Winkelmann, R., Albrecht, T., Goelzer, H., Golledge, N.R., Greve, R., Huybrechts, P., Jordan, J., Leguy, G., Martin, D., Morlighem, M., Pattyn, F., Pollard, D., Quiquet, A., Rodehacke, C., Seroussi, H., Sutter, J., Zhang, T., Van Breedam, J., Calov, R., DeConto, R., Dumas, C., Garbe, J., Gudmundsson, G.H., Hoffman, M.J., Humbert, A., Kleiner, T., Lipscomb, W.H., Meinshausen, M., Ng, E., Nowicki, S.M.J., Pergo, M., Price, S.F., Saito, F., Schlegel, N.J., Sun, S., van de Wal, R.S.W. "Projecting Antarctica's contribution to future sea level rise from basal ice shelf melt using linear response functions of 16 ice sheet models (LARMIP-2)." *Earth System Dynamics*, 11, 2020, 35–76.
- Levermann, A., Winkelmann, R., Nowicki, S.M.J., Fastook, J.L., Frieler, K., Greve, R., Hellmer, H.H., Martin, M.A., Meinshausen, M., Mengel, M., Payne, A.J., Pollard, D., Sato, T., Timmermann, R., Wang, W.L., Bindschadler, R.A. "Projecting Antarctic ice discharge using response functions from SeARISE ice-sheet models." *Earth System Dynamics*, 5, 2014, 271–293.
- Lin, N., Emanuel, K.A., Smith, J.A., Vanmarcke, E., 2010. "Risk assessment of hurricane storm surge for New York City." *Journal of Geophysical Research: Atmospheres*, 115, 2010.
- Lin, N., Marsooli, R., Colle, B.A. "Storm surge return levels induced by mid-to-late-twenty-first-century extratropical cyclones in the Northeastern United States." *Climatic Change*, 154, 2019, 143–158.
- Marsooli, R., Lin, N., Emanuel, K., Feng, K. "Climate change exacerbates hurricane flood hazards along US Atlantic and Gulf Coasts in spatially varying patterns." *Nature Communications*, 10, 2019, 3785.
- Meinshausen, N., Smith, S.J., Calvin, K., Daniel, J.S., Kainuma, M.L.T., Lamarque, J.-F., Matsumoto, K., Montzka, S.A., Raper, S.C.B., Riahi, K., Thomson, A., Velders, G.J.M., van Vuuren, D.P.P. "The RCP greenhouse gas concentrations and their extensions from 1765 to 2300." *Climatic Change*, 109, 2011, 213–241.
- Mitrovica, J.X., Gomez, N., Morrow, E., Hay, C., Latychev, K., Tamisiea, M.E. "On the robustness of predictions of sea level fingerprints." *Geophysical Journal International*, 187, 2011, 729–742.
- Moftakhar, H. R., AghaKouchak, A., Sanders, B. F., Allaire, M., & Matthew, R. A. "What Is Nuisance Flooding? Defining and Monitoring an Emerging Challenge." *Water Resources Research*, 54(7), 2018, 4218–4227.
- Moftakhar, H. R., AghaKouchak, A., Sanders, B. F., & Matthew, R. A. "Cumulative hazard: The case of nuisance flooding." *Earth's Future*, 5(2), 2017, 214–223.

- Moftakhari, H.R., AghaKouchak, A., Sanders, B.F., Feldman, D.L., Sweet, W., Matthew, R.A., Luke, A. "Increased nuisance flooding along the coasts of the United States due to sea level rise: Past and future." *Geophysical Research Letters*, 42, 2015, 9846–9852.
- Moore, J.C., Grinsted, A., Zwinger, T., Jevrejeva, S., 2013. Semiempirical and process-based global sea level projections. *Reviews of Geophysics*, 51, 484–522.
- Morlighem, M., Rignot, E., Binder, T., Blankenship, D., Drews, R., Eagles, G., Eisen, O., Ferraccioli, F., Forsberg, R., Fretwell, P., Goel, V., Greenbaum, J.S., Gudmundsson, H., Guo, J., Helm, V., Hofstede, C., Howat, I., Humbert, A., Jakob, W., Karlsson, N.B., Lee, W.S., Matsuoka, K., Millan, R., Mouginot, J., Paden, J., Pattyn, F., Roberts, J., Rosier, S., Ruppel, A., Seroussi, H., Smith, E.C., Steinhage, D., Sun, B., Broeke, M.R.v.d., Ommen, T.D.v., Wessem, M.v., Young, D.A. "Deep glacial troughs and stabilizing ridges unveiled beneath the margins of the Antarctic ice sheet." *Nature Geoscience*, 13, 2020, 132–137.
- Morlighem, M., Rignot, E., Mouginot, J., Seroussi, H., Larour, E. "Deeply incised submarine glacial valleys beneath the Greenland ice sheet." *Nature Geoscience*, 7, 2014, 418–422.
- Mouche, R., Forte, A.M., Mitrovica, J.X., Rowley, D.B., Quéré, S., Simmons, N.A., Grand, S.P. "Dynamic topography and long-term sea-level variations: There is no such thing as a stable continental platform." *Earth and Planetary Science Letters*, 271, 2008, 101–108.
- Nadal-Caraballo, N.C., Melby, J.A., Gonzalez, V.M. *Coastal Storm Hazards from Virginia to Maine, North Atlantic Coast Comprehensive Study (NACCS)*. US Army Corps of Engineers, Coastal and Hydraulics Laboratory, 2015, 204.
- Nations, U., 2012. *World Population Prospects. Economics & Social Affairs*.
- Nations, U., 2014. *World Population Prospects: The 2012 Revision*. Paper No. ESA/P/WP.228, 2013.
- Nerem, R.S., Beckley, B.D., Fasullo, J.T., Hamlington, B.D., Masters, D., Mitchum, G.T. "Climate-change–driven accelerated sea-level rise detected in the altimeter era." *Proceedings of the National Academy of Sciences*, 2018.
- Oppenheimer, M., Glavovic, B.C., Hinkel, J., van de Wal, R., Magnan, A.K., Abd-Elgawad, A., Cai, R., M., C., DeConto, R.M., Ghosh, T., Hay, J., Isla, F., Marzeion, B., Meyssignac, B. "Sea Level Rise and Implications for Low-Lying Islands, Coasts and Communities." *IPCC Special Report on the Ocean and Cryosphere in a Changing Climate*, 2019.
- Orton, P., Georgas, N., Blumberg, A., Pullen, J. "Detailed modeling of recent severe storm tides in estuaries of the New York City region." *Journal of Geophysical Research: Oceans*, 117, 2012.
- Paolo, F.S., Fricker, H., Padman, L. "Volume loss from Antarctic ice shelves is accelerating." *Science*, 348(6232), 2015, 327–331.
- Parizek, B.R., Christianson, K., Alley, R.B., Voytenko, D., Vaňková, I., Dixon, T.H., Walker, R.T., Holland, D.M. "Ice-cliff failure via retrogressive slumping." *Geology*, 47, 2019, 1–4.
- Parris, A., Bromirski, P., Burkett, V., Cayan, D., Culver, M., Hall, J., Horton, R., Knuuti, K., Moss, R., Obeysekera, J., Sallenger, A., Weiss, J. *Global Sea Level Rise Scenarios for the US National Climate Assessment*. NOAA Tech Memo OAR CPO-1, 2012, 37.
- Pattyn, F., Ritz, C., Hanna, E., Asay-Davis, X., DeConto, R., Durand, G., Favier, L., Fettweis, X., Goelzer, H., Golledge, N.R., Kuipers Munneke, P., Lenaerts, J.T.M., Nowicki, S., Payne, A.J., Robinson, A., Seroussi, H., Trusel, L.D., van den Broeke, M. "The Greenland and Antarctic ice sheets under 1.5 °C global warming." *Nature Climate Change*, 8, 2018, 1053–1061.
- Peltier, W.R. "Global Glacial Isostasy and the Surface of the Ice-Age Earth: The ICE-5G(VM2) model and GRACE." *Annual Reviews of Earth and Planetary Sciences*, 32, 2004.
- Peng, D., Hill, E.M., Meltzner, A.J., Switzer, A.D. "Tide Gauge Records Show That the 18.61-Year Nodal Tidal Cycle Can Change High Water Levels by up to 30 cm." *Journal of Geophysical Research: Oceans*, 124, 2019, 736–749.
- Piecuch, C.G., Huybers, P., Hay, C.C., Kemp, A.C., Little, C.M., Mitrovica, J.X., Ponte, R.M., Tingley, M.P. "Origin of spatial variation in US East Coast sea-level trends during 1900–2017." *Nature*, 564, 2018, 400–404.
- Pollard, D., DeConto, R.M., Alley, R.B. "Potential Antarctic Ice Sheet retreat driven by hydrofracturing and ice cliff failure." *Earth and Planetary Science Letters*, 412, 2015, 112–121.

- Pörtner, H.-O., Roberts, D.C., Masson-Delmotte, V., Zhai, P., Tignor, M., Poloczanska, E., Mintenbeck, K., Alegria, A., Nicolai, M., Okem, A., Petzold, J., Rama, B., Weyer, N.M. *IPCC, 2019: IPCC Special Report on the Ocean and Cryosphere in a Changing Climate*. 2019.
- Rahmstorf, S., Perrette, M., Vermeer, M. "Testing the robustness of semi-empirical sea level projections." *Climate Dynamics*, 39, 2012, 861–875.
- Ray, R.D. "Secular changes of the M2 tide in the Gulf of Maine." *Continental Shelf Research*, 26, 2006, 422–427.
- Ray, R.D., Foster, G. "Future nuisance flooding at Boston caused by astronomical tides alone." *Earth's Future*, 4, 2016, 578–587.
- Ray, R.D., Merrifield, M.A. "The Semiannual and 4.4-Year Modulations of Extreme High Tides." *Journal of Geophysical Research: Oceans*, 124, 2019, 5907–5922.
- Redfield, A.C., Miller, A.R. "Water Levels Accompanying Atlantic Coast Hurricanes." *Interaction of Sea and Atmosphere: A Group of Contributions*. American Meteorological Society, Boston, MA, 1957, 1–23.
- Rignot, E., Mouginot, J., Morlighem, M., Seroussi, H., Scheuchl, B. "Widespread, rapid grounding line retreat of Pine Island, Thwaites, Smith, and Kohler glaciers, West Antarctica, from 1992 to 2011." *Geophysical Research Letters*, 41, 2014, 3502–3509.
- Ritz, C., Edwards, T.L., Durand, G., Payne, A.J., Peyaud, V., Hindmarsh, R.C.A. "Potential sea-level rise from Antarctic ice-sheet instability constrained by observations." *Nature*, 528, 2015, 115–118.
- Ryan, J.C., Hubbard, A., Stibal, M., Irvine-Fynn, T.D., Cook, J., Smith, L.C., Cameron, K., Box, J. "Dark zone of the Greenland Ice Sheet controlled by distributed biologically-active impurities." *Nature Communications*, 9, 2018, 1065.
- Scambos, T.A., Bell, R.E., Alley, R.B., Anandakrishnan, S., Bromwich, D.H., Brunt, K., Christianson, K., Creyts, T., Das, S.B., DeConto, R., Dutrieux, P., Fricker, H.A., Holland, D., MacGregor, J., Medley, B., Nicolas, J.P., Pollard, D., Siegfried, M.R., Smith, A.M., Steig, E.J., Trusel, L.D., Vaughan, D.G., Yager, P.L., Markowski, M.S. "How much, how fast? A science review and outlook for research on the instability of Antarctica's Thwaites Glacier in the 21st century." *Global and Planetary Change*, 153, 2017, 16–34.
- Schlegel, N.J., Seroussi, H., Schodlok, M.P., Larour, E.Y., Boening, C., Limonadi, D., Watkins, M.M., Morlighem, M., van den Broeke, M.R. "Exploration of Antarctic Ice Sheet 100-year contribution to sea level rise and associated model uncertainties using the ISSM framework." *The Cryosphere*, 12, 2018, 3511–3534.
- Schoof, C. "Ice sheet grounding line dynamics: Steady states, stability, and hysteresis." *Journal of Geophysical Research-Earth Surface*, 112, 2007, F03S28.
- Schwalm, C.R., Glendon, S., Duffy, P.B. "RCP8.5 tracks cumulative CO₂ emissions." *Proceedings of the National Academy of Sciences*, 117, 2020, 19656–19657.
- Shepherd, A., Gilbert, L., Muir, A.S., Konrad, H., McMillan, M., Slater, T., Briggs, K.H., Sundal, A.V., Hogg, A.E., Engdahl, M.E. "Trends in Antarctic Ice Sheet Elevation and Mass." *Geophysical Research Letters*, 46, 2019, 8174–8183.
- Shepherd, A., Ivins, E., Rignot, E., Smith, B., van den Broeke, M., Velicogna, I., Whitehouse, P., Briggs, K., Joughin, I., Krinner, G., Nowicki, S., Payne, T., Scambos, T., Schlegel, N., A, G., Agosta, C., Ahlstrøm, A., Babonis, G., Barletta, V., Blazquez, A., Bonin, J., Csatho, B., Cullather, R., Felikson, D., Fettweis, X., Forsberg, R., Gallee, H., Gardner, A., Gilbert, L., Groh, A., Gunter, B., Hanna, E., Harig, C., Helm, V., Horvath, A., Horwath, M., Khan, S., Kjeldsen, K.K., Konrad, H., Langen, P., Lecavalier, B., Loomis, B., Luthcke, S., McMillan, M., Melini, D., Mernild, S., Mohajerani, Y., Moore, P., Mouginot, J., Moyano, G., Muir, A., Nagler, T., Nield, G., Nilsson, J., Noel, B., Otosaka, I., Pattle, M.E., Peltier, W.R., Pie, N., Rietbroek, R., Rott, H., Sandberg-Sørensen, L., Sasgen, I., Save, H., Scheuchl, B., Schrama, E., Schröder, L., Seo, K.-W., Simonsen, S., Slater, T., Spada, G., Sutterley, T., Talpe, M., Tarasov, L., van de Berg, W.J., van der Wal, W., van Wessem, M., Vishwakarma, B.D., Wiese, D., Wouters, B., The, I.t. "Mass balance of the Antarctic Ice Sheet from 1992 to 2017." *Nature*, 558, 2018, 219–222.

- Shepherd, A., Ivins, E., Rignot, E., Smith, B., van den Broeke, M., Velicogna, I., Whitehouse, P., Briggs, K., Joughin, I., Krinner, G., Nowicki, S., Payne, T., Scambos, T., Schlegel, N., A., G., Agosta, C., Ahlstrøm, A., Babonis, G., Barletta, V.R., Bjørk, A.A., Blazquez, A., Bonin, J., Colgan, W., Csatho, B., Cullather, R., Engdahl, M.E., Felikson, D., Fettweis, X., Forsberg, R., Hogg, A.E., Gallee, H., Gardner, A., Gilbert, L., Gourmelen, N., Groh, A., Gunter, B., Hanna, E., Harig, C., Helm, V., Horvath, A., Horwath, M., Khan, S., Kjeldsen, K.K., Konrad, H., Langen, P.L., Lecavalier, B., Loomis, B., Luthcke, S., McMillan, M., Melini, D., Mernild, S., Mohajerani, Y., Moore, P., Mottram, R., Mouginot, J., Moyano, G., Muir, A., Nagler, T., Nield, G., Nilsson, J., Noël, B., Otosaka, I., Pattle, M.E., Peltier, W.R., Pie, N., Rietbroek, R., Rott, H., Sandberg Sørensen, L., Sasgen, I., Save, H., Scheuchl, B., Schrama, E., Schröder, L., Seo, K.-W., Simonsen, S.B., Slater, T., Spada, G., Sutterley, T., Talpe, M., Tarasov, L., van de Berg, W.J., van der Wal, W., van Wessem, M., Vishwakarma, B.D., Wiese, D., Wilton, D., Wagner, T., Wouters, B., Wuite, J., The, I.T. "Mass balance of the Greenland Ice Sheet from 1992 to 2018." *Nature*, 579, 2020, 233–239.
- Stocker, T.F., Qin, D., Plattner, G.-K., Tignor, M., Allen, S.K., Boschung, J., Nauels, A., Xia, Y., Bex, V., Midgley, P.M. "IPCC, 2013: Climate Change 2013: The Physical Science Basis. Contribution of Working Group I to the Fifth Assessment Report of the Intergovernmental Panel on Climate Change." *Cambridge University Press, Cambridge, United Kingdom and New York, NY, USA*, 2013, 1535.
- Sweet, W., Dusek, G., Carbin, G., Marra, J., Marcy, D., Simon, S. *2019 State of U.S. High Tide Flooding with a 2020 Outlook*. 2020.
- Sweet, W.V., Dusek, G.W., Obeysekera, J.T.B., Marra, J.J. "Patterns and projections of high tide flooding along the U.S. coastline using a common impact threshold." *NOAA Technical Report NOS CO-OPS*, 86, 2018.
- Sweet, W.V., R.E. Kopp, C. P. Weaver, J. Obeysekera, R. M. Horton, E.R. Thieler and C. Zervas. "Global and Regional Sea Level Rise Scenarios for the United States." *NOAA Technical Report. NOS CO-OPS*, 83, 2017.
- Sweet, W.V., Park, J. "From the extreme to the mean: Acceleration and tipping points of coastal inundation from sea level rise." *Earth's Future*, 2, 2014, 579-600.
- Sweet, W.V., Zervas, C.E., Gill, S. "Elevated East Coast Sea Levels Anomaly: June–July 2009." *NOAA Technical Report NOS CO-OPS*, 51, 2009.
- Talke, S.A., Jay, D.A. "Changing Tides: The Role of Natural and Anthropogenic Factors." *Annual Review of Marine Science*, 12, 2020, 121–151.
- Talke, S.A., Kemp, A.C., Woodruff, J. "Relative Sea Level, Tides, and Extreme Water Levels in Boston Harbor From 1825 to 2018." *Journal of Geophysical Research: Oceans*, 123, 2018, 3895–3914.
- Talke, S.A., Orton, P., Jay, D.A. "Increasing storm tides in New York Harbor, 1844–2013." *Geophysical Research Letters*, 41, 2014, 3149–3155.
- Taylor, K.E., Stouffer, R.J., Meehl, G.A. "An overview of CMIP5 and the experiment design." *Bulletin of the American Meteorological Society*, 93, 2012, 485–498.
- Tedesco, M., Doherty, S., Fettweis, X., Alexander, P., Jeyaratnam, J., Stroeve, J. "The darkening of the Greenland ice sheet: trends, drivers, and projections (1981–2100)." *The Cryosphere*, 10, 2016a, 477–496.
- Tedesco, M., Mote, T., Fettweis, X., Hanna, E., Jeyaratnam, J., Booth, J.F., Datta, R., Briggs, K. "Arctic cut-off high drives the poleward shift of a new Greenland melting record." *Nature Communications*, 7, 2016b, 11723.
- Thompson, P. R., Widlansky, M. J., Hamlington, B. D., Merrifield, M. A., Marra, J. J., Mitchum, G. T., & Sweet, W. "Rapid increases and extreme months in projections of United States high-tide flooding." *Nature Climate Change*, 11(7), 2021, 584–590.
- Thompson, P.R., Widlansky, M.J., Merrifield, M.A., Becker, J.M., Marra, J.J. "A statistical model for frequency of coastal flooding in Honolulu, Hawaii, during the 21st century." *Journal of Geophysical Research: Oceans*, 124, 2019, 2787–2802.
- Van De Plassche, O., Wright, A.J., Horton, B.P., Engelhart, S.E., Kemp, A.C., Mallinson, D., Kopp, R.E. "Estimating tectonic uplift of the Cape Fear Arch (south-eastern United States) using reconstructions of Holocene relative sea level." *Journal of Quaternary Science*, 29, 2014, 749–759.
- van den Broeke, M., Enderlin, E.M., Howat, I.M., Kiopers Munneke, P., Noel, B.P.Y., van de Berg, W.J., van Meijgaard, E., Wouters, B. "On the recent contribution of the Greenland ice sheet to sea level change." *The Cryosphere*, 10, 2016, 1933–1946.

- Van Tricht, K., Lhermitte, S., Lenaerts, J.T.M., Gorodetskaya, I.V., L'Ecuyer, T.S., Noël, B., van den Broeke, M.R., Turner, D.D., van Lipzig, N.P.M. "Clouds enhance Greenland ice sheet meltwater runoff." *Nature Communications*, 7, 2016, 10266.
- van Vuuren, D.P., Edmonds, J., Kainuma, M., Riahi, K., Thomson, A., Hibbard, K., Hurtt, G.C., Kram, T., Krey, V., Lamarque, J.F., Masui, T., Meinshausen, M., Nakicenovic, N., Smith, S.J., Rose, S.K. "The representative concentration pathways: an overview." *Climatic Change*, 109, 2011, 5–31.
- Vizcaino, M., Mikolajewicz, U., Ziemen, F., Rodehacke, C.B., Greve, R., van den Broeke, M.R. "Coupled simulations of Greenland Ice Sheet and climate change up to A.D. 2300." *Geophysical Research Letters*, 42, 2015, 3927–3935.
- Vousdoukas, M.I., Voukouvalas, E., Mentaschi, L., Dottori, F., Giardino, A., Bouziotas, D., Bianchi, A., Salamon, P., Feyen, L. "Developments in large-scale coastal flood hazard mapping." *Natural Hazards and Earth System Sciences*, 16, 2016, 1841–1853.
- Weertman, J. "Stability of the junction of an ice sheet and an ice shelf." *Journal of Glaciology*, 13, 1974, 3–11.
- Williams, J., Horsburgh, K.J., Williams, J.A., Proctor, R.N.F. "Tide and skew surge independence: New insights for flood risk." *Geophysical Research Letters*, 43, 2016, 6410–6417.
- Woodworth, P.L., Melet, A., Marcos, M., Ray, R.D., Wöppelmann, G., Sasaki, Y.N., Cirano, M., Hibbert, A., Huthnance, J.M., Monserrat, S., Merrifield, M.A. "Forcing Factors Affecting Sea Level Changes at the Coast." *Surveys in Geophysics*, 40, 2019, 1351–1397.
- Yin, J. "Century to multi-century sea level rise projections from CMIP5 models." *Geophysical Research Letters*, 2012, 39.
- Yin, J., Goddard, P.B. "Oceanic control of sea level rise patterns along the East Coast of the United States." *Geophysical Research Letters*, 40, 2013, 1-7.
- Yin, J., Schlesinger, M.E., Stouffer, R.J. "Model projections of rapid sea-level rise on the northeast coast of the United States." *Nature Geoscience*, 2, 2009, 262–266.
- Zervas, C., Gill, S., Sweet, W. "Estimating vertical land motion from long-term tide gauge records." *NOAA Technical Reports. NOS CO-OPS*, 65, 2013, 22.

Appendix: Supplementary Data

SUPPLEMENTARY DATA: TABLE 4.1

NOAA sea level rise scenarios at the Boston tide gauge (Station ID 8443970) used in Thompson et al. (2021)

Note: Thompson et al. (2021) projections only extend through 2100, but we include NOAA sea level rise projections through 2200 here. Thompson et al. interpolated NOAA decadal projections to monthly projections using a cubic spline function.

Source: Sweet, W.V., R.E. Kopp, C. P. Weaver, J. Obeysekera, R. M. Horton, E.R. Thieler and C. Zervas (2017), Global and Regional Sea Level Rise Scenarios for the United States. NOAA Tech. Rep. NOS CO-OPS 83. NOAA sea level rise scenarios are publicly available and were obtained from the NOAA CO-COPS website: <https://tidesandcurrents.noaa.gov/publications/tech rpt083.csv>

Columns 2 to 4 show relative sea level rise in centimeters above 2000 mean sea level.

Sea level rise scenarios correspond to the following scenario names:

- Intermediate Low = 0.5 to MED (50th percentile of scenario with 0.5 meters global mean sea level rise in 2100)
- Intermediate = 1.0 to MED (50th percentile of scenario with 1.0 meters global mean sea level rise in 2100)
- Intermediate High = 1.5 to MED (50th percentile of scenario with 1.5 meters global mean sea level rise in 2100)

Year	Intermediate Low	Intermediate	Intermediate High
2000	0	0	0
2010	6	8	11
2020	12	17	23
2030	17	26	35
2040	23	36	51
2050	29	49	69
2060	36	63	89
2070	42	77	112
2080	46	92	136
2090	51	108	162
2100	56	125	192
2120	63	140	237
2150	79	192	341
2200	99	281	549

SUPPLEMENTARY DATA: TABLE 4.2

Annual projections of high tide flooding days per year.

Six total scenarios: NOAA minor and moderate flood thresholds under three sea level rise scenarios (NOAA Intermediate Low, Intermediate, and Intermediate High).

Values are in number of days per year; columns show percentiles (e.g. 10 = 10th percentile, where there is a 90% chance that high tide flooding days will exceed the 10th percentile); rows show years.

Source: Thompson, P. R., Widlansky, M. J., Hamlington, B. D., Merrifield, M. A., Marra, J. J., Mitchum, G. T., & Sweet, W. (2021). Rapid increases and extreme months in projections of United States high-tide flooding. *Nature Climate Change*, 11(7), 584–590. <https://doi.org/10.1038/s41558-021-01077-8>

Sea level rise scenario: NOAA Intermediate Low flood threshold: NOAA minor

Year/Percentile	5	10	17	50	83	90	95
2010	12	14	16	23	30	33	36
2011	13	15	17	23	31	33	37
2012	15	17	19	26	34	37	40
2013	11	13	15	21	29	32	35
2014	12	14	16	22	30	33	36
2015	9	11	12	18	25	27	30
2016	12	14	16	22	29	32	36
2017	11	13	15	22	31	34	37
2018	12	14	17	24	33	37	41
2019	11	13	15	23	31	35	39
2020	12	15	17	24	33	36	40
2021	11	14	16	23	31	34	38
2022	11	13	16	23	32	35	40
2023	8	10	12	19	27	30	34
2024	10	12	14	21	29	33	37
2025	11	13	15	22	30	33	37
2026	13	15	17	25	35	39	43
2027	13	15	18	26	36	40	44
2028	15	18	21	29	40	44	48
2029	20	23	26	35	46	50	54
2030	25	28	31	41	53	57	62
2031	23	26	30	40	52	57	62
2032	21	25	28	39	51	56	61
2033	26	29	32	43	54	59	64
2034	28	31	35	46	58	63	68
2035	27	30	34	45	58	62	68

Sea level rise scenario: NOAA Intermediate Low flood threshold: NOAA minor

Year/Percentile	5	10	17	50	83	90	95
2036	25	29	32	44	57	62	68
2037	29	33	37	48	61	66	72
2038	30	34	38	49	62	67	73
2039	29	33	37	48	62	66	71
2040	26	30	33	44	57	62	67
2041	25	28	32	43	56	61	66
2042	29	32	36	47	60	65	70
2043	31	35	39	51	65	70	76
2044	29	33	37	49	62	66	72
2045	35	39	43	57	71	76	83
2046	38	42	47	60	74	79	85
2047	46	50	55	69	84	89	96
2048	42	47	51	64	77	82	88
2049	51	56	60	75	91	96	103
2050	51	56	61	75	91	96	103
2051	57	62	66	82	98	104	110
2052	57	61	65	79	95	100	106
2053	63	68	72	88	104	109	116
2054	62	68	73	87	103	109	115
2055	67	73	78	94	109	115	122
2056	60	65	69	84	100	105	111
2057	66	72	77	92	107	113	119
2058	58	64	69	84	99	105	111
2059	61	66	72	88	104	110	116
2060	60	66	71	85	100	105	111
2061	67	73	77	92	108	114	120
2062	67	72	78	93	108	114	121
2063	74	79	85	100	117	123	129
2064	80	86	92	108	125	130	137
2065	86	91	97	113	130	136	142
2066	83	89	94	110	126	132	138
2067	85	91	96	112	128	133	140
2068	98	103	109	125	143	149	155
2069	99	106	112	129	146	152	158
2070	98	104	109	126	143	148	155
2071	96	102	107	123	140	146	153

Sea level rise scenario: NOAA Intermediate Low flood threshold: NOAA minor

Year/Percentile	5	10	17	50	83	90	95
2072	108	114	120	137	153	158	165
2073	107	114	120	137	155	161	167
2074	105	110	116	133	150	156	162
2075	94	100	105	121	138	144	150
2076	102	108	114	130	146	152	158
2077	93	100	105	122	139	145	151
2078	96	103	108	125	143	149	156
2079	90	95	100	117	133	139	146
2080	101	107	112	129	146	152	159
2081	102	109	114	131	148	155	162
2082	113	119	125	143	160	166	172
2083	107	113	119	136	154	160	167
2084	113	119	125	142	159	165	172
2085	115	122	127	144	162	168	175
2086	126	133	139	156	174	180	187
2087	123	130	136	154	172	178	185
2088	132	139	145	162	180	186	193
2089	130	136	142	159	177	183	190
2090	139	145	152	169	187	192	199
2091	141	147	153	170	188	194	201
2092	137	143	149	167	186	192	199
2093	130	136	143	161	179	185	192
2094	129	136	142	159	177	183	189
2095	132	139	145	162	180	186	193
2096	131	137	143	161	179	185	191
2097	129	136	142	159	177	183	190
2098	129	136	142	159	177	183	190
2099	142	149	154	170	189	195	202
2100	140	147	154	173	191	197	204

**Sea level rise scenario: NOAA Intermediate Low flood threshold:
NOAA moderate**

Year/Percentile	5	10	17	50	83	90	95
2010	0	0	0	2	4	5	7
2011	0	0	0	1	3	4	5
2012	0	0	1	2	5	6	7
2013	0	0	0	1	3	4	5
2014	0	0	0	1	3	4	5
2015	0	0	0	1	2	3	4
2016	0	0	0	1	3	4	5
2017	0	0	0	1	3	4	6
2018	0	0	0	2	4	5	6
2019	0	0	0	1	3	4	6
2020	0	0	0	2	4	5	6
2021	0	0	0	1	4	5	6
2022	0	0	0	1	3	4	6
2023	0	0	0	1	2	3	4
2024	0	0	0	1	3	4	5
2025	0	0	0	2	4	5	6
2026	0	0	0	2	4	5	6
2027	0	0	0	1	3	4	6
2028	0	0	0	2	4	5	7
2029	0	1	1	4	7	8	10
2030	0	1	2	4	8	9	11
2031	0	1	1	3	6	8	10
2032	0	0	1	3	6	7	9
2033	1	1	2	4	8	9	11
2034	1	2	2	5	9	10	12
2035	0	1	2	4	8	9	11
2036	0	1	1	4	7	8	10
2037	1	1	2	5	8	10	12
2038	1	2	2	5	9	11	13
2039	1	1	2	5	9	11	13
2040	0	1	2	4	8	10	12
2041	0	1	1	4	7	8	10
2042	1	2	2	5	9	11	13
2043	1	2	3	6	10	12	14
2044	1	1	2	5	9	11	13
2045	1	2	2	5	10	12	14

**Sea level rise scenario: NOAA Intermediate Low flood threshold:
NOAA moderate**

Year/Percentile	5	10	17	50	83	90	95
2046	2	3	4	7	12	14	16
2047	3	4	6	10	16	18	21
2048	3	4	6	10	15	18	20
2049	3	4	6	10	16	18	21
2050	4	5	6	11	17	19	22
2051	5	7	8	13	20	22	25
2052	6	8	9	15	22	24	28
2053	6	7	9	15	22	25	29
2054	5	7	8	14	21	24	27
2055	6	8	10	15	23	25	29
2056	7	9	11	16	23	26	30
2057	7	9	11	17	25	28	31
2058	5	6	8	13	20	23	26
2059	5	7	8	14	20	23	26
2060	7	9	10	16	23	25	28
2061	8	10	12	18	26	30	33
2062	7	9	11	17	26	29	33
2063	7	9	11	18	26	29	33
2064	12	14	16	24	33	36	40
2065	16	18	21	29	38	42	46
2066	13	15	17	26	36	40	44
2067	12	15	17	25	35	39	43
2068	16	19	22	31	41	45	50
2069	21	24	27	36	47	51	56
2070	20	23	26	36	47	52	56
2071	19	22	25	35	46	49	54
2072	20	24	27	37	49	54	59
2073	23	26	29	39	51	55	60
2074	22	25	28	38	51	55	61
2075	20	23	26	36	47	51	56
2076	18	21	24	33	45	49	54
2077	16	18	21	30	40	43	48
2078	17	20	23	33	44	48	53
2079	18	21	24	33	44	48	52
2080	19	22	24	35	47	51	56
2081	19	22	25	35	46	51	56

**Sea level rise scenario: NOAA Intermediate Low flood threshold:
NOAA moderate**

Year/Percentile	5	10	17	50	83	90	95
2082	24	28	31	43	55	60	65
2083	27	30	34	45	58	62	67
2084	26	30	33	45	58	63	68
2085	25	29	33	45	59	64	70
2086	32	36	40	53	67	73	78
2087	35	39	43	55	69	73	79
2088	40	44	48	61	75	80	86
2089	37	42	46	60	74	80	85
2090	42	46	51	65	81	87	93
2091	43	48	53	66	81	86	92
2092	43	48	52	66	80	86	91
2093	38	43	47	61	76	81	86
2094	36	40	44	58	72	78	84
2095	37	41	45	58	73	79	85
2096	38	42	46	58	72	78	84
2097	38	43	47	61	75	80	87
2098	38	42	46	60	74	80	86
2099	43	47	52	65	81	87	93
2100	44	48	53	67	82	87	93

Sea level rise scenario: NOAA Intermediate flood threshold: NOAA minor

Year/Percentile	5	10	17	50	83	90	95
2010	15	18	20	27	35	38	42
2011	17	19	21	28	36	40	43
2012	19	21	24	31	40	43	47
2013	15	17	20	27	35	38	42
2014	17	19	22	29	37	40	44
2015	13	16	18	24	32	35	39
2016	18	20	23	30	38	41	45
2017	17	19	22	30	40	44	48
2018	19	22	25	34	45	49	54
2019	18	21	24	33	44	48	53
2020	20	23	26	36	46	50	55
2021	20	23	25	34	45	49	53
2022	21	24	27	36	48	52	57
2023	17	20	22	31	42	46	52

Sea level rise scenario: NOAA Intermediate flood threshold: NOAA minor

Year/Percentile	5	10	17	50	83	90	95
2024	20	24	27	36	48	52	57
2025	21	24	27	37	48	51	56
2026	26	30	33	44	57	61	67
2027	28	32	36	47	60	65	70
2028	33	37	42	54	68	73	79
2029	40	44	48	60	74	78	84
2030	48	53	57	70	85	90	96
2031	48	52	57	70	85	90	96
2032	49	54	58	73	89	95	101
2033	53	58	63	77	92	98	104
2034	57	62	68	82	98	104	110
2035	57	62	67	81	96	102	108
2036	59	65	69	85	101	106	113
2037	66	72	77	92	108	114	120
2038	68	73	79	94	110	116	123
2039	67	72	77	92	108	113	119
2040	64	69	74	89	105	110	117
2041	67	73	79	95	112	118	124
2042	73	78	84	100	117	123	129
2043	79	85	90	106	123	128	134
2044	77	82	88	104	120	126	132
2045	93	99	105	121	137	143	150
2046	98	104	110	127	144	149	155
2047	111	117	123	140	157	163	170
2048	106	112	118	134	152	158	164
2049	122	129	134	151	169	174	181
2050	127	133	139	156	173	179	187
2051	138	144	150	167	184	190	197
2052	135	141	147	165	183	189	196
2053	148	154	160	178	197	203	211
2054	149	156	162	180	198	204	211
2055	161	167	172	190	208	214	221
2056	154	160	166	183	201	207	214
2057	164	170	176	194	213	219	225
2058	155	162	168	186	205	211	218
2059	164	170	177	195	213	219	226
2060	167	173	179	197	215	221	227

Sea level rise scenario: NOAA Intermediate flood threshold: NOAA minor

Year/Percentile	5	10	17	50	83	90	95
2061	178	184	190	209	228	235	243
2062	180	187	193	212	231	237	245
2063	191	198	205	224	243	250	257
2064	205	213	219	239	257	263	270
2065	215	222	229	248	266	272	279
2066	214	222	228	247	265	271	278
2067	222	230	236	254	271	277	284
2068	242	249	255	273	291	297	303
2069	251	258	264	282	299	304	310
2070	253	259	265	283	299	304	310
2071	255	262	268	284	300	304	309
2072	275	282	288	304	318	323	328
2073	281	287	293	309	324	329	333
2074	282	289	294	309	323	327	331
2075	271	277	282	298	312	316	321
2076	288	294	300	314	327	331	335
2077	285	292	298	313	327	332	336
2078	293	300	306	320	333	336	340
2079	285	291	296	311	324	328	332
2080	305	310	315	327	338	342	345
2081	312	317	321	333	343	346	349
2082	326	330	334	343	351	353	355
2083	318	323	327	338	347	349	352
2084	330	334	337	346	353	355	357
2085	332	336	339	347	354	356	358
2086	344	347	349	355	360	361	362
2087	341	344	347	353	358	359	361
2088	348	350	352	358	361	362	363
2089	346	349	351	357	361	362	363
2090	352	354	356	360	363	363	364
2091	353	355	357	360	363	364	364
2092	355	357	358	362	364	364	365
2093	353	355	357	361	363	364	365
2094	354	355	357	361	363	364	365
2095	357	358	360	363	364	365	365
2096	358	359	360	363	365	365	365
2097	356	358	359	362	364	365	365

Sea level rise scenario: NOAA Intermediate flood threshold: NOAA minor

Year/Percentile	5	10	17	50	83	90	95
2098	356	358	359	362	364	365	365
2099	360	361	362	364	365	365	365
2100	361	362	363	364	365	365	365

Sea level rise scenario: NOAA Intermediate flood threshold: NOAA moderate

Year/Percentile	5	10	17	50	83	90	95
2010	0	0	1	3	5	6	8
2011	0	0	0	2	4	5	6
2012	0	1	1	3	6	7	8
2013	0	0	0	1	4	5	6
2014	0	0	0	2	4	5	6
2015	0	0	0	1	3	4	5
2016	0	0	1	2	5	6	7
2017	0	0	1	2	5	6	8
2018	0	0	1	3	6	7	8
2019	0	0	1	3	5	6	8
2020	0	1	1	3	6	7	9
2021	0	1	1	3	6	7	9
2022	0	0	1	3	6	7	9
2023	0	0	0	2	5	6	7
2024	0	0	1	3	6	7	8
2025	0	1	1	4	7	8	10
2026	1	1	2	4	8	10	11
2027	0	1	2	4	7	9	11
2028	1	2	2	5	9	11	13
2029	3	4	5	9	14	16	18
2030	4	5	6	11	16	19	21
2031	3	4	5	10	15	18	21
2032	3	4	5	9	15	17	20
2033	5	6	7	12	18	21	23
2034	6	7	9	14	21	23	26
2035	5	6	8	13	20	23	26
2036	4	6	7	12	19	22	25
2037	6	8	10	15	23	25	29
2038	8	9	11	18	25	28	31
2039	8	9	11	18	26	29	33

Sea level rise scenario: NOAA Intermediate flood threshold: NOAA moderate

Year/Percentile	5	10	17	50	83	90	95
2040	7	9	10	17	24	27	31
2041	6	8	10	16	23	26	30
2042	10	12	14	20	29	32	36
2043	11	14	16	24	33	37	40
2044	11	13	15	23	33	36	41
2045	14	16	19	28	39	43	47
2046	18	21	24	33	44	48	53
2047	25	29	32	43	55	59	65
2048	25	28	31	42	54	58	63
2049	30	34	38	51	65	70	76
2050	33	37	41	54	68	73	79
2051	40	44	48	62	77	83	89
2052	43	47	51	64	78	83	89
2053	50	55	59	74	90	95	102
2054	51	57	61	76	92	97	104
2055	59	64	69	84	100	106	113
2056	54	59	63	78	93	98	105
2057	63	68	73	88	104	109	116
2058	57	63	67	82	98	104	110
2059	62	67	72	89	105	111	118
2060	64	69	75	89	105	111	117
2061	73	79	84	99	116	122	128
2062	76	81	87	102	118	125	131
2063	86	92	98	114	131	136	143
2064	96	103	108	125	142	148	154
2065	104	110	116	133	149	155	162
2066	103	109	115	131	148	154	160
2067	109	115	120	136	153	159	166
2068	125	131	137	154	172	178	184
2069	131	138	145	163	181	186	193
2070	133	140	146	163	181	188	195
2071	135	142	148	166	184	190	197
2072	150	157	163	181	199	205	212
2073	158	164	170	189	207	213	220
2074	156	163	169	188	207	213	221
2075	151	158	164	183	202	208	215
2076	160	168	174	193	211	217	224

Sea level rise scenario: NOAA Intermediate flood threshold: NOAA moderate

Year/Percentile	5	10	17	50	83	90	95
2077	161	167	173	192	210	217	224
2078	167	174	180	199	219	225	232
2079	166	173	179	198	217	223	230
2080	181	188	195	215	235	242	249
2081	187	194	201	221	241	248	255
2082	205	213	219	240	260	267	274
2083	206	214	221	240	259	265	272
2084	219	226	233	253	272	278	285
2085	225	233	240	260	278	285	292
2086	245	254	261	281	299	305	311
2087	247	254	261	280	297	302	308
2088	265	272	278	295	310	315	320
2089	268	275	281	297	312	317	321
2090	283	290	296	312	325	329	334
2091	291	298	303	318	330	334	339
2092	292	298	303	318	331	334	339
2093	289	295	300	315	327	331	336
2094	292	298	304	318	331	334	338
2095	305	311	316	330	341	344	347
2096	306	312	317	331	342	345	348
2097	306	311	316	328	339	342	345
2098	308	313	318	330	340	343	346
2099	327	331	335	344	352	354	356
2100	329	334	337	347	354	356	358

Sea level rise scenario: NOAA Intermediate High flood threshold: NOAA minor

Year/Percentile	5	10	17	50	83	90	95
2010	20	23	25	34	43	46	50
2011	23	26	29	37	46	50	54
2012	26	29	32	40	50	53	57
2013	22	25	28	36	46	49	53
2014	26	29	32	41	51	55	59
2015	22	25	27	36	45	49	53
2016	28	31	34	43	53	56	60
2017	26	30	33	43	54	58	63
2018	31	34	38	50	63	67	73

Sea level rise scenario: NOAA Intermediate High flood threshold: NOAA minor

Year/Percentile	5	10	17	50	83	90	95
2019	30	34	38	50	63	68	73
2020	34	38	42	54	67	72	77
2021	33	36	40	51	64	69	74
2022	36	40	44	56	69	75	81
2023	31	35	39	51	64	69	75
2024	38	42	46	59	73	79	85
2025	37	41	45	58	71	75	81
2026	46	51	55	69	85	90	96
2027	50	55	60	74	89	95	101
2028	60	65	70	85	101	107	113
2029	67	72	77	92	107	113	119
2030	78	84	89	104	120	125	132
2031	79	84	89	105	121	126	133
2032	86	92	97	113	130	136	142
2033	92	98	104	120	137	143	149
2034	99	105	111	128	145	151	157
2035	98	104	109	125	141	147	154
2036	105	111	116	132	149	155	161
2037	117	123	129	146	163	168	175
2038	122	128	133	150	167	173	180
2039	119	125	131	147	165	171	178
2040	118	124	130	147	164	171	178
2041	128	134	140	157	174	180	187
2042	136	143	149	166	184	190	197
2043	141	148	154	172	190	196	202
2044	142	149	154	172	191	197	204
2045	160	167	174	192	210	216	223
2046	171	178	184	202	221	227	233
2047	186	193	200	218	237	244	251
2048	183	190	197	215	233	240	247
2049	206	213	220	239	258	264	271
2050	212	219	226	245	263	270	277
2051	227	235	241	261	280	286	293
2052	228	235	241	260	277	283	289
2053	249	256	262	279	296	302	308
2054	252	259	265	281	297	303	308
2055	269	277	282	299	314	319	324

Sea level rise scenario: NOAA Intermediate High flood threshold: NOAA minor

Year/Percentile	5	10	17	50	83	90	95
2056	258	265	271	289	305	311	316
2057	277	283	289	304	319	323	327
2058	271	277	283	298	312	317	321
2059	284	291	297	312	325	329	333
2060	287	293	300	315	327	331	335
2061	303	308	313	325	336	340	343
2062	303	309	314	326	336	339	343
2063	320	324	328	338	346	348	351
2064	330	334	337	346	353	355	357
2065	337	341	344	351	357	358	360
2066	334	338	341	348	354	356	358
2067	339	342	345	351	357	358	360
2068	351	353	355	359	362	363	364
2069	355	356	358	361	364	364	365
2070	353	355	356	360	363	364	364
2071	354	356	357	361	363	364	365
2072	359	360	361	363	365	365	365
2073	360	362	362	364	365	365	365
2074	358	360	361	363	365	365	365
2075	359	360	361	364	365	365	365
2076	361	362	363	365	365	365	365
2077	362	363	364	365	365	365	365
2078	361	362	363	364	365	365	365
2079	362	363	363	365	365	365	365
2080	363	364	364	365	365	365	365
2081	363	364	365	365	365	365	365
2082	363	364	364	365	365	365	365
2083	364	364	365	365	365	365	365
2084	365	365	365	365	365	365	365
2085	365	365	365	365	365	365	365
2086	365	365	365	365	365	365	365
2087	365	365	365	365	365	365	365
2088	365	365	365	365	365	365	365
2089	365	365	365	365	365	365	365
2090	365	365	365	365	365	365	365
2091	365	365	365	365	365	365	365
2092	365	365	365	365	365	365	365

Sea level rise scenario: NOAA Intermediate High flood threshold: NOAA minor

Year/Percentile	5	10	17	50	83	90	95
2093	365	365	365	365	365	365	365
2094	365	365	365	365	365	365	365
2095	365	365	365	365	365	365	365
2096	365	365	365	365	365	365	365
2097	365	365	365	365	365	365	365
2098	365	365	365	365	365	365	365
2099	365	365	365	365	365	365	365
2100	365	365	365	365	365	365	365

**Sea level rise scenario: NOAA Intermediate High flood threshold:
NOAA moderate**

Year/Percentile	5	10	17	50	83	90	95
2010	0	1	1	4	7	8	9
2011	0	0	1	3	6	7	8
2012	1	1	2	5	8	9	11
2013	0	0	1	3	5	7	8
2014	0	1	1	3	6	7	8
2015	0	0	1	2	5	6	7
2016	1	1	2	4	7	8	10
2017	1	1	2	4	8	10	11
2018	1	2	2	5	9	11	13
2019	1	1	2	5	9	10	12
2020	1	2	3	6	10	12	14
2021	1	2	3	6	11	13	15
2022	1	2	3	6	11	12	15
2023	1	1	2	5	9	10	12
2024	2	2	3	7	11	13	15
2025	2	3	4	8	13	15	17
2026	3	4	5	10	15	17	20
2027	3	4	5	10	16	18	21
2028	5	6	8	13	19	22	25
2029	9	11	12	19	26	29	32
2030	12	14	16	23	32	36	40
2031	11	14	16	24	33	37	41
2032	11	14	16	24	34	37	42
2033	16	19	21	30	40	43	47
2034	20	23	25	35	46	50	54

**Sea level rise scenario: NOAA Intermediate High flood threshold:
NOAA moderate**

Year/Percentile	5	10	17	50	83	90	95
2035	20	23	26	36	48	52	57
2036	20	24	27	37	50	54	59
2037	26	30	34	44	58	62	68
2038	30	34	38	49	62	67	73
2039	31	35	39	51	64	69	75
2040	30	34	38	50	64	69	74
2041	33	37	41	54	68	73	79
2042	39	44	48	61	76	81	86
2043	46	51	56	70	86	91	97
2044	47	52	56	70	85	91	97
2045	60	66	71	87	103	109	115
2046	67	73	78	93	110	115	122
2047	81	87	93	109	126	132	138
2048	78	84	90	106	123	128	134
2049	97	103	109	125	142	147	154
2050	102	108	114	130	148	154	161
2051	114	121	127	144	161	167	174
2052	113	120	125	142	160	166	173
2053	128	134	140	158	176	182	190
2054	132	138	144	161	179	185	192
2055	146	152	157	175	192	198	205
2056	140	147	153	170	188	194	200
2057	153	159	165	182	201	207	214
2058	147	153	159	178	196	203	210
2059	158	165	171	189	207	213	221
2060	164	171	178	195	213	219	225
2061	178	185	192	211	231	237	244
2062	184	192	199	218	236	243	250
2063	200	208	215	234	253	259	266
2064	219	227	233	253	272	277	284
2065	233	240	247	266	283	289	296
2066	237	244	251	269	286	292	297
2067	249	256	263	280	295	300	306
2068	274	281	287	303	317	322	327
2069	285	292	298	314	327	332	336
2070	290	296	301	315	328	332	336

**Sea level rise scenario: NOAA Intermediate High flood threshold:
NOAA moderate**

Year/Percentile	5	10	17	50	83	90	95
2071	294	300	304	318	330	333	337
2072	316	322	326	337	345	348	351
2073	324	329	333	343	351	353	355
2074	325	329	333	342	349	352	354
2075	317	322	326	336	345	348	351
2076	333	337	340	348	354	356	358
2077	337	340	343	351	357	358	360
2078	340	343	346	353	358	359	361
2079	337	340	343	351	356	358	360
2080	347	350	352	357	361	362	363
2081	351	354	355	360	363	363	364
2082	355	356	358	361	364	364	365
2083	354	356	358	361	364	364	365
2084	359	360	361	363	365	365	365
2085	359	360	361	364	365	365	365
2086	361	362	363	365	365	365	365
2087	360	362	362	364	365	365	365
2088	363	364	364	365	365	365	365
2089	363	364	364	365	365	365	365
2090	363	364	364	365	365	365	365
2091	363	364	364	365	365	365	365
2092	364	365	365	365	365	365	365
2093	364	365	365	365	365	365	365
2094	364	365	365	365	365	365	365
2095	365	365	365	365	365	365	365
2096	365	365	365	365	365	365	365
2097	365	365	365	365	365	365	365
2098	365	365	365	365	365	365	365
2099	365	365	365	365	365	365	365
2100	365	365	365	365	365	365	365

SUPPLEMENTARY DATA: TABLE 4.3

Projections of MEAN high tide flooding days per month in future pentads (five-year periods)

Six total scenarios: NOAA minor and moderate flood thresholds under three sea level rise scenarios (NOAA Intermediate Low, Intermediate, and Intermediate High)

Values are in number of days per month; columns show percentiles (e.g. 10 = 10th percentile, where there is a 90% chance that high tide flooding days will exceed the 10th percentile); rows show the first year of each pentad

Source: Thompson, P. R., Widlansky, M. J., Hamlington, B. D., Merrifield, M. A., Marra, J. J., Mitchum, G. T., & Sweet, W. (2021). Rapid increases and extreme months in projections of United States high-tide flooding. *Nature Climate Change*, 11(7), 584–590. <https://doi.org/10.1038/s41558-021-01077-8>

Sea level rise scenario: NOAA Intermediate Low flood threshold: NOAA minor

Year/Percentile	5	10	17	50	83	90	95
2010	1	1	1	1	2	2	2
2015	1	1	1	1	2	2	2
2020	1	1	1	1	2	2	2
2025	1	1	1	2	2	2	3
2030	2	2	2	3	4	4	4
2035	2	3	3	3	4	4	5
2040	2	3	3	3	4	4	5
2045	4	4	4	5	6	6	6
2050	5	5	6	6	7	7	8
2055	6	6	6	7	8	8	8
2060	6	6	7	7	8	9	9
2065	8	8	9	9	10	10	11
2070	9	9	10	10	11	12	12
2075	8	9	9	10	11	11	11
2080	9	10	10	11	12	12	12
2085	11	11	12	12	13	14	14
2090	12	12	12	13	14	15	15
2095	12	12	12	13	14	14	15
2100	11	12	12	14	15	16	17

Sea level rise scenario: NOAA Intermediate Low flood threshold: NOAA moderate

Year/Percentile	5	10	17	50	83	90	95
2010	0	0	0	0	0	0	0
2015	0	0	0	0	0	0	0
2020	0	0	0	0	0	0	0
2025	0	0	0	0	0	0	0

Sea level rise scenario: NOAA Intermediate Low flood threshold: NOAA moderate

Year/Percentile	5	10	17	50	83	90	95
2030	0	0	0	0	0	0	0
2035	0	0	0	0	0	0	0
2040	0	0	0	0	0	0	0
2045	0	0	0	0	0	1	1
2050	0	0	0	1	1	1	1
2055	0	0	1	1	1	1	1
2060	1	1	1	1	1	2	2
2065	1	1	2	2	2	3	3
2070	2	2	2	3	3	3	4
2075	1	2	2	2	3	3	3
2080	2	2	2	3	4	4	4
2085	3	3	3	4	5	5	5
2090	4	4	4	5	6	6	6
2095	3	4	4	5	5	6	6
2100	3	4	4	5	6	7	7

Sea level rise scenario: NOAA Intermediate flood threshold: NOAA minor

Year/Percentile	5	10	17	50	83	90	95
2010	1	2	2	2	2	2	2
2015	1	2	2	2	2	3	3
2020	2	2	2	2	3	3	3
2025	3	3	3	4	4	4	5
2030	5	5	5	6	6	7	7
2035	6	6	6	7	8	8	8
2040	6	7	7	8	9	9	9
2045	9	10	10	11	12	12	12
2050	12	12	13	14	15	15	15
2055	14	14	14	15	16	17	17
2060	16	16	17	17	19	19	19
2065	20	20	20	21	22	22	23
2070	23	23	23	24	25	25	26
2075	24	24	25	25	26	26	27
2080	27	27	27	28	28	28	28
2085	28	29	29	29	29	29	29
2090	29	29	29	30	30	30	30
2095	29	30	30	30	30	30	30
2100	30	30	30	30	30	30	30

Sea level rise scenario: NOAA Intermediate flood threshold: NOAA moderate

Year/Percentile	5	10	17	50	83	90	95
2010	0	0	0	0	0	0	0
2015	0	0	0	0	0	0	0
2020	0	0	0	0	0	0	0
2025	0	0	0	0	0	0	0
2030	0	0	0	0	1	1	1
2035	0	0	1	1	1	1	1
2040	1	1	1	1	2	2	2
2045	2	2	2	3	3	4	4
2050	4	4	4	5	6	6	6
2055	5	6	6	7	7	8	8
2060	7	7	8	8	9	9	10
2065	10	10	11	11	12	13	13
2070	13	13	13	14	15	16	16
2075	14	14	15	16	17	17	17
2080	17	17	18	19	20	20	21
2085	21	22	22	23	24	24	25
2090	24	25	25	26	27	27	27
2095	26	26	27	27	28	28	28
2100	27	27	28	28	29	29	29

Sea level rise scenario: NOAA Intermediate High flood threshold: NOAA minor

Year/Percentile	5	10	17	50	83	90	95
2010	2	2	2	3	3	3	3
2015	2	3	3	3	4	4	4
2020	3	3	3	4	5	5	5
2025	5	5	5	6	7	7	7
2030	8	8	8	9	10	10	10
2035	10	10	10	11	12	12	13
2040	12	12	12	13	14	14	15
2045	16	16	16	17	18	19	19
2050	20	20	21	22	23	23	23
2055	23	23	24	25	25	26	26
2060	26	26	26	27	27	28	28
2065	28	29	29	29	29	29	29
2070	29	30	30	30	30	30	30
2075	30	30	30	30	30	30	30

Sea level rise scenario: NOAA Intermediate Low flood threshold: NOAA moderate

Year/Percentile	5	10	17	50	83	90	95
2080	30	30	30	30	30	30	30
2085	30	30	30	30	30	30	30
2090	30	30	30	30	30	30	30
2095	30	30	30	30	30	30	30
2100	30	30	30	30	30	30	30

**Sea level rise scenario: NOAA Intermediate High flood threshold:
NOAA moderate**

Year/Percentile	5	10	17	50	83	90	95
2010	0	0	0	0	0	0	0
2015	0	0	0	0	0	0	0
2020	0	0	0	0	0	0	0
2025	0	0	0	1	1	1	1
2030	1	1	1	2	2	2	3
2035	2	2	3	3	4	4	4
2040	3	4	4	5	5	6	6
2045	7	7	7	8	9	9	10
2050	10	11	11	12	13	13	13
2055	13	13	13	14	15	16	16
2060	16	17	17	18	19	19	20
2065	22	22	22	23	24	24	25
2070	26	26	26	27	28	28	28
2075	28	28	28	28	29	29	29
2080	29	29	29	30	30	30	30
2085	30	30	30	30	30	30	30
2090	30	30	30	30	30	30	30
2095	30	30	30	30	30	30	30
2100	30	30	30	30	30	30	30

SUPPLEMENTARY DATA: TABLE 4.4

Projections of MAXIMUM high tide flooding days per month in future pentads (5-year periods)

Six total scenarios: NOAA minor and moderate flood thresholds under three sea level rise scenarios (NOAA Intermediate Low, Intermediate, and Intermediate High)

Values are in number of days per month; columns show percentiles (e.g. 10 = 10th percentile, where there is a 90% chance that high tide flooding days will exceed the 10th percentile); rows show the first year of each pentad

Source: Thompson, P. R., Widlansky, M. J., Hamlington, B. D., Merrifield, M. A., Marra, J. J., Mitchum, G. T., & Sweet, W. (2021). Rapid increases and extreme months in projections of United States high-tide flooding. *Nature Climate Change*, 11(7), 584–590. <https://doi.org/10.1038/s41558-021-01077-8>

Sea level rise scenario: NOAA Intermediate Low Flood threshold: NOAA minor

Year/Percentile	5	10	17	50	83	90	95
2010	7	8	8	10	12	13	14
2015	6	7	8	9	12	13	14
2020	6	7	7	9	12	13	14
2025	7	8	9	11	13	14	15
2030	10	10	11	13	16	17	18
2035	10	11	12	14	17	18	19
2040	11	11	12	14	17	18	19
2045	13	13	14	16	19	20	21
2050	15	15	16	18	21	22	23
2055	15	16	16	19	21	22	23
2060	16	17	17	19	22	23	24
2065	18	19	19	21	23	24	25
2070	19	20	20	22	24	25	26
2075	19	19	20	22	24	25	26
2080	19	20	21	23	25	26	26
2085	21	22	22	24	26	27	28
2090	22	23	23	25	27	28	29
2095	22	22	23	25	27	27	28
2100	18	19	20	22	24	25	26

Sea level rise scenario: NOAA Intermediate Low Flood threshold: NOAA moderate

Year/Percentile	5	10	17	50	83	90	95
2010	1	2	2	3	4	5	6
2015	1	1	2	3	4	5	5
2020	1	1	2	3	4	4	5
2025	1	2	2	3	5	5	6

Sea level rise scenario: NOAA Intermediate Low Flood threshold: NOAA moderate

2030	2	3	3	4	6	6	7
2035	2	3	3	4	6	7	8
2040	3	3	3	5	6	7	8
2045	4	4	4	6	8	9	10
2050	5	5	6	7	9	10	11
2055	5	6	6	8	10	11	12
2060	6	6	7	9	11	12	13
2065	8	8	9	11	13	14	15
2070	9	10	10	12	15	16	18
2075	9	9	10	12	15	16	17
2080	9	10	11	13	16	17	18
2085	11	12	13	15	18	19	20
2090	12	13	14	16	19	20	21
2095	12	13	13	16	18	19	20
2100	9	9	10	13	15	17	18

Sea level rise scenario: NOAA Intermediate Flood threshold: NOAA minor

Year/Percentile	5	10	17	50	83	90	95
2010	8	8	9	11	13	14	16
2015	8	9	9	11	14	15	16
2020	8	9	10	12	14	15	17
2025	11	11	12	14	17	18	19
2030	14	14	15	17	20	21	22
2035	15	16	17	19	21	22	23
2040	16	17	18	20	22	23	24
2045	19	20	21	23	25	26	27
2050	22	23	24	26	28	28	29
2055	24	25	25	27	29	29	30
2060	27	27	28	29	30	31	31
2065	29	30	30	31	31	31	31
2070	31	31	31	31	31	31	31
2075	31	31	31	31	31	31	31
2080	31	31	31	31	31	31	31
2085	31	31	31	31	31	31	31
2090	31	31	31	31	31	31	31
2095	31	31	31	31	31	31	31
2100	31	31	31	31	31	31	31

Sea level rise scenario: NOAA Intermediate Flood threshold: NOAA moderate

Year/Percentile	5	10	17	50	83	90	95
2010	2	2	2	3	5	5	6
2015	2	2	2	3	5	5	6
2020	2	2	2	3	5	6	6
2025	3	3	3	5	6	7	8
2030	4	5	5	7	9	10	11
2035	5	6	6	8	10	11	12
2040	6	7	7	9	12	13	14
2045	9	10	11	13	16	17	18
2050	13	13	14	17	19	20	21
2055	15	15	16	18	21	22	23
2060	17	18	18	20	23	24	25
2065	20	21	21	23	25	26	27
2070	23	24	24	26	28	28	29
2075	25	25	26	28	30	30	30
2080	28	28	29	30	31	31	31
2085	30	31	31	31	31	31	31
2090	31	31	31	31	31	31	31
2095	31	31	31	31	31	31	31
2100	31	31	31	31	31	31	31

Sea level rise scenario: NOAA Intermediate High Flood threshold: NOAA minor

Year/Percentile	5	10	17	50	83	90	95
2010	9	10	11	13	15	16	18
2015	10	11	11	14	16	17	19
2020	11	12	12	15	17	18	20
2025	14	15	15	18	20	21	22
2030	18	18	19	21	23	24	25
2035	20	20	21	23	25	26	27
2040	22	23	23	25	27	28	29
2045	26	27	28	29	30	31	31
2050	30	30	30	31	31	31	31
2055	31	31	31	31	31	31	31
2060	31	31	31	31	31	31	31
2065	31	31	31	31	31	31	31
2070	31	31	31	31	31	31	31
2075	31	31	31	31	31	31	31
2080	31	31	31	31	31	31	31

Sea level rise scenario: NOAA Intermediate High Flood threshold: NOAA minor

2085	31	31	31	31	31	31	31	31
2090	31	31	31	31	31	31	31	31
2095	31	31	31	31	31	31	31	31
2100	31	31	31	31	31	31	31	31

Sea level rise scenario: NOAA Intermediate High Flood threshold: NOAA moderate

Year/Percentile	5	10	17	50	83	90	95
2010	2	2	3	4	6	6	7
2015	2	3	3	4	6	7	8
2020	3	3	4	5	7	7	8
2025	4	5	5	7	9	10	11
2030	7	8	9	10	13	14	15
2035	10	11	11	13	16	17	19
2040	12	13	14	16	19	20	21
2045	17	18	18	20	23	24	25
2050	20	21	22	24	26	27	28
2055	23	24	24	26	28	29	29
2060	27	28	28	30	31	31	31
2065	30	31	31	31	31	31	31
2070	31	31	31	31	31	31	31
2075	31	31	31	31	31	31	31
2080	31	31	31	31	31	31	31
2085	31	31	31	31	31	31	31
2090	31	31	31	31	31	31	31
2095	31	31	31	31	31	31	31
2100	31	31	31	31	31	31	31

Climate Change Impacts and Projections for the Greater Boston Area

ELLEN DOUGLAS, PhD, PAUL KIRSHEN, PhD

Findings of the Greater Boston Research Advisory Group Report

During the writing of the inaugural Boston Research Advisory Group (BRAG) report both NASA and NOAA announced that 2015 was the warmest year on record, beating the previous record set in 2014, by 0.29 °F. Just five years later (during the writing of this report), NASA announced that 2020 had tied 2016 for the warmest year, breaking the previous record by a stunning 1.84 °F, and that the last seven years have been the warmest seven-year period on record.

These observations support the assertion made in the sixth and most recent assessment by the Intergovernmental Panel on Climate Change , which states, “It is unequivocal that human influence has warmed the atmosphere, ocean and land. Widespread and rapid changes in the atmosphere, ocean, cryosphere and biosphere have occurred.” Hence, the question is not whether the climate is changing, but what we’re going to do about it. At a minimum, we must focus efforts to get to net zero greenhouse gas (GHG) by 2050. It’s not too late to achieve that goal, but time is running out for us to prevent the worst-case scenarios suggested here.

This report is broken into four chapters and summarizes the most recent (as of late 2021) scientific understanding of climate risk factors pertinent to Greater Boston.



University of Massachusetts Boston
School for the Environment

**University of Massachusetts Boston
School for the Environment**
100 William T. Morrissey Blvd.
Boston, MA 02125-3393
(617) 287-5000
<https://environment.umb.edu>